

Cultural Heritage Science

Austin Nevin
Malgorzata Sawicki *Editors*

Heritage Wood

Investigation and
Conservation of Art on Wood



Springer

Cultural Heritage Science

Series editors

Klaas Jan van den Berg
Cultural Heritage Agency of the Netherlands
Amsterdam, The Netherlands

Aviva Burnstock
Courtauld Institute of Art
London, United Kingdom

Koen Janssens
Department of Chemistry, University of Antwerp
Antwerp, Belgium

Robert van Langh
Rijksmuseum
Amsterdam, The Netherlands

Jennifer Mass
Bard Graduate Center
New York, New York, USA

Austin Nevin
University of Gothenburg
Gothenburg, Sweden

Bertrand Lavedrine
Centre de Recherche sur la Conservation des Collections
Muséum National d'Histoire Naturelle
Paris, France

Bronwyn Ormsby
Conservation Science & Preventive Conservation, Tate Britain
London, United Kingdom

Matija Strlic
Institute for Sustainable Heritage, University College London
London, United Kingdom

More information about this series at <http://www.springer.com/series/13104>

Austin Nevin • Malgorzata Sawicki
Editors

Heritage Wood

Investigation and Conservation
of Art on Wood

 Springer

Editors

Austin Nevin
Department of Conservation
University of Gothenburg
Gothenburg, Sweden

Malgorzata Sawicki
Art Gallery of New South Wales
Sydney, NSW, Australia

ISSN 2366-6226

Cultural Heritage Science

ISBN 978-3-030-11053-6

<https://doi.org/10.1007/978-3-030-11054-3>

ISSN 2366-6234 (electronic)

ISBN 978-3-030-11054-3 (eBook)

© Springer Nature Switzerland AG 2019

This work is subject to copyright. All rights are reserved by the Publisher, whether the whole or part of the material is concerned, specifically the rights of translation, reprinting, reuse of illustrations, recitation, broadcasting, reproduction on microfilms or in any other physical way, and transmission or information storage and retrieval, electronic adaptation, computer software, or by similar or dissimilar methodology now known or hereafter developed.

The use of general descriptive names, registered names, trademarks, service marks, etc. in this publication does not imply, even in the absence of a specific statement, that such names are exempt from the relevant protective laws and regulations and therefore free for general use.

The publisher, the authors, and the editors are safe to assume that the advice and information in this book are believed to be true and accurate at the date of publication. Neither the publisher nor the authors or the editors give a warranty, express or implied, with respect to the material contained herein or for any errors or omissions that may have been made. The publisher remains neutral with regard to jurisdictional claims in published maps and institutional affiliations.

This Springer imprint is published by the registered company Springer Nature Switzerland AG.
The registered company address is: Gewerbestrasse 11, 6330 Cham, Switzerland

Preface

Wood is an intrinsically complex material that has been used to produce our cultural heritage since prehistory. Wooden structures, furniture, wooden sculpture, painted wood, gilded wood, varnished wood, lacquered wood, paintings on wooden supports, and other wooden artefacts are part of our common heritage. The preventive conservation, in-depth technical study, and treatment of wood and panel paintings are highlighted in this volume dedicated to Heritage Wood.

The aim of the book is to present new research on different works of art on wood. The international research spanning different disciplines is related to the conservation of wood and works on wooden substrates. The contributions range from the development of conservation materials and methods for cleaning and consolidation to the application of advanced instrumentation to the study of paintings. The 11 contributions in this volume are new research in preventive conservation, technical study, treatment, and assessment of works of art on wood in its many forms. These range from historical paintings to ceiling decorations and from Syrian rooms to finely carved objects.

Painted wood is of key importance and is featured prominently in the volume. Technical studies of painted works are presented on important panel paintings and allow their attribution, shedding light both on the use and limitations of portable instrumentation. New research related to climate and wood demonstrates the role of low temperatures for wood and the need to focus on equilibrium moisture content rather than RH in planning HVAC systems. New methods for cleaning gilding and consolidation of waterlogged wood are also featured in chapters.

A broad theme of the research presented in this volume is the close collaboration between art historians and scientists; whether engineers, physicists, biologists, and chemists or computer scientists, all working together with conservators and curators of the different types of materials, can lead to new research in conservation science and technical art history. The conservation and treatment of wood from different contexts and continents – from waterlogged wood to ecclesiastical objects – require careful selection of methods and often vastly different approaches, in which the ethics of conservation play as central a role as does the compatibility and stability of new materials. It is crucial that the conservator understands how organic solvents

affect gilded surfaces to assess their risks and benefits and the short- and long-term effects on gilding layers.

The advances in scientific research applied to heritage wood include new methods for analysis and conservation. It is our belief that through sharing and publishing technical studies and case studies of treatments, we will be better prepared to assess degradation and to determine the most suitable treatments in the future. We are confident that, with technologic innovation and a greater collaboration between scientific research and conservation practice, new solutions will be developed for the deeper understanding and sustainable treatment of heritage made of wood.

Gothenburg, Sweden
Sydney, NSW, Australia

Austin Nevin
Malgorzata Sawicki

Contents

1	An Investigation of the Feasibility of the Use of Gels and Emulsions in Cleaning of Gilded Wooden Surfaces. Part A: Removal of Brass-Based Overpainting	1
	Malgorzata Sawicki, Emma Rouse, Sofia Lo Bianco, and Seela Kautto	
2	An Investigation of the Feasibility of the Use of Gels and Emulsions in Cleaning of Gilded Wooden Surfaces. Part B: Cleaning of Soiled Oil-Gilding	37
	Malgorzata Sawicki, Emma Rouse, Sofia Lo Bianco, and Seela Kautto	
3	New Consolidants for the Conservation of Archeological Wood	65
	Zarah Walsh-Korb, Emma-Rose Janeček, Mark Jones, Luc Averous, and Oren A. Scherman	
4	Analytical Examination and Conservation of East Asian Lacquer Works from European Collections	79
	Václav Pitthard, Silvia Miklin-Kniefacz, Sabine Stanek, and Martina Griesser	
5	Technology for Technology's Sake: The Technical Study of Gothic Miniature Boxwood Carvings in the Thomson Collection at the Art Gallery of Ontario	93
	Lisa Ellis, Alexandra Suda, Ronald Martin, Elizabeth Moffatt, Jennifer Poulin, Heidi Sobol, Priam Givord, Craig Boyko, Ian Lefebvre, and Andrew J. Nelson	
6	The Use of a Copper Green Oil Paint in the Interiors of Eidsvoll Manor in Norway: Analysis of a Discoloured Architectural Paint from 1814	109
	Edwin Verweij, Ulrich Schade, and Hartmut Kutzke	

7	A Polychrome Wooden Interior from Damascus: A Multi-method Approach for the Identification of Manufacturing Techniques, Materials and Art Historical Background	123
	Petronella Kovács Mravik, Éva Galambos, Zsuzsanna Márton, Ivett Kisapáti, Julia Schultz, Attila Lajos Tóth, István Sajó, and Dániel Károly	
8	An Original Approach to Active Climate Control Based on Equilibrium Moisture Content (EMC) as Set Point in a Middle-Age Building in Palermo, Italy	143
	Paolo Dionisi-Vici and Daniela Romano	
9	The Influence of Low Temperature on Moisture Transport and Deformation in Wood: A Neglected Area of Research	165
	Charlotta Bylund Melin	
10	Conservation and Technological Research of a Polychrome Sculpture of <i>Christ on a Donkey</i> from the Workshop of Michel and Gregor Erhart	183
	Katarzyna Męczyńska and Anna Michnikowska	
11	Multi-Disciplinary Complex Research to Reconsider Basic Questions on Attribution and Dating of the <i>Last Judgment</i> Triptych from National Museum in Gdańsk by Rogier van der Weyden and Hans Memling	197
	Iwona Szmelter and Tomasz Ważny	

Abbreviations

CT	computer tomography
DTPA	diethylenetriaminepentaacetic acid
EDTA	ethylenediaminetetraacetic acid
ELISA	enzyme-linked immunosorbent assay
EMC	equilibrium moisture content
FSP	fibre saturation point
FTIR	Fourier-transform infrared spectroscopy
HVAC	heating, ventilation, and air conditioning
HVPD	high viscous polymeric dispersions
IIIF	international image interoperability framework
LIBS	laser-induced breakdown spectroscopy
MC	moisture content
MNIR	multispectral near-infrared reflectography
OCT	optical coherence tomography
OM	optical microscopy
PEG	poly(ethylene glycol)
Py-GC-MS	pyrolysis-gas chromatography-mass spectrometry
RH	relative humidity
SAXS	small-angle X-ray scattering
SEM-EDS	scanning electron microscopy-energy dispersive spectrometry
SR	synchrotron radiation
TAC	tri-ammonium citrate
TCSPC	time-correlated single photon counting
TD-GC-MS	thermal desorption-gas chromatography-mass spectrometry
TEA	triethanolamine
T _g	glass transition temperature
THM	thermally assisted hydrolysis and methylation

TMAH	tetramethylammonium hydroxide
UV	ultraviolet
VR	virtual reality
XANES	X-ray absorption near-edge structure spectroscopy
XRD	X-ray diffraction
XRF	X-ray fluorescence spectroscopy

Chapter 1

An Investigation of the Feasibility of the Use of Gels and Emulsions in Cleaning of Gilded Wooden Surfaces.

Part A: Removal of Brass-Based Overpainting



Malgorzata Sawicki, Emma Rouse, Sofia Lo Bianco, and Seela Kautto

Abstract The term ‘cleaning of gilded wooden surfaces’ should be understood broadly to account for their complexity. Each layer of a gilded surface requires assessment, and often, a separate cleaning methodology. Removal of overpainting is a part of the surface cleaning process of gilded wood. Many cleaning methods for gilded surfaces were adopted from other conservation fields, as there is little research in reference to cleaning of gilded wood. Two case studies involving nineteenth century gilded frames, focused on finding a suitable gel and application method to remove brass-based overpainting and surface dirt. This paper presents the findings from our investigation in regards to brass-based overpainting removal (Part A). The results of experiments into removal of soiling from gilded wooden surfaces are covered in a second paper (Part B). Two rigid gels reviewed in conservation literature were tested for removing brass-based overpainting from oil-gilded surfaces: Xanthan gum gel and poly(vinyl alcohol)-borax gel (PVOH-borax gel). Low-viscosity emulsions based on Pemulen TR-2 were also tested as they involve more straightforward clearing process than with viscous gels. Gels were evaluated according to application and removal methods, viscosity, texture, and cleaning efficiency. Rigid solvent gels and low-viscosity emulsions offer a viable alternative to free solvent application provided they can be easily removed from the surface, with minimal clearing requirements. Factors influencing the performance of gel systems include the thickness of the overpainting layers, the presence of a ‘barrier layer’ between the overpainting and gilding, the solubility of the overpainting binder, and the solubility characteristics of the solvent (its rate and power of swelling,

M. Sawicki (✉) · E. Rouse · S. L. Bianco
Art Gallery of New South Wales, Sydney, NSW, Australia
e-mail: margaret.sawicki@ag.nsw.gov.au

S. Kautto
Faculty of Culture/Degree Programme in Conservation, Helsinki Metropolia University of Applied Sciences, Helsinki, Finland

evaporation rate and application method). For the removal of overpainting from gilded wooden surfaces, fast-acting solvents with moderate swelling power are more appropriate than slow-acting solvents with strong swelling power. The latter can soften gilding layers beneath the overpainting. Important factors to consider are solvent volatility and the rate it diffuses into the overpainting.

Keywords Gilding · Gilded wood · Surface cleaning · Brass-based paint · Solvents gels · Solvent emulsions · Xanthan · PVOH-borax gel · Pemulen TR2 emulsion · Benzyl alcohol

1.1 Introduction

The gilding of wooden artefacts is an ancient craft that has endured for millennia. Gilded surfaces can be multifaceted to prepare and complex to clean. In other conservation fields ‘*cleaning starts with the decision to protect the surface*’ ([7]: 12) however, in the conservation of gilded objects, it starts with understanding the surface. The selection of appropriate cleaning methods and treatment procedures depends upon it.

Historically, to gild a wooden surface, 0.8–0.3 µm-thick gold leaf was laid over a specifically-prepared foundation [10]. This foundation determined the technique of gold leaf application, its appearance, and durability. Traditionally, several gilding techniques were often used in one object; alternating polished and matte gilt sequences created unique lustre and vibrational effects. Gilded surfaces were typically coated with a variety of varnishes and glazes to preserve them and to adjust their aesthetic qualities. With time, the natural ageing processes of the materials, abrasion and wear, and the accumulation of dirt, candle soot, and other atmospheric pollutants alter gilding. Regilding was often carried out to disguise such damages, obscuring the intricacy and details of the design.

Various alloys of gold with silver and copper have been used in gilding. The composition of gold leaf could also vary according to where it was mined or produced. White metals (i.e. silver, tin) and, more recently, brass leaf, toned with various glazes, were used to imitate gold leaf. Powdered forms of gold and other metals have also been used to create the appearance of a gilded surface. Furthermore, from the middle of the nineteenth century onwards, brass-based paint (brass particles suspended in diverse mediums) flourished as an alternative to gilding and as a restoration technique for gilded wood.

Consequently, the term ‘cleaning of gilded wooden surfaces’ should be understood broadly to account for their complexity. Each layer of a gilded surface requires assessment, and often, a separate cleaning methodology. The original techniques, any subsequent changes and restorations, and the degradation processes involved, should determine such a methodology. The layers of overpainting, their state of preservation as well as the nature and condition of the original surface underneath should be equally considered.

Regardless of the technique, gold leaf is uniformly easy to abrade and damage. Burnished water gilding is the most durable; the pressure applied by an agate tool during burnishing establishes a superior bond between the gold leaf and the foundation layer. Matte water gilding also shows good resistance to ageing and many matte water-gilded surfaces have been preserved well in museum collections. Rather than a delamination of the gold leaf, damages to matte water gilding are caused mainly by mechanical abrasion or insufficient bonding between the gesso foundation and wooden substrate.

Oil gilding is less durable due to the interrelated aging processes of its resinous-oily foundation layers (sealer and gold size), glazes and protective coatings. Nevertheless, the ageing processes of original varnishes – whether proteinaceous, resinous or oil – based – will impact the durability of any type of gilding. Conservation practice shows these protective layers can contribute to gold-leaf delamination. Contrarily, they may also protect the gold leaf during overpainting removal.

Removing overpainting is dictated by the solubility of the binding medium and the type of gilding underneath. Gilding that is in poor condition can seriously complicate a treatment. Overpainting is often thick, multi-layered and applied over regilding; therefore, the removal of non-original layers requires two or more cleaning systems to be used in conjunction with each other. A layer-by-layer approach to cleaning allows greater control and selectivity in treatments. Removing brass-based overpainting from oil-gilded surfaces is particularly challenging because the oil-gilding foundation layers often have the same solubility parameters as the overpainting medium.

Common methods for overpainting removal include:

- Free solvent cleaning: applied on swab, poultices or in combination.
- Solvent gels or emulsions.

1.1.1 Gel-Cleaning Systems

Little research has been conducted into modern cleaning systems in reference to gilding. Therefore, many cleaning methods for gilded wooden surfaces were adopted from other conservation fields (panel paintings, polychrome, objects, metals, etc.).

The term ‘gel’ refers to numerous jelly, paste and putty-like materials that offer different ways to deliver a cleaning solution onto an artworks surface. As Angelova et al. [2] explain *‘In an ideal situation, the solubilised material can be wicked up into a gel, allowing for it’s safe and efficient removal from the artwork surface.’*

The first gel systems were developed in the 1980s as enzyme gels, resin soaps, and Carbopol solvent gels [26, 30]. They were not successful in cleaning gilded wooden surfaces as they proved difficult to control over delicate and thin gilding.

Practice has shown cleaning gilded surfaces must be quick and able to be interrupted immediately if any risk of removing gold leaf is observed. Carbopol solvent

gels, enzyme gels or resin soaps do not meet these criteria; the lengthy gel-residue clearing processes can effectively remove the gold leaf as well.

Subsequently, free solvent use or solvent-saturated poultices persists despite widespread understanding of potential adverse effects of solvents on gilding (softening, swelling, leaching, blanching, desaturation, material extraction, changes in mechanical properties etc.) ([27]: 45–46). These adverse effects fortunately do not affect all types of gilding. Furthermore, varnishes and gold leaf can act as a protective barrier for foundation layers during cleaning. In many cases, free solvents offer more effective methods of removing brass-based overpainting, as they can diffuse deeper into thick overpainting and soften it.

Nevertheless, broader conservation research over the last 30 years into surface deterioration mechanisms, and methods of surface cleaning, forms a growing body of knowledge applicable to gilded wooden surfaces. Newly developed cleaning methods incorporate a layer-by-layer approach. An extensive choice of gelling materials and cleaning agents with different specifications, is now on offer [2].

The Getty Conservation Institute's (GCI) new research project on Cleaning Systems for Wooden Gilded Surfaces takes a comprehensive look at various cleaning methods and materials for gilding.

Gel systems are potentially safer for the practitioner, the object and the natural environment; they can reduce solvent evaporation and diffusion rates. While gels are complex to prepare, they do not have rigorous safety requirements and can provide a faster-acting, more controlled and selective cleaning option. For example; a particular soiling type can be targeted by addressing specific characteristics and preparing customised gels according to required pH, viscosity, combinations of solvents, and concentrations.

The rise of interest in gels in conservation [1–3, 12, 13, 21], prompted us to reinvestigate the use of gels for cleaning gilded surfaces on frames.

Gilded wooden surfaces vary and each case requires unique investigation. Cleaning methods and procedures suitable for one gilded object will not necessarily work for another. Nevertheless, the testing outlined in this paper can assist to develop gel cleaning methodologies.

1.1.2 Testing Methodology/Gel Selection for Brass-Based Paint Removal

Two case studies focused on finding a suitable gel and application method to remove brass-based overpainting and surface dirt. The ideal gel would not require significant swab action or agitation when applied to the gilded surface. It should not penetrate into the cracks of the composition ornament and be easily removed so the gold leaf underlying the overpainting would not be affected. For these reasons, rigid gels were initially selected. Highly-viscous gels that require extensive clearing are harder to control, therefore less suitable options for gilded surfaces.

Several types of gels discussed in conservation literature, were tested for the following applications:

- (a) Brass-based overpainting removal; a substitute to free solvent use;
- (b) A vehicle for water-based cleaning solutions, to remove soiling and ingrained dirt.

Gels were evaluated according to application and removal methods, viscosity, texture, and cleaning efficiency. This paper will present the findings from our investigation in regards to brass-based overpainting removal (Part A). The results of our gilded surface cleaning investigation are covered in a second paper (Part B).

Initially, two rigid gels reviewed in conservation literature were tested for removing brass-based overpainting: Xanthan gum gel and poly(vinyl alcohol)-borax gel (PVOH-borax gel). Low-viscosity emulsions based on Pemulen TR-2 were also tested as they involve more straightforward clearing process than with viscous gels [26] (see [Appendix](#) for gel/emulsion preparation recipes).

Xanthan gum and PVOH-borax gels were also selected for their capacity to hold a high percentage of polar solvents. Xanthan gum forms hydrophobic ‘pockets’ within its structure; that suspend molecules less polar than water. Water-miscible solvents (i.e. ethanol, acetone) can be incorporated directly into Xanthan gum gel at a percentage of up to 50% v/v, without adversely impacting the gel structure [31]. Xanthan gum has been described as a ‘*naturally occurring polymeric emulsifier*’ [31] and has a semi-solid texture once gelled.

PVOH-borax gels require three ingredients; poly(vinyl alcohol), borax and water. PVOH is formed by the hydrolysis of polyvinyl acetate. While fully hydrolysed PVOH is not soluble in organic solvents, partially hydrolysed PVOH can be solubilised in various polar solvents. The lower the degree of hydrolysis, the more solvent the system can incorporate [2]. PVOH at 75% of hydrolysis can accept up to 70% of organic liquid [1]. Kuraray L-10 PVOH, which was used for all tests, can hydrolyse at 71.5–73.5%. The putty-like texture of the gel allows it to be easily removed from contoured surfaces by lifting with a spatula [1].

Pemulen TR-2 (modified polyacrylic acid) has a chemical structure that allows it to form oil-in-water emulsions with non-water miscible solvents without need for a surfactant. [26]. Detailed explanations on the working capabilities of Pemulen and recommended formulas for solvent emulsions are offered by Stavroudis [26] and Wolbers [31].

Solvents were selected according to solubility tests and FTIR examination of the overpainting medium. Volatile polar solvents, such as acetone and methylated spirit (ethanol with up to 10% addition of methanol), have been found to be most effective in removing degraded overpainting layers from gilded wooden surfaces. Benzyl alcohol was also included in testing, as it is widely recommended and used in solvent gel and emulsion recipes due to its strong swelling power, low volatility and low toxicity [26].

1.2 Case Study 1: The frame for Thomas Miles Richardson, *Eagle Crag and Gate Crag, Borrowdale, Cumberland* 1875; dimensions: 82.5 × 111.0 × 7.5 cm

The original frame for the watercolour *Eagle Crag and Gate Crag, Borrowdale, Cumberland* (1875) by Thomas Miles Richardson had been heavily regilded and restored with brass-based paint (Fig. 1.1). The painting is significant for the Art Gallery of NSW collection being the first non-Australian artwork to be commissioned for the newly founded gallery [29]. Major conservation treatment of the frame focussed on removing overpainting and overgilding to restore definition to the original composition ornaments and reveal original gilding.

1.2.1 Examination

1.2.1.1 Cross-Sections

Cross-section samples embedded in polyester resin were analysed with reflected and ultraviolet light, identifying the following stratigraphy: (a) a layer of brass particles in a synthetic binder and two oil-gilding schemes (b) and (c) (Fig. 1.2a, b).



Fig. 1.1 Case study 1: the corner and a detail of the frame for the Thomas Miles Richardson painting ‘*Eagle Crag and Gate Crag, Borrowdale, Cumberland, 1875*’, before treatment

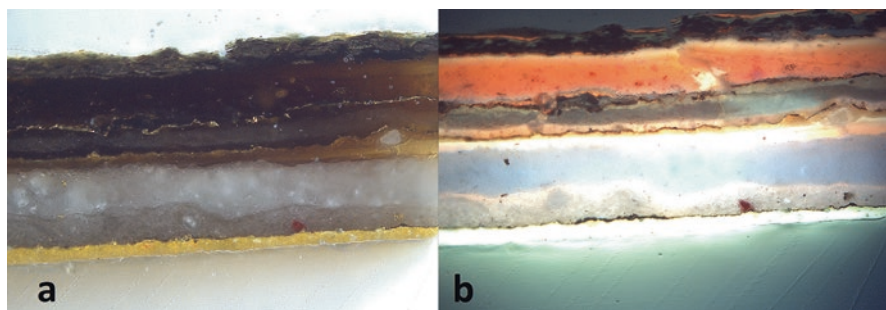


Fig. 1.2 Case study 1: the cross-section sample taken from outer scotia, viewed with reflected light (a) and UV luminescence (b) at 400× magnification

1.2.1.2 FTIR

Brass-based paint thin film samples were examined with FTIR in transmission mode.¹ The spectra showed strong absorption peaks at 1657 cm^{-1} (asymmetric stretch NO_2), 1280 cm^{-1} (symmetric stretch NO_2) and 841 cm^{-1} (N-O stretching) attributed to nitrocellulose. Strong vibration signals of the carbonyl group stretching at 1725 cm^{-1} , and C-O stretching at 1069 cm^{-1} as well as absorption peaks at 1460 cm^{-1} , 1122 cm^{-1} , and doublet at 749 cm^{-1} and 700 cm^{-1} can be assigned for alkyds or phthalate-type plasticiser [5, 6, 9, 15, 24] (Fig. 1.3).

1.2.1.3 Solvent Tests

Solvent tests were conducted with acetone, methylated spirit and a mixture of acetone and methylated spirit (1:1). The brass-based coating responded well to acetone and methylated spirit-saturated swabs revealing dark soiling underneath. Subsequently, acetone-saturated poultices were tested on the overpainting. The brass-based layer was easily softened after 30s of acetone exposure then removed with acetone-saturated swabs with no effect on the soiled-varnish and oil gilding layers underneath (Fig. 1.4).

The soiled-varnish layer was not soluble in solvents however it was sensitive to water and tri-ammonium citrate solutions (2% w/v). This suggests the layer is a soiled 'ormolu' (animal glue or animal glue with up to 10% v/v of diluted seedlac or shellac); a traditional varnish used for matte gilding (for more information see Part B).

¹FTIR spectra were collected using a Thermo Nicolet Nexus spectrometer attached to a Continuum IR microscope and MCT-A detector with KBr window ($11700\text{--}600\text{ cm}^{-1}$). The spectra were recorded in the range of $4000\text{--}550\text{ cm}^{-1}$ using 16 scans at 4 cm^{-1} resolution. A micro-compression cell with diamond window was used as a sample platform and samples were rolled flat with a FTIR roller prior to analysis.

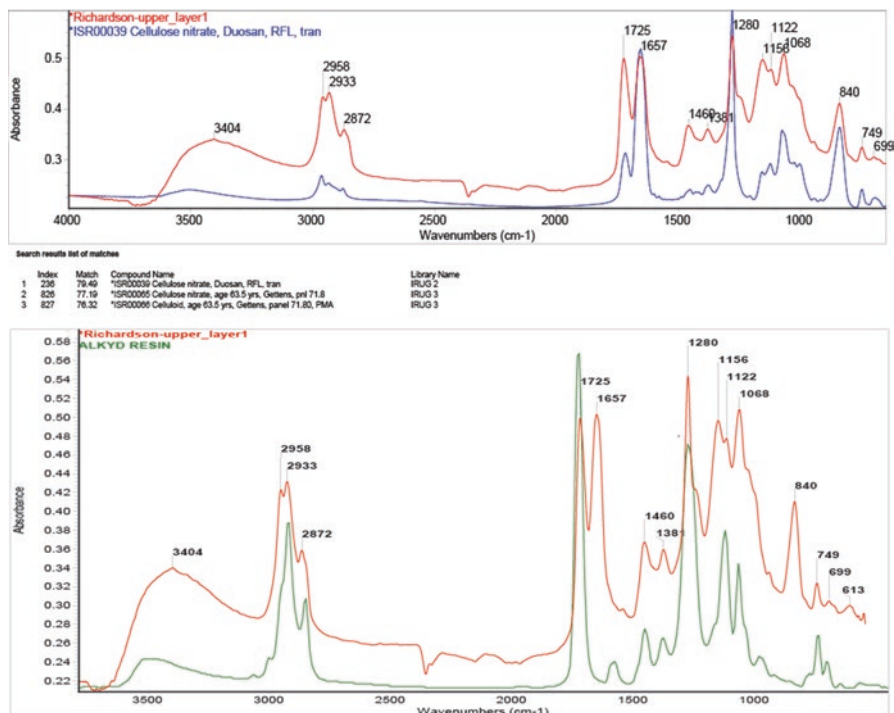


Fig. 1.3 Case study 1: FTIR spectra of the brass-based overpainting with references

1.2.2 Solvent Gel Testing – Removal of Brass-Based Overpainting (Table 1.1)

Xanthan gum solvent gels were applied to the surface by spatula or brush in a ~0.5 cm thick layer. The gel was covered with a sheet of Mylar to limit evaporation of the solvent. After the designated application time, the gel was removed with a spatula and the softened overpainting removed gently with a scalpel. The area was cleared with a dry cotton swab or a swab saturated with solvent.

To obtain the desired thickness, the PVOH-borax solvent gel was squeezed between two pieces of polyethylene sheet before it was applied to the surface. A piece of Mylar was placed over the gel during treatment to limit the evaporation of the solvent. After the desired application time, the gel could be lifted and removed with spatula (Fig. 1.5). There was no need for clearing. The softened brass-based paint could then be mechanically removed with a scalpel and swabs.

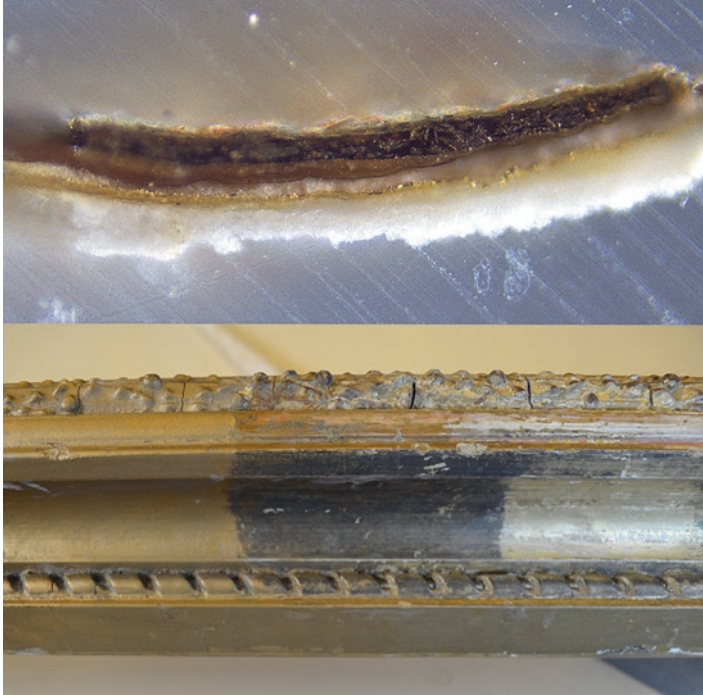


Fig. 1.4 Case study 1: upper image: the cross-section sample taken from outer scotia, viewed with reflected light at 400x magnification, lower image: outer scotia, results of solvent tests. The left-hand site section shows brass-based overpainting, the centre shows soiling exposed after removal of brass-based overpainting using acetone poultices followed by acetone swabs, the right-hand site section shows secondary (not original) oil-gilding revealed after removal of soiling with TAC solution

1.2.2.1 Results

Xanthan Gum Gel with Solvents

The gel was viscous and adhered well to the surface. Quick removal was not feasible; it was impossible to interrupt solvent action immediately and residues remained on the gilded surface which required clearing. Xanthan gum gel is not rigid enough to be easily removed without damage to the gold leaf.

Acetone

Xanthan gum gel with acetone solubilised the layers of brass-based overpainting. The underlying gilding was also softened and damaged when the gel was removed.

Table 1.1 Case study 1: Richardson frame – tests with solvent gels and emulsions for removal of brass-based overpainting

Gel tested	Area on frame tested	Application time	Application method	Removal method	Observation of gel texture	Results
Xanthan gum gel (4% w/v in water, pH 7) with Acetone (25% v/v).	Outer scotia	1; 3; 5 min	Spatula/ cotton swab	Cotton swab; dry and saturated with solvent	Low viscosity gel, conforms well to the overpainted surface. This consistency posed a risk of getting stuck in the cracks between ornament	Bronze overpaint could be removed after 3-5min of exposure to gel in all instances. The concentration of solvent used in the gel impacted how quickly the overpaint was solubilised; higher concentrations resulted in quicker reaction. However, the soiling and original gilding underneath were also affected; they were removed when gel residues were cleared using a swab barely dampened with acetone.
Xanthan gum gel (4% w/v in water, pH 7) with Acetone (30% v/v)						
Xanthan gum gel (4% w/v in water, pH 9) with Acetone (50% v/v)						
Xanthan gum gel (4% w/v in water, pH 8) with Methylated Spirits (50% v/v)					Low viscosity gel, conformed well to the overpainted surface.	Bronze overpaint could be removed after approximately 5min of exposure. The original gilding was also removed when gel residues were cleared using a swab barely dampened with methylated spirit.
Xanthan gum gel (4% w/v in water, pH 7) with benzyl alcohol (20% v/v) and EDTA (1% v/v),		5; 10; 20 min	Spatula	Cotton swab; dry and saturated with solvent	Low viscosity gel, conformed well to the overpainted surface.	5 min: isolated softening of brass-based paint occurred; which could be removed with benzyl-alcohol dampened swabs, removal was uneven and most of the brass-based paint remained. 10 min: bronze paint was softened and removed, however, the original gilding was also affected: the gilding foundation layers were softened as well and they could be removed with the swab.

<p>Cyclomethicone was applied by brush 1 minute before Xanthan gum gel (as above)</p>	<p>Taenia ornament</p>	<p>1; 3; 5 min</p>	<p>Spatula</p>	<p>Spatula</p>	<p>Gel was rigid, like a putty or plasticine. It could be manipulated into a sheet (~3mm thick) between two pieces of Mylar and then it could be easily applied over ornamented surface. It was easy to remove in one piece; it did not stick to the surface. There was no need for clearing.</p>	<p>The presence of Cyclomethicone slowed the softening of bronze paint. After 10 min brass-based paint could be removed with a benzyl alcohol dampened swab and after 20 min it could be removed with a scalpel. In both cases the soiling and gold leaf were also softened and removed with bronze paint. The presence of cyclomethicone did not protect the original layer of gold leaf.</p>
<p>10:90 acetone: PVOH/ borax gel</p>					<p>Gel was rigid, like a putty or plasticine. It could be manipulated into a sheet (~3mm thick) between two pieces of Mylar and then it could be easily applied over ornamented surface. It was easy to remove in one piece; it did not stick to the surface. There was no need for clearing.</p>	<p>Bronze paint swelled after 3 min; the area of brass-based paint that had been exposed to the gel could be mechanically removed with a scalpel. Very effective at solubilising brass-based paint.</p>
<p>50:50 acetone: PVOH/ borax gel</p>				<p>Spatula/ scalpel</p>	<p>Gel was rigid; easy to apply to any surface and to remove (as above).</p>	<p>When gel was applied to the surface of the frame the bronze paint began to soften within one minute. The area of brass-based paint that had been exposed to the gel could be mechanically removed with a scalpel.</p>

Fig. 1.5 Case study 1: testing PVOH-borax solvent gel; upper image shows how it can be applied and lower image shows how easy it can be lifted from the surface



Methylated Spirits

Xanthan gum with methylated spirits softened the brass-based overpainting producing results similar to the acetone gel. Removal with swabs damaged the underlying gilding.

Benzyl Alcohol and Ethylenediaminetetraacetic Acid (EDTA)

Benzyl alcohol in Xanthan gum gel had similar results. It worked slowly, however when it softened the thin layer of overpaint it also softened the soiling and gilding foundation layers underneath. The chelating agent EDTA was added to introduce a reaction with metallic particles in the overpainting to speed up the cleaning. Instead, it contributed to softening and dilution of the soiled-*varnish coating*. In areas where the *varnish coating* was thin (i.e. on the uppermost parts of moulding), this layer could be partially removed along with the gold leaf (Fig. 1.6).

Fig. 1.6 Case study 1: testing Xanthan gum gel with 20% v/v benzyl alcohol and 1% EDTA. The upper image shows it during the application time, while the lower image shows the surface after treatment; brass-based paint was removed together with soiling and most of gold leaf



Cyclomethicone was applied over the overpainting prior to the application of the gel to test its ability to protect the underlying gilding. Cyclomethicone slowed the softening of the brass-based overpainting, however the original layer of gilding was still vulnerable to damage when the gel was cleared with swabs.

PVOH-Borax gel

Acetone

Acetone was added to the PVOH-borax gel because it proved to be the most effective solvent for removing the overpainting. The 50% acetone gel proved most effective, softening the bronze paint rapidly. Within 1 min it softened and could be mechanically removed with a scalpel and swabs.

1.3 Case Study 2: The Frame for Charles Landelle 'Isemenie, Nymph of Diana' 1878, Dimensions: 177.6 × 131.5 × 15.0 cm

The frame for Charles Landelle's '*Isemenie Nymph of Diana*' (1878) purchased by the gallery in 1880 was originally constructed for the painting and manufactured in the late nineteenth Century. The rich plaster and composition ornaments were originally oil gilded, while the plain mouldings and corner-and-centre ribbons were matte and burnished water gilded over red and black bole foundations. Later, the frame was regilded. Cross-sections taken from the plain mouldings indicate two overgilding schemes; the latest layer appears characteristic of oil gilding techniques. In the twentieth century, the frame was covered with thick, brass-based overpainting to disguise damages to the gilding and ornament losses (Fig. 1.7). In 2014, the frame underwent conservation treatment to stabilise its construction. Treatment in 2018 aimed to remove the brass-based overpainting to reveal the gilded surface underneath.

Fig. 1.7 Case study 2: the corner of the frame for the Charles Landelle painting 'Isemenie, Nymph of Diana, 1878'. Upper image shows the corner prior to treatment; lower image shows the left-hand side member still covered with brass-based paint and the upper member after the overpaint was removed with acetone poultices, revealing soiled gilded surface, which was then cleaned first with Nd:YAG 1064 nm laser followed by 1% w/v Pemulen TR2 emulsion with 2% w/v EDTA (for details see Part B)



1.3.1 Examination

1.3.1.1 Cross-Sections

In 2018, a total of 12 samples from various locations on the frame underwent cross-section analysis (Fig. 1.8a, b). It appears the original, predominantly water gilded scheme, was later restored with oil gilding followed by brass-based overpainting (Fig. 1.8a, b).

1.3.1.2 FTIR

Brass-based paint thin film samples were examined with FTIR using transmission method. The spectra showed strong absorption at the regions of 1641 cm^{-1} , 1281 cm^{-1} , and 1072 cm^{-1} which could indicate cellulose nitrate component as well as strong carbonyl peak at 1729 cm^{-1} and an absorption signals at 1452 cm^{-1} , 1123 cm^{-1} and doublet at 747 cm^{-1} and 708 cm^{-1} indicating alkyds or phthalate-type plasticiser [5, 6, 8, 9, 15, 24] (Fig. 1.9).

1.3.1.3 Solvent Tests

Solvent testing was conducted on the brass-based paint layer with methylated spirit, acetone, a 1:1 mixture of both, as well as 1:1 acetone/white spirit and methylated spirit/white spirit mixtures. Acetone produced the best result.

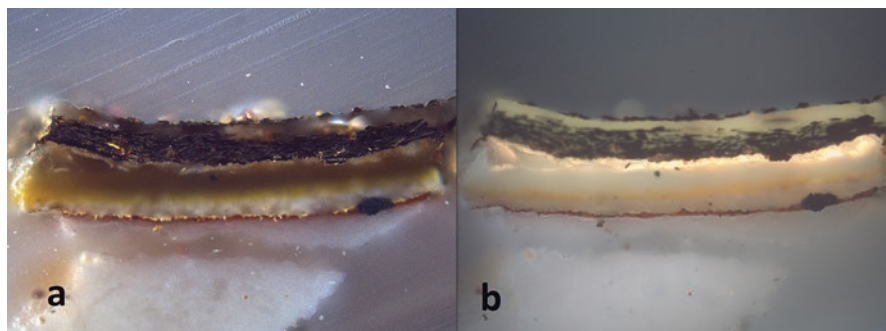


Fig. 1.8 Case study 2: cross-section sample of the plain inner moulding, under reflected (a) and ultraviolet (b) light, at 400 \times magnification, showed the surface stratigraphy as follow: (from the top) dirt layer, clear varnish layer, thick brass particles suspended in a nitrocellulose binder, thin dark dirt layer (probably soiled animal glue-based coating), gold leaf, gesso foundation saturated with oil gold-size and shellac, yellow ochre bole layer indicating another gilding scheme, white gesso layer, gold leaf, red bole layer and gesso layer

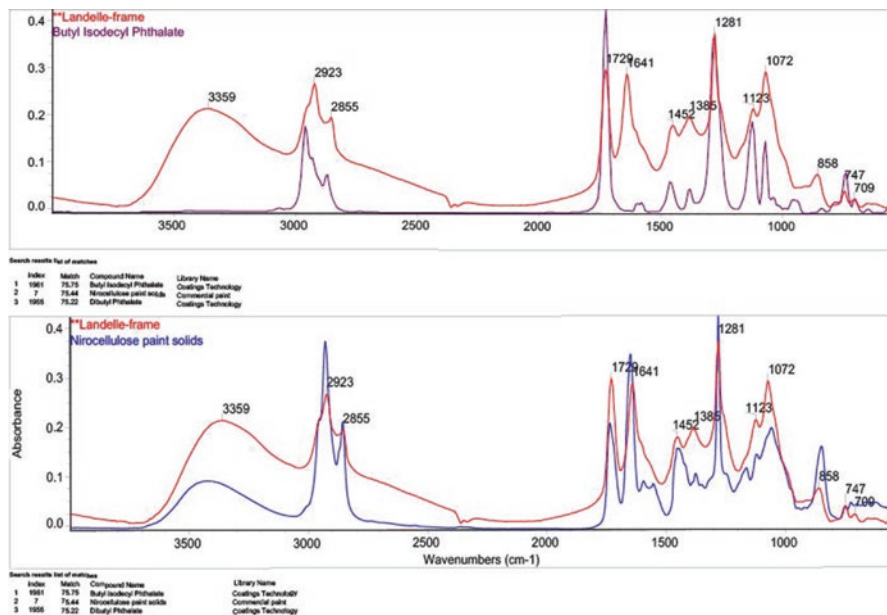


Fig. 1.9 Case study 2: FTIR spectra of the brass-based overpainting with references

The soiled-varnish layer beneath the overpainting was not affected by solvents, but was soluble in water or tri-ammonium citrate solution (2% w/v) suggesting that it is a proteinaceous ‘ormolu’ (as above).

1.3.2 Solvent Gel Testing – Removal of Brass-Based Overpainting

The overpainting was very thick, therefore a treatment was required that would diffuse into the surface rather than just provide surface-to-surface contact. The aim of this part of treatment was to remove overpainting and keep the soiled-varnish layer intact.

The project was conducted concurrently with Case 1. Initially both Xanthan gum and PVOH-borax gels with solvents were investigated as options for bronze paint removal.

Xanthan gum solvent gels were applied to the surface by brush in a ~0.5 cm thick layer. A layer of Mylar was applied over the gel to limit solvent evaporation. After contact time, the gel was cleared and the softened paint removed with a spatula and dry cotton swabs or swabs with solvents.

The PVOH-borax solvent gel was squeezed between two pieces of Mylar to the desired thickness and then applied over the overpainted surface. Mylar sheet was

laid over the gel to limit solvent evaporation. After contact time, the gel was removed from the surface with a spatula. The softened overpainting was then removed mechanically with a spatula and dry or solvent-saturated cotton swabs.

1.3.2.1 Results (Table 1.2)

Xanthan Gum Solvent Gels

Acetone

Xanthan gum gel with acetone (30% v/v) was tested on a small section at the outer scotia. The overpainting was softened and removed in two repeat applications. On the first application the solvent only partially diffused into the overpainting; the upper layer changed colour and softened. It was then removed with a spatula and dry cotton swabs. The second application worked faster; the action was difficult to control, and some softening of gilding foundation layers occurred in random areas. The gel texture provided limited control. Removal required repetitive action with a spatula and cotton swabs and residue clearance with solvents. Further tests on a larger area also produced problems with gel clearance. The second application of Xanthan gum-acetone gel softened some areas of gilding under the overpainting and it could be easily damaged during residue clearance. The results produced a surface that was patchy; partially cleaned and streaked with overpainting residue.

Benzyl alcohol

Benzyl alcohol's slower working time necessitated a contact time of over 30 min, to be monitored every 5–10 min. It was removed with a spatula, dry and solvent-saturated cotton swabs. Most overpainting was removed after 30 min, however soiling/gilding layers were also affected by the gel. The surface was patchy with overpainting residue; appearing partially cleaned. Due to its texture, the gel required prolonged swab action to remove and clear it, which aggravated the already softened gilding.

PVOH-Borax Gel with Solvent

Acetone

Removing PVOH-borax gel was straightforward; it was easily raised with a spatula and without the need for clearing. The first application softened only the upper layers of overpainting. Surprising, there was no evidence of the solvent having diffused deeper into the paint layers after a prolonged application. A repeat application of the gel to the same area (after the upper layer of paint was removed) proved more efficient. The gel was easy to control and removed without a residue. However, the second application softened the paint layer straight down to the soiled-varnish layer

Table 1.2 Case study 2: Landelle frame – tests with solvent gels and emulsions for removal of brass-based overpainting

Gel tested	Area on frame tested	Application/ check-up Time	Application method	Removal method	Observation of gel texture	Results
Xanthan gum gel (4% w/v in water, pH 8) with acetone (30% v/v)	the outer scotia at UM at RUC	5 min at both applications	Applied with spatula; two repeat applications; the diffusion of solvent in to the paint layer was not deep enough with one application.	Cleared with cotton swabs saturated with acetone at first application and with dry swab or swab with white spirit at the second application.	Viscous gel, well attached to the brass-based painted surface; it requires repeating clearing action	With first application only upper overpaint layer could be removed. Gel was applied again to the same area. The overpaint could be removed with second application, but the surface became sensitive to polar solvent; clearing of residue was performed with dry swab or swab with white spirit. Later tests on larger area showed problem with clearing – removal of gel after the second application could cause damage to the dark dirt layer under the paint and subsequently to gold leaf.
Xanthan gel (4% w/v in water, pH 8) with benzyl alcohol (20 % v/v)	the outer scotia at UM at RUC	5 min	Applied with spatula	Cleared with dry cotton swabs and benzyl alcohol	Viscous gel, well attached to the brass-based painted surface; it requires repeating clearing action	Great part of the overpainting removed, but random paint spots still present; problem with clearing; gel difficult to control.
		15 min				
		20 min				
		30 min				Most of the overpainting was removed, but some of the gold leaf could also be removed. Soiling/ gilding layers became already affected by the gel, although the surface was still patchy; partially cleaned and streaked with overpaint residue.

50:50 acetone: PVOH/borax gel	the outer scotia, LHSM, close to LUC	5, 10 min with first application; 5 min at the second application	Applied with spatula, covered with Mylar; two repeat applications; the diffusion of solvent in to the paint layers was not deep enough with one application.	Lifted up with spatula and removed mechanically with spatula and fingers; no clearing required.	Gel was like a putty or plasticine. It could be easily manipulated into desired thickness between two pieces of Mylar. It could be easily applied over ornamented surface. It was easy to remove; it did not stick to the surface. There was no needs for clearing.	With first application only upper layer of paint could be removed. Extended application time did not caused deeper diffusion into the paint layers. The overpaint could be removed with second application, but the gilded surface became also sensitive to polar solvent; removal of paint residue with cotton swabs was difficult, but not impossible; the process was slow.
	Outer scotia, RHSM	5 min 20 min	Applied with brush	Cleared with dry cotton swabs and swabs with benzyl alcohol	Low viscosity emulsion; it has to be applied in thin coat as it will incline to run off from the vertical surface.	Softening of the first layer of overpainting only was observed. Little progress - removal of the first layer of overpainting only.

(continued)

Table 1.2 (continued)

Gel tested	Area on frame tested	Application/ check-up Time	Application method	Removal method	Observation of gel texture	Results
1% (w/v) Pemulen TR2 pH 6.5 with 20 % (v/v) benzyl alcohol	Outer scotia, RHSM	30 min	Applied with brush	Cleared with dry cotton swabs and swabs with benzyl alcohol	Low viscosity emulsion; it has to be applied in thin coat as it will incline to run off from the vertical surface.	Random removal of all overpainting layers to the dirty gilded surface was observed.
		40 min				Most of the overpainting removed revealing dirty gilded surface, but many spots of the paint residue still present. Gilding foundation layers became slightly softened as well.
		45 min				Most of the overpainting removed, but spots of the paint residue still present. Gilding foundation layers softened as well.
		50 min				Most of the overpainting removed, but spots of the paint residue still present. Gilding foundation layers softened as well.
		60 min				Overpainting has been removed but the gold leaf was also removed in several areas.

<p>1% (w/v) Pemulen TR2 pH 6.5 with 30% (v/v) benzyl alcohol</p>	<p>Outer scotia, RHSM</p>	5 min	<p>Cleared with dry cotton swabs and swabs with benzyl alcohol</p>	<p>Low viscosity emulsion; it has to be applied in thin coat as it will incline to run off from the vertical surface.</p>	<p>Removal of the first layer of overpainting only was observed.</p>
		10 min			
		15 min			
		20 min			
		30 min			
40, 45 min	<p>All layers of overpainting are removed revealing dirty gilded surface, but many spots of the paint residue still present. Gilding foundation layers softened as well.</p>				
50 min	<p>Gilding layers are also affected. Overpainting has been removed but the gold leaf was also removed in several areas.</p>				

(continued)

Table 1.2 (continued)

Gel tested	Area on frame tested	Application/ check-up Time	Application method	Removal method	Observation of gel texture	Results
1% (w/v) Pemulen TR2 pH 8.0 with 20 % (v/v) benzyl alcohol	Outer scotia, RHSM	30 min	Applied with brush	Cleared with dry cotton swabs and alcohol	Low viscosity emulsion; it has to be applied in thin coat as it will incline to run off from the vertical surface.	Random removal of all overpainting layers to the dirty gilded surface was observed. No difference was noticed comparing to the action of a mixture with lower pH.
		40 min				Most of the overpainting removed revealing dirty gilded surface, but many spots of the paint residue still present. Gilding foundation layers slightly soften as well. No difference was noticed comparing to the action of a mixture with lower pH.
		50 min				Most of the overpainting removed revealing dirty gilded surface, but some spots of the paint residue still present. Gilding layers are also affected. No difference was noticed comparing to the action of a mixture with lower pH.

1% (w/v) Pemulen TR2 pH 6.5 with 10% (v/v) benzyl alcohol and EDTA (1% w/v)	Outer scotia, RHSM	5 min	Applied with brush	Cleared with dry cotton swabs and swabs with benzyl alcohol	Low viscosity emulsion; it has to be applied in thin coat as it will incline to run off from the vertical surface.	Removal of the first layer of overpainting only was observed.
		15 min				Little progress - bronze paint under the first clear layer of overpaint started softening.
		30 min				Most of the overpainting removed revealing dirty gilded surface, but many spots of the paint residue still present
		45 min				Good removal of the overpainting but some of the gold leaf can be also removed.

(continued)

Table 1.2 (continued)

Gel tested	Area on frame tested	Application/ check-up Time	Application method	Removal method	Observation of gel texture	Results
1% (w/v) Pemulen TR2 pH 6.5 with 20% (v/v) benzyl alcohol and EDTA (1% w/v)	Outer scotia, RHSM	5 min	Applied with brush	Cleared with dry cotton swabs and swabs with benzyl alcohol	Low viscosity emulsion; it has to be applied in thin coat as it will incline to run off from the vertical surface.	Removal of the first layer of overpainting only
		10 min				Random removal of all overpainting layers in a few areas
		15 min				Most of the overpainting removed revealing dirty gilded surface, but many spots of the paint residue still present. Gilding foundation layers became slightly soften as well.
		20 min				
		30 min				
	40 min		Most of the overpainting removed, but many spots of the paint residue still present. Gilding foundation layers soften as well.			
50 min		In small test: most of the overpainting removed. In bigger section: removal of the gold leaf also occurs; a mixture too strong – EDTA affects soiling layers: uppermost parts of soiled gilding removed with gilding. With longer application a mixture is difficult to control as it seems EDTA softened uppermost parts of soiling and eventually remove the gilding in random areas.				

Cyclomethicone was applied by brush 1 min before Pemulen TR2/20% (v/v) benzyl alcohol/ EDTA emulsion (as above)	30, 40 min	Applied with brush	Cleared with dry cotton swabs and benzyl alcohol	Low viscosity emulsion; it has to be applied in thin coat as it will incline to run off from the vertical surface.	Results as with a test without cyclomethicone
					Removal of the top layer of the bronze overpainting after 10 min, bronze paint under the first clear layer of overpaint started softening after 20 min
1% (w/v) Pemulen TR2 pH 6.5 with 30% (v/v) Benzyl alcohol - Without covering	10, 20 min	Applied with brush,	Cleared with dry cotton swabs and benzyl alcohol	Low viscosity emulsion; it has to be applied in thin coat as it will incline to run off from the vertical surface.	Removal of the top layer of the bronze overpainting and some removal of all overpainting layers
					Some removal of all overpainting layers; a mixture slightly more effective than without covering
1% (w/v) Pemulen TR2 pH 6.5 with 30% (v/v) benzyl alcohol - Lightly covered with plastic	10 min	Applied with brush	Cleared with dry cotton swabs and benzyl alcohol	Low viscosity emulsion; it has to be applied in thin coat as it will incline to run off from the vertical surface.	Removal of all overpainting layers occurs. A mixture slightly more effective than lightly covered or without covering.
					Most of the overpainting removed but many random spots of paint residue present. Gilding foundation layers became slightly soften as well.
	20 min				Most of overpainting removed, but gilding foundation layers soften as well and removal of the gold leaf occurs when the emulsion pours over the cleaned surface; a mixture difficult to control.
1% (w/v) Pemulen TR2 pH 6.5 with 30% (v/v) benzyl alcohol, - Covered with plastic	10 min		Cleared with dry cotton swabs and benzyl alcohol	Low viscosity emulsion; it has to be applied in thin coat as it will incline to run off from the vertical surface.	
					40 min

(continued)

Table 1.2 (continued)

Gel tested	Area on frame tested	Application/ check-up Time	Application method	Removal method	Observation of gel texture	Results
1% (w/v) Pemulen TR2 pH 6,5 with 30% (v/v) benzyl alcohol	Wider area of outer scotia, RHSM (10 x 10 cm)	20 min	Applied with brush	Cleared with dry cotton swabs and alcohol	Low viscosity emulsion; it has to be applied in thin coat as it will incline to run off from the vertical surface.	Bronze paint under the first clear layer of overpaint started softening. All layers of overpainting are affected; they are removed in many areas revealing dirty gilded surface, but many spots of the paint residue still present. Gilding foundation layers became slightly softened as well.
		30 min				
	40 min	All layers of overpainting are removed revealing dirty gilded surface, but many spots of the paint residue still present. Gilding layers are also affected where soiling layer is thinner or where an emulsion pours over previously cleaned surface.				
Acetone-saturated poultice (cotton bandage pocket packed with cotton wool), covered with polyethylene sheet	Wider area of outer scotia, RHSM (10 x 10 cm)	1, 3, 5 min			Poultice is applied as one piece and can be remove immediately if adverse reaction is observed.	Softened overpaint was successfully removed with scalpel, spatula, dry cotton swabs, and swabs with acetone. After 5 min application the entire surface could be cleared of brass-based overpaint up to the soiling layer. Soiling layer and gilding was not affected.

above the gilding. During overpainting removal, it became evident that gilding layers underneath had also softened and could be removed where the soiled-varnish layer was thin.

1.3.3 Further Solvent Emulsion Tests

The problems encountered with solvent gels necessitated a different approach. A low viscosity material, which could be easily removed from the surface without the need for lengthy clearing processes was required. Various Pemulen TR2 emulsions with solvents were prepared and applied to the overpainting by brush. After testing different application times, the gels were removed with dry swabs and then cleared with benzyl alcohol-saturated cotton swabs.

1.3.3.1 Results

1% (w/v) Pemulen TR2 Emulsion pH 6.5, with 10%, 20% and 30% (v/v) Benzyl Alcohol

All tested emulsions could be easily and quickly removed from the surface with cotton swabs. A higher benzyl alcohol content reduced their working time. Most of the overpainting could be removed with a 30% (v/v) benzyl alcohol emulsion after 40–50 min of application, but the soiled-varnish and gilding foundation were also softened; gold leaf could be removed in the areas where soiling was thin (Fig. 1.10b).

Tests of a 1% Pemulen TR2 emulsion with pH increased to 8 showed no observable difference in the efficacy of the gel.

1% v/v Pemulen TR2 pH 6,5 with 10% v/v and 20% v/v Benzyl Alcohol, and EDTA (1% v/v)

Most overpainting could be removed using both mixtures after 35–40 min of application time (Fig. 1.10a). Both materials performed well in small spot tests, but when applied over a wider area, the emulsions could remove both the dirt and gold leaf layers. The density and distribution of the soiled-varnish layer under the overpainting appeared uneven. The addition of EDTA to the Pemulen TR2 – benzyl alcohol emulsion contributed to softening and dilution of this coating. During clearing, this layer could be partially removed, along with the gold leaf, in areas where the varnish coating was thin, i.e. on the uppermost parts of moulding.

Cyclomethicone was also tested; it was brushed on the overpainted surface before the gel was applied. No difference in results was observed.

Theory suggests chelating agents can assist in overpainting removal by affecting the metal particles, however the addition of EDTA did not improve the solubility

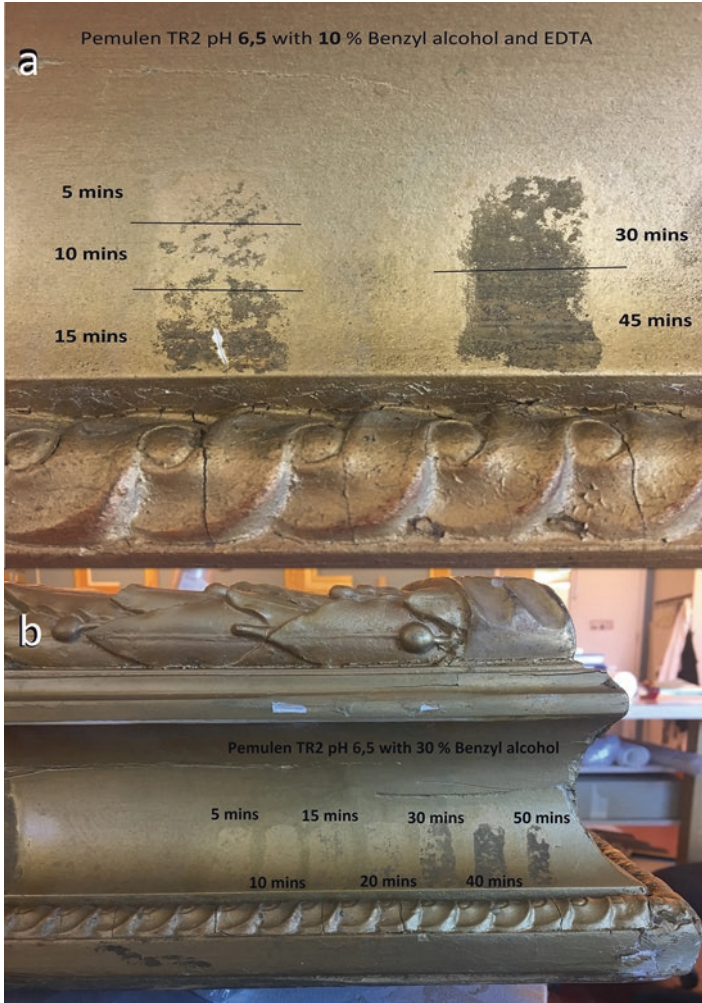


Fig. 1.10 Case study 2: testing 1% w/v Pemulen TR2 emulsions with benzyl alcohol (b) and benzyl alcohol with EDTA (a)

and removal of brass-based overpainting in these trials. These tests affirm the theory that the removal of brass-based overpainting is determined by the solubility of the overpainting medium, rather than the brass particles themselves.

1% Pemulen TR2 pH 6,5 with 30% Benzyl Alcohol, Uncovered, Covered Loosely with Plastic, and Covered Closely

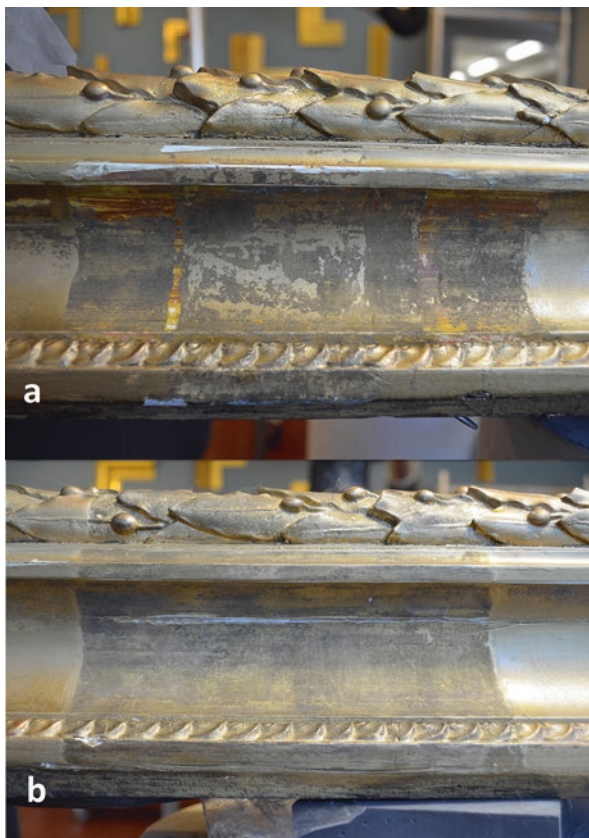
Following successes with Pemulen TR2 emulsion with 30% benzyl alcohol, subsequent trials explored whether application times can be reduced by covering the surface with a polyethylene sheet; to limit solvent evaporation and increase the

emulsions' efficacy. The same emulsion was applied to three discrete areas: one area left uncovered, a second covered loosely and the third covered closely. Close covering improved the gels efficiency; the paint softened and could be removed from the surface after 20 min. Unfortunately, the method also affected the dirt and gold leaf layers. Covering increased the speed of the reaction, however it was less controlled.

1% Pemulen TR2 pH 6,5 with 30% Benzyl Alcohol, Tested on a Wider Area, $10 \times 10 \text{ cm}^2$

Lastly, a 1% Pemulen TR2 emulsion with 30% benzyl alcohol was tested on a wider area of outer scotia (Fig. 1.11a). This was compared with a similar area cleaned with acetone poultices (Fig. 1.11b). The Pemulen TR2 emulsion produced an unevenly cleaned surface and paint residues remained. Some removal of the gold leaf was observed where cleaning treatments accidentally overlapped (i.e. at the edges of each gel swatch). Raised areas of moulding and the upper parts of scotia were more

Fig. 1.11 Case study 2: (a) results of testing 1% w/v Pemulen TR2 emulsion with 30% v/v benzyl alcohol on a wider area of the outer scotia moulding, (b) a similar area cleaned with acetone poultices



sensitive to treatment; the gold leaf could be removed after shorter application times compared with other areas. This may be due to variable thickness in the soiled-varnish layer.

By contrast, acetone poultices, followed by acetone swabs, produced an even result and exposed the soiled-varnish layer, free of paint residue. The short application time of acetone poultices did not affect the soiled-varnish and gilding layers. The soiled-varnish layer, which was not soluble in acetone, formed an isolation layer protecting the gold leaf beneath.

1.4 Discussion

The drawbacks of using free organic solvents for surface cleaning gilded objects are commonly understood by conservators. Prolonged penetration of solvents into surface layers can risk softening and damage to the gilding and its foundation layers, particularly in the case of oil gilding. Due to the volatile properties of these solvents, large quantities are often required. In addition, solvent toxicity necessitates the use of extraction systems and safety equipment. However, many treatments have proved, organic solvents when used with well-developed understanding of their properties and how they interact with the gilded surface, can provide effective and controlled removal of overpainting.

The common understanding of solubility, based on the Teas diagram, is delineated by polarity, hydrogen bonding and dispersion values. Alan Phenix argues that *'the Teas fractional solubility parameter system does not clearly reveal the particular chemical and/or physicochemical factors that contribute to the swelling action of any given solvent'* ([17]: 74). Phenix noticed that solvents with similar solubility parameters can have very different swelling powers. Therefore, the specific interactions occurring *'between a solvent and solute cannot be reliably described by the dispersion force-polar force/hydrogen bond approaches of Teas'* diagram ([17]: 74). Phenix proposed a classification of solvents in five groups determined by their swelling power (ΔA_{max} %) [4, 19] and the rate of swelling ($t_{1/2}$) [17], which show a strong reliance on the values of *a scale of hydrogen-bonding acceptor basicity* (β) and *an index of solvent polarity and polarizability* (π^*) of the KAT system [17].

According to Phenix' classification of solvents [17], acetone is classified as a very fast acting and low-to-moderate solvent in terms of swelling power, while benzyl alcohol is slow-acting with a very high swelling power.

It has been noted in conservation literature, the capacity for solvents to rapidly diffuse into a varnish or paint layer (such as acetone into brass-based paint) can be favourable in certain treatments [20]. The action is associated with fast solubilisation of the binder and it prevents solvent build-up in surface layers (i.e. in gilding foundation layers under the brass-based paint).

Conservation literature shows a strong correlation between the rate of swelling in a paint film and the thickness of the film, when using free solvents (the thicker the film, the slower the rate of swelling) [12, 20].

Both our case studies showed acetone poultices and acetone-saturated swabs worked rapidly, solubilising the medium and diffusing solvent into the overpainting layers, softening to a depth sufficient for overpainting removal without affecting underlying the soiled-varnish and oil gilding layers. This method offered controlled surface cleaning without damage to the gilding. In both cases, the soiled-varnish layer worked as a barrier to protect the underlying oil-gilding. The soiled-varnish was not soluble in acetone and therefore remained unaffected by the poultices. With prolonged or repeat applications of the hydrogels and emulsions, this protective layer could be softened by the water component of the gel systems and was not sufficient to protect the gilding.

Acetone in both Xanthan gum and PVOH-borax gels, applied for short periods, did not penetrate sufficiently into the thick overpainting; partly due to the high volatility of acetone (Case Study 2). When the application time was increased to 30 min, both acetone gels posed little risk of softening the soiled-varnish and oil gilding layers, demonstrating they affect only immediate surface layers. After partial removal of the overpainting, a repeat application of both gels, even for a short period, caused some removal of the soiled-varnish and gold leaf layers. This indicates underlying layers are at risk once the overpainting layers are thin (Case Study 1) or have been thinned (Case Study 2). The gilding layers were softened by the water-component of solvent gels, and the surface became too sensitive for these cleaning systems. While PVOH/borax gel was easily removed without the need for clearing, the clearing action required for Xanthan gum gel damaged the soiled-varnish and oil-gilding layers.

Alternatively, prolonged applications of less volatile, slow-acting benzyl alcohol could diffuse deeper into the overpainting, regardless of the gel or emulsion selected to carry it. White action of Xanthan gum gel with 10% benzyl alcohol was slower than Pemulen TR2 with 10% benzyl alcohol, both methods produced softening. Increasing the solvent content in Pemulen TR2 emulsion reduced the required application time. Longer application times allowed the solvent to diffuse deeper into the surface but caused some softening of the gilding and foundation layers. When benzyl alcohol began to act, it could not be controlled, and the gel-system did not differentiate between the overpainting, soiled-varnish and oil gilding layers. Close covering of the Pemulen TR2/benzyl alcohol emulsion sped up the softening process; however, this softening affected all layers.

A concentration of 1% Pemulen TR2 provided the most appropriate viscosity for curved surfaces and ornament, imparting the ability to conform to these surfaces and restrict penetration into cracks.

1.5 Conclusions

Xanthan gum gels, PVOH-borax gels, and Pemulen TR2 emulsions were trialled in two case-studies for their potential to remove brass-based overpainting from gilded wooden surfaces. Factors influencing the performance of gel systems include the

thickness of the overpainting layers, the presence of a 'barrier layer' between the overpainting and gilding, the solubility of the overpainting binder, and the solubility characteristics of the solvent (its rate and power of swelling, evaporation rate and application method). For the removal of overpainting from gilded wooden surfaces, fast-acting solvents with moderate swelling power are more appropriate than slow-acting solvents with strong swelling power. The latter can soften gilding layers beneath the overpainting. Important factor to consider are solvent volatility and the rate it diffuses into the overpainting.

Rigid solvent gels and emulsions offer a viable alternative to free solvent application provided they can be easily removed from the surface, with minimal clearing requirements. Gold leaf can protect foundation layers from softening, but it is a thin barrier and insufficient to withstand prolonged exposure to solvent gels, particularly in case of oil gilding. The presence of a proteinaceous 'barrier layer' (referred to in this article as a soiled-varnish layer) and strictly controlled application times, make it possible to reduce the softening of gilding foundation layers.

Polar and water-miscible solvents (acetone, ethanol etc.) are effective in removing overpainting from gilded surfaces. As stated in recent literature '*any polar solvent that is not miscible with the gel base or cyclomethicone can be emulsified into Velvesil Plus or the KSG gels*' ([26]: 216). Future research should look into the suitability of these materials for gilded surfaces.

Gel testing is a process of trial and error and there is no one correct method or material for wooden gilded objects. Each surface is different and requires thorough testing and examination so the gels can be tailored for the task at hand.

Our understanding of the effects of solvents on paint films has significantly increased, however the impact of free solvent use on gilded wooden surfaces still requires research. Highly polar solvents and aqueous cleaning agents such as chelators, may pose risks to oil-based coatings; this has been flagged in paintings conservation literature [11, 18, 19, 27] It has long been recognized that solvent swelling of an oil binder is a considerable risk for cleaning paintings [17]. Conservation scientists have expressed concern that organic solvents facilitate fatty acid and carboxylate migration in paint layers ([7, 16, 20, 23, 28]: 11). The migration of free fatty acids or the formation of fatty acids carboxylates in oil gilding should also be considered, particularly where gold leaf imitation or brass-powders are involved [22]. Sutherland's observations working with paintings from the seventeenth to nineteenth centuries are comforting, finding that the extraction of fatty acids, after prolonged exposure to polar solvents was small, and in some cases 'not observable' [20, 27].

It is crucial the conservator understand how organic solvents affect gilded surfaces; to assess their risks and benefits and the short and long-term effects on gilding layers. Numerous studies support the general trend away from prolonged exposure to solvents when cleaning heritage objects [27]. The conservation of gilded wooden surfaces should be no exception.

Materials

PVOH: Kuraray Poval Polyvinyl Alcohol L-10

Borax: Bare Essentials Borax

Pemulen TR2: Noveon, Inc. Pemulen

Triethanolamine TEA: Merck KGaA Triethanolamine

Citric Acid: Chem-Supply Citric Acid Anhydrous

Xanthan gum: Melbourne Food Ingredient Depot

EDTA: Ethylenediaminetetraacetic acid, Sigma-Aldrich

Appendix

Description of the solvent systems preparation included in the tests:

- A. 2% Pemulen TR2-TEA, pH 6.5 (stock solution) was formed according to the MCP recipe [25] as follows:

5 g Pemulen TR2 was mixed with 90 ml of deionised water; around 4.5 ml of TEA was added to adjust pH to 6.5 (little bit more for pH 8); then another 150 ml was incorporated to achieve a stock gel of ~2%.

1% Pemulen TR2-TEA, pH 6.5, was formed according to the Chris Stavroudis' instructions on YouTube:

5 ml of the 2% Pemulen TR2 stock solution was mixed with 2 ml citric system pH 6.5 (see below) and 3 ml deionised water on the magnetic plate with stirrer. The final mixture was 10 ml of 1% Pemulen TR2-TEA-citric system, pH 6.5.

- B. Citric system: Citric acid with Triethanolamine, pH 6,5

4,8 g citric acid was mixed with 70 ml of deionized water. Triethanolamine was added to adjust pH to 6,5 (approx. 4.5 ml) then an extra 20 ml of deionised water was added to make entire solution approx. 100 ml.

Emulsions:

- C. 1% Pemulen TR2-TEA, pH 6.5, + 10% (20%, 30%) benzyl alcohol was formed according to Chris Stavroudis instructions on the GCI YouTube channel:

5 ml of the 2% Pemulen TR2 stock solution was mixed with 2 ml citric system pH 6.5 (see above) and 3 ml deionised water on a magnetic plate with a stirrer. After approx. 5 min 1 ml (2 ml, 3 ml) benzyl alcohol was added and stirred again to form ~10% (~20%, ~30%) emulsion.

- D. 1% Pemulen TR2-TEA pH 6.5 + ~10%, (20%, 30%) benzyl alcohol + ethylenediaminetetraacetic acid (EDTA) pH 6,5 was formulated with influence of Chris Stavroudis MCP (as above):

5 ml of the 2% Pemulen TR2 stock solution was mixed with 2 ml of EDTA (5%) (replacement of citric system) and 3 ml deionised water on the magnetic plate with stirrer. 5 min later 1 ml (2 ml, 3 ml) of benzyl alcohol was added to form ~10% (~20%, ~30%) benzyl alcohol emulsion.

E. PVOH-Borax gels with acetone were prepared as follow ([1], p. 243).

90:10: For ~10 g batch, 0.6 g 75PVOH was solved in 6.37 g deionised water and 0.94 g solvent (acetone) at a moderate temperature ~50 °C for approx. 1 h. In a separate container 0.1 g borax (Bare Essentials Borax) was solved in 2 g of deionised water. Borax solution was added to PVOH mixture using magnetic stirrer until combined.

50:50: For ~20 g batch: 1 g 75PVOH was solved in 5.4 g deionised water and 9.4 g solvent (acetone) at ~50 °C for approx. 1 h, before adding the borax-water solution (0.2 g borax solved in 4 g deionised water).

F. 8% Xanthan gum stock gel was prepared by mixing 8 g of powder with 20 ml of deionised water, pH 7, and then top up with deionised water up to the final volume of 100 ml.

4% w/v Xanthan gum gel was used for all experiments.

For 25% solvent gel 25 ml of solvent was mixed with 25 ml of distilled water, pH 7, added to 50 ml of stock gel and stirred.

For 30% solvent gel 30 ml of solvent was mixed with 20 ml of distilled water, pH 7, added to 50 ml of stock gel and stirred.

For 50% solvent gel 50 ml of solvent was mixed 50 ml of stock gel and stirred.

Xanthan gum, with 20% benzyl alcohol 5% EDTA, pH 7, was prepared basing on an article by Doherty and Rivers 2017, p. 123.

10% EDTA stock solution was prepared by mixing 10 g EDTA in 100 ml distilled water, buffered with TEA to pH 7.

To make gel 50 ml EDTA (10%) was mixed with 30 ml of distilled water, pH 7, and 20 ml benzyl alcohol, and then 4 g of Xanthan powder and stirred with magnetic stirrer.

G. Acetone poultices were prepared as follows:

Large cotton bandage was folded to form patches; the size was determined by the area designated for treatment. The pocket was packed with cotton wool and saturated with solvent. During treatment, the poultice is covered with polyethylene sheet, to reduce evaporation. The poultice can be removed from the surface anytime and the treatment terminated immediately.

References

1. Angelova, L.V., Berrie, B.H., de Ghetaldi, K., Kerr A. and Weiss, R.G. 2015. Partially hydrolyzed poly(vinyl acetate)-borax-based gel-like materials for conservation of art: characterisation and applications. *Studies in Conservation* 60:227–44.
2. Angelova, L.V., Carretti, E., Berrie, B.H. and Weiss, R.G. 2017. Poly(vinyl alcohol)-borax 'gels': a flexible cleaning option. In Angelova, L.V., Ormsby, B., Townsend, J.H. and Wolbers, R. (eds) 1917. *Gels in the Conservation of Art*. Archetype Publications Ltd: 231–236.
3. Angelova, L.V., Ormsby, B., Townsend, J.H. and Wolbers, R. (eds) 1917. *Gels in the Conservation of Art*. Archetype Publications Ltd.

4. Doherty, E., and Rivers, S. 2017. The removal of lead- and oil-based overpaint from a plaster cast of *Hermes Fastening his Sandal*. In Angelova, L.V., Ormsby, B., Townsend, J.H. and Wolbers, R., (eds) 1917. *Gels in the Conservation of Art*. Archetype Publications Ltd: 121–126.
5. Cacic, S., Raskovic, L., Lacnjevac, C., Rajkovic, M., Barac, M. and Stojanovic, M., 2007. Physical-Mechanical Properties of Nitrodopes Affected by Ultra-Violet Radiation. *Sensors* ISSN1424-8220: MDPI; www.mdpi.org/sensors 2007, 7:2139–2156.
6. Giacomucci, L., F. Toja, P. Sammartin, L. Toniolo, B. Prieto, F. Vila, and F. Cappitelli, 2012. Degradation of nitrocellulose-based paint by *Desulfovibrio desulfuricans* ATCC13541. *Biodegradation* 23:705–716
7. Hackney, S., 2013. The Art and Science of Cleaning Paintings. In Mecklenburg, M. F., Charola, A. E., and Koestler, R. J., 2013. *New Insights into the Cleaning of Paintings*. Proceedings from the Cleaning 2010 International Conference, Universidad Politecnica de Valencia and Museum Conservation Institute, Smithsonian Institution Scholarly Press, Washington, D.C.: 11–15.
8. Kovalenko, V.I., Mukhamadeeva, R.M., Maklakova, L.N. and Gustavo, N.G., 1994. Interpretation of the IR Spectrum and Structure of Cellulose Nitrate. *Journal of Structural Chemistry*, July 1994; <https://www.researchgate.net/publication/243955019>
9. Learner, T.J.S. 2004. *Analysis of modern paints*. Los Angeles, CA: Getty Publications.
10. Lins, Andrew, 1991. *Basic Physical Properties of Gold Leaf*. Bigelow, D., Cornu, E., Landrey, G. J., Van Horne, C., (editors), 1991, *Gilded Wood: Conservation and History*. Sound View Press, Madison, Connecticut: 17–23.
11. Mansmann, K. 1998. Oberflächenreinigung mit Ammoniumcitrat. *Zeitschrift für Kunsttechnologie und Konservierung*, 12(2):220–237.
12. Mecklenburg, M. F., Tumosa, C. S. and Vicenzi, E. P, 2013a. The Influence of Pigments and Ion Migration on the Durability of Drying Oil and Alkyd Paints. In Mecklenburg, M. F., Charola, A. E., and Koestler, R. J., 2013. *New Insights into the Cleaning of Paintings*. Proceedings from the Cleaning 2010 International Conference, Universidad Politecnica de Valencia and Museum Conservation Institute, Smithsonian Institution Scholarly Press, Washington, D.C.: 59–67.
13. Mecklenburg, M. F., Charola, A. E., and Koestler, R. J., 2013b. *New Insights into the Cleaning of Paintings*. Proceedings from the Cleaning 2010 International Conference, Universidad Politecnica de Valencia and Museum Conservation Institute, Smithsonian Institution Scholarly Press, Washington, D.C.
14. Michalski, S., 1990. A physical model of the cleaning of oil paint. In Mills, J.S. and Smith, P., eds, *Cleaning, Retouching and Coatings. Technology and Practice for Easel Paintings and Polychrome Sculpture*. Preprints of the Contributions to the Brussels Congress, International Institute for Conservation of Historic and Artistic Works, London, 1990, pp. 85–92.
15. Noake, E., Lau D., and Nel, P. 2017. Identification of Cellulose Nitrate Based Adhesive Repairs in Archeological Pottery of the University of Melbourne’s Middle Eastern Archaeological Pottery Collection Using Portable FTIR-ATR Spectroscopy and PCA. *Heritage Science* 5:3 Springer Open Access: <https://link.springer.com/article/10.1186/s40494-016-0116-z>
16. Noble, P., and J. J. Boon. 2007. Metal Soap Degradation of Oil Paintings: Aggregates, Increased Transparency and Efflorescence. *AIC Paintings Specialty Group Postprints*, 19:1–15.
17. Phenix, A., 2013. Effects of Organic Solvents on Artists’ Oil Paint Films: Swelling. In: Mecklenburg, M. F., Charola, A. E., and Koestler, R. J. *New Insights into the Cleaning of Paintings*. Proceedings from the Cleaning 2010 International Conference, Universidad Politecnica de Valencia and Museum Conservation Institute, Smithsonian Institution Scholarly Press, Washington, D.C.: 69–76
18. Phenix, A., and A. Burnstock. 1992. The Removal of Surface Dirt on Paintings with Chelating Agents. *The Conservator*, 16:28–38. <https://doi.org/10.1080/01400096.1992.9635624>.
19. Phenix, A. 2002. The Swelling of Artists’ Paints in Organic Solvents. Part 2, Comparative Swelling Powers of Selected Organic Solvents and Solvent Mixtures. *Journal of the American Institute for Conservation*, 41:61–90. <https://doi.org/10.2307/3179897>
20. Phenix, A., and K. Sutherland. 2001. The Cleaning of Paintings: Effects of Organic Solvents on Oil Paint Films. *Reviews in Conservation*, 2:47–60.

21. Riedo, C., Caldera, F., Poli, T., and Chiantore, O., 2015. Poly(vinyl alcohol)-borate hydrogels with improved features for the cleaning of cultural heritage surfaces. *Heritage Science* 3(1): 23.
22. Sawicki, M., Rouse, E. and Limoges, S. 2017. Formation of metal soaps on brass-based coated frames: Nitrocellulose revisited. In: ICOM-CC 18th Triennial Conference Preprints, Copenhagen, 4–8 September 2017, ed. J. Bridgland, art. 2104. Paris: International Council of Museums.
23. Schilling, M., Khanjian, H. and Carson, D., 1997. Fatty acid and glycerol content of lipids; effects of ageing and solvent extraction on the composition of oil paints. *Techné* 5, pp. 71–8.
24. Selwitz, C.M., 1988. Cellulose nitrate in conservation. The Getty Conservation Institute.
25. Stavroudis, C., 2016. Cleaning of Acrylic Painted Surfaces, July 12–15, 2016, The John and Mable Ringling Museum of Art, Sarasota, Florida. MCP Recipes. The Getty Conservation Institute: https://www.getty.edu/conservation/our_projects/education/caps/modular_cleaning_recipes.pdf
26. Stavroudis, C., 2017. Gels: evolution in practice. In: Angelova, L.V., Ormsby, B., Townsend, J.H. and Wolbers, R., (eds) 1917. Gels in the Conservation of Art. Archetype Publications Ltd: 209–217.
27. Sutherland, K. 2000. The Extraction of Soluble Components from an Oil Paint Film by a Varnish Solution. *Studies in Conservation*, 45:54–62. <https://doi.org/10.2307/1506683>
28. Tumosa, C., Millard, J., Erhardt, D. and Mecklenburg, M., 1999. Effects of solvents on physical properties of paint films. ICOM Committee for Conservation, 12th Triennial Meeting, Lyon, pp. 347–52.
29. Victorian Watercolours from the Art Gallery of NSW, 2017. [Exhibition]. The Art Gallery of NSW 2 June – 3 Dec 2017.
30. Wolbers, C.R., Sterman, N. T. and Stavroudis, C. 1990. Notes for Workshop in New Methods in the Cleaning of Paintings. The Getty Conservation Institute, August 1990.
31. Wolbers, R., 2017. Terminology and properties of selected gels. In: Angelova, L.V., Ormsby, B., Townsend, J.H. and Wolbers, R., (eds) 1917. Gels in the Conservation of Art. Archetype Publications Ltd: 381–294.

Chapter 2

An Investigation of the Feasibility of the Use of Gels and Emulsions in Cleaning of Gilded Wooden Surfaces.

Part B: Cleaning of Soiled Oil-Gilding



Malgorzata Sawicki, Emma Rouse, Sofia Lo Bianco, and Seela Kautto

Abstract Experimental testing of various rigid gels and emulsions for removing soiling from gilded wooden surfaces were conducted using two nineteenth c. gilded frames. The gels and emulsions were selected according to their characteristics described in the conservation literature and involved Agar gels, Gellan gels, Xanthan gels, and PVOH-borax gel as well as low viscosity emulsions based on Pemulen TR2, with TAC and EDTA and with varied pH values. Two case studies have shown that hydrogels based on Agar and Gellan gum as well as Pemulen TR2 emulsions can be successfully used in the removal of soiling from gilded wooden surfaces, however each of the cleaning systems needs to be utilised with full understanding of the potential risk to the gilded surface. The option to increase the rigidity of gels can address one of the longstanding challenges of aqueous cleaning methods for gilded surfaces; that is the rate of water diffusion into the gilding's foundation layers. The rigid gels proved to be a good vehicle to deliver the chelating agents for removal of soiling from oil gilding, offering surface contact without diffusion into underlying layers. These methods can also decrease contact time between cleaning agents and the gilded surface, thus providing better control of treatments as well as reducing the needs for agitation of the gilded surface with cotton swabs. Low viscosity Pemulen TR2 emulsions provide similar opportunity without the need for repetitive clearing. Further testing is essential to obtain a better understanding and confidence in the working abilities of gel and emulsion systems for the cleaning of gilded wood.

Keywords Gilding · Gilded wood · Frames · Surface cleaning · Laser cleaning · Agar gel · Gellan gum gel · PVOH-borax gel · Xanthan gel · Pemulen TR2 emulsions

M. Sawicki (✉) · E. Rouse · S. L. Bianco
Art Gallery of New South Wales, Sydney, NSW, Australia
e-mail: margaret.sawicki@ag.nsw.gov.au

S. Kautto
Faculty of Culture/Degree Programme in Conservation, Helsinki Metropolia University of Applied Sciences, Helsinki, Finland

2.1 Introduction

Gilded wooden surfaces are often multifaceted: various gilding techniques can be used in one object and with time the surface can show different ageing characteristics. Dirty, damaged gilded surfaces were often regilded or coated with layers of overpainting, adding to the challenges and complexities of surface cleaning. Examining the stratigraphic layers of a gilded surface is essential prior to cleaning in order to understand the nature and symptoms of the various materials degradation.

Experimental testing of various gels and emulsions for removing overpainting from gilded wooden surfaces has been presented in the chapter entitled *An Investigation of the Feasibility of the Use of Gels and Emulsions in Cleaning of Wooden Gilded Surfaces. Part A: Removal of Brass-Based Overpainting*. For the purpose of our investigations, two nineteenth c. gilded, overpainted frames were used as case studies. Two rigid gels, reviewed in conservation literature, were tested for removing brass-based overpainting: Xanthan gum gel and poly(vinyl alcohol)-borax gel (PVOH-borax gel). In addition, low-viscosity emulsions based on Pemulen TR-2 were also tested proving that they involve a more straightforward clearing process than viscous gels [23]. The solvent gels and emulsions were evaluated according to their application and removal methods, viscosity, texture, and cleaning efficiency.

This paper will present the findings from our investigations involving selected gels and emulsions for the removal of soiling layers from gilded surfaces using the same two gilded frames as case studies.

2.2 Conservation Cleaning Methods Used for the Removal of Soiling from Gilded Wooden Surfaces

Soiling on gilded surfaces is often a build-up of atmospheric pollutants, dirt and dust over proteinaceous coatings applied originally to deepen the matte appearance of the both matte water gilded and oil-gilded surfaces. Nineteenth century treatises refer to this type of varnish as ‘sizing’ or ‘finishing size’ if it consists of parchment size or gelatine or alternatively as ‘ormolu’ if it includes a mixture of shellac or gamboge with the size¹.

¹ “80.—*The following is the manner in which the ormolu is prepared:*

Take a teaspoonful of either the tincture of gum benzoin or of white shellac varnish, and mix it in a cup with about twice or three times its bulk of the highest proof alcohol. Now have ready a hot solution of glue or of gelatine, of about the same strength as that of the finishing size. The quantity should be about one half a teacupful. This must be poured quickly and all at once into the solution of the gum benzoin or of shellac, and the result will be a perfect emulsion of the gum, which will be of a milky white appearance. This, of course, should be strained, and is to be applied as already described. If the first coat should appear spotty and

The ormolu or finishing size layer attracts dirt and soot, darkening the gilded surface over time.

Little research has been dedicated to cleaning methods in reference to gilded wooden surfaces and therefore most techniques have been adopted from other conservation fields. Current conservation practice incorporates the following cleaning approaches:

- Basic dry cleaning or dusting with brush;
- Mechanical removal i.e. with scalpel.
- Laser cleaning systems.
- Aqueous solutions, i.e. artificial saliva or water-based solutions of chelating agents (mainly tri-ammonium citrate, TAC, or ethylenediaminetetra-acetic acid (EDTA), with buffers and varied pH values, applied with swabs.
- Hydrogel systems and emulsions, with TAC or EDTA.

All gilded wooden surfaces are fragile and therefore each of the cleaning methods involves a certain degree of risk. Water gilding is particularly sensitive to water or polar solutions, but even aged oil gilding is prone to abrasions by prolonged movement of the aqueous solutions-saturated cotton swabs. Therefore, any cleaning action must be controlled, allowing the option to be terminated immediately if required. It should also involve as little agitation as possible, particularly where water based solutions are concerned.

2.2.1 Laser Systems for Cleaning of Gilded Wooden Surfaces

The Q-switched Nd:YAG 1064 nm photo-thermal laser cleaning system is the most common laser system used in the cleaning of heritage objects, including gilded wood surfaces. The portable variations of the system are popular due to their flexibility and simplicity of operation as well as effectiveness of treatment [20]. Recent studies reported that cleaning of gilded wooden objects with high soiling was successful using the Q-switched Nd:YAG 1064 nm at nanosecond laser pulses [21], while laser ablation using similar systems could delaminate brass-based overpainting, which then could be removed mechanically [22]. The morphological and colorimetric changes in gilded wooden surfaces induced by KrF excimer lasers at 248 nm (photochemical cleaning system) as well as Nd:YAG lasers at 532 and

streaky, a second one will be necessary. In applying either the finishing size or the ormolu, it is well to have a lump of alum convenient, to which, from time to time, the brush may be applied. This will, in the case of either, cause it to go on in a better manner and to lay more evenly. The ormolu, as prepared by the above method, will keep for any length of time. It may also be slightly colored, if it be desired to give the gold a deeper tinge. (Isaac H. Walker, 1884. The process of Gilding and Bronzing Picture Frames. New York, George F. Nesbitt & CO., Printers, Cor. Pearl and Pine Streets: 30–31)

1064 nm were studied to assess threshold values for both surface damage and colour changes in gold leaf [1, 2]. The Nd:YAG 355 nm laser was used successfully to remove soot from a silver-gilded icon [7]. Effective experiments with removal of brass-based overpaint and acrylic paints from gilded wood surfaces were carried out using Ti:Sapphire 250 kHz femtoseconds laser pulses, without heat propagation into the object. This system used laser-induced breakdown spectroscopy (LIBS) as a tool for determining the cease point for laser contaminant removal [13].

The Nd:YAG 1064 nm laser cleaning system is reportedly ‘self-limiting’ and offers controlled cleaning without over cleaning, if treatment is conducted below the damage threshold of the gilded surface. Selectivity of the cleaning process provides the ability to distinguish between contamination and original material; it can also produce a surface that is partially cleaned or under-cleaned. The cleaning process can be easily controlled by increasing or reducing ablation energy density; in practice, by increasing/ decreasing energy input, rate of impulses or a distance between the laser handpiece and the surface. It is probably the only cleaning system that offers ‘non-contact’ cleaning allowing gentle dirt removal from fragile gilded surfaces. It is an efficient technique and if suitable, it can save treatment time significantly.

This method is effective on water-gilded burnished surfaces, where the bond between gold leaf and the substrate is strong. Matte water-gilding is the most fragile surface, requiring lower fluence (the energy density) during treatment. Practice showed that shellac provides good protection for gold or silver leaf during laser cleaning. Removal of aged shellac is attainable, but it requires higher energy input, increasing the risk of damage to the underlying gold/ silver leaf [20].

The laser can be a useful tool for the removal of wax and acrylic resins residue from the gilding. In addition, laser cleaning is versatile and can be used in combination with other cleaning methods, i.e., the gilded surface can be first ‘under-cleaned’ with the laser ablation, followed by cleaning using hydrogels and emulsions or free chelating agent solutions on cotton swabs.

It has been also observed that laser cleaning is suitable particularly for undulated or ornamented gilded surfaces as circular imprints can become apparent in the partially-cleaned dirt layer on plain mouldings (‘under cleaning’ phase), corresponding with the field area affected by laser impulses.

2.2.2 Rigid Gels and Emulsions Systems for Dirt Removal

Rigid water-based gels have the advantage of saturating the dirt surface layer without leaving behind any visible residues. Rigid gels that can be applied and removed with a spatula also limit the aggravation of the surface with swabs. Viscous gels that require clearing would appear to be less controllable and therefore less suitable options for use on gilded surfaces.

The rigid gels and emulsions were selected in the subsequent two Case Studies according to their characteristics described in the conservation literature and involved Agar gels, Gellan gels, Xanthan gels, and PVOH-borax gel as well as low

viscosity emulsions based on Pemulen TR2, with and without chelating agents and with varied pH values.

2.2.2.1 Agar Gel

Agar consists of the carbohydrate forming structural components of seaweed. It can be melted above 85 °C and it will form gels at a temperature slightly above room temperature (32–45 °C). The process of melting and gel formation can be repeated many times, which is what makes Agar gels attractive for cleaning treatments [25]. The stability of gels however, can be affected by the temperature, pH level and sugar content. Prolong exposure to high temperatures can degrade gel strength. A pH value below 6.0 can cause precipitation of the agar, while higher sugar content can form harder gels, but of less cohesive texture [25]. At low concentrations (0.5%) Agar gels can form diluted solutions. Agar gels are characterised by their ability for high water retention, however, under pressure they are capable of exuding water through the gel surface, a phenomenon called syneresis [10, 25]. By increasing Agar concentration, the more rigid material can be obtained, with less possibility of the subsequent diffusion of water into the surface layers due to a formation of gel with a smaller pore size [10]. Conservation literature shows that 4% Agar solutions allow much less water diffusion into the surface than i.e. 2% solutions [9]. This would potentially be more beneficial for the gilded surfaces as it would offer surface-only contact treatment (less water diffusion into the gold-leaf underlying layers) and therefore better control of the cleaning process. In addition, it has been observed that in room temperature Agar gels form very rigid gels, which could be applied only to flat surfaces, however at temperatures elevated slightly above gel formation level (approximately 36–40 °C), the viscous substance can be brushed on the undulated surface and left to cool down. The subsequent gel can be then removed with spatula.

The contact time of agar gel with the proteinaceous dirt layer could have a significant impact on the efficiency of the treatment. It has been noticed that water soluble natural polymers such as gelatine behave as semipermeable membranes [9], which could be a critical factor in the cleaning process. With longer time contact, the surface could be more susceptible to osmotic processes causing a potential hazard to the gilding under the dirt layer. Moderately hypertonic conditions of cleaning (higher ion concentration in cleaning gel than in the surface dirt layer) would be recommended, as water which initially can wet the surface, will tend to migrate out of the dirt surface [9].

2.2.2.2 Gellan Gum Gel

Gellan gum is a polysaccharide gum that can be used as a gelling agent with aqueous liquids. The native (or 'high acyl') form contains acetate and glycate groups that can be stripped away forming the 'low acyl' structure [25]. The content of the acyl

groups determines the gel characteristics; ‘high acyl’ Gellan gum gels are soft and elastic, while ‘low acyl’ Gellan gum gels are firm and brittle [25], which theoretically would be more suitable for surface cleaning of gilding. The rigidity of the Gellan gum gel can be also influenced by the presence of Ca^{+2} ions; the higher the amount of Ca^{+2} ions the greater rigidity of the gel. However, in contrast to Agar gels, Gellan gum forms gels that are not thermo-reversible; once melted at 85–95 °C, Gellan gum will start to form gel upon cooling, and then can be reheated, but without changing the gel form. Similarly to Agar gel, Gellan gum gels are exposed to syneresis, and conservation literature has noted that this phenomenon affects particularly rigid gels [25].

Xanthan gel, PVOH-borax gel and Pemulen TR2 emulsions characteristics were described in paper Part A as well as elsewhere [3, 23, 25]. In reference to the removal of soiling from gilded surface Xanthan gel can offer an alternative to Agar or Gellan gels, while low-viscosity Pemulen TR2 emulsions can be a vehicle suited particularly to chelating agents. PVOH-borax gel proved to have the most-desired flexible texture for the removal of brass-based overpainting. In these trials, we intended to test its suitability for the direct removal of soiling from gilded surfaces.

2.2.3 Chelating Agents

Chelating agents, such as TAC, have been used for surface cleaning in heritage objects conservation since the 1980s. They have been shown to remove dirt consisting of both organic (lipidic) and inorganic components, due to the combination of metal ion chelation with deflocculation, peptization and favourable dispersion of oily material in the dirt layers [14].

The pH of an object’s surface and the pH of the chelating solution, impact the success and efficiency of this cleaning agent. At high pH, citric acid becomes fully dissociated and the participation of the OH group increases. This shifts the equilibrium towards the formation of a stable chelate complex, and influences the effectiveness of the cleaning solution [14].

While citric acid salts are weak chelators, EDTA is considered a stronger chelating agent, characterised with a high ability to sequester metal ions, i.e. in corrosion oxides or soiling, forming metal-EDTA complexes and allowing them to be removed from the surface. EDTA is the most common component of the gel cleaning systems. It has been reported that EDTA-containing agar gels extracted twice the quantity of green copper stains in comparison to pure gels [6]. The affinity of EDTA to form stable complexes with Fe^{+3} ions however, at pH c. 4.0–7.0 [19] could be of concern if the cleaning of water-gilded surfaces is considered, due to possibility of affecting its iron-rich bole foundation.

Chelating compounds should be used at the lowest possible active concentration to avoid potential damage occurring to the surface of an object. The application method can greatly impact the effectiveness of a cleaning agent. When applied

using a swab application method, chelating agents are not easily removed from undulations in an objects surface, even after clearance with water [14]. For this reason, rigid gels would be a more suitable application method to use on gilded ornamented wooden surfaces, as it is imperative that the chelating agents can be cleared from the gilded surface below.

Practice shows that soiled gilded surface has a slightly acidic pH, ~5.5 and effective cleaning usually can be achieved with water solutions pH 6.5 or higher. Conservation literature reports that citrates help to remove organic material from surfaces, particularly solutions with a higher pH value [14]. Strongly alkaline reagents however, should be avoided due to potential saponification of the oil medium which could pose a serious risk to oil-gilded surfaces.

In this investigation, both TAC and EDTA were incorporated into gels and emulsions to assess the effectiveness and practicality of these systems in delivering chelating agents to enhance the removal of soiling from gilded surfaces.

2.3 Case Study 1: The Frame for Thomas Miles Richardson, Eagle Crag and Gate Crag, Borrowdale, Cumberland 1875; dimensions: 82.5 × 111.0 × 7.5 cm

The findings of cross-section examination, FTIR analysis and solvent testing on the brass-based overpainting are detailed in paper Part A.

2.3.1 Solvent Tests of Soiling Layer

The removal of brass-based overpainting revealed a dark layer of dirt over the gilded surface of the frame. The initial examination of the cross-sections samples showed that the gilding layers underneath consisted of two oil gilding schemes. The dirt layer, showed sensitivity to TAC solutions. It could be removed with 4% (w/v) solution of TAC, at pH 8, applied with a cotton swab and cleared with white spirits. This application method revealed a well-preserved oil-gilded surface underneath, but required agitation of the surface (with a swab). Although TAC solubilised the dirt layer found on the gilded surface of this frame, it first had to be applied using a cotton swab to saturate the dirt layer and then re-applied to remove dirt and accretions.

2.3.2 Gel Testing: Removal of Ingrained Dirt and Soiling Tests (Table 2.1)

Table 2.1 Case study 1: Richardson frame – tests with gels and emulsions for removal of ingrained dirt and soiling

Gel tested	Area on frame tested	Application time	Application method	Removal method	Observation of gel texture	Soiling removal results
75PVOH-borax gel with TAC (~0.9% w/v)	N/A	N/A	N/A	N/A	Polyvinyl alcohol / water solution would not combine with the TAC solution; the mixture was cloudy and foamy and upon an addition of a borax solution the mixture separated in to two phases; the gel could not be formed. This gel was made twice with the same results and could not be used in the tests	N/A
Xanthan gum gel (3.75% w/v), with TAC (2.5% w/v), pH 7.5	Outer scotia	5 min	Dry cotton swab; spatula	Cotton swab; dry and saturated with solvent	Xanthan gum is emulsion-like in texture as it could not be removed in a single sheet like more rigid gels. This consistency posed a risk of getting stuck in the cracks between ornament	The gel effectively solubilised the dirt layer on the surface, which then could be removed with cotton swabs, but gold leaf could also be removed

(continued)

Table 2.1 (continued)

Gel tested	Area on frame tested	Application time	Application method	Removal method	Observation of gel texture	Soiling removal results
Agar gel (4% w/v) with TAC (1.25% w/v), pH 7.5		3; 5; 10 min	Gel can be cooled until it forms a semi-solid paste. This can be brushed onto the surface of the object and removed in a semi-solid state	Gel was removed using a spatula and the surface was cleared with a cotton swab moistened with triammonium citrate solution, followed by a cotton swab with white spirits	In the semi-solid state the gel texture shows still good flexibility and surface contact	Once the gel cooled and hardened, it could be removed with a spatula, leaving minimal residue on the surface. The dirt layer was softened and removed with cotton swabs during subsequent clearing. Oil gilding below remained intact
Agar gel (2% w/v), with TAC (1.25% w/v), pH 7.5		3; 5 min	Gel was applied by brush, when still warm and in the fluid form	After hardening, gel was removed using a spatula and the surface was cleared with a cotton swab moistened with triammonium citrate solution, followed by a cotton swab with white spirits	Gel was fluid when first applied to the surface of the frame. After it hardened (~1 min), the gel became rigid and conformed well to frame surface	Once the gel cooled and hardened, it could be removed with a spatula, leaving minimal residue on the surface. The dirt layer was softened and removed with cotton swabs during subsequent clearing. Oil gilding below remained intact. The gel delivered more water into the system than the 4% agar solution, which meant it had to be removed faster so as not to damage the gilding below

(continued)

Table 2.1 (continued)

Gel tested	Area on frame tested	Application time	Application method	Removal method	Observation of gel texture	Soiling removal results
Gellan gum low acyl gel (3% w/v), with TAC (0.83% w/v), pH 7.5	N/A	N/A`	N/A	N/A	When hot, the gel had a runny consistency. However once it had set, the gel was rigid and not malleable. It was too rigid to apply to the uneven moulding of the frame, as it could not make consistent contact with the surface	N/A
Gellan gum low acyl gel (3% w/v), with TAC (1.25% w/v), pH 8.0						
Gellan gum high acyl gel (1.64% w/v), with TAC (1.67% w/v), pH 8.0	Outer scotia	5; 10 min	Gel was applied by brush, when still hot and in the fluid form	After hardening, gel was removed using a spatula and the surface was cleared with a swab moistened with triammonium citrate, followed by white spirits	In the fluid form the gel was easy to work with. When left for 5-10 min the Gellan gel became very rigid, but had moulded well to the shape of the frame below. It could easily be removed with a spatula	When left on the surface for 5 min, both gels effectively softened the dirt layer, which could be then removed with swabs without disrupting the oil gilding. After longer application (10 min), the layer of gilding below soiling could also be removed during cleaning of dirt with cotton swabs
Gellan gum low acyl gel (2% w/v), with TAC (2.5% w/v), pH 8.0						

2.3.2.1 Agar Gel with TAC

Agar (2%; 4% w/v) gels were made and tested with 1.25% w/v concentrations of TAC at pH 7.5. Agar was applied directly to the surface with a paint brush after heating it to 40 °C and left on the surface for intervals of 3 and 5 min.

After the gel hardened, it could easily be removed with a spatula. Agar gel with TAC was found to effectively solubilise the ingrained dirt and soiling, which could be then easily removed with cotton swabs moistened with 1.25% w/v TAC solution. Finally, the area was cleared with white spirit applied with a swab. Both 2% and 4% w/v gels worked well, however the 2% w/v gel delivered more water into the system than the 4% w/v gel and as a result had to be removed after a shorter exposure time, to avoid damaging the gilding or softening the composition ornament below. For this reason, 4% w/v agar gel was favoured for the treatment of this frame (Figs. 2.1 and 2.2).

2.3.2.2 Gellan Gel with TAC

Both low and high acyl Gellan gels were tested by applying them in a rigid form when cold as well as brushing them to small areas of the dirty surface when still hot. The results varied.

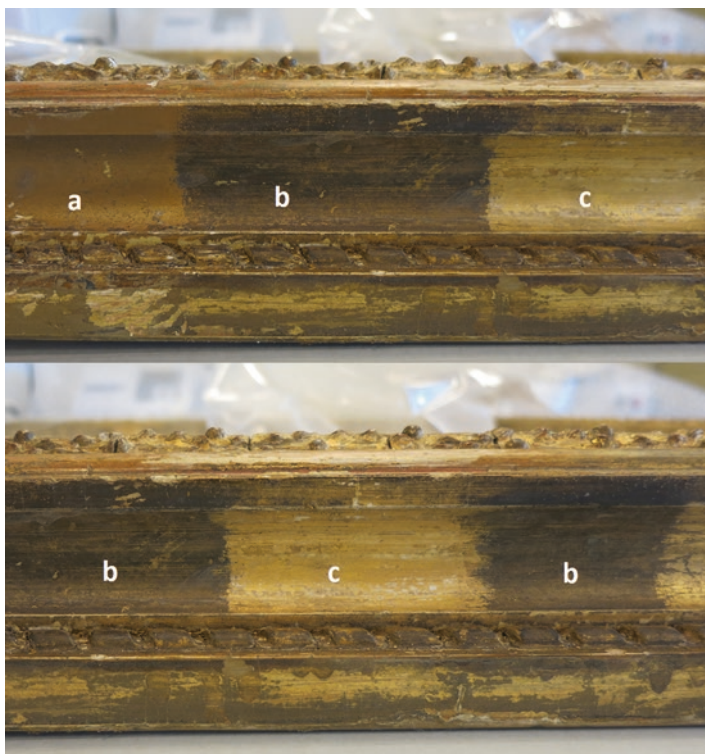
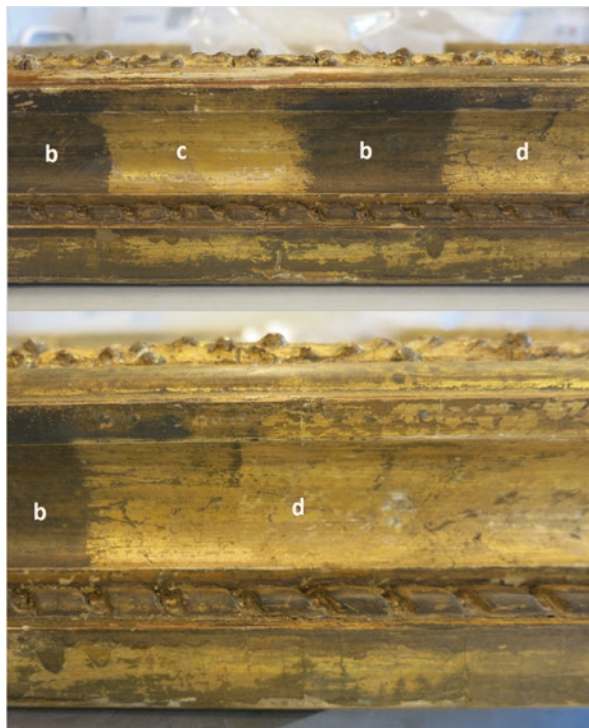


Fig. 2.1 Case study 1; the outer moulding of the frame for the Thomas Miles Richardson painting 'Eagle Crag and Gate Crag, Borrowdale, Cumberland, 1875' in varied cleaning stages: (a) the surface with brass-based overpainting, (b) the surface with soiling after brass-based overpainting was removed, (c) the oil-gilded surface after the dirt was removed with 4% w/v Agar gel, with 1.25% w/v TAC, pH 7.5

Fig. 2.2 Case study 1; the outer moulding of the Richardson frame during cleaning tests with Agar gel: **(b)** the surface with soiling after brass-based overpainting was removed, **(c)** the oil-gilded surface after the dirt was removed with 4% w/v Agar gel, with 1.25% w/v TAC, pH 7.5, **(d)** the oil-gilded surface after the dirt was removed with Agar gel showing some residue of the brass-based paint, which later was cleaned with acetone



Hot solutions of Gellan gels with TAC were poured into the rectangular containers and allowed to set. Once cool, these gels formed very rigid blocks that could be cut into small pieces and applied to the surface. However, it was difficult to apply them to curved, irregular or ornamented surfaces. The gel lacked flexibility that would allow close contact with the dirt layer. On flat surfaces Gellan gel was found to be effective in removing the soiling; the gel was easily lifted using a spatula and the softened dirt was removed with TAC moistened swabs, followed by white spirit. However, the motion of rolling a swab across the surface could potentially disturb and damage the gilding.

The most effective way of working with Gellan on irregular frame surfaces was to apply it with a brush while still in the warm phase. Once the Gellan had fully dissolved, the transparent mixture could be applied with a brush directly onto the soiled areas of the frame's surface (Fig. 2.3). Once cool, (~5 min), the gel hardened into a solid layer that could be removed with a spatula, leaving behind the softened dirt. The soiling was then removed using a swab dampened with TAC solution (at the same concentration and pH as was used in the gel) and the area was cleared with white spirit.

Both high and low acyl Gellan effectively saturated the soiling, but 2% w/v low acyl Gellan gel seemed to have the best working properties in our trials. All



Fig. 2.3 Case study 1; the outer moulding of the Richardson frame. Tests with Gellan gum gels: left hand side gel was applied with a brush while still in the warm phase, while the right hand side gel was applied in small pieces after setting, once cool

concentrations of TAC were effective, however even the lowest concentrations could have an adverse effect on gilding, which could be removed along with the softened soiling if the gel was kept on the surface for a longer time (10 min).

2.3.2.3 Xanthan Gel with TAC

Xanthan gum (3.75% w/v) with TAC (2.5% w/v) in water was made and tested on the frame's surface. The gel effectively softened the soiling after exposure for 3 min, but during clearance, the gold leaf was also removed. This gel had a viscous texture and there was a risk it would get stuck in the cracks between cracked ornaments. For this reason, trials with Xanthan gum were not pursued as it did not have the desired, rigid consistency.

2.3.2.4 PVOH-Borax Gel

With our experiments we were not able to incorporate TAC solutions (~0.9% w/v, at pH 8.0%) in the PVOH-Borax system. This gel was made twice with the same results whereby the gel was not forming and remaining in separate phases upon the addition of the borax solution.

2.4 Case Study 2: The Frame for Charles Landelle 'Isemenie, Nymph of Diana' 1878; dimensions: 177.6 × 131.5 × 15.0 cm

The findings of cross-section examination, FTIR analysis and solvent testing on the brass-based overpainting are detailed in paper Part A.

The conductivity of the dirt layer was measured three times after bronze paint removal, with the results of 119, 260 and 300 Microsiemens respectively, while pH of the dirt layer achieved the value of 5.7.

2.4.1 Solvent Tests of Soiling Layer

Removal of the brass-based overpainting revealed a thick, dark layer of dirt on the gilded surface of the frame. Cross-sections indicated the original gilding scheme consisted predominantly of water gilding followed by a later oil-gilding restoration. In cleaning tests, the soiling layer showed sensitivity to water and responded best to a 5% w/v aqueous solution of TAC with a pH level between 7.5 and 8.0 (Fig. 2.4).

2.4.2 Laser Cleaning

The dark soiling was particularly intense at the inner moulding of the lower member of the frame. Therefore this area was cleaned first with the Nd: YAG 1064 Lynton Phoenix laser system using a fluence of 0.2–0.3 J/cm² per pulse, with the repetition rate 5–15 Hz. This fluence allowed for an 'underclean' of the gilded surface (Fig. 2.5).



Fig. 2.4 Case study 2; the outer scotia moulding of the Landelle frame. Brass-based overpainting was partially removed exposing soiling underneath. The lighter rectangular section shows oil-gilding revealed after cleaning with swabs saturated with a 5% w/v aqueous solution of TAC with a pH level between 7.5 and 8.0



Fig. 2.5 Case study 2; after brass-based overpaint was removed, the inner mouldings of the lower member of the frame were cleaned with the Nd: YAG 1064 Lynton Phoenix laser system using a fluence under the damage threshold of the gilded surface, allowing for an ‘underclean’ finish

2.4.3 Gel Testing – Removal of Ingrained Dirt and Soiling Tests (Table 2.2)

The soiling layer was likely composed of atmospheric pollutants such as soot, and dirt bound up in an intentionally applied proteinaceous coating (i.e. ormolu). The density of this soiling layer varied significantly across the frame, and the distribution and condition of the proteinaceous coating also seemed to vary. Both these factors influenced the success and subsequently, the methodology adopted when using the gels and Pemulen TR2 emulsions for surface cleaning.

Gels were tested at various pH and concentrations (of gelling agent and chelating agent) for various intervals of time, starting with 1 min for sensitive surfaces and sometimes as long as 10 min for surfaces with heavier soiling.

Table 2.2 Case Study 2: Landelle frame – tests with gels and emulsions for removal of ingrained dirt and soiling

Gel tested	Area on frame tested	Application time	Application method	Removal method	Observation of gel texture	Results
Emulsions						
1% w/v Pemulen TR-2, 0.5% w/v EDTA pH 6.5	Outer scotia	3 min	Brushed directly on surface	Gel removed with dry swab. Futher cleaning with 0.5% EDTA in distilled water. Cleared with distilled water	Glue-like texture	Satisfactory removal of dirt revealing gilding underneath, white border marks formed at edges of tested section
		5 min	Brush application over cyclomethicone film	Gel removed with dry swab. Futher cleaning with 1% EDTA in distilled water. Cleared with distilled water		More efficient at removing dirt than 3 min, white border marks appeared at edges of tested section
		7 min	Brush application over cyclomethicone film	Gel removed with dry swab. Futher cleaning with 1% EDTA in distilled water. Cleared with distilled water		Effective removal of dirt, revealing gilding underneath, white border marks appeared at the edges of the tested section. No significant improvement from 5 min application

(continued)

Table 2.2 (continued)

Gel tested	Area on frame tested	Application time	Application method	Removal method	Observation of gel texture	Results
1% w/v Pemulen TR-2, 1% w/v EDTA, pH 6.5	Outer scotia	5 min	By brush over cyclomethicone film		Glue-like texture	Good removal of dirt revealing gilding underneath; no white border marks at the edges of the tested section
1% w/v Pemulen TR-2 TEA 1% w/v EDTA. pH 8.0	Outer scotia	5 min	By brush over cyclomethicone film		Glue-like texture	Good removal of dirt but it is not as effective as pH 6.5
Hydrogels						
~3% w/v Gellan gum gel, <1% TAC pH 7.5	Outer scotia	3 min	Cold gellan gum gel (from refrigerator) cut into squares and applied directly to the soiled gilding	Cleared with distilled water	Flexible yet firm film	No result
		5 min				No result
		7 min				No result
		10 min				No result
3% w/v Gellan gum low acyl gel, 1.25% w/v TAC pH 8.0	Outer scotia	3 min	Cold gellan gum gel (from refrigerator) cut into squares and applied directly to the soiled gilding	Cleared with distilled water	Flexible yet firm film	No result
		5 min				No result
		7 min				Some dirt on swab. No visible change to gilded surface
		10 min				Some dirt on swab. Limited removal of soiling at the edges of the Gellan square

(continued)

Table 2.2 (continued)

Gel tested	Area on frame tested	Application time	Application method	Removal method	Observation of gel texture	Results
2% w/v Gellan gum low acyl gel, 2.5% w/v TAC pH 8.0	Outer scotia	3 min	Cold gellan gum gel (from refrigerator) cut into squares and applied directly to the soiled gilding.	Cleared with distilled water	Flexible yet firm film	Slight removal of soiling at edges of Gellan square
		5 min				Effective removal at the corners of the Gellan square
		7 min				Effective removal at the corners of the Gellan square
		10 min				Very effective. In order to ensure consistent removal and contact with the curved surface, the Gellan square would need to be weighted
4% w/v agar gel, 1.25% w/v TAC pH 8.0	Ornament	3 min	Warmed to 40 °C. applied with a brush.	Cleared with distilled water	Gel was fluid when first applied to the surface of the frame. After it hardened (~1 min), the gel became rigid and conformed well to frame surface	Consistent, effective removal
		5 min				Consistent, effective removal. No major difference between 3 and 5 min

(continued)

Table 2.2 (continued)

Gel tested	Area on frame tested	Application time	Application method	Removal method	Observation of gel texture	Results
4% w/v agar gel, 3% w/v TAC pH 8.0	Ornament	5 min	Warmed to 40 °C. applied with a brush.	Cleared with distilled water	Gel was fluid when first applied to the surface of the frame. After it hardened (~1 min), the gel became rigid and conformed well to frame surface	Very effective. Unlike previous tests, removal of dirt occurs when the gel is cleared with distilled water on the swab

The gels were trialled on flat, curved and contoured surfaces of the frame to determine how viscosity, rigidity and other gel properties would influence their success when cleaning the various shapes of the frame profile. These areas included the outer scotia, the torus ornament of top moulding and ornament on the inner scotia.

Cyclomethicone was also tested beneath applications of Agar gel and Pemulen TR-2 by being brushed directly over the soiled surface.

2.4.3.1 Agar Gel with TAC

After heating to 40 °C, 4% w/v Agar gels with 1.25% w/v and 3% w/v TAC respectively at pH 8.0 were applied directly to the surface with a paint brush. The gels were left on the surface for intervals of three and 5 min. The gels were then removed with a spatula and distilled water-saturated cotton swabs or TAC solution-saturated swabs followed by swabs with distilled water. The removal of dirt occurred during the first clearing of the gel with distilled water on cotton swabs. Surprisingly, increasing of TAC concentration did not improve cleaning efficacy.

Agar gel produced good results and this system proved to be a good candidate for future projects involving the cleaning of gilded wood surfaces.

Cylcomethicone was observed to have little impact on the effectiveness of the cleaning method.

2.4.3.2 Gellan Gel with TAC

Small squares of Low Acyl Gellan were cut from pre-cast, refrigerated sheets of the gel. The squares were applied cold. Conductivity of Gellan gels has been maintained at around 3700 Microsiemens, approximately 10–20 times the dirt surface conductivity, as suggested by the conservation literature [16].

The following concentrations of Gellan and TAC were tested on the concave surface of the outer scotia: 3% w/v Gellan gel with <1% TAC at pH 7.5, 3% w/v Gellan gel with 1.25% w/v TAC at pH 8.0, and 2% w/v Gellan gel with 2.5% w/v TAC solution at pH 8.0 gels. These formulations were trialled at intervals of three, five, seven and 10 min. After removing the Gellan gel, the softened dirt layer was removed with dry swabs and the area was cleared with distilled water. This method produced very limited success. As the Gellan gel was cast flat, it would not conform to the curved surface of the outer scotia. Cleaning only occurred at the corners and edges of the Gellan gel squares: the only areas that made consistent contact with the frames surface.

2.4.3.3 Pemulen TR2 Emulsion with EDTA

Pemulen TR2 emulsions were prepared according to the Chis Stavroudis' Modular Cleaning Program. 2% w/v stock solution was prepared and subsequent mixtures from this stock were then adjusted to a range of concentrations and pH levels.

EDTA was tested at concentrations ranging from 0.5%, 0.75%, 2% w/v, with pH levels between 6.5 and 8.0. A pH of 6.5 was found to be most effective (Fig. 2.6). Pemulen solutions were tested on the surface for intervals of 3, 5, 7 and 10 min. The gel was removed with a dry swab, followed by further swab cleaning with EDTA and then clearance with distilled water. According to the condition of the surface, it varied whether the bulk of dirt removal occurred with the dry swab or subsequent treatment with EDTA (Fig. 2.7).



Fig. 2.6 Case study 2; the outer scotia moulding. Preliminary tests with the 1% w/v Pemulen TR2 emulsions with 0.5% w/v EDTA, pH 6.5, showed a formation of white border marks at the edges of the tested sections



Fig. 2.7 Case study 2; the outer mouldings of the Landelle frame during the removal of soiling using the 1% w/v Pemulen TR2 emulsion with 1% w/v EDTA, pH 6.5

All Pemulen TR2/ EDTA mixtures were tested over an application of cyclomethicone to determine its effectiveness as a protective barrier layer. Results varied. Cyclomethicone appeared to assist in the actual removal of soiling from the ornaments, where the dirt layer was thinner, however little impact was observed in tests conducted on the outer scotia, where accumulation of dirt was greater.

Overall, the Pemulen TR2/ EDTA system was the most effective for the safe removal of soiling from the oil-gilded surface (Figs. 2.8 and 2.9). Depending on the level of soiling and the sensitivity of the gilding, the final application time ranged from 1 to 3 min.

In heavily soiled areas, follow-up cleaning with EDTA needed to be done soon after the gel was cleared: as its effectiveness diminished as time passed. A streaked and irregular pattern often remained after the gel and soiling were cleared. This may be due to uneven distribution and varying properties of the proteinaceous-based coating.

2.5 Discussion

The success of wet-cleaning water-sensitive surfaces is determined by two factors: the properties of the water (pH, ion concentration, conductivity, and additives such as chelators, surfactants or specific salts), and the application method (free solutions on cotton swabs, emulsions, viscous gels, rigid gels) [8].

Water-gilded wooden surfaces are very sensitive to cleaning with aqueous solutions due to the hydrophilic nature of the foundation layers under the gold leaf. Extremely thin gold leaf is permeable enough to allow water to diffuse through it

Fig. 2.8 Case study 2; the inner part of the Landelle frame during cleaning with the 1% w/v Pemulen TR2 emulsion with 1% w/v EDTA, pH 6.5



Fig. 2.9 Case study 2; a fragment of the outer mouldings of the Landelle frame after surface cleaning

into the foundation layers. Oil-gilding should theoretically be more resistant to water-damage, however practice has shown that prolonged applications of aqueous solutions can have a similar impact on these surfaces. Conservation literature on soiled oil films also reports that in order to avoid the swelling and extraction of ionic materials, any cleaning solution should maintain conductivity parameters that are 10–20 times the surface conductivity of the oil-based film [16].

The tests discussed here show that both rigid hydrogels (Agar and Gellan gels) and Pemulen TR2 emulsions can be used in removing soiling from gilded wooden surfaces, but their suitability and subsequent success is determined by the nature of the surface and the application method.

None of the systems could remove the soiling without subsequent swab agitation. Each gel and emulsion worked as moisture/ chelating agent vehicles allowing softening of the dirt layers, but their removal required additional working with dry or moisten swabs. The effectiveness of the systems was time dependent. However, the systems proved to be more effective in removal of soiling from the gilded wooden surfaces than by using only free aqueous solutions on swabs.

Gellan gum gels were by far the most rigid of all gels tested. As Gellan gum gel could not be reversed from a solid state to a liquid state after it had formed, it must be used immediately after being made, if it is to be brushed onto a surface. If the Gellan gum was brushed onto all surfaces immediately after being made, it would be on the surface for too long and this may affect the gilding below. If the Gellan gum gel was made into sheets for later usage, the gel pieces will lack flexibility and may not have enough contact with the ornamented or uneven surface and hence, would not be an effective carrier for the aqueous solution or chelating agents.

Agar gel has been found to be the most versatile. It can be cooled until it forms a semi-solid paste, which then can be brushed onto the surface of the object and later removed with a spatula. Agar gel can be also brushed on to the surface when still in the liquid state, just slightly above gelling temperature (for most types ~36–40 °C), assuring close contact with undulated surface. It is also a very efficient method as the reheating process can be repeated several times.

Xanthan gum was found to have the least-controllable emulsion-like texture as it could not be removed in a single sheet like other rigid gels. Its viscous consistency could have an adverse effect on gilded surface, particularly if it is richly ornamented and badly cracked.

Pemulen TR2 emulsions have been found to be the most efficient of all the systems. They were only slightly thicker than free chelating agent solutions, but the texture allowed them close contact with the surface without penetrating under the surface through the cracks. They were easily removed from the surface, allowing good control of the cleaning process.

Although it is likely that the dirt layer could react just to the water content of the gels, the contact with the surface would have to be much longer for effective dirt removal and therefore hazardous for gilding. In addition, water itself would not remove ionic and fatty deposits from the surface. The addition of chelating agents enhanced the cleaning efficacy by both dissolving and softening the dirt and shortening the gels/emulsions contact time with the surface. There was no significant difference observed between gels and emulsions with the TAC or EDTA components, but it was observed that although higher content of chelating agent could shorten the reaction time, it could also have an adverse effect on gilding. In general, the effective cleaning was achieved using lower concentrations of chelating agents in gels and emulsions than it required at cleaning using free solutions on swabs.

It is probable that in case study 2, the patches of soiling that were harder to clean corresponded with parts of the ormolu coating containing greater amounts of resin, and were therefore more resistant to solubilising, requiring repetition of the treatment in following days, after the resting period.

It has been flagged by researchers at the Shelburne Museum, that despite the addition of triethanolamine (TEA) as a buffer, the pH of a Pemulen TR2 emulsion can drop by half a unit over-night [17]. This was confirmed in our tests, finding a solution at the pH value of 6.5 dropping to 6. Therefore, the solution needs to be monitored and adjusted where required.

Khandekar [12] has observed that triethanolamine (TEA) can have the enhancing action in surface cleaning while used as a buffer, therefore the potential impact of this component in the cleaning mechanism of gels and emulsions with chelating solutions should not be ignored.

Decreasing the contact-time between water and the surface is crucial for a successful treatment. Silicone solvents (cyclomethicones) are advocated for by Stavroudis [24] and Cremonesi [8] for extra protection during cleaning with aqueous solutions by forming temporary hydrophobization of the surface and restricting diffusion of water under the surface. With low dissolving ability, low surface tension and slow evaporation, cyclomethicones can 'wet' the surface under the soiling layer [[10]] providing protection for the gilded surface during cleaning using aqueous solutions. However, the above case studies showed that the dirt layer must be relatively thin to find this method effective; while application of cyclomethicone assisted in cleaning of the ornamented passages, it had a little effect in the removal of soiling from the outer scotia moulding on the Landelle frame (case study 2).

It has been also noted in other studies that the oxidised aged surface can show higher hydrophilic character, and in consequence higher sensitivity to water [[10]]. This could be a drawback in cleaning gilded wooden surfaces using gels and emulsions, which require repeated water clearing after the application.

PVOH-Borax gels are highly viscous polymeric dispersions (HVPD) with a very high shear elastic modulus allowing one to peel the settled material easily from the cleaned surface, without leaving residues and the need for clearing [4, 5, 18]; a feature not observed with other tested materials. Therefore, its lack of compatibility with TAC solutions was disappointing. It has been noticed in the literature that the pH level plays a crucial role in the PVOH-borax gel formation, and changes in the pH equilibrium of the system can obscure formation of gel. With a pH level below 8.0 gel will not form, while with a pH above 9.0 gel could become more rigid or the system will separate into two phases [3, 4]. High salt concentration in the system can have a similar effect. It is possible that the TAC solution concentrations in the above trials were too high. Angelova [3] observed that incorporating chelating salts in the PVOH-borax system '*demands fine tuning*' ([3]: 233). The change of the ion balance in the 'liquid part' of the mixture can cause disruption in the polymer chain formation and crosslinking of borates, resulting in an excessively rigid gel or separation of it into two phases. Increasing the concentration of the chelating agents in the gel system correlates with increasing the strength of the gel network. Angelova was

able to incorporate not more than 0.5 wt% EDTA into the 80PVOH-borax system [4]. Indeed this system requires further experiments with chelating agents in the future.

Future tests could include experiments using rigid gel formation with an addition of a citrate–diethylenetriaminepentaacetic acid (DTPA) chelator, which has been recognised as a particularly effective agent for the removal of carbon-based materials such as soot, organic soils, combustions residue [15].

For highly water-sensitive surfaces Cremonesi [10] proposed the use of grated Agar, which can provide even further control and reduction of water release to the treated surface. This method could also be effective using rigid Gellan gel and therefore is planned to be tested using both systems in the future.

2.6 Conclusion

These two case studies have shown that hydrogels based on Agar and Gellan gum as well as Pemulen TR2 emulsions can be successfully used in the removal of soiling from gilded wooden surfaces, however each of the cleaning systems needs to be utilised with caution and full understanding of the potential risk to the gilded surface.

The option to increase the rigidity of gels can address one of the longstanding challenges of aqueous cleaning methods for gilded surfaces; that is the rate of water diffusion into the gilding's foundation layers. The above tests showed that rigid gels proved to be a good vehicle to deliver the chelating agents for removal of soiling from oil gilding, offering surface contact without diffusion into underlying layers. These methods can also decrease contact time between cleaning agents and the gilded surface, therefore providing better control and safety in treatments as well as reducing the needs for agitation of the surface with cotton swabs. Low viscosity Pemulen TR2 emulsions provide similar opportunity without the need for repetitive clearing.

It has been recognised that the above tests form just a prelude for further experiments with these cleaning methods for removal of soiling from varied gilded wooden surfaces. Further testing is essential to obtain a better understanding and confidence in the working abilities of gel and emulsion systems for the cleaning of gilded wood.

Materials

PVOH: Kuraray Poval Polyvinyl Alcohol L-10

Borax: Bare Essentials Borax

Pemulen TR2: Noveon, Inc. Pemulen

Triethanolamine TEA: Merck KGaA Triethanolamine

Citric Acid: Chem-Supply Citric Acid Anhydrous

Xanthan gum: Melbourne Food Ingredient Depot

EDTA Ethylenediaminetetraacetic acid: Sigma-Aldrich

Gellan Gum Powder Low Acyl, High Acyl: The Melbourne Food Ingredient Depot

Agar Agar: The Melbourne Food Ingredient Depot

Appendix

Description of the hydrogel systems preparation included in the tests:

- A. Agar gel: 4 g (or 2 g) of Agar Agar powder was dissolved in 75 ml of deionised water over high heat (~150C) using magnetic stirrer. All particles of Agar were solved prior to adding 25 ml of TAC 5% w/v solution. Once combined the gel was allowed to cool down to approximately 40C before applying it to the dirty surface of the frame.
- B. Gellan Gum gel (low acyl or high acyl):
 - (a) ~3.2% w/v, with TAC, 0.83% w/v, pH 7.5: 5 g of Gellan Gum Powder was added to 100 ml water adjusted with TEA to pH 7.5, and left to stand overnight. The mixture was then dissolved over heat with a magnetic stirring bead. 50 ml of 2.5% w/v TAC, pH 7.5 was then gradually added.
 - (b) ~3% w/v, with TAC, 1.25% w/v, pH 8.0: 3 g of Gellan Gum Powder was added to 75 ml of hot water adjusted with TEA to pH 8.0, and microwaved for ~2 min. The mixture was then heated on hotplate at ~100C, and stirred with magnetic stirring bead for about 1 h. 25 ml of 5% w/v TAC, pH 8.0 was then slightly heated and gradually added.
 - (c) 1.64% w/v, with TAC, 1.67%, pH 8.0: 2.5 g of Gellan Gum Powder was added to 50 ml of hot water adjusted with TEA to pH 8.0, and dissolved over heat with magnetic stirring bead. 100 ml of 2.5% w/v TAC, pH 8.0 was then slightly heated and gradually added.
 - (d) 2% w/v, with TAC, 2.5% w/v, pH 8.0: 3 g of Gellan Gum Powder was added to 75 ml of hot water adjusted with TEA to pH 8.0, and left to stand for 1 h. The mixture was then dissolved in microwave and 75 ml of 5% w/v TAC, pH 8.0 was then heated and gradually added.
- C. Xanthan Gum gel was made according to the literature recommendations to use 4% for best consistency and working properties ([11], p.123): 7.5% Xanthan gum stock gel was prepared by mixing 7.5 g of powder with 20 ml of deionised water, pH 7.5 (adjusted with TEA), and then top up with deionised water up to the final volume of 100 ml. Then 5 ml of Xanthan stock gel was mixed with 5 ml of TAC, 5% w/v, pH 7.5.
- D. Pemulen TR2 emulsions and EDTA solutions: see: Sawicki M. et al. Chap. 1 in this volume, Part A, Appendix.
- E. PVOH-borax system with ~0.9% TAC (unsuccessful): 2 g of 75PVOH (Kuraray Poval polyvinyl alcohol L-10) was dissolved in 18.75 g of deionised water over moderate heat (<~50 °C) and then mixed gradually with 18.75 g g of 2.5% TAC solution. The mixture was cloudy and foamy. In a separate container 0.5 g of borax was dissolved in 10 g of deionised water. When borax was added to the PVOH-TAC solution separation of the components occurred.

References

1. Acquaviva S., D'Anna E., De Giorgi M.L., Della Patria A. and Pezzati L. 2008. Morphological and colorimetric changes induced by UV laser radiation on metal leaves. In: Casillejo M., Moreno P., Oujja M., Radvan R., Ruiz J., (eds), 2008. *Lasers in Conservation of Artworks*. Taylor & Francis Group, London, ISBN 978-0-415-47596-9: 317–322.
2. Acquaviva S., D'Anna E., De Giorgi M.L., Della Patria A., Pezzati L., Pasca D., Vicari L., Bloisi F., Califano V. 2007. Laser cleaning of gilded wood: a comparative study of colour variations induced by irradiation at difference wavelengths. *Applied Surface Science* Vol. 253, Issue 19: 7715–7718.
3. Angelova LV, Carretti E, Berrie BH and Weiss RG 2017. Poly(vinyl alcohol)-borax 'gels': a flexible cleaning option. In Angelova L.V., Ormsby B., Townsend J.H. and Wolbers R, (eds), *Gels in the Conservation of Art*. Archetype Publications Ltd.: 231–236.
4. Angelova L.V., Berrie B.H., de Ghetaldi K., Kerr A. and Weiss R.G. 2015. Partially hydrolyzed poly(vinyl acetate)-borax-based gel-like materials for conservation of art: characterisation and applications. *Studies in Conservation* 60:227–44
5. Baglioni P., Berit D., Bonini M., Carretti E., Perez M.D.C.C., Chelazzi D., Dei L., Fratini E., Giorgi R., Natali I. and Arroyo M.C., 2012. Gels for the Conservation of Cultural heritage. *MRS Online Proceedings Library*, Cambridge Journals, Cambridge University press: 1–11.
6. Bertasa M., Chiantore, O., Poli, T., Riedo, C., di Tullio, V., Canevali, C., Sansonetti, A. and Scalalone, D. 2017. A study of commercial agar gels as cleaning materials. In Angelova, L.V., Ormsby, B., Townsend, J.H. and Wolbers, R, (eds), *Gels in the Conservation of Art*. Archetype Publications Ltd: 11–18.
7. Bordalo R., Morais P.J., Gouveia H., and Young C. 2006. Laser Cleaning of Easel Paintings: An Overview. *Laser Chemistry*, Volume 2006, Article ID 90279, Hindawi Publishing Corporation, 9 pages: doi: <https://doi.org/10.1155/2006/90279>
8. Cremonesi P. 2018. Combination of a Liquid-Dispensing and Micro-Aspiration Device for the Cleaning of Sensitive Painted Surfaces, *Studies in Conservation*, 63:6; 315–325, DOI: <https://doi.org/10.1080/00393630.2017.1396029>
9. Cremonesi P. and Casoli A. 2017. Thermo-reversible rigid agar hydrogels: their properties and action in cleaning. In Angelova L.V., Ormsby B., Townsend J.H. and Wolbers R, (eds), *Gels in the Conservation of Art*. Archetype Publications Ltd: 19–27.
10. Cremonesi P. 2016. Surface cleaning? Yes, freshly grated Agar gel, please. *Studies in Conservation*, 61:6, 362–367, DOI: <https://doi.org/10.1179/2047058415Y.0000000026>
11. Doherty E. and Rivers S. 2017. The Removal of Lead and Oil-based Overpaint from a plaster cast of Hermes Fastening His Sandal. In Angelova L.V., Ormsby B., Townsend J.H. and Wolbers R, (eds), *Gels in the Conservation of Art*. Archetype Publications Ltd: 122–125.
12. Khandekar N. 2000. A survey of the conservation literature relating to the development of aqueous gel cleaning on painted and varnished surfaces. *Studies in Conservation*, 45:sup3, 10–20, DOI: <https://doi.org/10.1179/sic.2000.45.s3.003>
13. Kono M., Baldwin K.G.H., Wain A., Sawicki M., Malkiel I. K. and Rode A.V. 2013. High repetition rate laser restoration and monitoring of large area gilded surfaces. *Lasers in the Conservation of Artworks IX*, Archetype Publication, Ltd, London: 45–52.
14. Morrison R., Bagley-Young A., Burnstock A., van den Berg K.J. and van Keulen H. 2007. An Investigation of Parameters for the Use of Citrate Solutions for Surface Cleaning Unvarnished Paintings. *Studies in Conservation*, 52:255–270.
15. Moskalik-Detalle A., Assoun J., Joseph F., Martiny M-L and Monfort M. 2017. Conservation of murals by Eugene Delacroix at Saint Sulpice, Paris. In Angelova L.V., Ormsby B., Townsend J.H. and Wolbers R, (eds), *Gels in the Conservation of Art*. Archetype Publications Ltd: 200–208.
16. Ormsby B. and Learner T. 2009. The effects of wet surface cleaning treatments on acrylic emulsion artists' paints – a review of recent scientific research. *Studies in Conservation*, 54:sup1, 29–41, DOI: <https://doi.org/10.1179/sic.2009.54.Supplement-1.29>

17. Ravenel N. 2000. How to make the gel, Pemulen TR2. accessed 20 June, 2018, <http://pemulentr2.pbworks.com/w/page/15636418/How%20to%20make%20the%20gel>
18. Riedo C., Caldera F., Poli T. and Chiantore O. 2015. Poly(vinyl alcohol)-borate hydrogels with improved features for the cleaning of cultural heritage surfaces. *Heritage Science* 3(1): 23.
19. Rives S. and Umney N., 2003. Conservation of Furniture. Butterworth-Heinemann, Oxford.
20. Sawicki M., Bramwell–Davis V. and Dabrowa B. 2011. Laser cleaning from a practical perspective: Cleaning tests of varied gilded-wood surfaces using Nd:YAG Compact Phoenix laser system. *AICCM Bulletin* Volume 32, 2011: 44–53
21. Schmidt A.B., Pentzien S., Conradi A., Krüger J., Roth C., Beier O., Hartmann A., Grünler B. 2017. Decontamination of biocidal loaded wooden artworks by means of laser and plasma processing. Lasers in the Conservation of Artworks XI, Proceedings of LACONA XI, P. Targowski et al. (Eds.), NCU Press, Toruń 2017, DOI: <https://doi.org/10.12775/3875-4.17>
22. Striber J., Jovanović V., Jovanović M. 2017. Easel paintings on canvas and panel: application of Nd:YAG laser at 355 nm, 1064 nm and UV, IR and visible light for the development of new methodologies in conservation. Lasers in the Conservation of Artworks XI, Proceedings of LACONA XI, P. Targowski et al. (Eds.), NCU Press, Toruń 2017, DOI: <https://doi.org/10.12775/3875-4.20>
23. Stavroudis C. 2017. Gels: evolution in practice. In Angelova L.V., Ormsby B., Townsend J.H. and Wolbers R, (eds), Gels in the Conservation of Art. Archetype Publications Ltd: 209–217.
24. Stavroudis C. 2016. Cleaning of Acrylic Painted Surfaces, July 12–15, 2016, The John and Mable Ringling Museum of Art, Sarasota, Florida. MCP Recipes. The Getty Conservation Institute: https://www.getty.edu/conservation/our_projects/education/caps/modular_cleaning_recipes.pdf
25. Wolbers R. 2017. Terminology and properties of selected gels. In: Angelova L.V., Ormsby B., Townsend J.H. and Wolbers R, (eds.). 1917. Gels in the Conservation of Art. Archetype Publications Ltd: 381–294.

Chapter 3

New Consolidants for the Conservation of Archeological Wood



Zarah Walsh-Korb, Emma-Rose Janeček, Mark Jones, Luc Averous,
and Oren A. Scherman

Abstract The preservation of cultural heritage is of great importance worldwide and, as such, has been the focus of an increasing number of research projects in recent years. In spite of considerable efforts around the world, significant problems have arisen with the conservation of many shipwrecks. The most common issues facing conservators are structural instability upon drying and biological degradation stemming from the aquatic flora and fauna active around the excavation site. However, many important artefacts – such as the sixteenth century warship *Mary Rose* – also suffer from metal ion saturation from degraded bolts and fittings. In most cases Fe^{3+} is the greatest problem, which catalyses the production of sulfuric and oxalic acid in the waterlogged timbers, adding chemical degradation to the potential conservation issues. Moreover, the Fe^{3+} also feeds biological degradation by providing bacteria with an iron source for sustained growth. As such, multi-functional consolidants are greatly needed to tackle not only the many-pronged conservation issues already visible, but also to prevent others from evolving over time. This paper discusses the recent successes in the development of such materials from

Z. Walsh-Korb (✉)

BioTeam, ECPM/ICPEES, UMR CNRS 7515, Université de Strasbourg, Strasbourg, France

Melville Laboratory for Polymer Synthesis, Department of Chemistry, University of Cambridge, Cambridge, UK

e-mail: zarah.walsh2@mail.dcu.ie

E.-R. Janeček

Melville Laboratory for Polymer Synthesis, Department of Chemistry, University of Cambridge, Cambridge, UK

Institute of Materials, Ecole Polytechnique Federale de Lausanne, Lausanne, Switzerland

M. Jones

The Mary Rose Trust, Portsmouth, UK

L. Averous

BioTeam, ECPM/ICPEES, UMR CNRS 7515, Université de Strasbourg, Strasbourg, France

O. A. Scherman

Melville Laboratory for Polymer Synthesis, Department of Chemistry, University of Cambridge, Cambridge, UK

sustainable, bio-based sources and some potential areas for the future development of these tools.

Keywords Waterlogged archaeological wood · *Mary rose* · Poly(ethylene glycol) · Bio-based polymers · Supramolecular materials · Conservation

3.1 Background

Although the timbers of the sixteenth century warship *Mary Rose* are generally well conserved there are three major problems facing conservators: structural instability upon drying, biological activity in the timbers and high concentrations of iron present from the degradation of bolts and fittings in the ship, which contribute to the chemical degradation of wood [1–7, 10]. Current conservation strategies involve spray treating with increasingly concentrated solutions of poly(ethylene glycol) (PEG) in water that have been doped with a broad spectrum biocide. The spray treatment of the *Mary Rose*, which has recently concluded, is shown in Fig. 3.1.

PEG became popular in the early twentieth century, with the large-scale industrialisation of the chemical industry, and represented a major advance over the alum treatments that had been used previously. The alum conservation method had involved immersing artefacts in concentrated alum (potassium aluminium sulphate) solutions at 90 °C, the alum then recrystallised within the timbers and prevented dimensional changes on drying. Unfortunately, artefacts conserved in this manner suffer over time from the generation of sulfuric acid by the alum. The significantly reduced pH within the wood, often as low as pH 1, has resulted in mechanically weak timbers that require further stabilisation [8]. The introduction of PEG to conservation science, with its low cost and relatively low toxicity, represented a significant advance in conservation technology compared to alum. PEG treatment works by solvent displacement. Spraying solutions of PEG at the wood or soaking the wood in PEG replaces the water in the timbers with PEG molecules. Structural instability during the drying process is, therefore, reduced as the vapour pressure of PEG is significantly higher than water. Thus the wood dries, while the fragile cells are supported by the PEG within.

However, in recent years several disadvantages of PEG have become apparent. In particular, its ability to act as a solid-state ion transporter [9] its degradation to acidic by-products [4, 5, 10, 11] the need for additives to provide anti-bacterial properties or remove iron, [3, 12] and the cost of long-term use. Moreover, the long-term use of PEG in wood conservation was found to increase the likelihood of plasticisation of the timbers, leading to eventual brittleness and further instability [13, 14]. These drawbacks all point to the need for new treatments to be designed. As PEG does not counter-act the presence of iron in the timbers, the chemically induced degradation of the *Mary Rose* is currently left unchecked.

In recent years there has been much interest in the use of non-synthetic materials for conservation and several research groups have investigated the use of bio-based



Fig. 3.1 The sixteenth century warship *Mary Rose* undergoing spray treatment with solutions of PEG200 and PEG2000 at HM Naval Base dry-dock in Portsmouth, UK. (Image reproduced with permission from the Mary Rose Trust)

polymers as alternative consolidants [15–17]. While these materials certainly pave the way for the future improvements in the consolidation of waterlogged wooden artefacts, they still lack the multi-functionality required to be minimally invasive to the artefact while producing the maximum conservative effect. A new conservation treatment is presented here based on a supramolecular polymer network constructed from chitosan and guar [18]. This material is a dynamically cross-linked 3-dimensional bio-based polymer network. Cross-linking of the guar and chitosan network is provided by host-guest ternary complexation using a macromolecular host unit known as cucurbit[8]uril and complementary guest molecules methyl viologen (guar) and naphthyl units (chitosan), providing the basic dynamic structure, Fig. 3.2. Metal-ligand interactions implemented by a strong Fe^{3+} chelator pen-

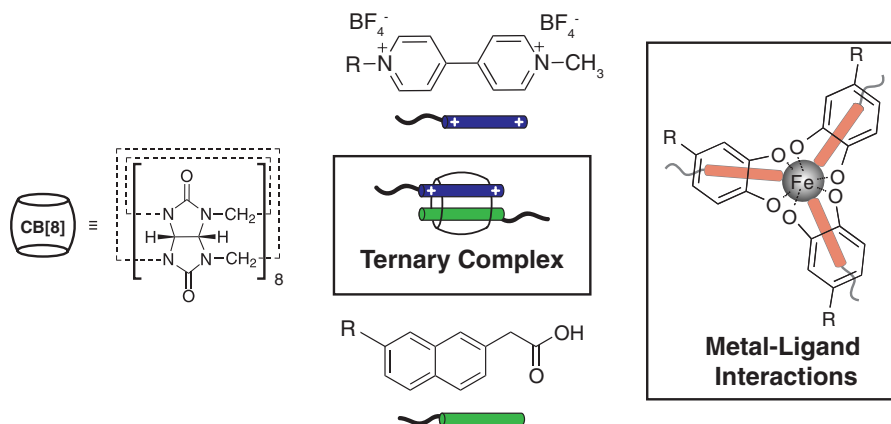


Fig. 3.2 Schematics and structures of the ternary complexation between methyl viologen (blue bar), 2-naphthylacetic acid (green bar) inside the cucurbit[8]uril macromolecular host (barrel) and the metal-ligand interactions promoted by the dihydroxyphenylacetic acid unit (red bar) around Fe^{3+} centres

dant from the chitosan backbone (Fig. 3.2), give the functional material the ability to chelate and trap iron while increasing structural stability. Thus, allowing the material to adapt to the chemical environment of the wood.

The inclusion of methyl viologen as a guest molecule also enhances the antibacterial character of the polymer network and will provide the material with increased biological resistance relative to conventional conservation treatments (Fig. 3.2). The polymer is known as *PolyCatNap* due to the incorporation of catechol (*Cat*), promoting the formation of metal-ligand interactions, and naphthol (*Nap*), allowing for the host-guest complexation, onto the backbones of the bio-based polymers used to construct the network. Exploiting environmentally compatible bio-based materials with reversible cross-links through host-guest chemistry and metal-ligand interactions makes a safer, greener alternative to current strategies and will potentially extend the lifetime of many precious waterlogged wooden artefacts under conservation around the world. [15, 16, 19].

3.2 Experimental Results

A number of analytical and instrumental techniques have been used to verify the ability of *PolyCatNap* to chelate iron and its structural stability. As a first step, accelerated ageing tests were performed on the polymeric components of the supramolecular consolidant and compared with the results obtained from PEG under the same conditions, which were adapted from a paper by [11]. Under these conditions PEG showed an increase in acidity of 2 pH units when tested before and after the experiment. Whereas, with the chitosan and guar, no change in pH was observed

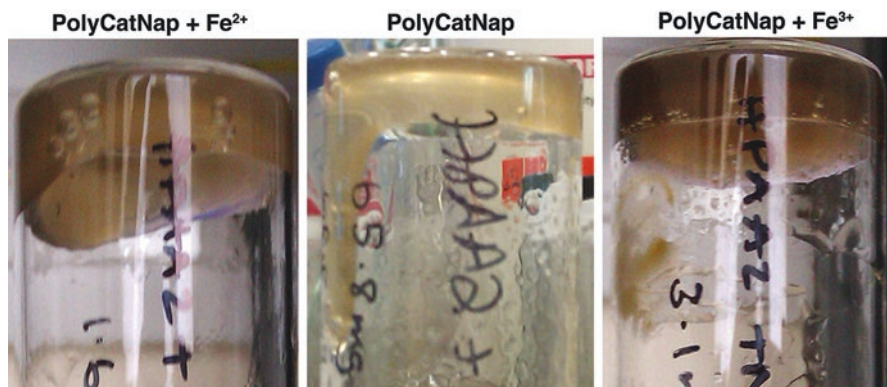


Fig. 3.3 (a) *PolyCatNap* with the addition of 1 mM FeSO_4 (Fe^{2+}), (b) *PolyCatNap* immediately after preparation and (c) *PolyCatNap* with the addition of 1 mM $\text{Fe}_2(\text{SO}_4)_3$ (Fe^{3+})

over the duration of the experiment [17]. Additionally, there was no observed change in the Fourier-transform infrared (FTIR) spectrum for the bio-based polymers while the PEG showed an increase in the carboxylic acid peak, which explains the increase in acidity of the PEG solution. Secondly, chelation of iron (Fe^{3+}) by the consolidant material was confirmed by colour change of the strong iron-chelator functionalised polymer chain; additionally, an increase in viscosity of the polymeric material was observed in the presence of Fe^{3+} . This can be seen in Fig. 3.3.

Figure 3.3b shows the liquid polymer directly after preparation, while Fig. 3.3a shows the solution after the addition of Fe^{2+} and Fig. 3.3c after the addition of Fe^{3+} . The initial consistency of the polymer solution resembles thick honey, upon the addition of Fe^{3+} the solution becomes a gel as the metal-ligand interactions begin to form around the Fe^{3+} centre adding another layer of structure to the material and increasing its strength. Interestingly, upon addition of Fe^{2+} the material becomes significantly weaker than even the original polymer before the addition of any metal ions. Although the catechol units have no affinity for the Fe^{2+} , the amine groups on the chitosan backbone do and can ‘mop up’ the available Fe^{2+} . This alters the orientation of the chitosan chains and prevents the guests of the ternary complex unit from coming into direct contact with one another, thus, weakening the material.

Rheological measurements confirm these observations and show that the complex viscosity of the new consolidant is higher than that of PEG and increases further in the presence of Fe^{3+} , confirming its ability to trap iron and structurally stabilise timbers [18]. While iron sulfate is the most common iron salt in the timbers, the response of the consolidant to other iron salts, specifically nitrate, citrate, chloride, oxide and phosphate, was also tested (Fig. 3.4).

The rheological response of iron (II) sulfate (FeSO_4), iron (III) chloride (FeCl_3) and iron (II) citrate (FeCit) were found to be equal to or weaker than the response of the polymer solution alone, Fig. 3.4a, c. On the other hand, *PolyCatNap* in the presence of iron (III) oxide (Fe_2O_3), iron (III) phosphate (FePO_4), iron (III) nitrate (FeNO_3) and iron (III) sulfate ($\text{Fe}_2(\text{SO}_4)_3$), displayed enhanced mechanical properties

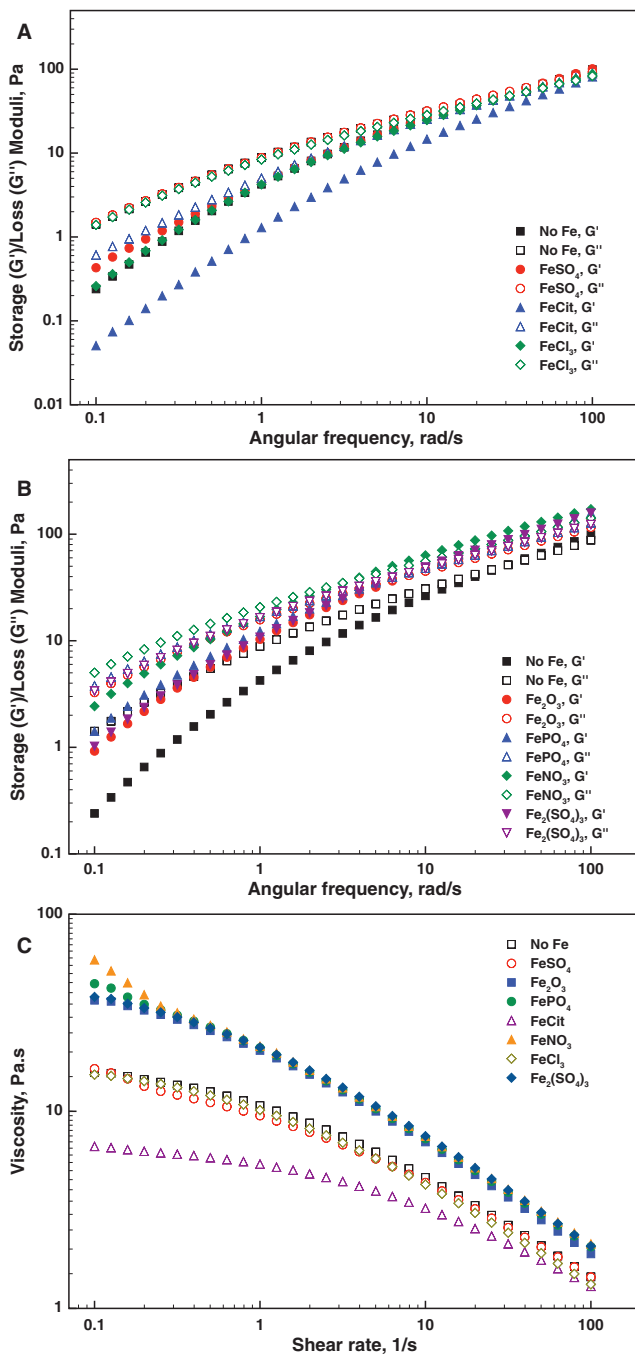


Fig. 3.4 Rheological study of the effect of counter-ions, plots of storage (G') and loss (G'') moduli (Pa) as a function of angular frequency (rad/s) where the addition of Fe produces (a) no significant change and (b) a significant change from the iron-free solution and (c) plot of viscosity (Pa.s) as a function of shear rate (1/s) for all samples

with a viscous liquid to gel transition at lower angular frequencies and a higher viscosity relative to shear rate, than the metal-free solution, Fig. 3.4b, c. This is important as the 3+ oxidation state is that in which the iron can catalyse the production of acid in the timbers. To expand, the material always showed an increase in complex viscosity and the storage and loss moduli of a gel at lower angular frequencies once Fe^{3+} was present. This is extremely promising as there is also the possibility of iron phosphates, oxides and nitrates in the timbers, in addition to sulfates. Disappointingly, the same does not appear true for chlorides, of which there is also a large amount present in the timbers. Further investigation will be required to understand why this appears to be the case. However, in general, the counter-ion does not significantly affect the response of the consolidant, and iron can be chelated as long as it is in the correct oxidation state.

The viscous liquid-to-gel transition evident in the rheological analysis was confirmed by small angle X-ray scattering (SAXS) for the polymer networks containing iron (III) sulfate. The material structure becomes more ordered in the presence of Fe^{3+} , which correlates with the addition of the extra metal-ligand cross-links. [18]. Interestingly, after several days the solutions containing iron in the 2+ oxidation state appeared to resemble the solutions containing Fe^{3+} . Further study of the Fe content of the solutions using X-ray absorption near edge structure (XANES) spectroscopy elucidated that after several days the Fe^{2+} in the solutions had been fully oxidised to Fe^{3+} (Fig. 3.5).

This ability of the polymer to oxidise the iron to the 3+ oxidation state, and subsequently chelate the iron within the polymer network, is particularly useful for the stemming of the iron-catalysed degradation. As such not only the available Fe^{3+} is

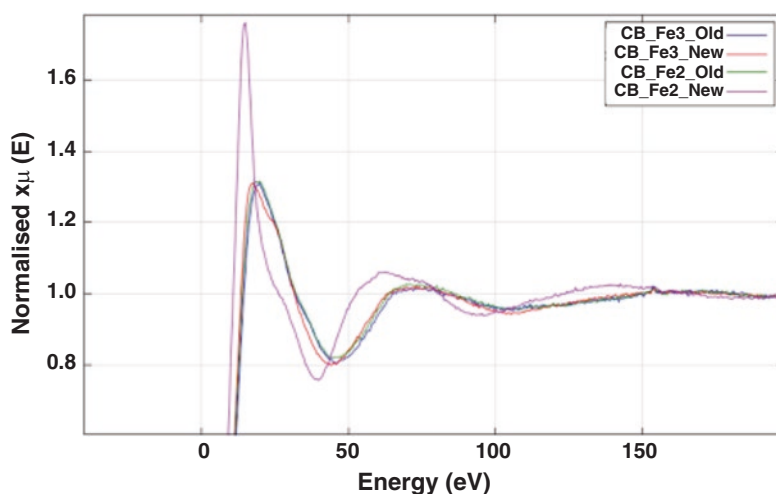


Fig. 3.5 XANES spectra of (pink) freshly prepared *PolyCatNap* containing 1 mM Fe^{2+} , (red) freshly prepared *PolyCatNap* containing 1 mM Fe^{3+} , (green) *PolyCatNap* containing 1 mM Fe^{2+} after several weeks, (blue) *PolyCatNap* containing 1 mM Fe^{3+} after several weeks

taken up into the network but adjacent Fe^{2+} can be converted to Fe^{3+} and chelated before it is naturally oxidised and used to generate acid in the timbers.

These analyses have all shown that the new consolidant can react to the chemical environment of the wood, that is the metal content, and based on this adapt its mechanical properties, which will in turn effect the mechanical stability of the wood. Lastly, bacterial enumeration experiments show that the supramolecular polymer network material can effectively hinder the growth of several strains of bacteria including *Staphylococcus aureus*, *Escherichia coli* and *Pseudomonas aeruginosa*, which is extremely promising for the treatment of bacteria in the ship's timbers [18]. Thus, the new *PolyCatNap* consolidant can be used to treat all three major conservation issues in waterlogged wood simultaneously.

3.3 Treatment of Artefacts

As an example of treatment potential, the supramolecular polymer material was applied to the surface of an arrow found with the *Mary Rose*, with high concentrations of iron salts on the surface, Fig. 3.6.

During the optimisation of the *PolyCatNap* networks, two different naphthyl-containing units (2-naphthoic acid (2-NPA) and 2-naphthylacetic acid (2-NPAA)) were tested to determine if the distance between the naphthol and the chitosan backbone altered the material properties of the final network. The solid content of the polymeric network (4 wt. % or 8 wt. %) was also optimised to determine the concentration that best removes surface iron deposits. The naphthol unit is separated from the chitosan backbone by either one (2-NPA) or two (2-NPAA) methyl units. The 2-NPA is denoted as **1** in Fig. 3.6 and was prepared at a concentration of 4 wt. % total polymer solids in a 1 vol. % solution of acetic acid at pH 6.5. The 2-NPAA is both **2** and **3** in Fig. 3.6, where **2** is a 4 wt. % polymer solution and **3** is an 8 wt. % polymer solution, both prepared in the same acetic acid solution. The supramolecular consolidants were applied to the surface, allowed to dry and the films removed from the surface. In doing so the surface iron deposits would also ideally be removed leaving the wood surface undamaged. This was only possible with **3** (Fig. 3.6b–d), as **1** and **2** were difficult to remove from the surface and left a polymer residue on the artefact.

It can be seen in Fig. 3.6b–d that on the edges of the treatment area there is a small white deposit, this is believed to be the formation of a surface salt but further tests are required to determine its exact composition and cause. These negative effects were not observed with polymer **3**, which was easy to remove from the surface and, as can be clearly seen in Fig. 3.6c, d leaves no white deposit formed on the treated area of the artefact. It is possible that the slightly increased spacing between the functional unit and the backbone allows more efficient cross-linking of the network and as such a more stable material.

Under the area where polymer **3** was removed, it is also evident that the colour of the arrow has changed from orange (indicative of the iron salts) to the brown

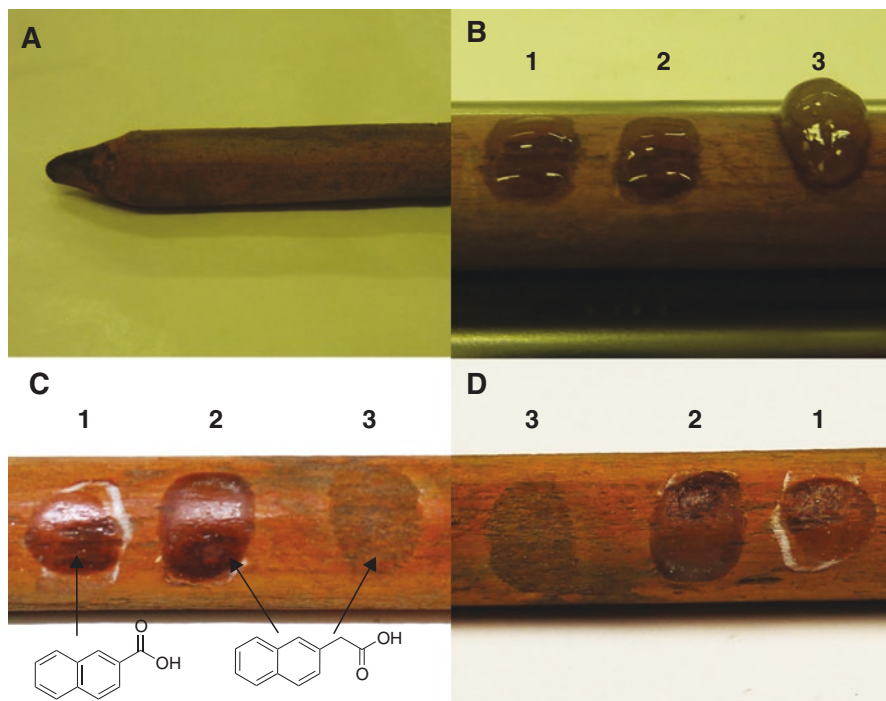


Fig. 3.6 An arrow, found with the *Mary Rose*, with significant surface iron deposits being treated with the supramolecular polymer consolidants; (1) 4 wt. % *PolyCatNap* with 2-NPA (2) 4 wt. % *PolyCatNap* with 2-NPAA, (3) 8 wt. % *PolyCatNap* with 2-NPAA. The images shows the arrow before treatment (a), directly after treatment (b), after 7 days showing also the structures of the 2-NPA (left) and 2-NPAA (right) units used in the optimisation study (c) and after 28 days (d)

colour of the original wood. The polymer likely encapsulated the surface salts in the matrix and allowed facile removal of the salts from the surface without damage to the surface of the artefact. However, such a thick polymer gel could not be used to penetrate the wood and chelate the iron content within the timbers. As such, future experiments will involve studying the diffusion of the material at lower solid content through an archaeological timber sample to determine the feasibility of using *PolyCatNap* as an internal treatment alternative to PEG spraying.

3.4 Impact for the Museum Community

While the synthesis and isolation of the cross-linking unit in this supramolecular system, the molecule cucurbit[8]uril, is patented the molecule is commercially available and the preparation of the consolidant network is detailed in Walsh et al. [18]. Free, open access to research across the museum community is essential for the optimisation of this material. It is quite clear from preliminary studies that this

material works very well for artefacts such as those found with the *Mary Rose*, their degree of degradation and the biological and iron content is suitably counter-acted by this material. However, this is only one artefact and open access to this material across the museum community will help us understand how widely applicable this material can be. This will allow us to determine if these materials really have the potential to outperform PEG treatments as the standard treatment in the first stages of conservation.

3.5 Areas for Further Development

While a large number of artefacts are affected by iron-catalysed degradation processes, without exception all large waterlogged wooden objects are subject to mechanical instability during drying. One of the key issues with preventing mechanical instability in treated objects is the weight of the consolidant used [21]. With this in mind several recent papers have focussed on maximising the mechanical stability by minimising the weight of the consolidant. Again, bio-based polymers show great promise in mitigating the issue of consolidant weight, despite the fact that the individual polymer chains are generally longer than the oligomeric PEG consolidants. The reason for this is their tendency to form networks within the wood, resembling woods' own structure, which lends support to the damaged wood without adding extensive weight [16, 18, 20]. An image of such bio-based polymer networks, specifically chitosan and alginate, within the treated wood is shown in Fig. 3.7.

Our current work is focussed on expanding the range of adaptable consolidants to react to mechanical changes in the wood in addition to the chemical changes induced by the presence of iron. It is well described in the literature that the distribution of load in waterlogged wooden artefacts rarely remains static over time. [21]. Thus, materials must not only react to chemical changes within the wood but also changes in load distribution. Ideally, the mechanical properties of these materials should

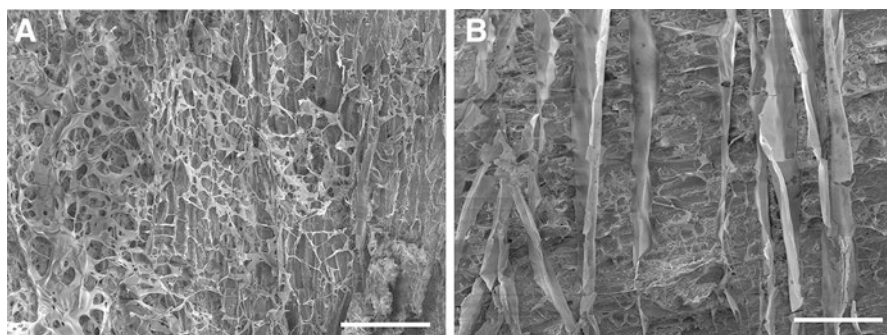


Fig. 3.7 Scanning electron micrographs of archaeological wood treated with (a) a 0.5 wt. % chitosan solution and (b) a 0.5 wt. % solution of sodium alginate

increase as the compressive load on the wood increases. We are particularly interested in the development of new structurally superior consolidant materials based on chitosan and alginate. These mixed, bio-based materials combine the naturally antibacterial properties of chitosan and the excellent mechanical properties of alginates. In preliminary work, networks based on varying concentrations of these two bio-based polymers showed enhanced mechanical stability in their base form, greater than the initial mechanical properties of *PolyCatNap*. Additionally, they show excellent mechanical adaptability to a number of metal ions and combinations of metal ions in solution, an important property as there is unlikely to be just one metal ion within a specific artefact, particularly when Na, Ca and K are so abundant in Nature. Current research is focussing on how to introduce these materials into the wood without effecting the excellent materials properties of the network.

Furthermore, the chemistry of developing such adaptable consolidants is not the only obstacle to their realisation. The analytical instrumentation used to determine the presence of the consolidant in the wood during the treatment process is another significant limitation. Lignin, cellulose and PEG have such distinctly different chemical signals that any number of analytical techniques can differentiate them from one another, allowing the conservator to localise the presence of PEG within the wood. Using bio-based, and specifically polysaccharide-based, consolidants present significant obstacles to the detection of the material within the wood. In particular, the major issue is the difficulty in making a real-time assessment of consolidation progress *in situ* without the need for destructive sampling. Thus, we are not only focussed on understanding the structural behaviour of polymer networks under stress but also on incorporating bio-based optical tags within these materials. Such hybrid, functional materials will function as a green, sustainable sensor that reacts to mechanical changes in the wood with a clear optical signal. As such, the wood under conservation can be monitored *in situ* and catastrophic failure due to excess load can be prevented in good time.

3.6 Conclusion

It is clear that there are many advantages to the replacement of PEG with materials such as *PolyCatNap* and other bio-based (e.g. chitosan/alginate-based) materials. The major advantage of these adaptable networks is their ability to react to and counter-act conservation issues as they present themselves, specifically iron catalysed degradation, biological activity and mechanical instability. Additionally, being primarily sourced from bio-based materials, they are cost-effective, do not form acidic degradation products, can remove surface iron deposits quickly and without damage to the artefact and appear to show diffusion capabilities within the wood. The advent of a new generation of renewable, reversible, greener, more compatible conservation treatments for the preservation of wooden artefacts of historical importance is a significant gain for the museum community and further research on this topic will be of great importance in years to come.

Acknowledgements The research leading to these results has received funding from the People Programme (Marie Curie Actions) of the European Union's 7th Framework Programme (FP7/2007-2013) under REA grant agreement n. PCOFUND-GA-2013-609102, through the PRESTIGE programme coordinated by Campus France, awarded to ZWK (PRESTIGE-2016-2-0008). ZWK acknowledges the help of Drs J.T. Hodgkinson, M. Welch, J. Sedlmair, A. Koutsoubas, and Profs. D.R. Spring, C.J. Hirschmugl, C. Toprakcioglu, A. Dent and J.R. Nitschke in the characterisation and development of these materials. ZWK and OAS acknowledge financial support from the *Mary Rose* Trust, the Engineering and Physical Sciences Research Council (EPSRC) UK and the European Research Council (ERC) (Starting Investigator Award No. 240619, ASPIRe). OAS also acknowledges the Walters-Kundert Charitable Trust for a Next Generation Fellowship. ERJ thanks the EPSRC for a doctoral training grant.

References

1. Bjordal, C.G., T. Nilsson, G. Daniel. 1999. Microbial decay of waterlogged archaeological wood found in Sweden applicable to archaeology and conservation. *Int. Biodeterior. Biodegrad.* 43, 63–73.
2. Sandstrom, M., F. Jalilehvand, I. Persson, U. Gelius, P. Frank, I. Hall-Roth, I. 2002. Deterioration of the seventeenth-century warship *Vasa* by internal formation of sulphuric acid. *Nature* 415, 893–897.
3. Fors, Y. and M. Sandstrom. 2006. Sulfur and iron in shipwrecks cause conservation concerns. *Chem. Soc. Rev.* 35, 399–415.
4. Almkvist, G. and I. Persson. 2008. Fenton-induced degradation of polyethylene glycol and oak holocellulose. A model experiment in comparison to changes observed in conserved waterlogged wood. *Holzforschung* 62, 704–708.
5. Almkvist, G. and I. Persson. 2008. Analysis of acids and degradation products related to iron and sulfur in the Swedish warship *Vasa*. *Holzforschung*, 62, 694–703.
6. May, E. and M. Jones. 2008. Molecular Bacterial Diversity in the Timbers of the Tudor Warship the *Mary Rose*. 204–218 In: eds May, E. and M. Jones. *Heritage Microbiology and Science: Microbes, Monuments and Maritime Materials*. Cambridge: Royal Society of Chemistry.
7. Bjurhager, I., H. Halonen, E.L. Lindfors, T. Iversen, G. Almkvist, E.K. Gamstedt and L.A. Berglund. 2012. State of degradation in archaeological oak from the 17th century *Vasa* ship: Substantial strength loss correlates with reduction in holo(cellulose) molecular weight. *Biomacromol.* 13, 2521–2527
8. Braovac, S. and H. Kutzke. 2012. The presence of sulfuric acid in alum-conserved wood – Origin and consequences. *J. Cult. Herit.* 13, S203–S208.
9. Gray, F. M. 1997. *Polymer Electrolytes*. RSC Materials Monographs. Cambridge: Royal Society of Chemistry.
10. Almkvist, G and I. Persson, I. 2008c. Degradation of polyethylene glycol and hemicellulose in the *Vasa*. *Holzforschung* 62, 64–70.
11. Mortensen, M.N., H. Egsgaard, S. Hvilsted, Y. Shashoua, and J. Glastrup. 2007. Characterisation of the polyethylene glycol impregnation of the Swedish warship *Vasa* and one of the Danish *Skuldev* Viking ships. *J. Archaeol. Sci.* 34, 1211–1218.
12. Berko, A., A.D. Smith, A M. Jones, E.J. Schofield, J.F.W. Mosselmanns and A.V. Chadwick. 2009. XAS studies of the effectiveness of iron chelating treatments of *Mary Rose* timbers. *J. Phys. Conf. Ser.* 190, 012147.
13. Bardet, M., G. Gerbaud, Q.-K. Trân, and S. Hediger. 2007. Study of interaction between polyethylene glycol and archaeological wood components by C-13 high-resolution solid-state CP-MAS NMR. *J. Archaeol. Sci.* 34, 1670–1676.

14. Bardet, M., G. Gerbaud, C. Doan, M. Giffard, S. Hediger, G. De Paepe, and Q.-K. Tr an. 2012. Dynamics property recovery of archaeological-wood fibers treated with polyethylene glycol demonstrated by high-resolution solid-state NMR. *Cellulose* 19, 1537–1545.
15. Cipriani, G., A. Salvini, P. Baglioni, and E. Bucciarelli. 2010. Cellulose as a renewable resource for the synthesis of wood consolidants. *J. Appl. Polym. Sci.* 118, 2939–2950.
16. Christensen, M., H. Kutzke and F.K. Hansen. 2012. New materials used for the consolidation of archaeological wood – past attempts, present struggles, and future requirements. *J. Cult. Herit.* 13, S183–S190.
17. Walsh, Z., E.R. Jane ek, M. Jones and O.A. Scherman. 2017. Natural polymers as alternative consolidants for the preservation of waterlogged archaeological wood. *Stud. Conservat.* 62, 173–183.
18. Walsh, Z., E.R. Jane ek, J.T. Hodgkinson, J. Sedlmair, A. Koutsoubas, D.R. Spring, M. Welch, C.J. Hirschmugl, C. Toprakcioglu, M. Jones, J.R. Nitschke, and O.A. Scherman. 2014. Supramolecular polymer networks as next generation consolidants for archaeological wood conservation. *Proc. Nat. Acad. Sci. USA* 111, 17743–17748.
19. Raafat, D., K.von Barga, A. Haas, and H.-G. Sahl. 2008. Insights into the mode of action of chitosan as an antibacterial compound. *Appl. Environ. Microbiol.* 74, 3764–3773.
20. Christensen, M., E. Larn y, H. Kutzke and F.K. Hansen. 2015. Treatment of waterlogged archaeological wood using chitosan- and modified chitosan solutions. Part 1: Chemical compatibility and microstructure. *J. Am. Inst. Conservat.* 54, 3–13.
21. Lechner, T., I. Bjurhager, R.I. Klinger. 2013. Strategy for developing a future support system for the *Vasa* warship and evaluating its mechanical properties. *Herit. Sci.*, 1, 35–45

Chapter 4

Analytical Examination and Conservation of East Asian Lacquer Works from European Collections



Václav Pitthard, Silvia Miklin-Kniefacz, Sabine Stanek, and Martina Griesser

Abstract The study summarises results of a comprehensive research regarding scientific examination of coatings and foundations of selected exceptional pieces of East Asian lacquer works from the sixteenth to the nineteenth century, which helped to prepare and subsequently conduct the relevant conservation treatment. Particularly, a Japanese Namban cabinet from the collections of the Kunsthistorisches Museum Vienna (KHM, Kunstammer), two Japanese lacquer cabinets and two Japanese lacquer chests from the Imperial Furniture Collection, Vienna, two lacquer cabinets from the Liechtenstein City Palace, Vienna, three lacquer boxes, a table and a cabinet from a private collection, Austria, and a series of lacquer panels from the Chinese Pavilion at Drottningholm Palace, Stockholm, Sweden, were examined in past years. These comprehensive investigations by means of optical and SEM microscopy and (Py)-GC/MS techniques helped to identify both the stratigraphical layout and the detailed composition of the studied coatings, and revealed that the objects of East Asian origin were often restored and covered using European materials as well as pieces of East Asian artefacts were incorporated in European furniture pieces.

Keywords East Asian lacquers · European varnishes · Optical and SEM microscopy · Pyrolysis-gas chromatography/mass spectrometry (Py-GC/MS)

V. Pitthard (✉) · S. Stanek · M. Griesser
Conservation Science Department, Kunsthistorisches Museum, Vienna, Austria
e-mail: vaclav.pitthard@khm.at; sabine.stanek@khm.at; martina.griesser@khm.at;
<http://www.khm.at>

S. Miklin-Kniefacz
Atelier for conservation and restoration (metals, brush), Vienna, Austria; <http://www.urushi.at>

4.1 Introduction

The interest in collecting East Asian artefacts has been fashionable among European aristocratic houses from the sixteenth century since the Portuguese and later the Dutch and the English obtained a monopoly for trading with China and Japan, where lacquer has been used for thousands of years as a durable and beautiful coating material. As European imitations and replicas were produced later, it has always been fundamental for assigning the provenance of these objects to accurately define not only the coating technique, but also the composition of the surface varnishes and lacquers as well. Examinations of the lacquer objects revealed that besides of East Asian lacquers varieties of other materials were used to obtain a durable lacquer layer. Diverse drying oils, proteinaceous or polysaccharide based materials applied as organic binding media – together with various substrates and pigments – occurred when studying the grounds, lacquer layers or upper coatings. Combining optical microscopy and GC/MS appeared to be a suitable analytical approach to detect and identify such complex organic mixtures [8]. East Asian lacquer originates from the sap of lac trees growing in different regions of East Asia and is tapped from the tree just like maple syrup. Initially the juice is hazy, but becomes dark brown and translucent after polymerisation. When applied to objects by brush, it takes a damp atmosphere to harden [17]. The species of lacquer tree and the local environment strongly affect the components of the lacquer. According to the tree origin there are three types of lacquers – trees *Toxicodendron vernicifluum* originating in Japan, China and Korea, *Rhus succedanea* from Vietnam and Taiwan and *Melanorrhoea usitata* from Thailand and Burma. They all contain a latex material composed of phenol derivatives, water, plant gum and laccase enzyme. The enzyme reacts as catalyst of the actual lacquer polymerisation. Because lacquer films are insoluble in most common solvents, only a few analytical techniques including pyrolysis are appropriate for their analysis. Pyrolysis-GC-MS is effective because it can discriminate between pyrolysis products of lacquers. The phenol derivative of *Toxicodendron vernicifluum* is urushiol, that of *Rhus succedanea* laccol and the one of *Melanorrhoea usitata* is thitsiol. These monomers are considered as the most characteristic markers to distinguish between different lacquers [1, 5, 6, 12, 13].

4.2 Experimental

After a primary on site examination a set of samples was taken for the subsequent investigations of the artefacts studied (see Table 4.1 for details). Samples were initially examined by optical microscopy (OM) with a stereomicroscope Stemi 2000-C, Zeiss, Germany, and subsequently, a set of samples prepared as cross-sections: small particles were embedded in epoxy resin and polished after curing. These sections were used for microscopic investigations and histochemical staining [3, 14] to identify and map the presence of binders in the multi-layered structure. The microscopic

Table 4.1 Index of objects, analytical techniques applied and summary of results

Collection	Object description	Analytical methods	Results/composition
Kunstammer, Kunsthistorisches Museum, Vienna, Austria	Sixteenth century Namban lacquer cabinet decorated with mother-of-pearl inlays (KK_5421)	Cross-section, microchemical tests, GC/MS, THM-Py-GC/MS	Lacquer layer: urushiol and thitsiol with perilla oil, carbon interlayer; starch based ground with earth pigments
Imperial Furniture Collection, Vienna, Austria	Seventeenth century Japanese <i>makie</i> cabinet, Kyoto (?) (MD 035838), one of a pair	Cross-section, microchemical tests, GC/MS, THM-Py-GC/MS	Resinous varnish based on sandarac and shellac. Lacquer layer: urushiol and linseed oil
	Seventeenth century Japanese <i>makie</i> chests, Kyoto (?), pair MD 037696 and MD 037697	Cross-section, microchemical tests, GC/MS, THM-Py-GC/MS	No varnish Lacquer layer with urushiol and drying oil Ground layer with urushiol, drying oil and animal glue
Liechtenstein City Palace, Vienna, Austria	Namban chest, Japan, 1630–50 (MO 17)	Cross-section, SEM, GC/MS	Varnish: linseed oil with traces of pine resin
	Japanese <i>makie</i> cabinet, 1660–1690, Kyoto (?), one of a pair (MO 1839)	Cross-section, SEM, GC/MS	Varnish: stand oil, sandarac, shellac and Burgundy pitch
Private collection, Austria	Japanese Namban lacquer box, around 1600 (K 164)	Cross-section, microchemical tests, GC/MS	Varnish based on linseed oil, amber, Venice turpentine and pine resin Ground: drying oil, no urushiol or other ingredients
	Nineteenth century Chinese lacquer tea box, Canton (9952)	Cross-section, microchemical tests, GC/MS	Pig blood based ground
	Eighteenth century Chinese jewellery box (M 122)	Cross-section, microchemical tests, GC/MS	Upper coating: with cedrol (no urushiol) Ground: pig blood based
	Corner cabinet from Jacques Dubois, Paris 1760, with Seventeenth century Japanese panel (M 73/1), one of a pair nineteenth century table, one of a pair European Japanning (M 198/1)	Cross-section, microchemical tests, GC/MS Cross-section, microchemical tests, GC/MS	Upper coating based on drying oil, shellac, sandarac and pine resin, Ground with animal glue and probably some Asian lacquer Lacquer layer: linseed oil, pine resin and shellac

(continued)

Table 4.1 (continued)

Collection	Object description	Analytical methods	Results/composition
Chinese Pavilion, Drottningholm Palace, Stockholm, Sweden	Chinese lacquer panel, eighteenth century Panel 10.5, type A (decorated with landscapes)	Cross-section, microchemical tests, GC/MS, THM-Py-GC/MS	Varnish: shellac, linseed oil and pine resin Lacquer layer: laccol, drying oil and cedar oil Ground: based on pig blood
	Chinese lacquer panel, eighteenth century Panel 4.2, type B (decorated with flowers and butterflies)	Cross-section, microchemical tests, SEM, GC/MS	Varnish: shellac, linseed oil and pine resin, Pigments: realgar (As ₂ S ₂), mica and a blue pigment
	Part of a Chinese screen, eighteenth century Panel 1, type C (decorated with palace scenes)	Cross-section, microchemical tests, SEM, GC/MS	Varnish: shellac, linseed oil and pine resin Lacquer layer: laccol, drying oil and cedar oil Ground: based on pig blood Pigments: cinnabar, red iron oxide

studies were carried out under incident light either using polarised light or in the dark field mode, but also using UV-fluorescence. Where necessary the microscopic investigations were complemented by scanning electron microscopy (SEM) studies to identify the inorganic components of the ground layers and decorative elements. A FEI Quanta 200 F electron microscope equipped with an EDAX X-ray detection system was applied. Another set of samples was directly used for gas chromatography/mass spectrometry (GC/MS) to detect lipids and resins as well as proteinaceous binding media. Pyrolysis (THM-Py-GC/MS) was applied to identify the different East Asian lacquers. The presence of oil, resin, proteins, and polysaccharides was proved by special wet-microchemical tests for samples, which were not analysed by optical microscopy (OM). To detect the presence of starch and blood as a binder in the ground layers spot tests were used for material characterisation.

The latter analysis is based on an enzymatic reaction of peroxidase: addition of H₂O₂ causes haemoglobin to decompose into water and oxygen. The latter oxidises benzidine, which becomes visible by a change of colour to a blueish-green shade [9]. The GC/MS analytical procedure for the analysis of lipids is based on the transesterification of fatty acids and the determination of their relative ratios to identify particular lipids, the analytical procedure for the analysis of resinous binding media is based on the esterification of resinous acids followed by the identification of particular resins according to their resinous acid methyl esters and the analytical procedure for the analysis of proteinaceous materials is based on an acidic hydrolysis of proteins to liberate amino acids, followed by the derivatisation and quantitative determination of amino acids as their silyl derivatives [11]. The procedure for thermal assisted hydrolysis and methylation pyrolysis (THM-Py-GC/MS) with

TMAH analysis was performed on two different systems using either a Curie-point pyromat located in our department or a double-shot pyrolyzer employed in the frame of our collaboration with the Academy of Fine Arts Vienna. Experimental details on the analytical instruments used and the most important measurement parameters are given in Table 4.2. The analyses of western lacquers based on resinous or oleo-resinous varnishes were performed by means of gas chromatography-mass spectrometry technique (GC/MS) while the pyrolysis (Py-GC/MS) enabled to differentiate aged Asian lacquers according to their various chemical compositions, and so to trace the trade and production of the lacquers.

Table 4.2 Experimental parameters of analyses

Method	Instrumentations	Parameters/conditions
Optical microscopy (OM)	Zeiss Axioplan 2 microscope fitted with a Sony Power HAD video system	Incident light, 100 W halogen lamp and 100 W high pressure mercury lamp for UV light (UV filter 365 nm) and blue light (filter 450–490 nm) use
Scanning electron microscopy with energy dispersive X-ray detection (SEM-EDX)	FEI Quanta 200 F with EDAX X-ray detection system	High vacuum, acceleration voltage 20 kV
Gas chromatography-mass spectrometry (GC-MS)	6890 N gas chromatograph connected to a quadrupole mass spectrometer, model 5973 N (both Agilent Technologies, USA)	Transesterification with a 0.2 M methanolic solution of Meth-Prep II (20 μ L), DB-5 MS [poly (5% phenyl-95% methylsiloxane), J&W, USA] capillary column (0.25 mm \times 0.25 μ m \times 30 m), the temperature program from 50 $^{\circ}$ C (1 min) to 320 $^{\circ}$ C (12 min) at 10 $^{\circ}$ C.min $^{-1}$ for lipids and resins. Hydrolysis with 6 M hydrochloric acid (HCl, 100 μ L) at 105 $^{\circ}$ C for 24 h, followed by silylation with a pyridine – pyridine hydrochloride mixture (15 μ L) and a silylation reagent (MTBSTFA, 30 μ L) at 60 $^{\circ}$ C for 1 h. Temperature program (80 $^{\circ}$ C (1 min) to 280 $^{\circ}$ C (1 min) at 6 $^{\circ}$ C.min $^{-1}$) for proteins
Thermal assisted hydrolysis and methylation pyrolysis (THM-Py-GC/MS)	Curie-point pyromat, (GSG, Germany) attached to a gas chromatograph and mass spectrometer GC/MS (Agilent, USA)	1 μ L of 25% aqueous TMAH (Fluka, Germany). Pyrolysis was performed at 764 $^{\circ}$ C for 20 s. DB-5 MS [poly (5% phenyl-95% methylsiloxane), J&W, USA] capillary column (0.25 mm \times 0.25 μ m \times 30 m), the temperature program from 50 $^{\circ}$ C (1 min) to 320 $^{\circ}$ C (12 min) at 10 $^{\circ}$ C.min $^{-1}$
Thermal assisted hydrolysis and methylation pyrolysis (THM-Py-GC/MS)	Double-shot pyrolyzer PY-2020iD (Frontier Lab, Japan) attached to a gas chromatograph and mass spectrometer GC/MS-QP2010 Plus (Shimadzu, Japan)	3 μ L of 25% aqueous TMAH (Aldrich, USA). Pyrolysis was performed at 500 $^{\circ}$ C. Ultra alloy [5% diphenyl-95% dimethyl siloxane, Shimadzu, Japan] capillary column (0.25 mm \times 0.25 μ m \times 30 m), temperature program (40 $^{\circ}$ C (1 min) to 280 $^{\circ}$ C (20 min) at 10 $^{\circ}$ C.min $^{-1}$)

4.3 Results and Discussion

During the preparation of the conservation concepts, the Conservation Science Department of the Kunsthistorisches Museum has often been involved to assist conservators in better understanding the composition of the materials and the applied coating techniques. In the frame of this close collaboration, a Japanese Namban cabinet of the Kunsthistorisches Museum Vienna (KHM, *Kunstammer Wien*), two Japanese lacquer cabinets and two Japanese lacquer chests from the Imperial Furniture Collection, Vienna, two lacquer cabinets from the Liechtenstein City Palace, Vienna, three lacquer boxes, a table and a cabinet from a private collection, Austria, and a series of Chinese lacquer panels from the Chinese Pavilion at Drottningholm Palace, Stockholm, Sweden, were studied. An overview of the results on the compositions of the individual artefacts is given in Table 4.1. According to the provenance, this set of objects can be divided into three groups: Chinese, Japanese, and European origin, respectively. For this paper, one object of each group was selected for a closer discussion in the following.

4.3.1 Chinese Lacquer Object: Example 1

A set of East Asian lacquer objects and furniture pieces belonging to a remarkable private collection in Austria could be sampled during different studies. The investigations served to identify the materials and to plan the conservation measures. The Tea box (9952) is a typical Canton lacquer object from the nineteenth century (1820–1850, Qing dynasty). The box with lid contains another box made of tin, in which the tea was stored. The black lacquer surface of the outer wooden box is decorated with very fine gold and silver paintings (*miaojin*), depicting scenes with persons drinking, tasting and trading tea; some details are executed with red lacquer. The foundation layer taken from the edge of the top side of the Chinese lacquer tea box (Fig. 4.1a–b.) was analysed by both microchemical test and GC/MS. The sample was firstly treated with hydrogen peroxide and benzidine, the positive presence of blood was indicated by a blue coloration appearance. The comparison of chromatographic profiles of amino acids obtained by hydrolysis of a blood reference standard and the sample (Fig. 4.2.) proved that the ground contains blood – according to the literature and traditional recipes, pig blood was commonly used by Chinese lacquer artists [7].



Fig. 4.1 Chinese lacquer tea box, 1820–1850, Canton (private collection), (a); sampling spot on the back edge of the lid (sample E10/1), (b). (Photo © S. Miklin-Kniefacz)

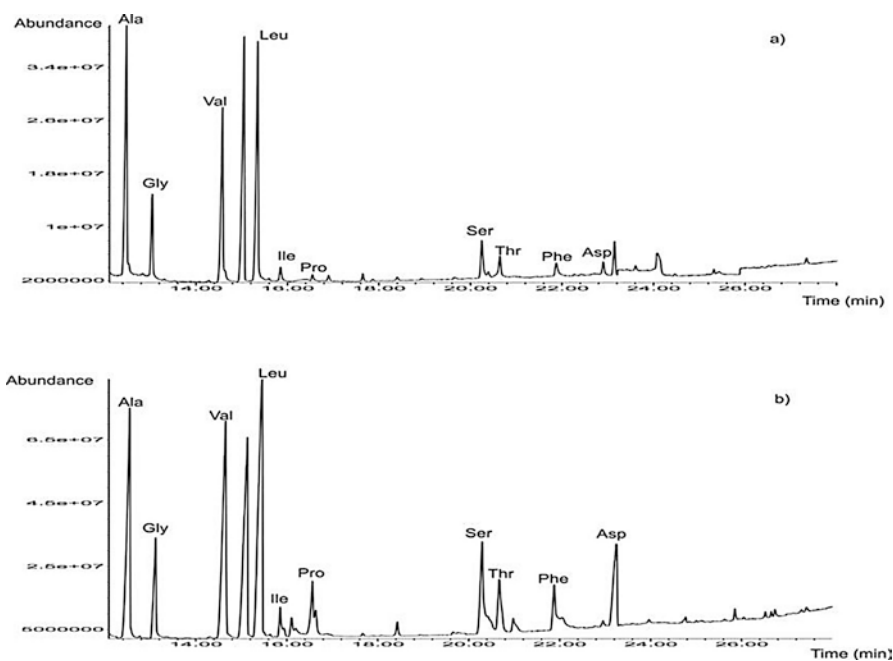


Fig. 4.2 Total ion chromatograms of the ground layer (a) and a pig blood reference standard (b). Note: amino acids from pig blood (*Ala* alanine, *Gly* glycine, *Val* valine, *Leu* leucine, *Ile* isoleucine, *Pro* proline, *Ser* serine, *Thr* threonine, *Phe* phenylalanine, *Asp* aspartic acid). (Photo © Kunsthistorisches Museum Vienna)

4.3.2 Japanese Lacquer Object: Example 2

The Japanese Namban cabinet KK_5421 (Fig. 4.3a) at the Kunsthistorisches Museum Vienna, dated 1580–1607/11, was originally part of the Kunstkammer collection of Ambras Castle, Innsbruck, Tyrol, although it is not mentioned in the 1596 inventory of the heritage of Archduke Ferdinand II of Tyrol, as suggested in most descriptions [4]. However, it could also be one of the cabinets listed in the inventory of the Kunstkammer in Prague of Emperor Rudolf II from 1607/11, which probably was transferred from Prague to Ambras via the Viennese Schatzkammer during the baroque period. The cabinet is a typical Namban lacquer work with flat gold and silver *makie* and mother-of-pearl inlay on a black-lacquered ground with designs of plants, flowers and animals and gilded copper fittings. Its wooden base is probably a Japanese cypress (dimensions: H: 31 × W: 42.5 × D: 29 cm). Its conservation for the re-opening of the new galleries of the Kunstkammer collections in the Kunsthistorisches Museum included cleaning and consolidation with *mugi-urushi*, improvement of the old fillings and retouching of the split on the backside with both Japanese and western materials, and aesthetic integration of the big lacquer losses.

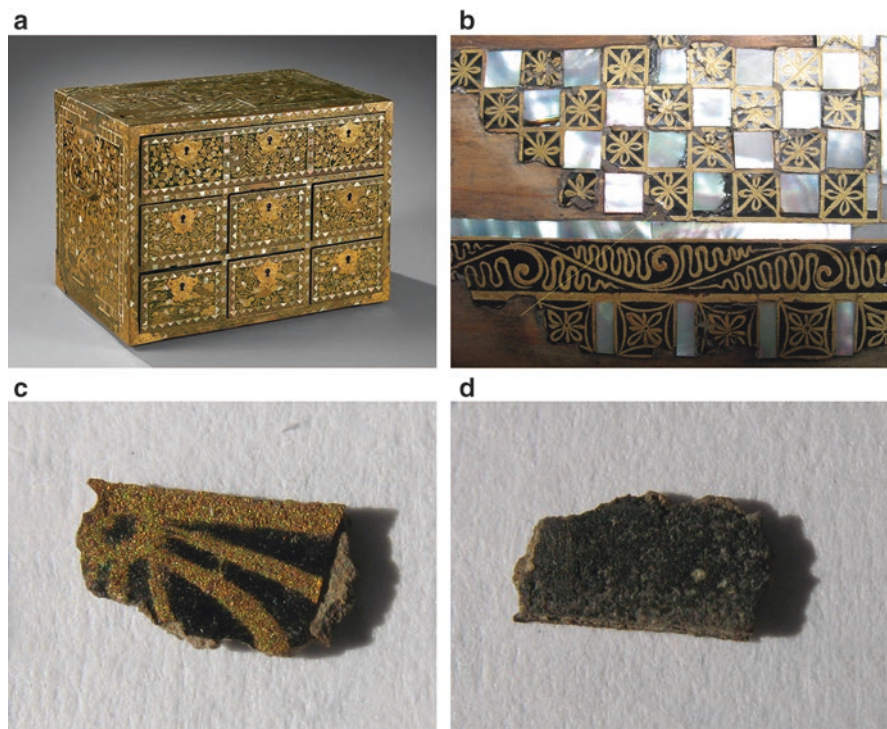


Fig. 4.3 Namban lacquer cabinet (KK_5421), Kunstkammer Vienna (a); a detail of the topside of the cabinet (sampling spot of sample P2) (b); sample P2 (see cross section, Fig. 4.5) (c); reverse side of sample P2 (d). (Photo © Kunsthistorisches Museum Vienna, © S. Miklin-Kniefacz)

In parallel to the conservation the analyses of two samples were performed to get new information about the stratigraphy and the composition of the layers as far as possible, namely the composition of the lacquer itself as well as the binder of the ground (Fig. 4.3b–d.).

The urushi lacquer tapped from the *Toxicodendron vernicifluum* trees was detected by THM-pyrolysis-GC/MS technique according to the characteristic markers pentadecylcatechol and pentadecenylcatechol and the oxidation product methyl 8-(2,3-dimethoxyphenyl) octanoate (Mazzeic acid) (see Fig. 4.4.); while traces of thitsi lacquer collected from the *Melanorrhoea usitata* trees were detected by the presence of the marker compounds 3-(10-phenyldecyl) catechol and 3-(12-phenyldodecyl) catechol [2, 10, 12, 13]. Besides the two Anacard lacquers drying oil, probably perilla oil, was identified. The very thin black layers situated between the lacquer layers, underneath the ground and beneath the mother-of-pearl could not be identified so far.

Microscopic examination of the cross-section (Fig. 4.5a–c.) showed the presence of a coarse ground layer with a thin black layer insulating the first lacquer layer. The observation of the cross-section under UV-light helped to distinguish the two overlying lacquer layers, which appeared as a single dark structure in visible light. The following red layer with dark red and bright red particles is finished with a thin gold powder application on top, as described in Table 4.3.

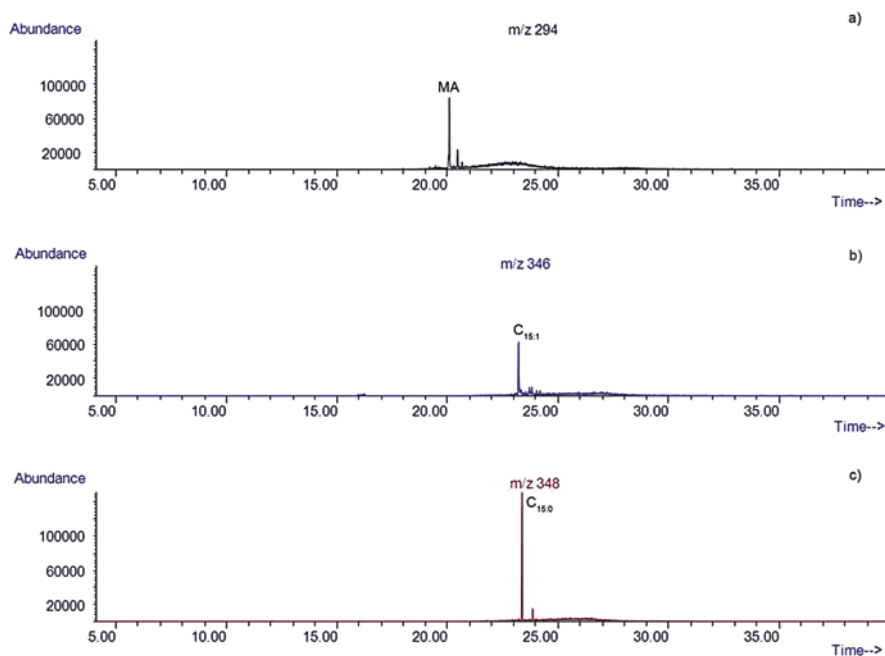


Fig. 4.4 The ion extracted pyrogram at m/z 294, 346, 348 of the sample from the Namban lacquer cabinet (KK_5421) showing the pyrolytic products of urushiol: m/z 294, Mazzeic acid methyl ester (a); m/z 346, $C_{15.1}$ – catechol methylated (b); m/z 348, $C_{15.0}$ – catechol methylated (c). (Photo © Kunsthistorisches Museum Vienna)

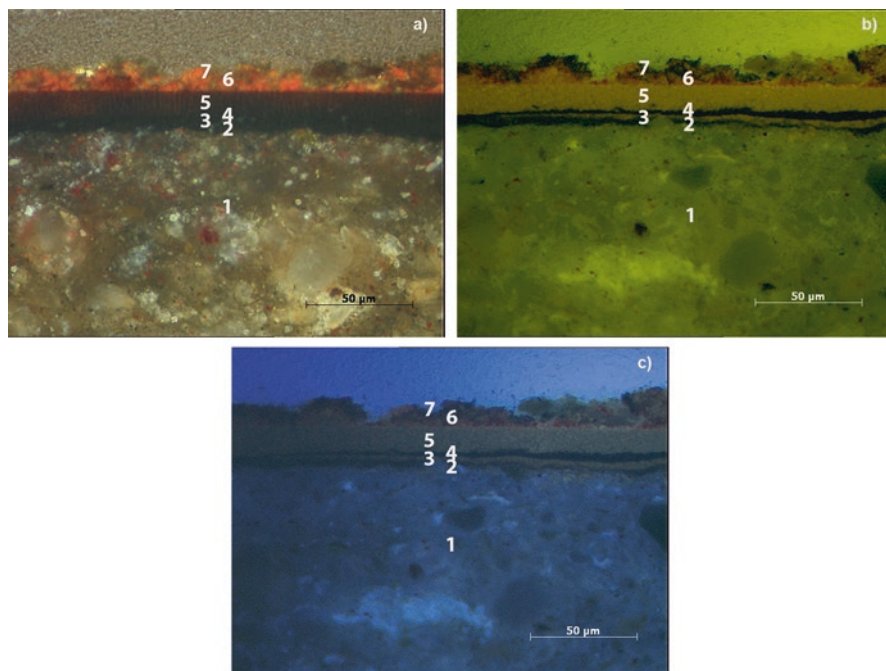


Fig. 4.5 Cross-section of a sample from the Namban lacquer cabinet (KK_5421) showing the stratigraphy of the ground, lacquer layers and golden decoration under Visible Light Illumination, Polarisation, 500 × (a); Blue Light Illumination, 500 × (b); Ultra Violet Illumination, 500 × (c). For description of stratigraphy see Table 4.3. (Photo © Kunsthistorisches Museum Vienna)

Table 4.3 Stratigraphy of Sample from Namban lacquer cabinet (KK_5421) seen in Fig. 4.5a–c

Layer	Name	Description
7	Gold	Layer of gold powder (particles)
6	Red size	Red layer, dark and brighter red particles, inhomogeneous, iron oxide (XRF)
5	Upper lacquer	Thin layer, UV-fluorescence like milk coffee
4	Black outline	Dark thin layer2, carbonic
3	Lower lacquer	Thin layer, UV-fluorescence like milk coffee
2	Black outline	Dark thin layer1, carbonic
1	Ground	Thick tan-grey ground layer with coarse particles (white, yellow, red and black), claylike

4.3.3 *European Furniture with Incorporated Japanese Lacquer Plate: Example 3*

The eighteenth century French cabinet (M73/1) made by Jacques Dubois in Paris around 1760 is another exceptional piece from the same private collection as the above mentioned tea box. A Japanese lacquer panel is inserted in the front door (Fig. 4.6a-c). The corner cabinet is one of a pair and obviously the doors have been



Fig. 4.6 Cabinet by Jacques Dubois with incorporated Japanese panel (M 73/1), private collection, (a) Front door under UV, sample E3/P2, (b); Sampling spot for ground layer E3/P1, (c). (Photo © S. Miklin-Kniefacz)

used before for a Japanese lacquer cabinet with two doors and a big lock plate in the centre (the traces are still visible, now on the side). The door panels are Japanese export lacquer, produced between 1640 and 1690, and have been sliced down to 5 mm, bent and transferred to the new corner cabinet. The decoration is highly elaborated with *takamakie* and *hiramakie* techniques, using different gold and silver powders and small *kirikane* plates, depicting a landscape with huts and trees. The analyses should answer the question of the composition of the ground layer to support suggestions for consolidation materials as well as the composition of the varnish to be able to decide about the surface treatment. GC/MS investigations of the ground layer showed that it is based on animal glue. The European varnish or coating is composed of drying oil, shellac, sandarac resin and pine resin. As shown in Fig. 4.7, oxidation products of dehydroabietic acid indicate the presence of pine resin, while totarol, methyl sandaracopimarate and methyl hydroxy-sandaracopimarate were main markers to detect sandarac. Shellac was detected according to a series of shellac acids [8, 15, 16].

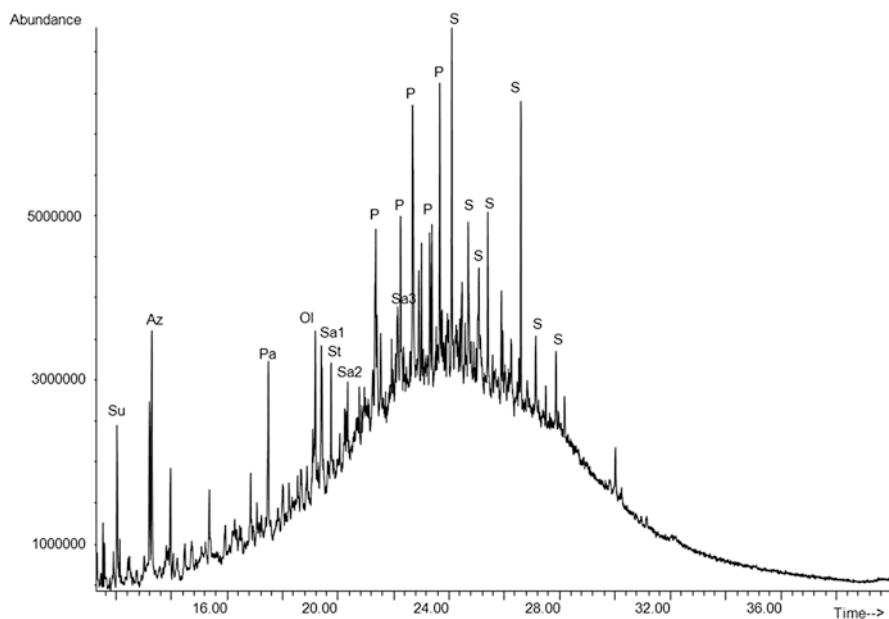


Fig. 4.7 Total ion chromatogram of the coating from the Jacques Dubois cabinet (M 73/1). Note: fatty acids from drying oil (*Su* suberic acid, *Az* azelaic acid, *Pa* palmitic acid, *Ol* oleic acid, *St* stearic acid); *P* pine resin diterpenes; sandarac components (*Sa1* = totarol, *Sa2* = methyl sandaracopimarate, *Sa3* = methyl hydroxy-sandaracopimarate); *S* shellac acids. (Photo © Kunsthistorisches Museum Vienna)

4.4 Conclusion

For conservation issues very often the composition of the ground and the later varnishes are of higher interest than the lacquer itself, because consolidation and surface treatment are the most frequent problems to be solved. The scientific study using gas chromatographic analysis combined with microscopic investigations not only gives reliable results on the composition and layout of materials used on Asian lacquer furniture, but also unveiled a few interesting facts. The ground layers of Chinese pieces often contain blood while the Japanese ones are rather based on animal glue or starch. Furthermore, Asian lacquer artefacts were regularly restored applying European materials as well as parts of Asian artefacts were incorporated in European furniture.

Material List

Benzidine, tetramethylammonium hydroxide (TMAH), pyridine (Fluka Chemie AG, Switzerland)

Hydrogen peroxide (Riedel-deHaën, Germany)

Methanol, N-text-butyldimethylsilyl-N-methyltrifluoroacetamide (MTBSTFA), pyridine, toluene (Sigma-Aldrich, Austria)

Meth-Prep II (m-trifluoromethylphenyl) trimethylammonium hydroxide (TFTMAH, Alltech Associates, Belgium)

Acknowledgements The authors wish to thank all the colleagues of the Kunsthistorisches Museum Vienna and the Academy of Fine Arts Vienna (special thanks to Shuya Wei), the University of Applied Arts, Vienna, the Liechtenstein City Palace, Vienna, the Imperial Furniture Collection, Vienna, and the Drottningholm Palace, Stockholm, involved in this research for their assistance and co-operation. In addition, we want to thank The Getty Conservation Institute and especially Michael Schilling and the RADICAL team for their support. The Austrian Science Fund (FWF, Project No. L187-N11) is gratefully acknowledged for the financial funding.

References

1. Frade J.C., M.I. Ribeiro, J. Graça T. Vasconcelos and J. Rodrigues J. 2010. Chemotaxonomic application of Py-GC/MS: Identification of lacquer trees. *Journal of Analytical and Applied Pyrolysis* 89: 117–121.
2. Heginbotham A. and M. Schilling. 2011. New evidence for the use of Southeast Asian raw materials in seventeenth century Japanese export lacquer. In Rivers, S., Faulkner, R. & Pretzel, B. eds. 2011. *East Asian Lacquer: Material Culture, Science and Conservation*. London: Archetype Publications Ltd. in association with Victoria and Albert Museum. Kopplin, M. 2002. *Lacquerware in Asia, today and yesterday*. UNESCO Publishing: 178.
3. Jütte W. 1989–91. Mikrochemischer Nachweis natürlicher Harze mit Alkannafarbstoffen in Querschleifen von Malschichtproben. Wien. In: Wiener Berichte über Naturwissenschaft in der Kunst (6–8). Vendl Alfred, Pichler Bernhard, Weber Johannes, Erlach Rudolf, Banik Gerhard.

4. Kühnenthal M. 2000. *Japaners and European Lacquerware*, ed. M. Kühnenthal, München: Bayerisches Landesamt für Denkmalpflege.
5. Le Hô A.S. M. Regert, O. Marescot, C. Duhamel, J. Langlois, T. Miyakoshi. C. Genty and M. Sablier. 2012. Molecular Criteria for Discriminating Museum Asian Lacquerware from Different Vegetal Origins by Pyrolysis Gas Chromatography/Mass Spectrometry. *Analytica Chimica Acta* 710: 9–16.
6. Lu R. Y. Kamiya, T. Miyakoshi. 2006. Applied Analysis of Lacquer Films Based on Pyrolysis-Gas Chromatography/Mass Spectrometry. *Talanta* 70: 370–376.
7. Miklin-Kniefacz S. V. Pitthard, W. Parson, C. Berger, S. Stanek, M. Griesser S. Kuckova. 2016. Searching for blood in Chinese lacquerware, *Studies in Conservation* 61: sup3, 45–51.
8. Mills J.S. and R.White. 1994. *The organic chemistry of museum objects*. Oxford: Butterworth-Heinemann.
9. Odegaard N. S. Carroll, W.S. Zimmt. 2005. Material characterization tests for objects of art and archaeology. London: Archetype Publications Ltd.
10. Pitthard V. S. Stanek, M. Griesser, C. Jordan, S. Miklin-Kniefacz. 2016. Technical investigations of an 18th century Chinese imperial carved lacquer screen – valuable contribution to the conservation strategy. *Studies in Conservation* 61: sup3, 97–108.
11. Pitthard V. S. Wei, S. Miklin-Kniefacz, S. Stanek, M. Griesser and M. Schreiner. 2010. Scientific Investigations of Antique Lacquers from a 17th-Century Japanese Ornamental Cabinet. *Archaeometry* 52(6): 1044–1056.
12. Schilling M.R. 2012. Anacard marker compounds. Recent Advances in Characterizing Asian Lacquers (RAdiCAL) workshop, 22–26 October 2012, Getty Conservation Institute, Los Angeles. Personal communication.
13. Schilling M.R. and A. Heginbotham. 2016. Beyond the basics: A systematic approach for comprehensive analysis of organic materials in Asian lacquers, *Studies in Conservation* 61: sup3, 3–27.
14. Schramm H.P. and B. Hering. 1995. Historische Malmaterialien und ihre Identifizierung. Stuttgart: Ferdinand Enke Verlag.
15. Sutherland K. 2010. Bleached Shellac Picture Varnishes: Characterization and Case Studies. *Journal of the Institute of Conservation* 33(2): 129–145.
16. Sutherland K. J.C. Del Rio. 2014. Characterisation and discrimination of various types of lac resin using gas chromatography mass spectrometry techniques with quaternary ammonium reagents. *Journal of Chromatography A*, 1338: 149–163.
17. Webb M. 2007. *Lacquer Technology and Conservation*. Oxford: Butterworth-Heinemann.

Chapter 5

Technology for Technology's Sake: The Technical Study of Gothic Miniature Boxwood Carvings in the Thomson Collection at the Art Gallery of Ontario



Lisa Ellis, Alexandra Suda, Ronald Martin, Elizabeth Moffatt,
Jennifer Poulin, Heidi Sobol, Priam Givord, Craig Boyko, Ian Lefebvre,
and Andrew J. Nelson

Abstract This paper describes the evolution and results of a technical study that focused initially on the Thomson Collection of miniature boxwood carvings at the Art Gallery of Ontario (AGO). This work eventually became the AGO's impetus for its participation in an international exhibit "Small Wonders," organized with the Rijksmuseum and the Metropolitan Museum of Art. The technical work on early sixteenth century miniature boxwood carvings, which includes both prayer beads and miniature altarpieces, started with X-radiography at the Royal Ontario Museum, followed with in-house photography using a cutting edge but now somewhat more common specialized macro set-up, and ultimately micro-computed tomography (CT) scanning, or high-resolution X-ray micro-computed tomography at Sustainable Archaeology, Western University, London Ontario and Advanced 3D Analysis software (ORS) at the AGO. Secondary digital files were used in "Small Wonders: the VR Experience," wherein users could enter into a dramatically magnified virtual prayer bead. Scientific analysis of a selection of the artifacts' coatings, polychromy and adhesives was undertaken by the Canadian Conservation Institute using Fourier

L. Ellis (✉) · A. Suda · C. Boyko · I. Lefebvre
Art Gallery of Ontario, Toronto, ON, Canada
e-mail: lisa.ellis@ago.ca

R. Martin · A. J. Nelson
Departments of Anthropology and Chemistry, The University of Western Ontario,
London, ON, Canada

E. Moffatt · J. Poulin
Canadian Conservation Institute, Ottawa, ON, Canada

H. Sobol
Royal Ontario Museum, Toronto, ON, Canada

P. Givord
Computational Designer, Toronto, ON, Canada

transform infrared spectroscopy (FTIR); scanning electron microscopy-energy dispersive spectrometry (SEM-EDS); thermal desorption-gas chromatography-mass spectrometry (TD-GC-MS); and Raman spectroscopy.

Keywords Technical study · Boxwood · Miniature carving · Prayer beads · Nuts · Micro CT scanning · Advanced 3D analysis software

5.1 Introduction

This paper presents the results of several years of interdisciplinary collaborative research on a corpus of sixteenth century objects of religious devotion (*small wonders*). These objects include prayer beads and miniature altar pieces that are united by the presentation of remarkably intricate scenes microcarved in boxwood. Starting as a focused study on the Thomson collection of Gothic boxwood miniatures at the AGO, the study ultimately made a significant contribution to a major international exhibition, “Small Wonders,” shortlisted in 2017 by Apollo Magazine as an “Exhibition of the Year.” The exhibition generated two print catalogues [1, 2], one of which was recognized by the New York Times as one of “The Best Art Books” of 2017; an online database which won “Outstanding Digital Publication” in 2017 by the Association of Art Museum Curators; and a virtual reality experience which was awarded an Honorable Mention Media and Technology MUSE Award by the American Association of Museums. The AGO also received the Canadian Museums Association’s Conservation Award of Outstanding Achievement in 2017 for its critical role in the development of the “Small Wonders” (Fig. 5.1).

The success of the gothic boxwood miniature research project and its reception owes a great deal to timing, technology and teamwork. Technological developments perfectly meshed with research goals: the size and complexity of the artworks being studied were perfect subjects for the scientific instrumentation and software available. While access to micro-CT instrumentation initially presented some challenges, developments in desktop computation meant that the datasets of the artworks could be manipulated by the principal investigator in the conservation studio in close proximity to the objects [3]. The photographers’ software and related hardware improved to such a degree over the course of the project that the scope of their work was able to expand significantly due to the exponential reduction of the hours necessary for post capture processing. At the same time, the technologies used to study the boxwood miniatures also acted as vehicles that allowed the public to gain access to these beloved carvings in a variety of media, namely the on-line database, featuring high resolution images; two print catalogues featuring these images and outlining technical findings [1, 2]; animations created using micro-CT data and revealing construction techniques; and a virtual reality (VR) experience into which the viewer virtually enters into and deconstructs one of the Thomson Collection prayer beads.

Initiated as a collaborative project at the AGO between curator Alexandra Suda and conservator Lisa Ellis, this research focused on the world’s largest collection of



Fig. 5.1 Small Wonders exhibit at the Art Gallery of Ontario, November 5, 2016–January 22, 2017

early sixteenth century boxwood miniature carvings, found in the Thomson Collection of European Art at the AGO. Both were intrigued by the mysterious construction of these objects, as are the majority of museum visitors who notice the tiny artworks in the many museums where they are presented as *objects of wonder*. As the scope of the initial research project expanded, additional researchers with specialized imaging and analytical skills and corresponding instrumentation joined the team from the Chemistry and Anthropology Departments at the University of Western Ontario; the Royal Ontario Museum; and the Canadian Conservation Institute (CCI).

Contained within the Thomson collection of European Art at the AGO, the objects of interest are ten late Gothic/early Renaissance Northern European prayer beads, two associated miniature altarpieces, and a later, seventeenth century Italian group of even tinier carvings by Ottaviano Jannella (Fig. 5.2). The entire group was investigated with the goal of understanding the intricacies of construction and potentially identifying production workshops and perhaps even individual sculptors of the sixteenth century works. Greatly outnumbering the other types of objects, the prayer beads showed promise in answering the question about their makers: there appeared to be several different kinds of these objects, characterized by different construction techniques and therefore likely made by different workshops and sculptors.

The micro-CT scanning and resulting images processed with Advanced 3D Analysis software produced very promising material early on in the project's evolu-



Fig. 5.2 View of Thomson Collection miniature Gothic boxwood carvings on permanent view at the Art Gallery of Ontario

tion. Findings were shared with other museums with similar objects in an effort to persuade them to research their own collections in a collaboration with the AGO. A major travelling and international exhibition called “Small Wonders” was created by curators Alexandra Suda (AGO), Barbara Boehm (Metropolitan Museum of Art (the MET)) and Frits Scholten (Rijksmuseum) to showcase their collections. At that time, Pete Dandridge, Conservator, Department of Objects Conservation at the MET joined the technical research project. His extraordinarily deep experience in understanding the manufacture of medieval objects along with materials and restoration practices perfectly complemented the research underway. The technical investigation of the works was published jointly by Ellis and Dandridge in a chapter in the exhibition catalogue [2] and in a guidebook to the collections of the AGO and MET [1].

AGO photographers Craig Boyko and Ian Lefebvre travelled around the world to capture high resolution images of as many of the miniature boxwoods as possible to be used first in research, exhibition didactics and marketing, and ultimately in the two major publications associated with the project and the on-line database. The objects were shot using the same light source and camera and processed with the same software in a predetermined set of views in such a way as to allow the resulting images to be comparable. The photographs are now available in a publicly accessible database (ago.boxwood.ca) which operates using IIIF, the International Image Interoperability Framework (iiif.io), designed to allow experts and novice users to view, compare and annotate the high resolution images.

5.2 Description of the Thomson Collection Prayer Beads

Two of the Thomson prayer beads are carved in the shape of human skulls. The remaining eight are more or less in the form of two hemispheres joined at their equators with a wide band, the outside diameters of which range from approximately 3–10 cm. The exteriors of the prayer beads are pierced with ornate patterns inspired by gothic tracery. Some have Latin scripts carved around their circumference. All are hinged with metal pins. While some retain what appear to be original fittings made with precious metals, such as escutcheons and chains, others have been stripped of these or sport newer restored hardware. Opening the objects reveals minutely sculpted reliefs which are held by pegs in the hollowed out hemispheres that make up the outer shells. Close inspection reveals that some of the reliefs are composed of are comprised of numerous wooden elements joined together, some more subtly than others and some with indiscernible joinery.

While the sculpted, pierced exteriors of the prayer beads are impressively delicate and beautiful, they were designed to protect the even more fragile interiors of the beads that have been proven to be awe inspiring and unforgettable to the AGO's and other collections' visitors, and presumably previous owners. The more simply constructed beads' interiors consist of a single, circular plane of wood into which a low relief has been carved. The more complex prayer beads' interiors, however, are made of a number of elements, some impossibly small and delicate such as spears and flagpoles, which appear barely thicker than a hair. The reliefs bring to life narrative scenes, mostly Christological, which grab the viewer's attention: many of the tiny figures in the foregrounds are almost completely carved in the round. Tiny groupings in low relief in the background are typically obscured by closer elements which defy and frustrate the viewer's desire to understand their construction (Fig. 5.3).

Ellis and Dandridge ultimately used micro-CT scanning coupled with Advanced 3D Analysis software along with close examination to determine that there are two strategies at work in the complex prayer bead relief scenes [1, 2]. Some of the scenes are carved into of joined layers or discs of pierced boxwood that are held within the outer tracery carved shell by tiny pegs. Some of the interior carvings use a more or less single shell of boxwood into which strategically placed cutouts allow the carver to access areas that would otherwise be impossible to reach with tools if the carving was worked only from the front. The cutouts or "windows" thus created are subsequently filled with carved elements and are then held in place with joinery and/or pegs. The most complex interior reliefs are made up of three to five major interlocking elements with sometimes tens of additional elements used to further embellish the final composition, such as spikes, stars and buttons which are pressure fitted into drilled holes (Fig. 5.4).

Fig. 5.3 Prayer bead.
AGO ID 29365. The
Thomson collection at the
Art Gallery of Ontario



5.3 Examination Using Microscopy and Macro Photography

Visual examination of the prayer beads can be frustrating, depending, of course, on the viewer's eyesight and available lighting. The works are of such a small size that for many, only the general composition is evident, particularly when the objects are viewed within a museum vitrine. For the smallest carvings, sometimes even the number of figures and objects portrayed can be difficult to discern. While the construction of the simpler prayer beads is evident upon close examination, many of these exquisite wooden carvings were only understandable once they had been micro-CT scanned. Not only are the objects tiny, but the sculptor intentionally obscured the joins for the cutouts in the most sophisticated examples.

The need to search for more powerful imaging tools became evident long before the inception of the project in 2011. Closer examination at the AGO by Ellis who first encountered the works in 2007, began with a Zeiss stereo microscope, with a maximum magnification of 20 \times . While she was able to manipulate objects to gain better viewing angles along with improved fiber optic lighting to understand composition and clues of construction, such as pegs and joins, it was impossible to see some of the joins and intersections of the interlocking pieces the sculptor had carefully hidden from sight. Perhaps most frustrating were the tantalizing glimpses made available through ages old lacunae in the prayer beads' outer shells that only partially revealed construction methodologies.

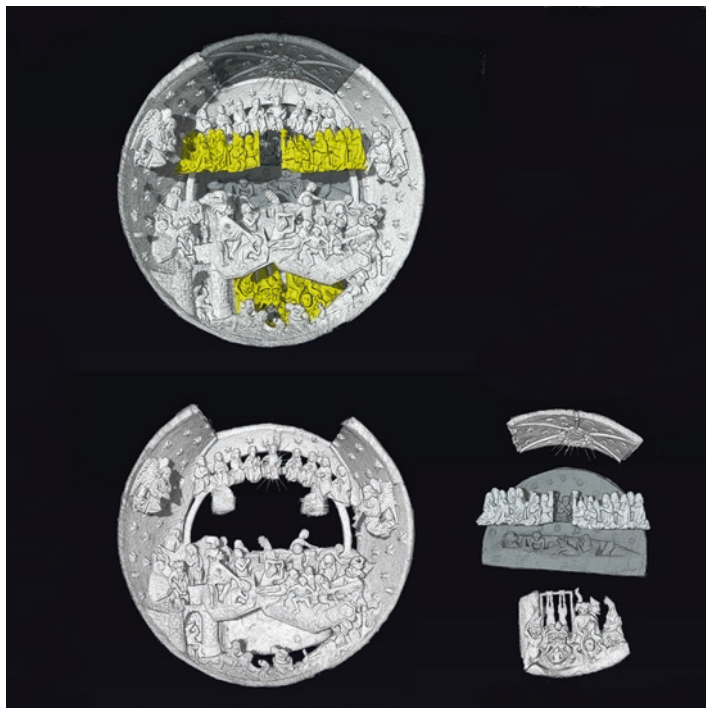


Fig. 5.4 Prayer bead. AGO ID 29365 Rendering of upper relief created using ORS Advanced 3D Analysis software and micro-CT scan. Composite parts in shades of grey and yellow shown together at top; bottom views show same relief separated into its major components digitally

5.4 Specialized Photography

One of the surprising and contradictory aspects about understanding such diminutive art objects is the difficulty in appreciating the work as a whole. As the tiny scale of the carving requires microscopy to discern details pertinent to the scenes being depicted, and the overall composition can be lost to the viewer. An obvious solution to this is to have macro photographs for reference. However, there are significant challenges in photographing small, detailed objects with deep relief, such as the prayer beads. Using a traditional photography setup, the resolution of the image is sacrificed, as the small aperture required to achieve the desired depth of field results in a softer image. The diminutive size of the prayer beads results in poor quality images where entire passages may be lost in haziness.

In order to overcome these obstacles, the AGO photography department started using a technique called focus stacking: this was a cutting edge technology at the start of the project, and has now gained wide acceptance in commercial and museum photography studios. In this technique, a single photographic image is assembled from a series of images, each focused on a different incremental plane through the

depth of the object. The images are shot with a wide aperture in order to reduce diffraction.

The AGO's photography department used a Phase One 645DF camera body, 120 mm Phase One Macro lens and the Leaf Aptus-II 12 digital back to produce 80 megapixel images with files sizes ranging around 250 MB. While focus stacked images were once assembled manually in different computer applications, it was a time-consuming process which, depending on the operator, could take hours for a single image. A number of different focus stacking applications, including Adobe Photoshop, were tested at the AGO and the results compared. The purpose-built focus stacking software, Helicon Focus, yielded the most reliable images, perhaps due to its wide variety of adjustable parameters. The resulting macro photographs of the prayer beads are phenomenal, and of such fine resolution that they can be increased to poster size without loss of detail (Fig. 5.5).

The research value of this kind of imaging was immediately clear. The photographers, along with input from the rest of the AGO team, developed a style guide, outlining equipment, lighting and views of the object to be captured, to share with other institutions so that comparable images could be produced. While some of the larger institutions with dedicated photo studios, such as the MET, committed their own resources to the project and were able to follow the style guide, other institutions granted access and makeshift studio space to the AGO photographers Boyko

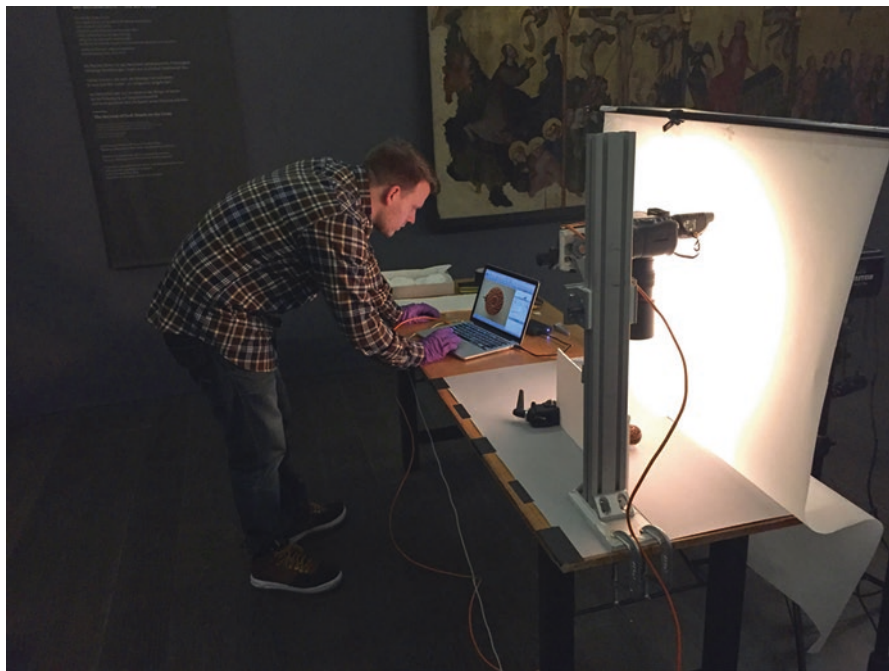


Fig. 5.5 AGO photographer Craig Boyko in a makeshift studio capturing high resolution stacked images

and Lefebvre. These include the Art Institute of Chicago; Bergbau und Gotikmuseum, Leogang Austria; Detroit Institute of Arts; Devonshire Collection, Chatsworth; Kunstgewerbemuseum, Staatliche Museen zu Berlin; Loyola University Museum of Art; Musée du Louvre; Museum Catharijneconvent; Mayer van den Bergh Museum, Antwerp; Museum voor Religieuze Kunst; The Wernher Foundation, English Heritage, Ranger's House, London; Rijksmuseum, Amsterdam; Seattle Art Museum; Staatliche Kunstsammlungen Dresden; The State Hermitage Museum; Thyssen-Bornemisza Collections; Victoria and Albert Museum; and the Wallace Collection.

5.5 X-Radiography

The first attempt to understand internal features of the miniature boxwoods began with X-Radiography. The AGO conservation department does not have a suitable instrument, and the conservation department at the nearby Royal Ontario Museum kindly offered use of their Faxitron, a cabinet X-Ray machine. The Faxitron is equipped with a relatively low kilovoltage and has a relatively small cabinet size. Developed for looking at tissue samples in operating theaters, it is particularly useful in the museum context for imaging small natural history and organic samples that fit in the cabinet and that are not particularly radio-opaque.

Time on the Faxitron was limited by practical factors: one workday was devoted to this project and thus determined the number of views of the prayer beads. Shot in the open position to reduce overlapping elements in the projections, each prayer bead was X-radiographed three times. All prayer beads were placed in the same three positions to provide projections from the anterior posterior, or front; the lateral or side; and at an oblique angle.

The X-ray images revealed many secrets about the prayer beads' construction (Fig. 5.6). Most surprising were the differences between the interior construction of the two skull beads. One of the skull's interiors is made up of stacked layers that contribute to the interior relief, while the other bead appears, though very similar at first glance, to have an entirely different construction. The interior has been carved from the frontal plane of the relief, out of the skull shaped mass of wood. Based on the X-radiography and subsequent study of associated works in other institutions, Suda identified the two skulls to be the work of ancillary workshops, supplying objects emulating the larger corpus of miniature boxwood carvings in response to a desire for and the dearth of miniature boxwood carvings [4].

Although the X-radiographs are extremely fine, they are two dimensional images of three dimensional objects. Thus, there is inevitably superimposition of some structures on others and subtleties of construction can be difficult to determine. While the Faxitron proved an excellent tool during the early investigation of the prayer beads, outstanding questions about the more complicated prayer beads' construction still remained.

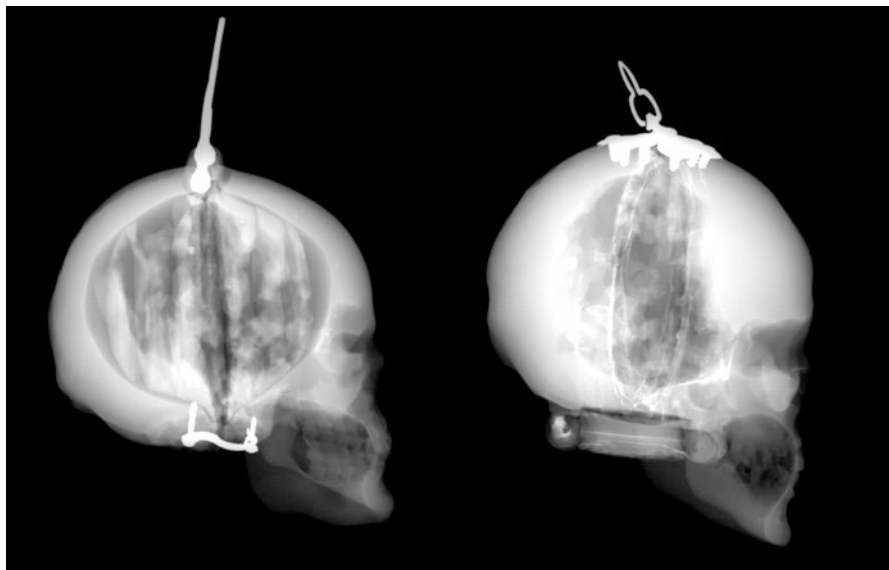


Fig. 5.6 Prayer beads AGO ID 29282 and 29283. X-Radiographs revealing different strategies in the carving of the inner reliefs

5.6 Micro CT Scanning

A prayer bead in the Rijksmuseum had been successfully imaged using synchrotron-based computer X-ray microtomography [5] and although the prayer beads in the Thomson Collection were also excellent candidates for this kind of imaging, there were a number of challenges. These included securing time at a synchrotron facility and consideration of the implicit risk involved in travelling with a large number of delicate artworks. Dr. Wallet, a senior scientist at the Rijksmuseum, kindly suggested considering micro-CT scanning as a lower resolution but adequate tool.

Micro-CT scanning, or high-resolution X-ray tomography, essentially produces the same output as medical computerized tomography or CT scanning, but it uses a different process and it produces images of considerably higher resolution. Both use computers to assemble X-radiographs taken from different angles of the subject being scanned into a 3D volume. The clinical scanner creates slices or cross-sections in the axial plane, which can be reformatted along different planes, or combined to create three-dimensional or volumetric models [6]. The micro-CT scanner takes many individual projections to calculate a volume using a back-projection algorithm [7], which can then be manipulated in many different ways, including producing slices like the clinical scanner. Both can produce 3D models that can be manipulated in virtual space.

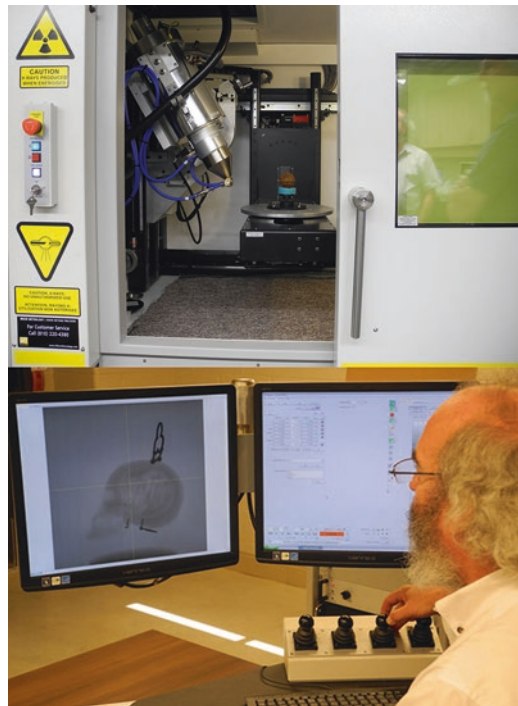
Micro-CT scanning refers specifically to scanners which can deliver output in which voxels (3D isometric pixels) size can be measured in the sub-100 micron range [6]. This is a relatively new technology and is made possible by the enormous

capacity of computer memory and the extremely fine mechanical engineering that enables such high-resolution capture and manipulation. Elliot and Dover [8] developed the first micro-CT system in the early 1980s to examine the structure of a shell, with units first becoming commercially available in the 1990s [9].

A number of different institutions and manufacturers were contacted in the search for a suitable instrument to study the AGO miniature boxwoods. It became apparent that limiting factors included chamber size and the environment within the chamber. Even though some machines were developed for *in vivo* examination of laboratory specimens such as rats, the comfort of the specimen was evidently not of primary concern, with high temperatures being produced by the hardware during the scanning process. The sudden increased temperature in the chambers of some of the instruments ruled out their use as the risk to the boxwood prayer beads would be too great. In addition, many *in vivo* scanners have very small bores, which are not large enough to accommodate the AGO's larger prayer beads or the miniature altarpieces.

Fortuitously, the search for a suitable scanner ended with an introduction to Dr. Andrew Nelson at the Sustainable Archaeology (SA) facility in the Department of Anthropology at Western University, in London, Ontario, approximately 200 km west of Toronto (<http://www.sustainablearchaeology.org/>) (Fig. 5.7). The SA houses a Nikon Metrology XT H 225 micro-tomographic (micro-CT) scanner, capable of scanning the beads at a minimum resolution of 37 micron voxels. The micro-CT

Fig. 5.7 Prayer bead in micro CT scanner at Department of Sustainable Archaeology, Western University



scanner is used for non-invasive studies of archaeological and bioarchaeological materials (and now artworks) revealing a sample's internal structures and features. The scanner can investigate objects with a maximum volume close to that of a human head.

Most importantly for the purposes of this study, the environment in the imaging chamber, which is sizable, contains a cooling system, and so is not subjected to high temperatures and corresponding reductions in relative humidity. The HOBO U12 Temp/RH/Light/External Data Logger (Onset Computer Corporation) was used to record the chamber's environment to ensure that conditions therein were stable and would not damage these sensitive artworks. Over a test period of 10 h, the data logger showed a slight increase in temperature from approximately 22–24 °C with a corresponding decrease in relative humidity from approximately 50% to 46%.

The scans were initially read and manipulated at the SA with licensed software, Volume Graphics, VGStudio Max 2.2. For further processing, the data was exported in industry standard DICOM format so that it could be read using free downloaded software called ImageJ, which was initially used on site at the AGO to manipulate the images. Subsequently, an Advanced 3D Analysis software, ORS Visual SI, developed by Object Research Systems, (<http://theobjects.com>), was used at the AGO to manipulate the datasets: segmentation tools were used to virtually dissect the prayer beads and miniature altarpieces into their composite pieces. Exported files capturing only the surface morphology in “meshes” were used by Priam Givord to create the creation of “Small Wonders: the Virtual Reality Experience” a co-production between the AGO, the Canadian Film Centre Media Lab and Seneca College (Fig. 5.8).

The value of the micro-CT scans and corresponding digital assets was immediately recognized. Scrolling through successive slices of the volume captured in the dataset clearly revealed the construction secrets of these superlative carvings. Joining techniques including tongue and groove, rabbets and butt joints secured with pegs became visible. The problems associated with overlapping elements in the X-radiographs were no longer an issue at all.

The imaging technique provided unequivocal answers and was instrumental in solving a small but significant mystery concerning one of the collection's skull shaped prayer beads. The carved hasp of the bead became of special interest after Suda, along with a former colleague at the MET, re attributed its heraldic device carved in relief to Albrecht of Mainz, Archbishop of Mainz and Magdeburg from 1513–1545. This led to questions surrounding the production of the bead: had it been commissioned specifically for Albrecht, or perhaps the hasp had been added later, after the bead was already complete? While X-radiographs of this area were difficult to interpret, the micro CT scans show that without a doubt, the clasp with the attribution to Albrecht was added after the prayer bead had already been made (Fig. 5.9).



Fig. 5.8 Scene of a visitor in the “Small Wonders: the VR Experience” at the AGO. The screen in the background repeats the user’s view

5.7 Scientific Analysis

In order to understand the original manufacture and subsequent repairs and restorations to the prayer beads, minute samples of adhesives, coatings and polychrome decoration were analysed. Elizabeth Moffatt and Jennifer Poulin at the Canadian Conservation Institute, undertook this analysis using a variety of scientific instrumentation, including: Fourier transform infrared spectroscopy (FTIR); scanning electron microscopy-energy dispersive spectrometry (SEM-EDS); thermal desorption-gas chromatography-mass spectrometry (TD-GC-MS); and Raman spectroscopy.

The following coatings have been identified: shellac, beeswax, pine resin, and a labdane resin. Adhesives may eventually help link a prayer bead to a specific restorer or school of restoration, or be used to date a restoration. Animal glue, a typical wood adhesive, has been found, along with the much more modern poly(vinyl acetate), and even a polyester resin.

A remarkable aspect of these wooden art objects is an overall lack of polychromy. It seems that the prayer beads were intended to show off their maker’s virtuosic skill in carving and joining elements and so were left bare of gesso and paint. There are, however, some notable exceptions to this. One of the more complex Thomson prayer beads, AGO ID number 29365, has a polychromed passage under a ledge, in an area depicting hell (Fig. 5.10). The painted areas here are subtle and mostly hidden from view: a red paint is used to embellish carved flames and a dark bluish

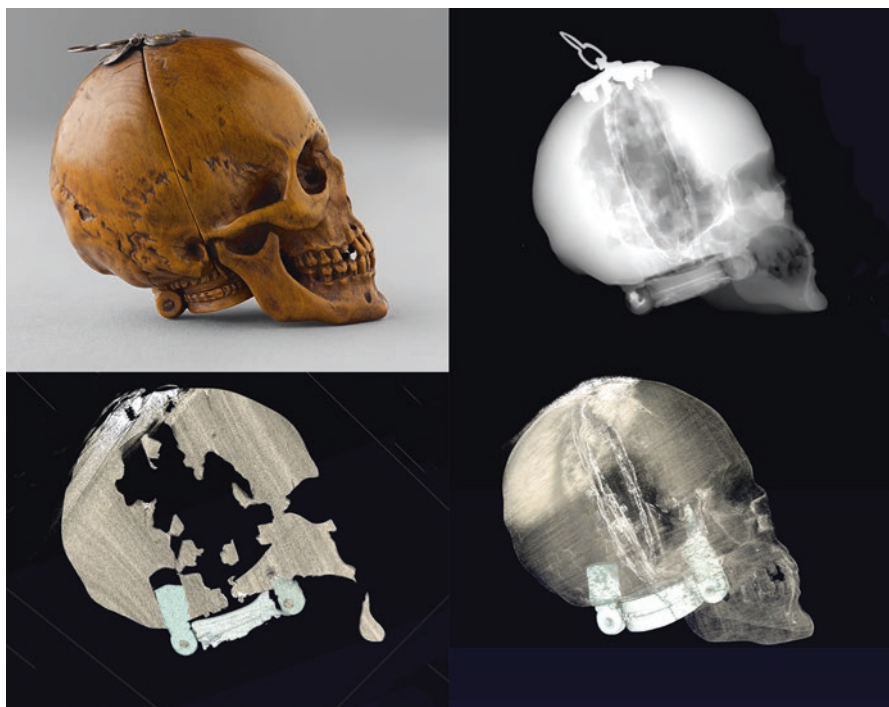


Fig. 5.9 Prayer bead AGO ID 29282. Upper left, photograph; upper right, X-radiograph; lower left, micro-CT slice showing insertion of pegs in skull; lower right, rendering created using ORS Advanced 3D Analysis software and micro-CT scan, the hasp and pegs are visible in situ as the density of the rest of the object has been reduced visually

black pigment coats the interior walls of the cavern like area. Traces of these two paints were identified by the Canadian Conservation Institute (CCI) as a carbon-based black pigment with a protein binding medium and a red paint consisting of a mixture of a red lake, gypsum and a protein. The red pigment's organic colorant was characterized using TD-GC-MS as a compound extracted from kermes. A protein derived from wool found in the red pigment suggests that it was extracted from a dyed wooden textile, a practice associated with the production of pigments used in medieval manuscript illuminations [10]. The use of polychromy in this prayer bead links it convincingly to a prayer bead found in the collection of the British Museum's Waddeson Bequest [11].

5.8 Conclusion

The technical study of the AGO's Thomson Collection of Gothic miniature box-woods has been a resounding success, underscoring the fortuitous intersection of recent advances in technology and the authors' ambition to uncover the mysterious



Fig. 5.10 Prayer bead AGO ID 29365, has a polychromed passage where a red paint is used to embellish carved flames and a dark bluish black pigment coats the interior walls of the cavern like area

construction of these objects. The challenges these works present to modern analysts is a tribute to those who produced them. Macro photography, X-radiography and micro-CT scanning were all necessary to deconstruct these tiny objects, with the latter ultimately being the decisive tool in fully understanding their construction. The scientific analysis of coatings, paints and adhesives was also essential in creating a full picture of the objects, not only of their manufacture, but also giving insight into each object's history of use and restoration. The array of high-technology deployed for this study, and the details it revealed about their construction also causes us to reflect on the remarkable skills of the medieval artisans who made these beads with the simplest of tools and only primitive crystal lenses for magnification.

While at first proving more challenging than originally anticipated, the technical study of the prayer beads prompted partnerships with several organizations in order to gain access to cutting edge technologies and expert knowledge. The AGO's new connections to the Departments of Chemistry and Anthropology at the University of Western Ontario and renewed connections with our other partners, have proven not only informative, but inspiring for future collaborative ventures.

The value of the work described in this paper is corroborated by the exhibition "Small Wonders" and its overwhelmingly positive reception. The discovery and sharing of the Gothic miniature boxwood carvings' secrets using dramatically magnified images of the works, computer animations and the Virtual Reality experience did not detract from their former seductive mystery, as some feared, but rather made them even more intriguing to a wider range of audiences.

Acknowledgments For their support of the technical work carried out on the Thomson Collection, the authors would like to acknowledge the extraordinary support of the AGO, and in particular, Maria Sullivan, Angela Glover, Wendy Hebditch and Margaret Haupt of the Art Gallery of Ontario and Annick Lapotre and David Franklin of TWAL. The online catalogue raisonné and digital photography campaign was made possible through the generous support of Thomson Works of Art. We would also like to acknowledge the dedicated staff and support of the Sustainable Archaeology facility, particularly Zoe Morris and Rhonda Bathurst, at the University of Western Ontario and the staff at ORS, in particular Eric Fournier. Further thanks are owed to exhibition partners at the Metropolitan Museum of Art and the Rijksmuseum as well as the support of the Canadian Film Centre's Media Lab and Seneca College for the development and distribution of "Small Wonders: the VR Experience."

References

1. Boehm B. P. Dandridge, L. Ellis and A. Suda. 2016. *Small Wonders: Gothic Boxwood Miniatures*, eds. L. Ellis and A. Suda. Toronto: AGO Research.
2. Scholten, F. Ed. *Small Wonders: Late-Gothic Boxwood Micro-Carvings from the Low Countries*, 514–573. Amsterdam: Rijksmuseum Publications Department.
3. Ellis L. A. Suda, R.M. Martin, E. Moffatt, J. Poulin, and A. Nelson. 2017. The Virtual Deconstruction of a Prayer Bead in the Thomson Collection at the Art Gallery of Ontario with Micro-CT Scanning and Advanced 3D Analysis Software. In *Prayer-Nuts, Private Devotion and Early Modern Art Collecting*, 22. Abegg-Stiftung eds. E. Wetter and F. Scholten, 208–217, Riggisber: Riggisberger Berichte.
4. Suda A. (2017) Sixteenth-Century Micro-Carving and Exceptions to the Norm: Three Case Studies. In: *Prayer-Nuts, Private Devotion and Early Modern Art Collecting*, Riggisberger Berichte 22: 186–207, E. Wetter and F. Scholten F (eds), Riggisber: Abegg-Stiftung.
5. Peter Reischig, Jorik Blaas, Charl Botha, Alberto Bravin, Liisa Porra, Christian Nemoz, Arie Wallert, Joris Dik, (2009) A note on medieval microfabrication: the visualization of a prayer nut by synchrotron-based computer X-ray tomography. *Journal of Synchrotron Radiation* 16 (2):310-313
6. Kalender, W.A. 2011. *Computed Tomography. Fundamentals, System Technology, Image Quality, Applications*. Erlangen: Publicis Publishing.
7. Holdsworth D.W. and M.M. Thorton. 2002. Micro-CT in small animal and specimen imaging. *Trends in Biotechnology* 20: S34–S39.
8. Elliott, J.C. and S.D. Dover. 1982. X-ray microtomography. *Journal of Microscopy* 126 (2): 11–213.
9. Elliott, J.C. G. Davis and S. D. Dover. 2008. X-ray microtomography, past and present. In *Developments in X-Ray Tomography VI*, ed. S.R. Stock Proc. of SPIE 7078 (707803): 0277–786.
10. Moffatt E. and J. Poulin. 2012. *Analysis of Coatings on Prayer Beads in the Thomson Collection, Part I*, for the Art Gallery of Ontario. CCI Report No. CSD 4971.1, CCI 123806
11. Suda A., and L. Ellis . 2012. *Curator's Project: Investigating Miniature Boxwood Carving at the Art Gallery of Ontario in Toronto*. Codart EZine. 2 Spring 2013. <http://ezine.codart.nl/17/issue/45/artikel/investigating-miniature-boxwood-carving-at-the-art-gallery-of-ontario-in-toronto/?id=119>. Accessed: 30/03/2019.

Chapter 6

The Use of a Copper Green Oil Paint in the Interiors of Eidsvoll Manor in Norway: Analysis of a Discoloured Architectural Paint from 1814



Edwin Verweij, Ulrich Schade, and Hartmut Kutzke

Abstract The late eighteenth century Eidsvoll manor house in Norway was modernised in the first two decades of the nineteenth century. The house and its interiors were colour examined during an architectural paint research. Two colour schemes from the early nineteenth century were found; a light greyish lead white and a green copper-based oil paint. The green colour scheme had discoloured severely. In this paper we discuss the results of synchrotron based infrared spectroscopy experiments on the green paint, which consisted of a verdigris pigment used in oil with lead white and chalk. The analytical results are compared with contemporary recipes found in painters' handbooks around 1800 and seems to be darker than any recipe provided.

Keywords Verdigris pigment · Metal soap · Synchrotron infrared spectroscopy

E. Verweij (✉)

Norwegian Institute for Cultural Heritage Research, Oslo, Norway

e-mail: edwin.verweij@niku.no

U. Schade

Helmholtz-Zentrum Berlin für Materialien und Energie, Institute Methods for Material Development, Berlin, Germany

e-mail: ulrich.schade@helmholtz-berlin.de

H. Kutzke

Museum of Cultural History, University of Oslo, Oslo, Norway

e-mail: hartmut.kutzke@khm.uio.no

© Springer Nature Switzerland AG 2019

A. Nevin, M. Sawicki (eds.), *Heritage Wood*, Cultural Heritage Science,

https://doi.org/10.1007/978-3-030-11054-3_6

6.1 Introduction

The Eidsvoll manor house, situated 60 km north of Oslo in Norway, was built in the eighteenth century and modernised in the first two decades of the nineteenth century (Fig. 6.1). The renovation of the interiors was still ongoing when a constitutional meeting was held at the Eidsvoll manor in 1814 to establish Norway's independence [1].

During research on the architectural paint, executed by the Norwegian institute for cultural heritage research (NIKU) in Oslo between 2006 and 2012, the house and its interior were examined [2, 3]. Two main colour schemes from the period around 1814 were found in the interiors, a light greyish lead white and a green copper-based oil paint. These original colour schemes have been reconstructed for the bicentennial commemoration in 2014 (Fig. 6.2). Archival material about the house and the original colour schemes was scarce, therefore additional analysis was performed to determine the exact nature of the paints and the materials that were used.

In this paper we will focus on the green colour scheme that was found in three rooms on the ground floor: the Billiard room (Biljardstuen), the Library (Bibliotheket) and the Study (Lesekabinettet). One intact window frame was discovered on the north wall of the billiard room, revealing the 1814 colour scheme untouched, since this window near the entrance had been covered in order to make a blind window. The interiors have undergone two major restorations in conjunction with the 1914 and 1964 commemoration where most of the previous colour schemes were both chemically and mechanically removed. The widow frame enabled us to examine



Fig. 6.1 Exterior of Eidsvoll Manor with the billiard room located on the ground floor to the right



Fig. 6.2 The billiard room seen towards the northwest with the blind window in the far-left corner

and determine the paint, its colour and consistency in more detail. The colour scheme has a brownish appearance but on closer inspection, small areas with a slightly more greenish colour can be recognised. On the paint surface itself, coarse pigments can be observed and/or small elements of corrosion. In the cross-sections seen in Figs. 6.3 and 6.4, all layers seem to be opaque with no clearly transparent materials and/or glazing layers visible.

6.2 Methods and Analysis

To examine the paint layers in detail, exposures were made on site and sample material were taken. This enabled light microscopic (LM) examination of the stratigraphy, polarization microscopy (PLM) and scanning electron microscopy with an energy dispersive X-ray analyzer attached (SEM-EDX) for pigment identification. Uncast sample material allowed for synchrotron based infrared microscopy (SR-FTIR). The cross-section microscopy was performed at the conservation studio of NIKU by comparing the colour schemes based on physical characteristics like colour, texture, thickness and the presence of dirt layers and/or surface deterioration.

The first colour Scheme (I), applied in the eighteenth century when the window frame originally was mounted, has a ‘warm greyish’ colour tone and consists of four, separately applied, paint layers. Dark spots, presumably soot, dust and dirt,

Fig. 6.3 An eighteenth-century window frame left untouched since the beginning of the nineteenth century



suggests that this paint surface has been exposed over a longer period. A second colour Scheme (II) was applied in two coats, a light grey and a finer light greyish white paint layer (Fig. 6.5).

The early nineteenth century green colour scheme (III) seems to have been applied in two paint sessions; a light grey basecoat (7) with two (8, 9) or sometimes three (10) layers of a green paint with the same consistency (Fig. 6.6). The build-up of this colour scheme was confirmed by sample material taken from the window reveal that was installed simultaneously with new panelling in the room. These locations show only the paint layers 7–10 and not the previous, eighteenth century, paint layers (0–6).

In polarisation microscopy the discolouration of the bluish green particles is clearly visible, and some have transformed into a reddish-brown colour (Fig. 6.7). Other particles have discoloured into a semi-transparent colour which, combined with the yellowing of the binding media, has resulted into a brownish colour. The original lightness, intensity of the colour and saturation of the green colour scheme is there for unknown. Size measurements of the green pigment indicate that the pigments were coarsely ground. Most particles are between 16 and 24 μm in size (coarse), with some lumps between 72 and 96 μm (very coarse) [6]. Most of the particles vary from being rectangular e.g., 40 \times 80 – 32 μm to more rounded e.g., 42 \times 40 or 48 \times 48 μm .

Fig. 6.4 Discoloured oil paint with coarsely grinded pigments giving texture to the paint surface with corrosion products at the edges and on the profiles of the mouldings



Now, after over 200 years, this green colour has changed into a brownish colour. The chromatic coordinates are determined by visual colour coding and colour measurements carried out with an X-Rite Eye-One Pro (i1) spectrophotometer and compared with the Natural Colour System from NCS Colour AB/SCI Sweden, see Table 6.1. The nearest colour swatch using the Natural Colour System (NCS) varies from NCS S 7020-Y20R to 8010-Y30R for the darkest areas. The lightest areas, still showing traces of a green colour scheme, are coded ranging between NCS S 5020-Y and 5020-G90Y. Green corrosion products are coded between NCS S 4030-Y and 5020-Y.

The high spatial resolution down to the diffraction limit provided by synchrotron based infrared microscopy gives the possibility to study the forming of deterioration products like metal soaps on a microscopic level in such a detail as it is not possible by using conventional infrared spectroscopy. The advantages of using synchrotron infrared spectroscopy in the study of cultural heritage objects were proved in several studies [4, 5]. Synchrotron based infrared microscopy was performed at the IRIS beamline at the Helmholtz-Zentrum Berlin (BESSY II), using a Nicolet Continuum microscope with an aperture size of $12 \times 12 \mu\text{m}^2$.

Analyses of the embedded and carbon coated samples were carried out using a JEOL JSM-840 electron scanning microscope equipped with an Oxford 6506 EDX detector. In the top coat, see layer 8–10 in Fig. 6.6, the elements copper (Cu), lead (Pb) and calcium (Ca) were found; indicating the presence of a copper pigment mixed with lead white and chalk. By means of infrared microscopy the binding

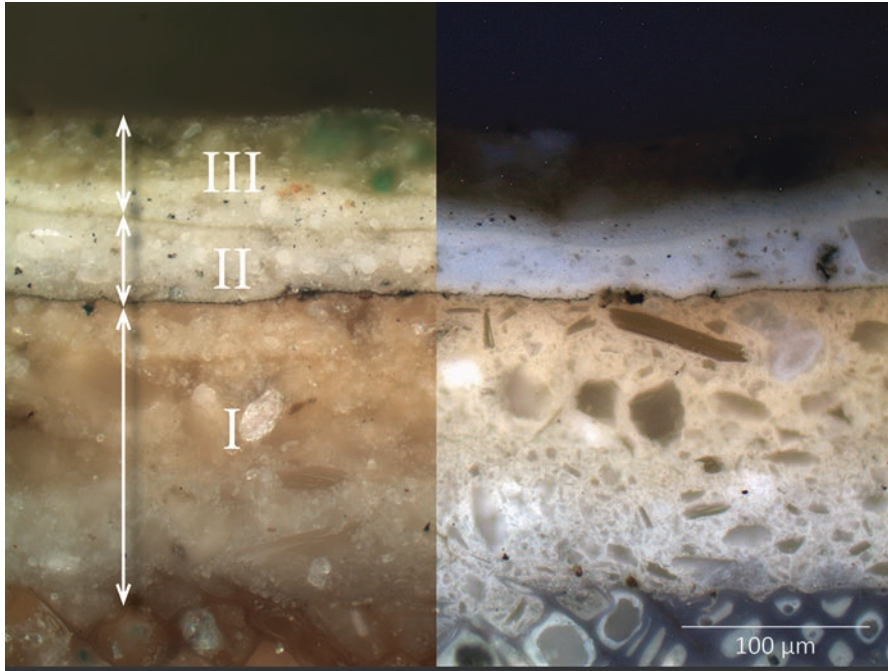
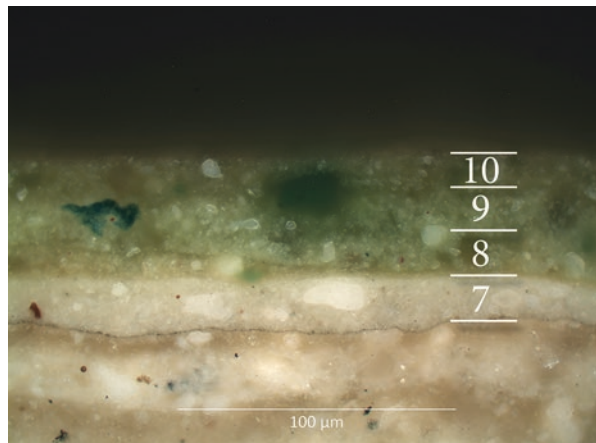


Fig. 6.5 Paint build-up of two eighteenth century colour schemes (I) and (II) underneath the early nineteenth century green colour scheme (III) examined under normal light (left) and ultraviolet light conditions (right). Micrograph Eidsvoll INT117-17 (250×)

Fig. 6.6 The green paint coat applied in three layers (8–9) on a thin greyish basecoat (7) to form the third colour scheme (III). Micrograph EIDSVOLL_ INT117-17 (250×)



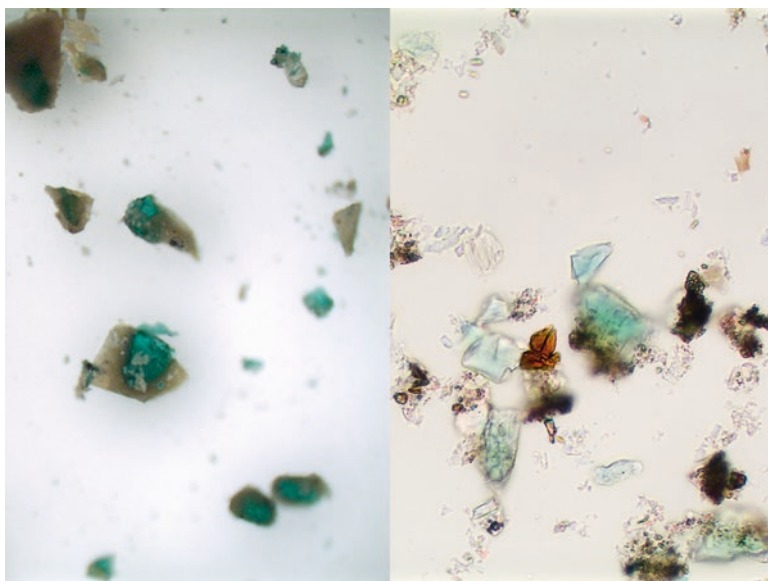





Fig. 6.7 Green verdigris pigments isolated from the topcoat examined under normal light (left) and in transmitted light (right) showing the discoloration into brown. Micrograph Eidsvoll INT117-17 (250×)

Table 6.1 Colour measurements of the discoloured green paint from 1814 found in the billiard room at Eidsvoll manor

Eidsvoll Billiard room	Window frame interior 117 Swatch	CIE lab values			Natural colour system
		L*	a*	b*	NCS S
Aged colour 117_K (brown)		30,68	5,12	10,60	7020-Y20R 8010-Y30R
Aged colour 117_Sd (green)		42,68	2,83	20,45	5020-Y 5020-G90Y
Corrosion product 117_Sl (green)		47,92	2,38	26,45	4030-Y 5020-Y

CIE $L^*a^*b^*$ (CIELAB) is a color space specified by the International Commission on Illumination (French Commission internationale de l'éclairage, hence its CIE initialism). It describes all the colors visible to the human eye and was created to serve as a device-independent model to be used as a reference.

The three coordinates of CIELAB represent the lightness of the color ($L^*=0$ yields black and $L^*=100$ indicates diffuse white; specular white may be higher), its position between red/magenta and green (a^* , negative values indicate green while positive values indicate magenta) and its position between yellow and blue (b^* , negative values indicate blue and positive values indicate yellow). The asterisk (*) after L, a and b are pronounced star and are part of the full name, since they represent L^* , a^* and b^* , to distinguish them from Hunter's L, a, and b, described above

media was identified as oil. No indications were found for the presence of a resin or resinates. The spectra of the green particles from the top layer indicate a reaction between verdigris and oil, resulting in a copper oleate (Fig. 6.8 and Table 6.2).

The formation of an oleate can clearly be recognized by the replacement of the band assigned to the C=O stretching vibration at around 1700 cm^{-1} in the pure oil by the -COO^- stretching signal around $1550\text{--}1600\text{ cm}^{-1}$ in the metal soap. Decreasing of the wavenumbers is caused by the mesomeric effect in the carboxylate group. Additionally, the C-O stretching band is shifted from 1300 to 1400 cm^{-1} [7]. It is expected that the broad band related to the O-H stretching vibration in the region between 3200 and 3600 cm^{-1} disappears during oleate formation. However, due to the presence of pure oil or other components containing -OH it may still be visible in paint samples.

While the formation of metal soaps is well-known from paintings, their occurrence is hardly ever being reported for interiors. Lead soaps were observed on a surface of a bone black paint on a seventeenth century ceiling in the Johan de Witt house in The Hague [8].

6.3 Paint Techniques for Use in Interiors

The verdigris pigment mixed with oil and/or resin, gives a (semi-)transparent coating. This can be applied as a coloured transparent finish over opaque paint layers or as a glaze over e.g., gold and silver foils; a technique often found on easel paintings and polychromed sculpture. It is mentioned as a decorative painting technique for

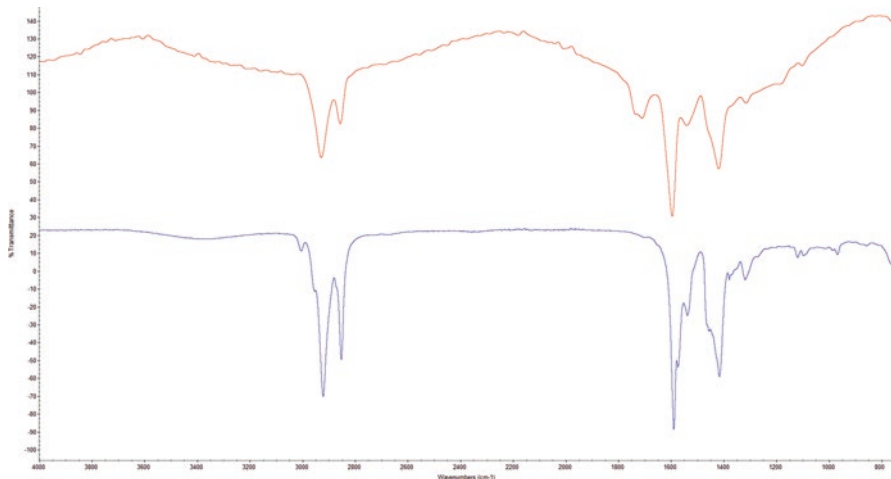


Fig. 6.8 The spectrum of a greenish particle taken from the top layer of paint indicates a reaction between verdigris and oil, resulting in a copper oleate (above). The copper oleate reference (below) was prepared following the prescription given by Corbeil and Robinet [18]

Table 6.2 Infrared wavenumbers (cm^{-1}) for Eidsvoll interior sample 117-17 and a copper oleate reference

Eidsvoll interior sample 117-17	Copper oleate reference	Assignment
2929	2922	$\nu_s \text{CH}_2$ [7]
2854	2852	$\nu_a \text{CH}_2$ [7]
1741		Polymerisation products of linseed oil [17]
1709		$\nu \text{C}=\text{O}$ (oleic acid) [7]
1592	1588	$\nu_a \text{COO}$ [7]
1539	1537	
1458	1455	δCH_2 [17]
1416	1415	$\nu \text{C-O}$ carboxylic acid products [17]
1312	1314	
1174		
1102		
	712	

use in interiors but is not very common, with only a few cases reported which include eighteenth century examples in Monticello, USA, Danton House, UK., Colonial Williamsburg, USA.

The pigment verdigris itself is produced by the corrosion of copper and copper alloys exposed to the atmosphere and/or organic acids. Verdigris paint is known to change over time, due to the transformation of the organo-copper complexes and the formation of copper-oleates and copper salts. A gradual change of the substance and colour starts even during the manufacturing of the paint and continues during the curing period within the binding medium. The reason for the colour change, from a bluish colour to a bright green, has been studied extensively, but the transformation over time into a brownish colour is still subject of debate [9–11].

6.3.1 Paint Sources

Descriptions of how to paint interiors in a green colour, with the use of verdigris, seem to be sparse at the end of the eighteenth and beginning of the nineteenth century. However, some recipes can be found in painters' handbooks. The hiding power of verdigris itself is not very high but can be improved by adding a little lead white to the paint mixture.

For the Eidsvoll manor, neither archival sources nor contemporary descriptions of the paintwork have survived from the building period. General information on Norwegian building- and paint techniques are reported [11]. For this paper, additional sources were studied to compare our findings with similar painting techniques described in Dutch, Swedish and Norwegian paint handbooks [12–15] and a detailed British study on interior house paints and colours and technology [16].

In the United Kingdom, in the eighteenth century, one of main green colours would be made by mixing two different pigments; a yellow ochre with a Prussian blue, these were sometimes described as ‘inferior’ greens ([16]: 159). With the use of verdigris, a range of green colours could be made, where different shades would get their own colour name like grass green or willow green ([16]: 165). For example, mixing equal proportions of verdigris and lead white would give this grass green colour. Prices of verdigris varied depending on the availability, production facilities, lack of natural resources and/or import restrictions. In 1806, for example, it was about four to five times more expensive than that of lead white and it was the most expensive green in 1812 and could be bought either as a dry pigment, in a spirit based medium or in a varnish.

In a Dutch painter’s handbook, written by the painter Lambertus Simis, the Spanish green pigment (verdigris) is considered among the most resistant and durable paints. This is most often used outdoors and is not recommended for interior work due to fact that it becomes ‘very ugly and dirty’ [Simis: 56]. A recipe for a light green can be made by mixing five ounces of thickly ground green with at least four and a half or at most five ounces of ground lead white [Simis: 54]. After application it will have a light blue colour, but some days into the drying process this will change into its final greenish colour (Simis: 56). The distilled version of the same Spanish green is considered much purer, better, cleaner and even more resistant. This paint quality is applied only in interiors. It is made into a house paint by grinding the pigments with oil of turpentine and adding a mastic varnish, or with a resin. This paint was used as a glazing technique on silver, glossy surfaces, for hatchings, to accentuate borderlines or for the decoration of furniture but only when a little (lead) white was mixed into the mixture.

The use of green pigments in the eighteenth century or the beginning of the nineteenth century in Norway has been reported during architectural paint research at several houses.¹ Pigment and/or binding media analysis were not performed during these investigations and it is therefore unknown whether these interior paints were made using verdigris pigment and/or other (copper) pigments.

A handwritten notebook by a Norwegian painter, Simen Syvertsen contains recipes for several green colours, for example, by taking equal amounts of Spanish green and lead white (1:1) and grinding them in raw oil. A boiled oil should be added during application and painted on a light grey ground made of black mixed with lead white. The price for Spanish green was a quarter that of distilled Spanish green, while lead white would cost three times more than ordinary Spanish green.

¹Damsgård manor Laksevåg/Bergen (1730–1780), Kjosgård Kristiansand (1786), Gulskogen manor Drammen (1802–1804), Frydenlund (now at Gamle Bergen) Bergen (1799), Strømsbo gård Arendal (1805–1810), Kalleviggården Arendal (1812–1815), Ladegård Trondheim (1811), and Søndre Brekke Skien (1777/1811–1813).

In a Swedish painter's handbook published by Johan Conrad Gütle in 1799, three different recipes can be found. Two paints are made by mixing linseed oil in combination with oil of turpentine and varnish but the third one describes a recipe for 'a green paint for e.g., on wood'. This is obtained by mixing one pound of green with two pounds of lead white (1:2) after they have been ground separately in nut oil and heating them evenly. Since the open air can quickly lead to the green becoming darker over time, it is advised to even use three pounds of lead white (1:3) [Gütle:127]. For mixing 'A beautiful mixed green paint colour for painting outside spaces' lead white is mixed with distilled Spanish green with the addition of a mixture of oil and oil of turpentine (1:1) and the addition of a Dutch varnish (Gütle:126).

From the end of the eighteenth century, the costs for painting interiors could be estimated by the amount of work involved; painting twice, three or four times in oil. The application of four coats of an oil paint with the use of verdigris would have been the most expensive, while a 'dull dead green by mixture' would cost much less. Since saturated colours would require greater use of pigments these paints would be even more expensive [16].

6.3.2 *Paint Reconstruction by Mixing the Analysed Components and Visual Matching*

The grey base coat layer of the colour schemes at Eidsvoll show great similarities with the recipe given by Syvertsen in 1787. All contemporary recipes seem to consist of an equal amount of verdigris to lead white (1,1), or the proportion of lead white is even larger 1:3, 1:4 or even 1:5. The Eidsvoll colours applied seems to be darker than a mixture of green of lead white mixed one to one with verdigris. During the paint matching and reconstruction attempts described in Table 6.3 and shown in Figs. 6.9 and 6.10 it became clear that equal parts of ground green pigment with lead white (w:w) would result in a very light green colour that would not have aged into the paint found at Eidsvoll.

Table 6.3 Paint matching by mixing linseed oil with verdigris, chalk and lead white paint based on late eight- and early nineteenth paint recipes. (v:w:w:w)

Green paint mock-ups	First coating	Second coating
30	2:2:1:1	2:2:1:1
31	2:1:1:2	3:1:1:2
32	2:1:1:3	3:1:1:3
33	2:1:1:4	3:1:1:4
34	1:4:1:1	4:4:1:1



Fig. 6.9 Second coat of newly mixed paint (right) applied over dried first coat (left). Paint based on contemporary recipes of green verdigris pigments mixtures with lead white in different ratios

Fig. 6.10 The final paint mixture applied on a mock-up moulding with only one paint layer (top left) and two paint layers (bottom right) to visualize thickness and transparency



6.4 Conclusion

In the second half of the eighteenth century the fashion to paint in flat or ‘dead’ finishes, meaning a matt surface, became widespread and was the preferred finish for high quality work. This tradition seems to have disappeared in the beginning of the nineteenth century ([16]: 102).

Analysis confirmed that the paint used at Eidsvoll was made using four different ingredients, green verdigris with a small amount of white lead and some chalk mixed into a drying oil. No resin was found in the paint samples. In the micrographs of the sample material, the amount of green pigment is much higher than the amount of lead white. Although the paint has changed over time, it was probably never a

very light green colour; the original lightness, intensity of the colour and saturation of the green colour scheme is however unknown.

The painted surfaces at Eidsvoll have certainly lost their original bright sheen but there are still traces of a glossy appearance. According to contemporary recipes, the paints that were applied, seem to have been mixed using a recipe for exterior paints. But the appearance and colour of these kind of paints would, as Simis already wrote, become 'very ugly and dirty', since it would discolour into a brownish colour.

Paint mock-ups indicate that ground green mixed with ground white (3:1) would result in a colour scheme resembling that of the paintwork that was executed in 1814. The use of dark green paints in interiors has been reported, both by historians and architectural paint researchers, and occurred in the first quarter of the nineteenth century. Known problems with the discolouration of some green pigments, especially with the use of verdigris, might have been one reason to avoid using these colour schemes. By the middle of the nineteenth century, the use of verdigris for interior decoration had practically disappeared.

Acknowledgements The authors wish to thank the Helmholtz-Zentrum Berlin, Germany for allocation of synchrotron beam time. A travel grant provided by the SYNKNØYT program of the Norwegian Research Council (project number 143564) for one of the authors (HK) is gratefully acknowledged. Thanks also to NIKU, for funding additional analysis (project number 15620301-21) for the Eidsvoll project, Jon Brønne, for providing copies of Scandinavian painters' handbooks found at archives and libraries and personal communication, Helena Grundberg, for help with the translation of the Swedish manuscript and Annelies van Loon for discussions on the use and ageing of verdigris.

References

1. Risåsen, G-T: Eidsvollsbygningen. Carsten Anker og Grunnlovens hus. Damm, Oslo (2005).
2. Solberg, K. and Risåsen, G.T. 2008, Eidsvollsbygningen tilbake til 1814. Rapport over fargeundersøkelser og bygningshistorie. Oslo (part 1) Unpublished report.
3. Solberg, K., Verweij, E., and Risåsen, G.T. 2011, Eidsvollsbygningen tilbake til 1814. Rapport over fargeundersøkelse og bygningshistorie, Oslo (part 2) Unpublished report.
4. Salvado, N. S. Butí, MJ Tobin, E Pantos, AJ Prag, and T Pradell 2005. Advantages of the use of SR-FT-IR microspectroscopy: Applications to cultural heritage. *Anal. Chem.* 77, 3444-3451
5. Cotte, M., P Dumas, Y. Taniguchi, E. Checroun, P. Walter and J. Susini, 2009. Recent applications and current trends in Cultural Heritage Science using synchrotron-based Fourier transform infrared micro- spectroscopy. *C.R. Physique* 10, 590-600 (2009).
6. Feller, R. and M Beyard. 1986.: Terminology and procedures used in the systematic examination of pigment particles with the polarizing microscope. In: *Artists' pigments: a handbook of their history and characteristics* 1:285-298, Cambridge University Press/National Gallery of Art, Washington, DC.
7. Robinet, L. and M Corbeil 2003.: The characterization of metal soaps. *Studies in Conservation* 48, 23-40.
8. Van Loon, A. and Boon, J. 2005. : The whitening of oil paints films containing bone black In: 14th triennial meeting The Hague, 511-518 ICOM Committee for Conservation: preprints volume 1/ed. I. Verger, James & James, London (2005).
9. Scott, D. 2002: *Copper and bronze in art. Corrosion, colorants, conservation.* Getty Publications, Los Angeles (2002).

10. Gunn, M., G Chottard, E Rivière, J-J Girerd and J-C. Chottard 2002: Chemical reactions between copper pigments and oleoresinous media. *Studies in Conservation* 47, 12–23.
11. Eikema-Hommes, M. van 2004.: Verdigris glazes in historical oil paintings: recipes and techniques. In: *Changing pictures. Discoloration in 15th–17th century oil paintings*. Archetype, London, 51–90.
12. Drange, T. H.O. Aanensen and J. Braenne, 1980: *Gamle Trehus. Historikk, reparasjon og vedlikehold*. Universitetsforlaget/Gyldendal Norsk Forlag, Oslo (1980)
13. Simis, L. 1829: *Over den aart en de eigenschap der groene verwen*. In: *Grondig onderwijs in de schilder-en verw-kunst*, 54–60, 2nd ed. Gartman, Amsterdam (1801/1829).
14. Gütle, J.C. 1799: *Grundelig anvisning at förfärdiga goda fernissor jamte konsten at latera och förgulla*, Holmberg, Stockholm (1799).
15. Syvertsen, S. 1787: *Oppskriftsbok for maling og dekor* (manuscript). Universitetsbibliotheket, Oslo (1787)
16. Bristow, I.C. 1996. Green pigments (3). In: *Interior house-painting colours and technology 1615–1840*, 22–24, Yale University Press, New Haven (1996).
17. Meilunas, R.J.; Bentsen, J.G. & Steinberg, A.: Analysis of aged paint binders by FTIR spectroscopy. *Stud. Cons.* 35 (1990) 33-51.
18. Marie-Claude Corbeil, Laurianne Robinet, (2002) X-ray powder diffraction data for selected metal soaps. *Powder Diffraction* 17 (1):52-60

Chapter 7

A Polychrome Wooden Interior from Damascus: A Multi-method Approach for the Identification of Manufacturing Techniques, Materials and Art Historical Background



Petronella Kovács Mravik, Éva Galambos, Zsuzsanna Márton, Ivett Kisapáti, Julia Schultz, Attila Lajos Tóth, István Sajó, and Dániel Károly

Abstract The polychrome wooden interior from Damascus (1802–1803 CE) was purchased by Budapest’s Museum of Applied Arts in 1885. The wooden panelling is ornamented in the ‘ajami technique using gesso relief with painted, metal-gilded and glazed surfaces in various colours and patterns. Based on ongoing conservation work, this paper presents the room’s history and findings concerning the materials and manufacturing techniques used to make it. It shows that red lead, vermillion, smalt, indigo, lead white, verdigris, and different arsenic sulphides were used as pigments. Presumably, aloe was used in the orange, verdigris in the green glaze and cochineal in the red lake. Collagen, ovalbumin and gums were identified in the paint as binders. Although the appearance of the originally brilliant and matte surfaces cannot be recovered, after restoration the interior will still be a highlight of MAA’s planned Islamic Museum.

P. Kovács Mravik (✉) · É. Galambos · I. Kisapáti
Conservation Department, Hungarian University of Fine Arts, Budapest, Hungary

Z. Márton
Department of Environmental and Laser Spectroscopy, University of Pécs, Pécs, Hungary

J. Schultz
Laboratory for Archaeometry, State Academy for Art and Design, Stuttgart, Germany

A. L. Tóth
Institute of Technical Physics and Materials Science, Hungarian Academy of Sciences, Budapest, Hungary

I. Sajó
Szentágotthai Research Centre, University of Pécs, Pécs, Hungary

D. Károly
Faculty of Science and Technology, Nottingham Trent University, Nottingham, UK

Keywords ‘ajami · Arsenic sulphides · Collagen · ‘Damascus room’ · ELISA · Gum · Ovalbumin · Smalt

7.1 History of the Room

The Hungarian Museum of Applied Arts (MAA) was established in 1872 on the model of the South Kensington Museum (Victoria and Albert Museum) and the Österreichisches Museum für Kunst und Industrie (Museum für angewandte Kunst). The rapid development of the manufacturing industry and the emergence of modern industrial production eclipsed the craft industry during the nineteenth century. The new technical procedures provided wide opportunities regarding form and material but the other hand also ignored artistic demands. The main purpose behind the establishment of the MMA was to shape and develop public taste and to show to craftsmen the artistic possibilities through collections of artefacts from different nations and ages at a time of industrial expansion. The collection was originally built up through donations by Hungarian private individuals and by various institutions abroad, as well as through specific purchases. The MAA curators regularly travelled abroad on the lookout for new acquisitions. Documents about their activity can be found in the archives of the museum, including the business correspondence concerning the purchase of an ‘old Arabian room’ displayed at the Antwerp Universal Exhibition in 1885. Having received an inquiry as to its price, the British firm exhibiting the room, Mawe and Co., wrote the following to the museum: ‘We will let your museum have the room and content for £300, we packing it for you and paying duty. It would be a great acquisition to your Museum, and is a much finer room than the one in the South Kensington Museum London, and for which nearly double the price we ask you, was paid’.¹ The museum decided to buy the room, albeit without its proffered contents, as the museum’s secretary, informed the company: ‘... we should take in consideration old Arabian room without contents, not only have we great many objects to put in, but I do not remember to have seen among mentioned objects, many of great artistic value or special interest’.² However, the British company would have liked to have sold the objects exhibited in the room, in order to avoid having to ship them back to London. The museum insisted on its decision, behind which lay financial and existing collection policy considerations: ‘... the Museum is quite unable to by contents of Arabian room, first of all the founds [sic] of the Museum are completely exhausted secondly we have Persian carpets of very fine rate, embroideries, copper wares and all sort of oriental objects quite sufficient to the room.’³ Following a donation from the First National Savings

¹ Letter from the Mawe and Co., MAA Archive, 172/1885

² Letter from the MAA to Mawe and Co., MAA Archive, 172/1885.

³ Letter from the MAA to Mawe and Co., MAA Archive, 256/1885.



Fig. 7.1 The ‘old Arabian room’ at the first exhibition in 1886. (Archive©MAA, Budapest)

Bank Association of Pest, the marvellous painted wooden interior was finally purchased for £175.⁴

The museum did not have an own building at that time, its exhibitions were staged in rooms in the National Museum and it also leased spaces at the Hall of Exhibitions. After its arrival in Pest, the ‘Arabian room’ was first shown to the general public at the latter. (Fig. 7.1).

The palace of the Museum of Applied Arts was inaugurated by Francis Joseph, emperor of Austria and king of Hungary, in 1896. At that time, only art objects of Hungarian origin were exhibited. A year later the exhibition was enlarged and the ‘old Arabian room’ was also presented in the right hand archway of the building’s splendid, central glass-topped hall ([9], 12).

The origins of the room and details of the house from which it was taken are not exactly known, only that, it is one of the two rooms sent to Mawe and Co. by their agent in Damascus. ‘There is no particular history to the two rooms which we have sent you in 1884–1885. They come from Mouslim houses and probably they were rooms of the favourites of the Harim’.⁵ It was one of the first of this type of item to be owned by a museum but nevertheless did not attract much international attention

⁴Letter from the MAA to Mawe and Co., MAA Archive, 308/1885.

⁵Letter of Mawe and Co., MAA Archive, 49/1886.



Fig. 7.2 Inscription board with the date of manufacture. (Image: G. Nyíri©MAA, Budapest)

until recently. Only a few publications, connected with the exhibitions at which it was shown, mention it ([3], 201–207; [4], 19). This was probably due to the fact that the room, now called the ‘Damascus room’, was only twice put on display following its original showings, namely at the 1955 exhibition ‘Applied Arts of the Near and Middle East’ at the MAA and at Eger Castle Museum in 1962. Since then, it has remained in the storerooms of the MAA.

7.2 Description of the Room

A survey, performed in 2010, and a provisional assembling of the elements of the interior, showed that the panelling – richly painted and decorated using the ‘ajami technique – was made in AH 1217 (1802–1803), as written on one of the inscription boards, originally covered the walls of a rectangular room measuring about 4 × 5.5 m. (Fig. 7.2).⁶

There are two types of numbering on the reverse side of the elements. One type was put on by the masters making the objects so that the verses would be in the correct order and is marked with strokes and a circle, as mentioned by Scharrachs [14]. The other type was added at the time of the dismantling work in Damascus or on the occasion of the Antwerp exhibition. (Fig. 7.3).⁷

As a result of the survey, it was found that the room is still complete with all its wooden elements. The walls are broken up by shelved niches, integrated cabinets, a

⁶The survey was carried out by Erzsébet Vadászi, curator of the MAA, József Balázs, Mária Fodor, Mária Szilágyi and Petronella Kovács Mravik wooden restorers MA.

⁷Letter of Mawe and Co., MAA Archive, 269/1885.



Fig. 7.3 Two numbering types on the reverse side of the panelling. (Image: G. Nyíri©MAA, Budapest)

masabb, five windows with wooden grilles (three of them with pairs of outer window shutters), and an entrance door. The height of the room will be calculable after restoration all of the elements. An arch and two consoles divided it into two parts—for the ‘ataba’ and the ‘tazar’. Two decorated painted ceilings with adhered carvings and small mirror fragments belong to the ensemble which formerly covered the walls of an upper-floor room of a residence in Damascus. This is assumed on the basis of the size and location of the entrance door, the space in the panelling for the opening of the door, and the depth of the wooden window frames which confirm that the wall was only 20 cm thick. The upper-floor walls of Damascus houses are always thinner than the ground-floor ones, which are normally 70 cm in width.⁸

The decoration of the ‘ataba’ differs from that of the ‘tazar’. The panels and cornices of the ‘ataba’ are decorated with floral motifs only, while the elements of the main room feature stylised cityscapes as well. The two consoles are also decorated with cityscapes. The two parts also differ with regard to their main colour; pink is the dominant colour of the wall panelling of the ‘ataba’ while the ‘tazar’ framework is decorated with flower cartouches painted on an orange background (Figs. 7.4 and 7.5).

This type of interior used to be typical in this region, but due to fire, war damage and changes in style few examples have survived *in situ* with many having also been sold by art dealers to museums and private collections. Another such interior, the so-called ‘Turkish room’ (probably also from Damascus) was also in Hungarian ownership. It was purchased by at auction by Count János Erdődy Pálffy in 1902 from the estate of the one-time king of Serbia Milan I Obrenović. The Count used the panelling as wall decoration in his study at his castle in Bajmóc (today Bojnice, Slovakia) ([5], 45).

⁸Personal communication with Scharrachs.



Fig. 7.4 Detail of a panel of the 'ataba' decorated only with flowers, before restoration. (Image: P. Kovács Mravik©MAA, Budapest)



Fig. 7.5 Stylized cityscape on a panel of the tazar, after restoration. (Image: P. Kovács Mravik©MMA, Budapest)

The 'ajami' technique and the use of different sheet metals decorated with diverse lustrous colours, is very typical for these interiors. According to Scharrahs research, the 'Damascus room' at the MAA is very similar to three other rooms preserved *in situ* in Damascus and to a room in the Aga Khan Museum, Toronto ([13], 334–335). One of them is dated to the same time as the 'Damascus room' of the MAA and another to 1800-1. The five interiors are so very similar to each other

in terms of style, floral and other decorative motifs and elements that it is conceivable that they might even originate from the same workshop.

7.3 Materials and Techniques

Only a few publications have ever provided scientifically based findings of painting techniques of the 'ajami rooms preserved *in situ* or in collections. These studies and historical Persian treatises served as the bases for comparison during the research into the Damascus room of MAA.

Microscopic identification showed that elements of the wooden panelling are made from poplar.⁹ Characteristic features of the painted wooden elements of these rooms, such as joins to lengthen the boards, iron nails to fix the boards together and to attach carved elements to them, and various materials (e.g. bundles of hemp fibres, paper, and leftover textiles) to fill or cover the gaps between the boards [12], 135 are also observable on the 'Damascus room'. The painting technique and the materials used were studied using X-ray fluorescence spectrometry (XRF), polarised light microscopy (PLM), fluorescence microscopy, scanning electron microscopy with energy-dispersive X-ray spectroscopy (SEM-EDX), X-ray diffraction (XRD), Fourier transform infrared spectroscopy (FTIR), and Raman spectroscopy. The types of binding media employed were investigated using micro-chemical tests on cross-sections, and using FTIR and Enzyme-linked Immunosorbent Assay (ELISA). Two darkened varnish layers, applied most likely in Damascus and later on during repair work preceding the earlier exhibitions, cover the painted and glazed surfaces and complicate the interpretation of the analytical results. Red lead, vermilion and organic red lake used to create different shades of red paint, usually painted one on top of the other, and the application of their mixture are also characteristic of these rooms. Smalt is the main pigment for dark blue, while a mixture of smalt and lead white or indigo and lead white was observed in the samples taken from light blue motifs. The green parts of the floral motifs painted with dark green contained orpiment and indigo. The pigments of a greenish line on the edge of some panels were identified as a mixture of verdigris, smalt and lead white. Orpiment provides the yellow colour and lead red the orange colour of the flowers, while lead white, in some places mixed with gypsum, was used for the white lines and different motifs. Red and green glazes were also used over opaque paints to add depth and contour to the flowers and other decorative motifs. Gypsum bound with animal glue is a characteristic material of 'ajami decoration; it was also applied as ground layer for the cityscapes and in some other places, but not on all wooden surfaces of the panelling. Two other white layers containing lead white and gypsum were put on the gypsum base before the motifs of the cityscapes were painted. The pink background colour on the boards of the 'ataba' is painted on an orange colour lead red base

⁹The investigation was carried out by József Balázs wooden objects restorer, National Centre for Conservation and Conservation Training (NCCCT).

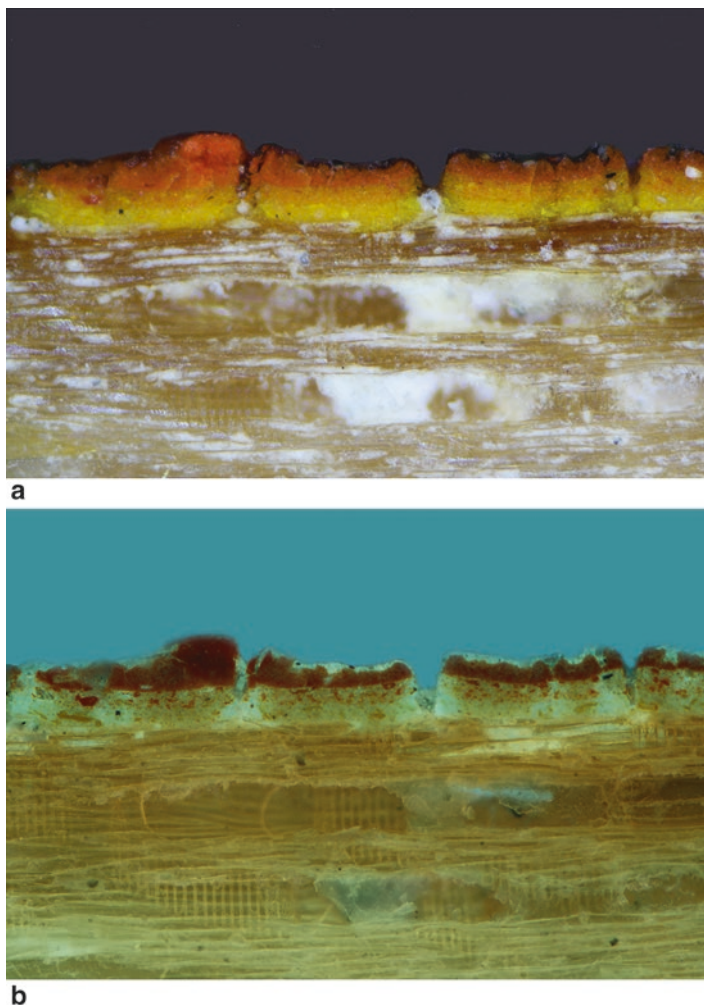


Fig. 7.6 (a–b) Cross-section of the layers containing arsenic compounds: under visible light (a), under UV light (b). (Image: P. Kovács Mravik©MAA, Budapest)

layer, while the stratigraphy of the orange background of the cartouches on the panels of the tazar is more complex. There are three layers on top of one another containing various arsenic compounds according to the results of the Raman spectroscopy and XRD.¹⁰ The first is a yellow layer painted directly onto the wood

¹⁰The investigation of the arsenic-containing layers was carried out with a Thermo Scientific DXR Raman microscope at 780 excitation by Zsuzsanna Márton and Ivett Kisapáti on cross sections of embedded micro samples. The XRD measurements were performed by István Sajó on powder samples scratched from the paint layers, with a Philips PW 3710/PW 105 type Bragg-Brentano diffractometer using Cu K α radiation, graphite monochromator and proportional counter

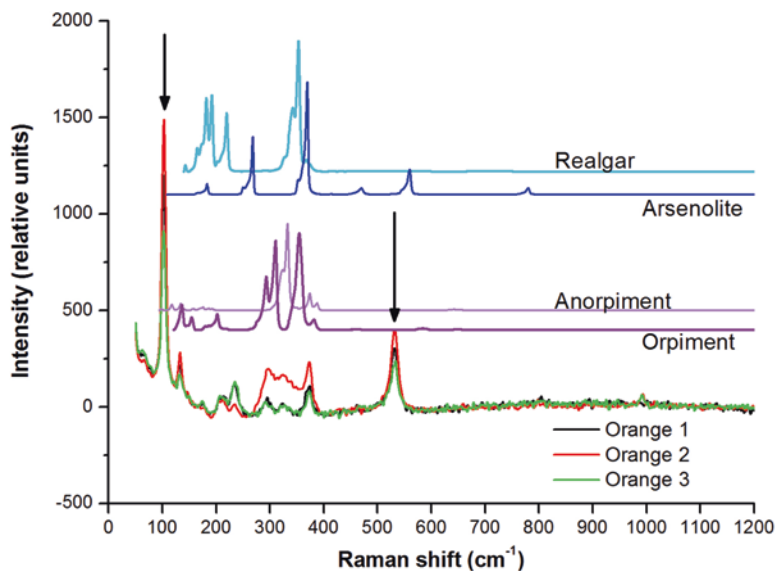


Fig. 7.7 Raman spectra of the uppermost orange layer and RRUFF database spectra of realgar, arsenolite, orpiment and anorpiment. The arrows indicate spectral lines that are attributed to some additive different from any of the above arsenic pigments. (According to the spectra from Vermeulen [19], fig. 4, the indicated peaks cannot originate from pararealgar)

that contains orpiment; the second layer is a slightly darker yellow, also mainly containing orpiment and furthermore some arsenolite. The uppermost layer is orange and is a mixture of orpiment, anorpiment, arsenolite, realgar, and a material that gives strong Raman bands at 116 and 542 cm⁻¹, and a wide band between 290 and 400 cm⁻¹. (Figs. 7.6a–b and 7.7) The anorpiment is a triclinic modification of orpiment [6], while the colourless arsenolite can form from orpiment following light exposure, similarly to realgar, which due to effects of light and air can become pararealgar, then arsenolite [2, 17].¹¹ According to the investigations of Vermeulen et al. various binders have different influence on the degradation of arsenic sulphide pigments [18]. With XRD analysis some gypsum was found in the bottom and in the top layers. The difference between the findings of XRD and the results of Raman analysis, can be derived from the different preparation of the samples.

It was observed under UV on the microscopic cross-section, that the colour of, and the measure of, the pigments in the three layers are also different with the measures of the pigments of the uppermost layer are much smaller. (Fig. 7.6a, b) Whether the fineness of the grains plays a part in the orange colour of this layer, is a question requiring further investigations. Historical Persian treatises mentioned that, ‘If you wish the orpiment red, grind it first carefully, the more one grinds it dry

¹¹ It is a good evidence for this that the samples of the first yellow layer, covered with two other paint layers, did not contain any arsenolite, but samples from the uncovered part of the same paint contain arsenolite as well.

the redder is grows' ([7], 200). According to other authors it is more likely that the red orpiment mentioned in the above treatises is presumably realgar [8]. In plane polarised light the colour of the particles taken from the orange paint layer are orange-red; under crossed polarised light they have distinctive, strong orange internal reflection; hence, the body colour masks, the interference colours which is a phenomenon characteristic of realgar.

The painted surfaces of the wooden panels which were once bright blue became brownish or grey for nowadays. The main pigment of these paint layers is smalt, to which a mixture of collagen, gum and ovalbumin was used as binding medium, according to the results of ELISA tests. Several factors may affect the color change of the smalt pigment. Resin based coatings can influence the optical appearance of the paint layers bounded with collagen or egg, because they fill up the spaces between the pigment particles, thereby changing the light absorbing and reflective properties of the paint layer. Degraded coatings cause optical changes as well, while the components of the coating, penetrated into the paint layer, reacting with the binding media or with the pigments, can trigger processes that effect the colour of the pigment. Another phenomenon observed is the discoloration of the binding medium by the metal ions of the pigment. The smalt pigment often degrades through leaching of potassium, which leads to a change in cobalt coordination from tetrahedral to octahedral, and causes the loss of the blue colour. The reasons of the colour change of smalt were investigated and published by several authors, but most of them deal with smalt samples taken from European paintings ([10, 11], [16], 56–70). The few studies, dealing with painting technique of 'Damascus rooms' attributed the colour change of the smalt only to the optical effects of later added coatings. Although Scharrachs mentions that the pigment itself may change, she states that this has not yet been investigated and proven for this type of objects ([14], 171). Due to lack of this, the 'Damascus room' of the MAA gave a good opportunity to investigate the degradation of smalt on this rare type of object. Samples taken from blue paint layers, and reference samples of two smalt pigments were investigated by SEM-EDX and micro-Raman spectroscopy.¹² Varying degrees of potassium leaching from the pigment grains has been demonstrated by mapping, line profile and EDX measurements.¹³ (Fig. 7.8a–f, Tables 7.1 and 7.2).

Micro-Raman spectroscopy also successfully proved the potassium leaching, causing changes in the structure of the pigments. (Fig. 7.9) The investigation was carried out with a Thermo Scientific DXR Raman spectrometer, using a 780 nm laser. The symmetrical bending Si-O-Si vibrations, are at 460 cm^{-1} , and they appeared in all spectra with $1\text{--}2\text{ cm}^{-1}$ wavelength shifts. Another important vibration is Si-O⁻, which is coordinated with potassium, and its presence and intensity in the

¹²Very fine smalt, Kremer pigment; and smalt of unknown origin from the pigment collection of the NCCCT.

¹³The investigations were carried out by Attila Lajos Tóth and Petronella Kovács Mravik with a HEOL JSM25 SEM/Brucker Quantax EDX, and by Dániel Károly with a Hitachi S-4700 FE-SEM/EDX, in the frame of his BA studies at the University of Szeged, supervisor: Dr. Ákos Kukovecz, associate professor.

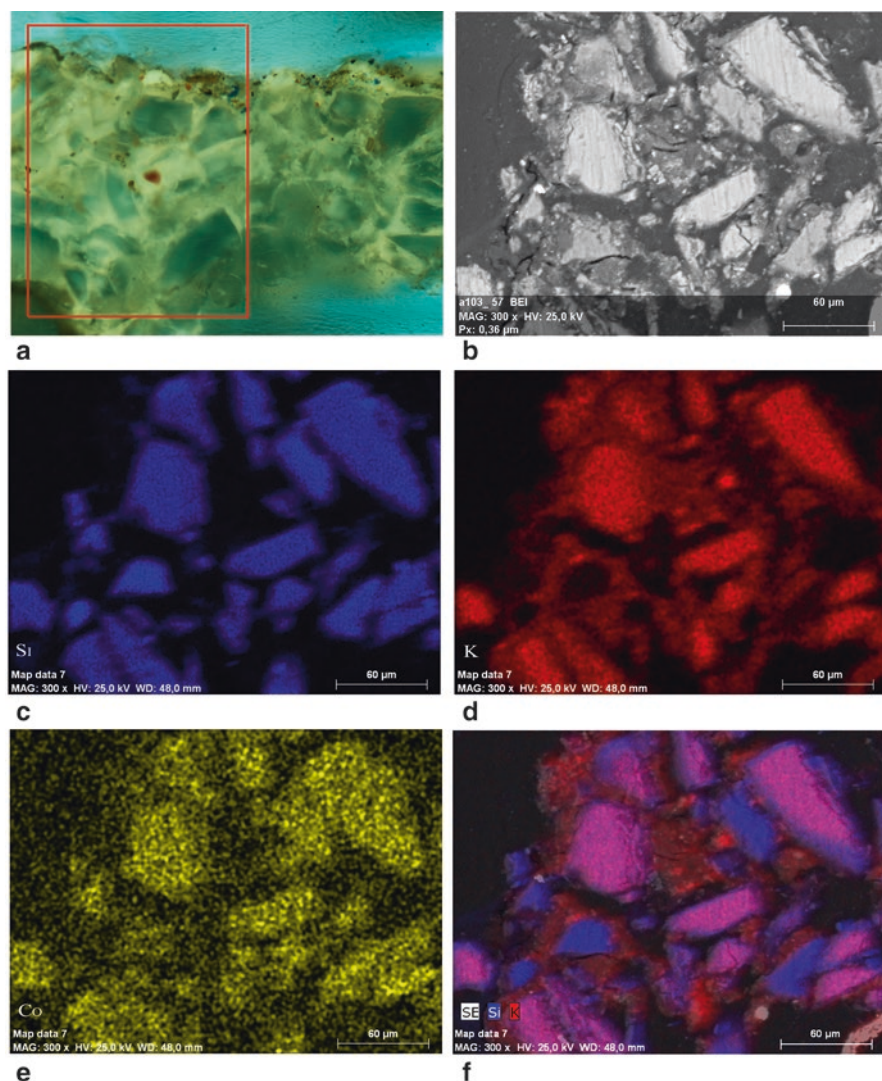


Fig. 7.8 (a–f) Cross section of a sample from the small layer under UV light (a) backscattered SEM image of it (b), EDX maps: of silicon (c), of potassium (d), of cobalt (e) and of silicon and potassium (f)

spectrum provides information on the amount of potassium that is coordinated to the pigment structure. This vibration was visible in each spectrum of the investigated pigments. It appeared in the Kremer smalt sample at 1095 cm^{-1} , that its intensity was broadly similar to the Si-O-Si vibration. (Fig. 7.9a) The spectra of the three altered pigment particles from the ‘Damascus room’ were broadly similar, but the deviation from the reference sample in Si-O⁻ was significant. (Fig. 7.9b–d).

Table 7.1 Results of the SEM-EDX investigation

Wt%	O	Na	Al	Si	P	S	Cl	K	Ca	Fe	Co	Ni	As	Pb
Elemental composition of some degraded smalt grains taken from the smalt-containing paint layer														
Grain core	44.85			30.30		3.92		7.52	4.34	2.63	1.13	1.59	3.71	
Grain rim	46.48			38.64				2.76	1.01	4.43	2.04	0.82	3.81	
Grain core	46.98			31.14	0.93	4.67	0.83	5.59	3.4	1.67	0.75	1.17	2.86	
Grain rim	45.91			33.62		2.92		2.92	5.8	2.2	3.37	1.6	3.83	
Grain core	45.18			37.07				3.5	1.29	5.11	2.42	0.93	4.49	
Grain rim	49.02			38.79		1.93	0.67	3.44	1.43	1.56	0.62	0.74	1.8	
Elemental composition of some degraded smalt grains taken from the light blue pigment layer containing also lead white														
Grain core	44.24			35.72			0.51	8.18	1.06	4.39	1.79	0.69	3.42	
Grain rim	46.95			39.13				2.73	0.79	4.37	1.91	0.88	3.25	
Grain core	45.8		0.52	37.27				5.25	0.94	4.22	1.74	0.77	3.49	
Grain rim	45.84			37.98				2.92	1.29	4.28	1.87	0.81	2.07	2.94
Elemental composition of reference smalt samples														
Kremer very fine smalt	62.46		0.61	28.41				5.59			2.89			
Kremer very fine smalt	59.4	1.22	0.62	26.41				8.19			4.13			
Smalt from the pigment collection	59.09	12.67	1.05	20.3				5.12		0.11	1.64			
Smalt from the pigment collection	61.38	5.29	0.87	28.37				3.91			0.16			

Table 7.2 Summary of analytical results

	Pigment/ colorant	Binder	Methods	Comments
Paint				
Red 1	Red lead, often in combination with vermilion	Ovalbumin, collagen, gums	PLM, SEM-EDX, ELISA	The ELISA is not suitable for detection of egg yolk and whole egg
Red 2	Vermilion	Ovalbumin, collagen, gums	PLM, SEM-EDX, ELISA	The ELISA is not suitable for detection of egg yolk and whole egg
Pink	Organic red lake (probable cochineal)/lead white	Collagen, gums	PLM, SEM-EDX, ELISA	SEM-EDX suggested Al and Ca content probable from the manufacturing technique of cochineal
Violet	Organic red lake	Ovalbumin, collagen, gums	PLM, SEM-EDX, ELISA	The ELISA is not suitable for detection of egg yolk and whole egg
Blue	Smalt	Ovalbumin, collagen, gums	PLM, SEM-EDX, RAMAN, ELISA	The ELISA is not suitable for detection of egg yolk and whole egg
Light blue	Indigo/lead white smalt/lead white	Ovalbumin (?) collagen, gums	PLM, SEM-EDX, RAMAN, ELISA	The ELISA is not suitable for detection of egg yolk and whole egg
Green 1	Indigo/Orpiment	Collagen, gums	PLM, SEM-EDX, RAMAN, ELISA	
Green2	Smalt/verdigris/lead white	Ovalbumin, collagen, gums	PLM, SEM-EDX, ELISA	The ELISA is not suitable for detection of egg yolk and whole egg
Yellow	Orpiment	Collagen, ovalbumin (?)	PLM, SEM-EDX, RAMAN, XRD, ELISA	The sample was taken from uncovered paint layer XRD detected some gypsum too. The ELISA is not suitable for detection of egg yolk and whole egg
Dark yellow	Orpiment/anorpiment	Collagen, gums (?)	PLM, SEM-EDX, RAMAN, XRD, ELISA	Mainly orpiment
Orange1	Various arsenic compounds	Collagen, gums (?)	PLM, SEM-EDX, RAMAN, XRD, ELISA	According to the results of RAMAN and XRD orpiment, anorpiment, realgar, pararealgar, arsenite, XRD detected some gypsum too
Orange2	Red lead/lead white/gypsum	–	PLM, SEM-EDX	

(continued)

Table 7.2 (continued)

	Pigment/ colorant	Binder	Methods	Comments
Black	Carbon black	Ovalbumin, collagen, gums	PLM, ELISA	The ELISA is not suitable for detection of egg yolk and whole egg
White	Lead white	Collagen, gums	PLM, SEM-EDX, RAMAN, ELISA	
White 2	Lead white/ gypsum		PLM, SEM-EDX	Used on top of the gypsum ground layer on the parts with cityscapes
Glazes				
Green	Verdigris	Drying oil- Pinacea resin	PLM, FTIR	Sample likely contaminated from uppevarnishes. Verdigris, based on the PLM investigation of grain particles, with Raman could not detected a clear spectrum of verdigris
Red	Cochineal (probable)	Drying oil- Pinacea resin	PLM, FTIR	Sample likely contaminated from uppevarnishes PLM: red organic pigment and small grains probable from the manufacturing technique
Orange	Aloe (probable)	Drying oil- Pinacea resin	PLM, FTIR	Sample likely contaminated from uppevarnishes PLM: round, drop-like, slightly brownish yellow particles, isotropic, refractive index: around 1.5
Yellow		Drying oil- Pinacea resin	PLM, FTIR	Sample likely contaminated from uppevarnishes. No pigments or colorants were found in the samples.
Blue	Smalte	Ovalbumin, collagen, gums	PLM, RAMAN, ELISA	The ELISA is not suitable for detection of egg yolk and whole egg
Preparation layer				
Ground and 'ajami	Gypsum	Collagen, gums		Sample likely contaminated from upper paint layer.
Metal leafs				
Tin			XRF, SEM-EDX	
Brass	5.9 at% Cu and 0.6 at% Zn		XRF, SEM-EDX	

(continued)

Table 7.2 (continued)

	Pigment/ colorant	Binder	Methods	Comments
Coating layers				
Uppermost coating		Pinacea resin	FTIR, RAMAN	
Lower coating			PLM	PLM: bluish-white under UV light on cross sections

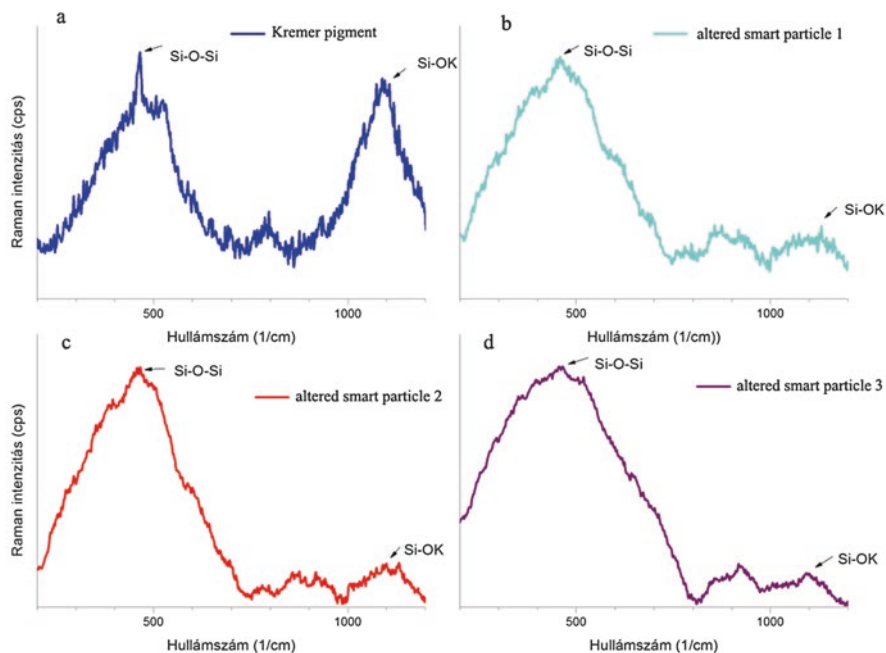


Fig. 7.9 Micro-Raman spectra of the Kremer pigment (a), and of three altered smart particles of micro-samples taken from the paint layer of the ‘Damascus Room’ of the MAA (b–d)

Most of the ‘ajami motifs on the “Damascus room” of the MAA are covered with tin foil, but the doors, ceilings, inscriptions, and curved tables also have parts decorated with brass leaf as well. The tin foils are overlaid with yellow, orange, red, green and blue glazes. According to the PLM investigation of the prepared particle samples smart gives the colour of the blue, verdigris of the green glaze, while the red and the yellow glazes are of organic origin, probably cochineal and aloe. Added colorant could not have been detected with PLM in the yellow glaze. The tin foil has turned dark in many places even under the glazes. Another corrosion phenomenon is that the brass leaf applied on ‘ajami parts have lost their metallic character, and now look like a greenish paint in appearance. (Fig. 7.5) The discoloration of the size and the gypsum layer and the remains of the brass leaf could be seen under UV on the cross-sections. The penetration of copper ions into the adhesive and the gypsum

layer was also revealed using SEM/EDX. Brass leaf applied directly on painted surfaces, such as some of the floral motifs, retained their shiny appearance.

Collagen was confirmed as the binding media for the ground layer, which correlates well with other studies of 'ajami interiors [1, 15]. However, traces of gums were also identified which are most likely the result of contamination from the paint layer above. For the pink, white/1, yellow/orange, and green/1 colours a mixture of collagen and gum was identified using ELISA, whereas for blue, black, white/2, red, green/2, light blue, and violet colours a mixture of collagen, gum and ovalbumin was analysed. Even though all of the samples from the Damascus room in Budapest were taken from the front of the panels, where the presence of later consolidation or coating layers was to be expected, the use of a distemper system (animal glue and a plant gum, some egg as an emulsifier and maybe even a little oil to produce matte and stable paint layers) was not unlikely. Recent ELISA analysis carried out on samples taken from the Damascus room in Dresden also identified gum, egg (ovalbumin) and collagen as components of two paint layers. In comparison to the extensive analysis of the Damascus room at the Metropolitan Museum in New York [1] where no gum was found, this finding might be indicative of a change of manufacturing techniques, as the room in the Met is nearly 100 years older than either the room in Budapest or the one in Dresden. Alternatively, it may also show a characteristic feature of the work of a particular atelier or artist, but more research needs to be done in order to clarify the finding in question. Historical Persian treatise do mention the use of gum Arabic for grinding pigments, however this material has also historically been used as a binding medium for both the painting of wood and paper ([7], 200).

7.4 Conservation Treatment

The 'Damascus room' has been assembled and dismantled several times in the past. Both the wooden support and the paint layers are affected by pest infestation, mechanical damage and environmental impact. Cracks and gaps in the wood have occurred. The paint layers have suffered blistering and peeling. Additionally, the characteristic light and bright appearance of the paint has become dark and dull, on account of later varnishing over of the entire panelling. The conservation program of the interior started in 2008 with the restoration of a frame of one of the niches as a degree project¹⁴ at the Hungarian University of Fine Arts. The other elements of the same wall of the 'tazar' were restored in 2012–2013.¹⁵ A mixture of bone and skin glue was used to repair the broken elements. The varnishes, and paints applied later, were removed with ethyl acetate, in some places with a 1:1 mixture of ethanol and acetone. Because of the similar solubility of both the varnishes and the glazes, this had to be done very carefully. Only a thin brownish layer, most likely caused by

¹⁴Restorer student: Attila Bodó, supervisor: hon. professor Petronella Kovács Mravik DLA

¹⁵Restorers: Petronella Kovács Mravik and Mária Fodor.



Fig. 7.10 The restored panelling of one wall of the ‘tazar’. (Image: G. Nyíri©MAA, Budapest)

the binding media of an earlier consolidation, remained on the surface after the removal. (Fig. 7.5). This layer could not be removed, due to its similar solubility properties to those of the original paint layers. This phenomenon has previously been observed in other Syrian interiors. Fish glue was used to consolidate the flaking paint layers; plaster of Paris mixed with animal glue was applied to make good the losses of ‘ajami and of the ground layer. A moderate retouching was carried out with watercolours on flat painted areas, and with pigments mixed with lacquer to match the lustre on the metal foils, employing a mixture of 120 g shellac, 20 g sandarac, 10 g mastic. Finally, the painted surfaces were coated with a protective layer of Paraloid® B-67 in white spirit. (Fig. 7.10).

7.5 Conclusion

This case study let to further information being collected regarding the manufacturing techniques and materials of similar rare objects whose preservation in their land of origin is now endangered due to the critical war and conflict. The techniques and materials identified are mostly consistent with those identified in previous studies. However, the use of plant gums in combination with animal glue and egg as a distemper system needs further study in order to clarify possible changes in manufacturing techniques or working practices. A comparative in-depth study of the ‘Damascus room’ of MAA and the other four rooms mentioned in this paper, which are all of a similar age, might assist in answering this question. The results of the investigations of the smalt pigment showed its degradation, which would draw attention to the application of aqueous solutions for cleaning surfaces painted with

this moisture-sensitive pigment. The glass-based pigment is sensitive also to dryness, so it is important to consider also this when storing items of the ‘Damascus room’.

References

1. Baumeister M., Edelstein, B., Rizzo, A., Gambirasi A., Hayes, T., Keppler, R. and Schultz, J. 2010. ‘A splendid welcome to the “house of praises, glorious deeds and magnanimity”’. *Conservation and the Eastern Mediterranean. IIC Contributions to the Istanbul Congress, 20–24 September 2010*. Rozeik, C., Roy, A. and Saunders, D. (eds), London: IIC. 126–133.
2. Daniels, V., Leach, B. 2004. The Occurrence and Alteration of Realgar on Ancient Egyptian Papyri. *Studies in Conservation* Vol. 49. No. 2. 73–84.
3. Dr. Boncz, Ö. 1886. ‘Az Iparművészeti Múzeum arab szobája’. *Művészeti Ipar*, 1885/1886. I. 201–207.
4. Fehérvári, G. 1955. ‘Islamic applied arts exhibition in Budapest’. *The Islamic Review*, London, November, 19.
5. Horváth H. 2007. *Gróf Pálffy János műgyűjteménye*. Művészettörténeti füzetek 29. Budapest: Akadémiai Kiadó, 45.
6. Kampf, A. R., Downs, R.T., Housley, R. M., Jenkins, R. A., Hyršl, J. 2011. ‘Anorpiment, AS₂S₃, the triclinic dimorph of orpiment’ *Mineralogical Magazine*, December, Vol. 75. (6), 2857–2867. DOI <https://doi.org/10.1180/minmag.2011.075.6.2857>
7. Minorsky, V. 1959 (trans) *Calligraphers and Painter: A Treatise by Qadi Ahmad, Son of Mir Munshi (circa ah1015/ad1606) 1606*. Freer Gallery of Art Occasional Papers, Vol. 3. No. 2. Washington DC: Freer Gallery of Art, 200
8. Purington, N., Watters, M. ‘A Study of the Materials Used by medieval Persian Painters.’ *JAIC*, Volume 30, Number 2, Article 2, 125–144.
9. Radisics, J. 1898. *Ideiglenes- kalauz. Az Országos Magyar Iparművészeti Múzeum Gyűjteményeiben*. 2nd ed. Budapest, 12.
10. Robinet, L. Spring, M., Pagès-Camagna, S., Vantelon, D., Trcera, N., 2011. ‘Investigation of the discoloration of smalt pigment in historic paintings by micro X-ray absorption spectroscopy at the Co-K edge.’ *Analytical Chemistry*, 83. 5145–5152.
11. Robinet, L. Spring, M., Pagès-Camagna, S. 2013. ‘Vibrational spectroscopy correlated with elemental analysis for the investigation of smalt pigment and its alteration in paintings.’ *Analytical Methods*, 5. 4628–4638.
12. Scharrahs A. 2010. ‘Insight to a sophisticated painting technique: Three Polychrome wooden interiors from Ottoman Syria in German collections and field research in Damascus.’ *Conservation and the Eastern Mediterranean. IIC Contributions to the Istanbul Congress, 20–24 September 2010*. Rozeik, C., Roy, A. and Saunders, D. (eds) London: IIC. 134–139.
13. Scharrahs, A. 2012. ‘Zur Kunsttechnik und Erhaltungsproblematik von polychromen Vertäfelungen in Empfangsräumen (ağamī-Zimmern) syrischer Stadthäuser des 17. – 19. Jahrhunderts’. Ph.D. Dissertation. Hochschule für Bildende Künste, Dresden
14. Scharrahs A. 2013 *Damascene ‘Ajami Rooms: Forgotten Jewels of Interior Design*, London: Archetype Publications
15. Schultz et al 2010: Schultz, J., Arslanoglu, J., Petersen, K. (2010): ‘The use of ELISA for the identification of proteins using the example of a Damascene reception room in The Metropolitan Museum of Art’, *Conservation and the Eastern Mediterranean. IIC Contributions to the Istanbul Congress, 20–24 September 2010*. Rozeik, C., Roy, A. and Saunders, D. (eds) London: IIC. 269.

16. Spring, M., Higgitt, C., Saunders, D. 2005. 'Investigation of Pigment-Medium Interaction Processes in Oil Paint containing Degraded Smalt.' *National Gallery Technical Bulletin*, 26. 56–70.
17. Trentelman, K., Stodulski, L., and Pavlosky, M. 1996. 'Characterization of pararealgar and other light-induced transformation products from realgar by Raman microspectroscopy'. *Analytical Chemistry*, 68. 1755–1761.
18. Vermeulen, M., Jansens, K., Sanyova, J., Rahemi, V., McGlinchey, Ch., De Wael, K. 2018a. 'Assesing the stability of arsenic sulphide pigments and influence the binding media on their degradation by means of spectroscopic and electrochemical techniques.' *Microchemical Journal*, 138, 82–91.
19. Vermeulen, M., Saverwyns, S., Coudray, A., Jansens, K., Sanyova, J. 2018b. 'Identification by Raman spectroscopy of pararealgar as a starting material in the synthesis of amorphous arsenic sulphide pigments.' *Dyes and Pigments*, 149. 290–297.

Chapter 8

An Original Approach to Active Climate Control Based on Equilibrium Moisture Content (EMC) as Set Point in a Middle-Age Building in Palermo, Italy



Paolo Dionisi-Vici and Daniela Romano

Abstract In the frame of a more sustainable approach to climate control, a long term strategy has been developed and is under advanced phase of implementation by technical staff of the University of Palermo in an important building, Palazzo Steri, owned by the University. The monumental room under climate control, the *Sala dei Baroni* (also known as *Sala Magna*), has a precious wooden ceiling where the previously loadbearing elements are covered with wooden painted panels. Many of them, painted in the fourteenth c, underwent important restorations in the past due to climate related damage (cracks, warpings, paint layer delamination) and biological infestations. The room is currently undergoing an important installation, using an HVAC system designed differently from the standard approach to climate control. The adopted design approach deals with the control of the air surrounding the wooden artifact as a function of the potential Equilibrium Moisture Content (EMC) that the panels could achieve. EMC is a synthetic parameter useful in correlating the response of panel paintings to climate fluctuations, and the behaviour of wooden objects may be better expressed as a function of EMC than to Relative Humidity (RH) fluctuations alone. Indeed, the correlation between a specified climate expressed with a parameter that takes into account both T and RH as experienced by wood is more correct. In this case-study the benefits of such an approach are even greater: due to the fact that it is possible to obtain the same EMC values with different combinations of Temperature and Relative Humidity values, the climate can be kept stable around the objects in the way the objects would feel it, meanings that the same EMC values (or hygro-mechanical stability of the artifacts) can be obtained in different seasons by adapting the Relative Humidity to the cor-

P. Dionisi-Vici (✉)
Free-lance conservation scientist, Massa, Italy
e-mail: paolo.dionisivici@gmail.com

D. Romano
University of Palermo, Palermo, Italy
e-mail: daniela.romano@unipa.it

responding EMC value, letting the system free to follow the Temperature seasonal variations without compromising its stability.

The expected improvements of such a design are:

- energy efficiency,
- greater stability,
- better use of the HVAC systems,
- better comfort for the visitors during the year, with smaller differences between the indoor and the outdoor climate.

Keywords Microclimate monitoring · Equilibrium moisture content · Sustainability · Preventive conservation · Wooden cultural heritage

8.1 Methodological Approach

The Equilibrium Moisture Content (EMC) is the moisture content that wood is able to achieve in a dynamic equilibrium with the environmental conditions (Temperature (T) and Relative Humidity (RH)) of the air where an artifact is placed. There are several equations that can be used to estimate this value using T and RH as data input; as an example we cite equations proposed by Hailwood-Horrobin [1] (Fig. 8.1), Brunauer, Emmett and Teller [2], Guggenheim-Anderson-de Boer [3–5], Avramidis [21], and Dionisi-Vici et al. [6].

Unlike the individual parameters considered separately, the EMC provides a family of isothermal curves experimentally determined and then processed accord-

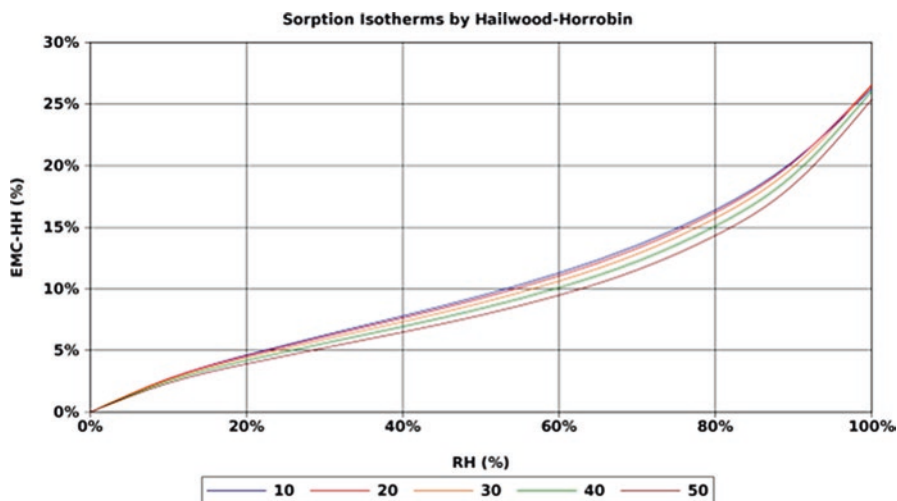


Fig. 8.1 The Hailwood-Horrobin wood isotherm curves

ing to mathematical model, taking into account the physical mode of interaction of the wood material with the RH and T that characterize the microclimate.

The premise of this work, that aims to minimize the effects of climatic variations on deformation response and related stress of wooden cultural heritage objects and to optimize the energy resources necessary to air-conditioning the exhibiting environment, relies on the assumption that there are multiple couples of T and RH that can achieve the same EMC.

While on the level of standards [7, 8] and in technical reference literature [ASHRAE, chapter 21] the interaction between RH and T are considered separately [9], and recommendations focus only on the maintenance of stable conditions of the two values separately in a more or less strict fluctuation range, this paper proposes to consider the values of EMC as benchmarks, achieving even large seasonal temperature changes that will be followed by the corresponding RH fluctuations in order to maintain a stable moisture content.

The benefits of such an approach are self-evident when considering the optimization of the use of resources for the operation of air conditioning systems, that can be run to achieve thermal conditions closer to external temperatures. A further benefit is provided by the well-being that the occupants of the museum site will experience, without being affected by the thermal shocks that normally occur at the entrance and at the exit of the museum sites in which rigidly fixed temperature values are pursued, without relation to the particular conditions of the area where the site is located. In this sense, this approach proposes a peaceful coexistence of conservation needs, sustainability from the point of view of energy usage and well-being of the visitors.

The current approaches to the choice of microclimate set points are decided on one hand on rigid climatic parameters set points [7] and on the other hand avoiding to actively control the microclimate, whenever verified (but *ex post* and with the difficulties tied to establish objective damage definition criteria [10]) that the previous so called “historical” climate has not produced visible damage to the object [8]. These two extreme approaches involve two different points of view, one focusing on the protection at any cost of the objects, the other one highlighting the benefits of a more environmentally and financially sustainable climate control, introducing the concept of the inevitability of degradation. The latter necessitates a philosophical approach that leaves curators to decide if “the progress of damage [is] considered insignificant” [11].

Other research has been carried out in order to investigate potentially different strategies about climate set points in museums and microclimate analysis in conditioned and uncontrolled exhibiting sites [12–14, 22]. New technological solutions for very stable active climate control in sealed micro-environments are being developed [15].

The strategy adopted in this work allows the thorough protection of wooden panels from the occurrence of mechanical damage related to thermo-hygrometric variations, without however forcing air conditioning systems to perform expensive cycles to maintain conditions that are in many cases unnecessarily energetically burdensome. This approach represents an uncommon integration of preventive conservation of wooden cultural heritage and active climate control design from an

engineering point of view, with the aim to adapt technology to the specific needs of wooden heritage.

The work has been performed in two phases. The first deals with an analysis of 1 year of microclimate data logged in the hall, in order to characterize the level of fluctuations; this kind of approach has become a useful mine of information for sophisticated analysis. The second part focuses on the choice of the range of climate fluctuations to be set as references for the new HVAC system and how its performance will be optimized according to the newly adopted approach.

8.2 Microclimate Analysis

In January 2004, a working group, made up of Profs. S. Barbaro, C. Giaconia and S. Trapani and Eng. Alessia Cusumano of the Department of Energetic and Environmental Research of the Engineering Faculty of the University of Palermo [16, 17], was appointed to carry out micro-climatic investigations in three important rooms of the University of Palermo, including the *Sala dei Baroni* (also called *Sala Magna*) (Fig. 8.2), that is often used as a conference room and may contain, according to the building's fire emergency plan, up to 150 people.

In order to carry out investigations, five cordless sensors have been installed in the *Sala dei Baroni*, attached to the intrados of the ceiling taking care not to damage the painted areas. Six more cordless sensors have been installed in the air space above the wooden ceiling, in consideration of what emerged from a phytosanitary and entomological survey conducted by the Faculty of Agriculture of the University of Palermo (see Table 8.1 and Fig. 8.3). These sensors logged Temperature, Relative Humidity and surface temperature, with a sample rate of 6 min.

For the detection of carbon dioxide concentrations, an anthracometric laser-absorption probe in the infrared range was installed inside the room, on the wall between the tenth and ninth beams, at 2.5 m from the floor, on the side of the wall facing the internal courtyard. Monitoring was carried out between January 2004 and January 2005 during the normal activities carried out in the hall. It is therefore a precious snapshot of the real conditions of the environment of the wooden ceiling prior to restoration.

In this work, written several years later, the analysis carried out on data acquired during the aforementioned monitoring is described; it aims to correlate the various parameters detected in order to formulate hypotheses on the causes of microclimatic perturbations and in particular those of logged RH.

In fact, since the RH affects the wood's moisture content much more than T, we can consider its excessive instability as potentially harmful because of the warping processes that it can induce on the painted panels. With this aim, we have firstly tried to identify the phases in which the RH changed abruptly over the course of a single day, reporting on a psychrometric chart the initial and final values of T and RH of the aforementioned transformations, in order to evaluate the sensible and latent heat components. RH and T were then compared with data from carbon dioxide probes in order to identify the days and hours involved in conferences or other



Fig. 8.2 The Sala Magna ceiling in Palazzo Steri, Palermo (Italy)

Table 8.1 list of the probes installed in the *Sala Magna* and the channel # of the single sensors (not used in the text)

Probe #	Temperature channel #	RH channel #
<i>Under the ceiling</i>		
5	23	24
1	14	12
10	11	13
6	15	16
9	29	30
<i>Over the ceiling</i>		
67	31	32
84	33	34
90	35	36
113	37	38
114	39	40
116	43	44

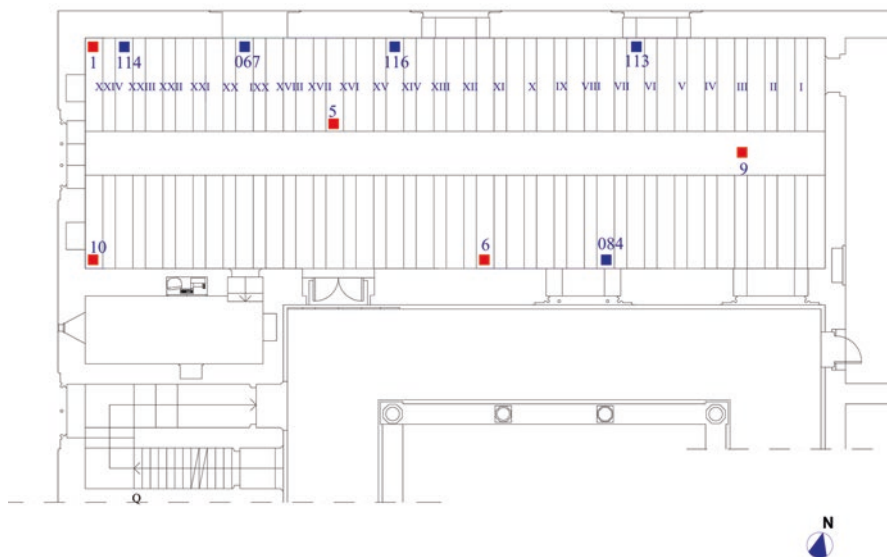


Fig. 8.3 Sensor distribution map on the ceiling: in red the sensors under the ceiling, in blue the ones over the ceiling

events and assess the impact of such events on the microclimate experienced by the wooden ceiling.

This analysis has been based on the distinction between the two different and coexisting modes of RH variation:

First, variations caused solely by changes in room temperature were considered. In these cases the absolute humidity air content remains constant and both Relative Humidity and Temperature vary.

This scenario can be ascribed to the heating by the fan coils or to the presence of cold or hot sources placed in the surrounding areas, like the pipes for heating and cooling of the upper room.

Second variations that do not depend on temperature changes but on air absolute humidity, i.e. the amount of vapor present in the air, expressed in grams of steam per kg of dry air, were examined.

In this second case, the input of perturbing elements coming from outside are presumed, such as:

- access to the hall of a conspicuous number of people, whose presence was detected during monitoring by the aforementioned anthracometric probe;
- input of more humid or drier external air that enters through the window frames and doors, as well as the permanent openings in the wall (see Figs. 8.4 and 8.5), like the rosettes of the three-light windows in the central window of the south-east wall, that have a total open area of about 0.3 square meters and are placed at an altitude of about 4.5 m from the ground. It can be estimated that the amount of air entering the room from the permanent openings can significantly modify, under certain conditions, its microclimate.



Fig. 8.4 Window with rosettes, south-east wall



Fig. 8.5 Door frame in the south-east wall

Usually both the above mentioned phenomena coexist, but in different proportions: therefore, on the psychrometric diagram showing the extremes of the variation, the mixed type transformation can be split in two different vectors.

8.2.1 Analysis of Data Collected by the Sensors Located Under the Ceiling During Winter Months

It should be noted that all the analyses were carried out starting from the hourly average values, without taking into account maximum and minimum values within each hour. The logged T values vary between 16 and 28 °C. The maximum values are reached during conferences. The RH values range between 20% and 60% (see Charts 8.1 and 8.2). It has been estimated from calculations made on the data collected by all the sensors that the RH remains below 40% for 30% of the monitoring period.

There are strong fluctuations in RH of up to 25% width over 24 h, but sometimes even within 3–4 h. Correlating the RH and T and carbon dioxide ones, three types of phenomena are revealed:

1. Significant decreases in RH occur together with sudden increases in temperature above the normal winter set-point (20–22 °C) without occupants and can be ascribed to the operation of the fan coils heating system, since in such cases absolute humidity variations are negligible and there are no variations of carbon

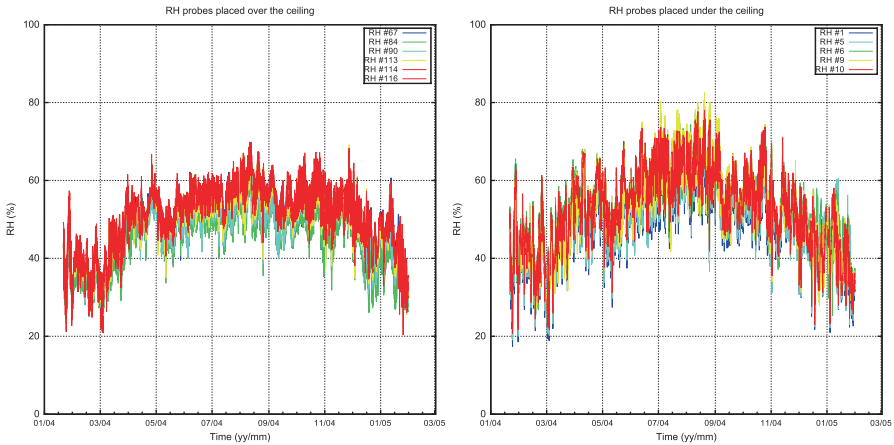


Chart 8.1 General view of the RH values logged by the sensors over (left) and under (right) the ceiling

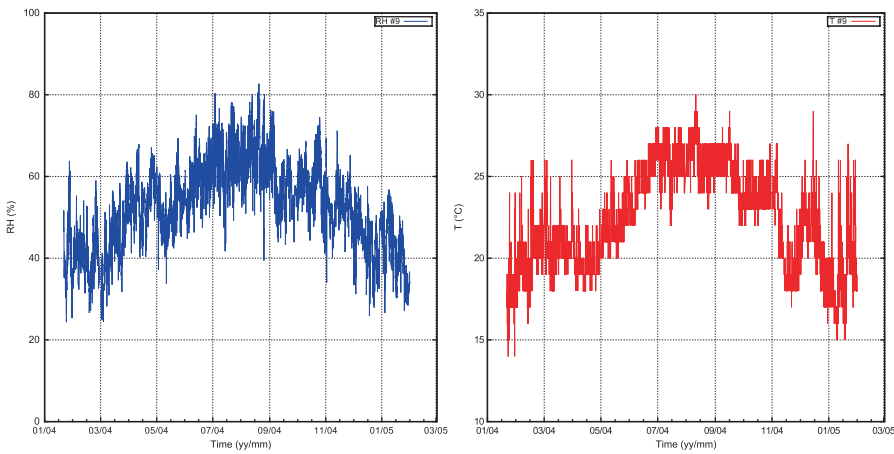


Chart 8.2 Sensor #9 RH (left) and T (right) values

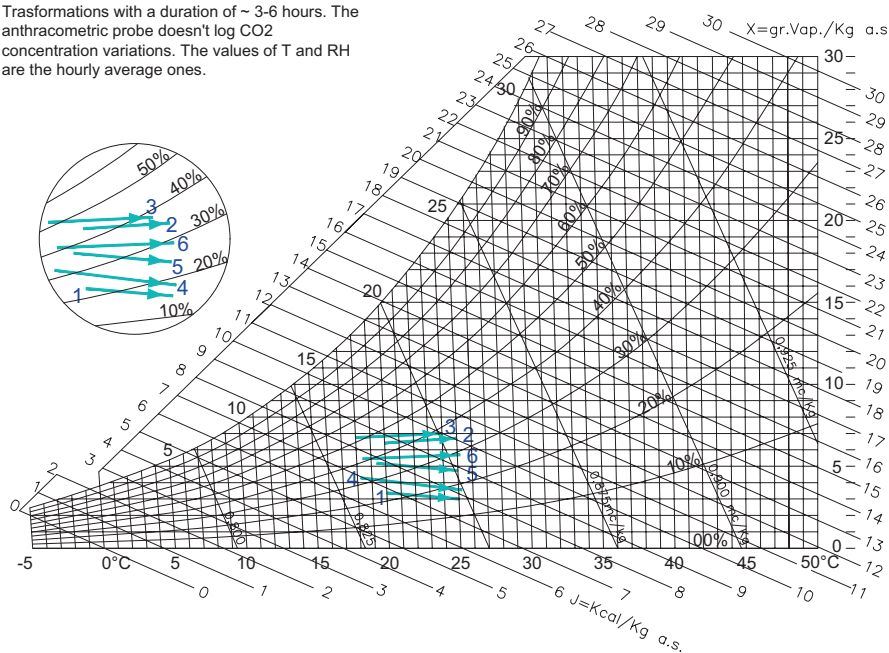
dioxide (see Chart 8.3, where the lines of the considered transformations tend to be parallel to the temperature axis).

2. When the room is occupied, in parallel to the increase in percentage of carbon dioxide, there is a considerable increase in absolute humidity which affects the RH due to changes in the room Temperature, that usually increases. In the hours following public events, the reverse process usually takes place, i.e. a rapid lowering of the temperature and absolute humidity (see Chart 8.4a).
3. At other times the variations in RH can not be related to the operation of the heating system since they mainly represent increases in latent heat and are not due to the presence of people. Furthermore, sometimes they happen at night: in this

CHART 8.3

WINTER MONTHS, PROBES CHANNELS: RH 30 AND T 29 (SENSOR #9).

Trasformations with a duration of ~ 3-6 hours. The anthracometric probe doesn't log CO2 concentration variations. The values of T and RH are the hourly average ones.

**LEGEND**

- 1) 04/01/05 11:00-13:00
- 2) 06/02/04 10:00-15:00
- 3) 16/02/04 08:00-15:00
- 4) 18/02/04 08:00-13:00
- 5) 03/03/04 16:00-20:00
- 6) 08/03/04 10:00-16:00

Chart 8.3 Psychrometric chart displaying the transformations in winter months without occupants as logged by sensor #9 and with fan coils operating in intermittent mode

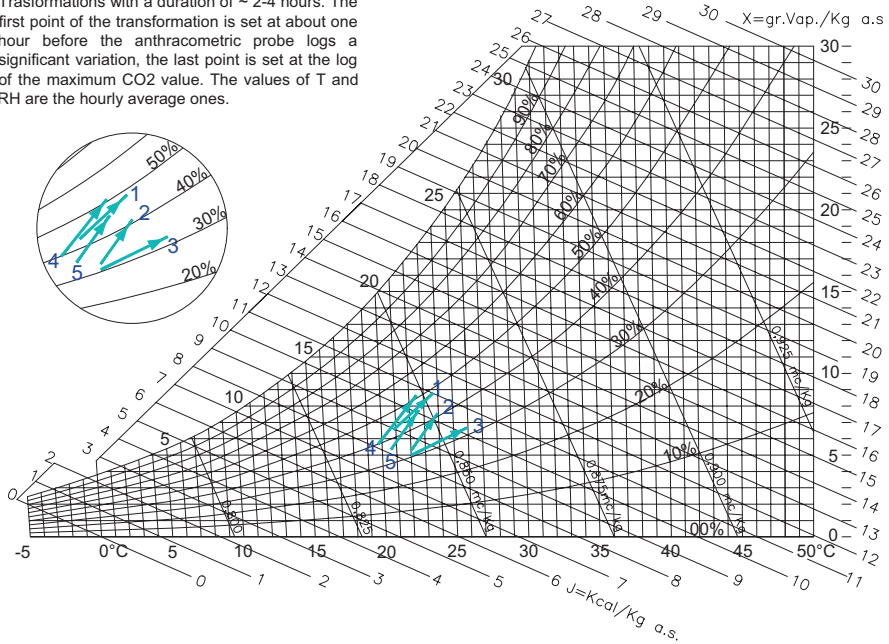
case it is possible to correlate them to the return of air from outside through windows or permanent openings.

Observing Chart 8.4b, it is evident that in these cases the lines of the considered transformations tend to become vertical.

CHART N. 8.4a

WINTER MONTHS, PROBES CHANNELS: RH 30 AND T 29 (SENSOR #9), DURING THE PUBLIC EVENTS.

Trasformations with a duration of ~ 2-4 hours. The first point of the transformation is set at about one hour before the anthracometric probe logs a significant variation, the last point is set at the log of the maximum CO2 value. The values of T and RH are the hourly average ones.



LEGEND

- 1) 12/01/05 09:00 - 13:00 (max CO2 value 1607 ppm)
- 2) 25/01/05 16:00 - 20:00 (max CO2 value 1840 ppm)
- 3) 27/01/05 18:00 - 20:00 (max CO2 value 1338 ppm)
- 4) 11/03/04 09:00 - 13:00 (max CO2 value 1212 ppm)
- 5) 13/03/04 09:00 - 13:00 (max CO2 value 1170 ppm)

Chart 8.4a Psychrometric chart displaying the transformations in winter months during public events as logged by sensor #9

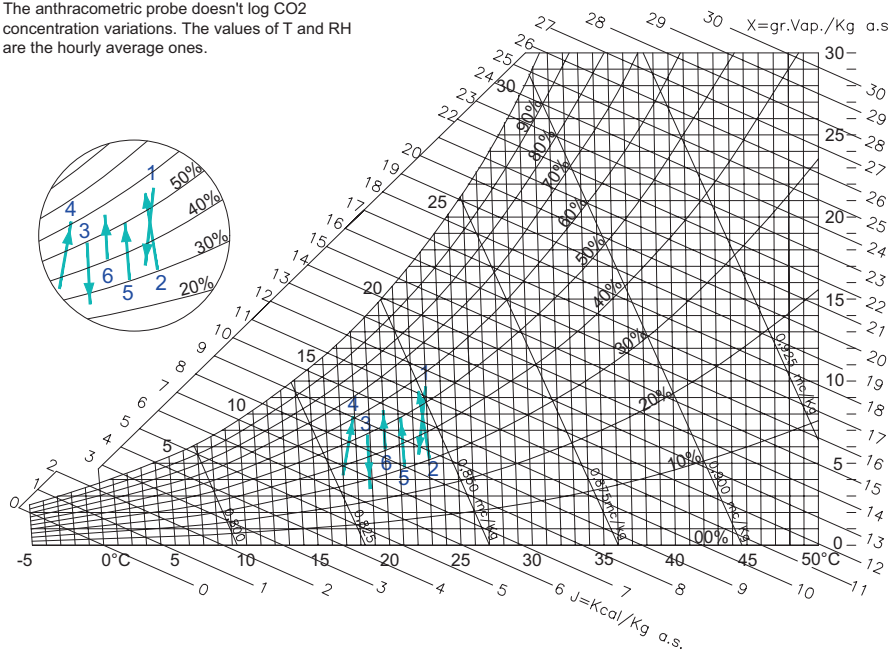
8.2.2 Analysis of Data Collected by the Sensors Located Under the Ceiling During Spring and Summer Months

In general, from April to July there is a progressive increase of Relative Humidity for which while even in May 70% is never exceeded, in July and August the value of 80% is sometimes exceeded. Even the minimum values increase, from 30% in the month of May, to 45% in the months of July and August, with some rare exceptions below this value (see Charts 8.1 and 8.2). Moreover, in the month of July and in August, the RH is between 60% and 75% for three quarters of the analyzed period. The daily trend of Temperatures is more uniform than during the winter months. However, the maximum daily temperature of the room increases gradually reaching 30 °C in July.

Significant drifts of RH within 24 h occur, similarly to winter period. These fluctuations become much more pronounced in the month of July and August. During

CHART 8.4b

WINTER MONTHS, PROBES CHANNELS: RH
30 AND T 29 (SENSOR #9)
Transformations with a duration of ~ 4 - 24 hours.
The anthracometric probe doesn't log CO₂
concentration variations. The values of T and RH
are the hourly average ones.

**LEGEND**

- 1) 03/12/04 01:00-06:00 (last conference 02/12/04 22:00-00:00)
- 2) 04/12/04 01:00-05:00
- 3) 03-04/01/05 21:00-10:00 (last conference 22/12/04 10:00-12:00)
- 4) 28-29/01/04 17:00-05:00
- 5) 22/02/04 00:00-22:00
- 6) 14/03/04 07:00-18:00

Chart 8.4b Psychrometric chart displaying the transformations in winter months without occupants as logged by sensor #9

congresses there is often a conspicuous increase in absolute humidity and also in Temperature, at least until the beginning of June; then in the hottest period, i.e. July, August and first half of September, Temperature increases are less wide while relative and absolute humidity fluctuations are more evident.

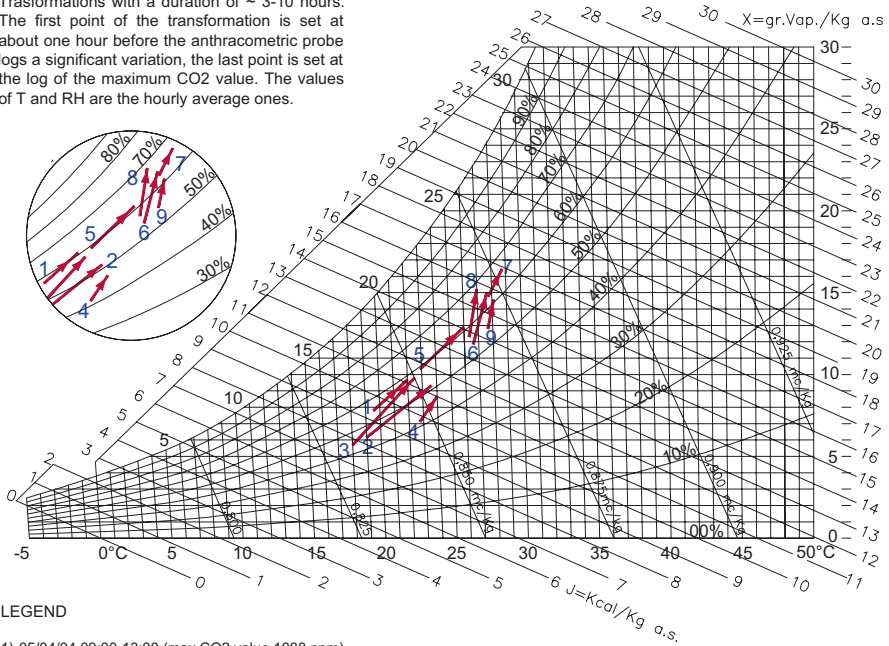
Looking at the diagram in Chart 8.5a, which highlights the transformations of the microclimate during the conferences in spring and summer, the transformations vectors tend to 'become vertical' in the hottest months: it is indeed possible that in these months the air conditioning system (fancoil-based) was in operation.

Exceptionally sometimes the conditions remained stable during a conference, i.e. during an event that occurred in the evening hours on July 17, 2004: in this case we can assume the presence of significant ventilation of the room through the window frames and the coexistence of external weather conditions, favorable to a sort of free-cooling.

CHART 8.5a

SPRING AND SUMMER MONTHS, PROBES CHANNELS: RH 30 AND T 29 (SENSOR #9), DURING PUBLIC EVENTS.

Transformations with a duration of ~ 3-10 hours. The first point of the transformation is set at about one hour before the anthracometric probe logs a significant variation, the last point is set at the log of the maximum CO2 value. The values of T and RH are the hourly average ones.



LEGEND

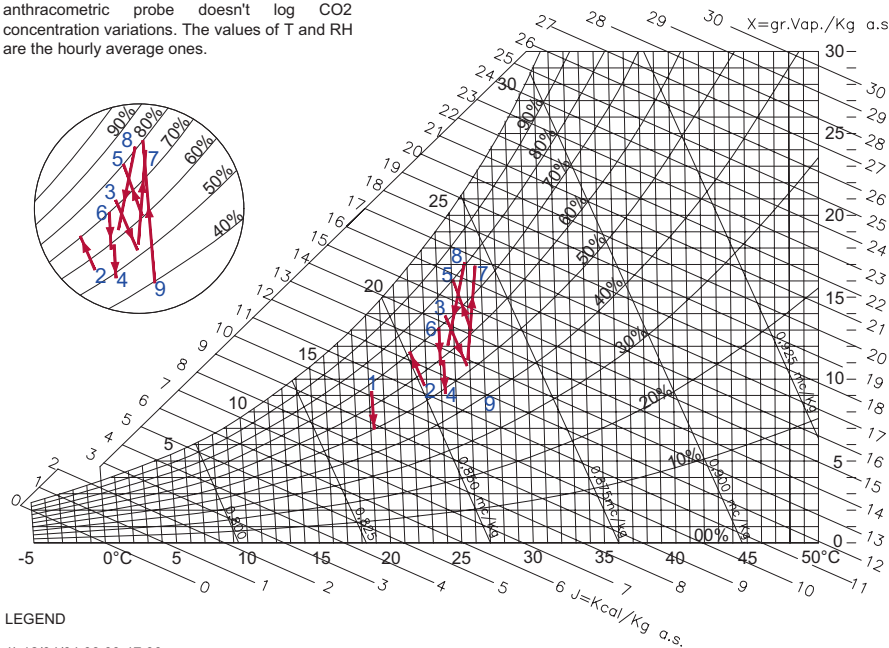
- 1) 05/04/04 09:00-13:00 (max CO2 value 1088 ppm)
- 2) 07/04/04 09:00-19:00 (max CO2 value 1018 ppm)
- 3) 15/04/04 08:00-17:00 (max CO2 value 1834 ppm)
- 4) 08/05/04 09:00-12:00 (max CO2 value 1051 ppm)
- 5) 07/06/04 08:00-12:00 (max CO2 value 1591 ppm)
- 6) 28/06/04 09:00-11:00 (max CO2 value 1105 ppm)
- 7) 01/07/04 09:00-17:00 (max CO2 value 716 ppm)
- 8) 09/07/04 07:00-11:00 (max CO2 value 1212 ppm)
- 9) 15/09/04 11:00-19:00 (max CO2 value 1826 ppm)

Chart 8.5a Psychrometric chart highlighting transformations of the microclimate during the conferences in spring and summer

Often the absolute humidity content varies independently from the presence of people (see Chart 8.5b): on August 26, 2004 over 24 h, RH passed from 39% to 80% (sensor # 9), while the temperature varied between 26 and 27 °C. The anthracometric probe does not detect the presence of people that day: it is therefore possible to hypothesize that this perturbation was due to the input of air with an unstable absolute humidity content.

CHART 8.5b

SPRING AND SUMMER MONTHS, PROBES CHANNELS: RH 30 AND T 29 (SENSOR #9).
Trasformations with a duration of ~3-17 h. The anthracometric probe doesn't log CO2 concentration variations. The values of T and RH are the hourly average ones.

**LEGEND**

- 1) 12/04/04 08:00-17:00
- 2) 21/05/04 08:00-20:00
- 3) 13-14/06/04 22:00-10:00
- 4) 20/06/04 06:00-09:00
- 5) 03-04/07/04 09:00-02:00
- 6) 16-17/07/04 15:00-08:00
- 7) 24/07/04 08:00-11:00
- 8) 13-14/08/04 03:00-07:00
- 9) 26/08/04 05:00-19:00

Chart 8.5b Psychrometric chart showing sharp variations, without presence of people; the variations were probably due to the input of air with an unstable absolute humidity content (probe #9)

8.2.3 Analysis Concerning the Data Collected by the Sensors Placed Above the Ceiling

In general, in the winter months the oscillation of RH it is between 20% and 60%, as in the case of the probes placed below the floor. In the spring and summer months the minimum values rise, generally remaining around 40%, as already observed for the microclimate logged below the floor. Also the maximum values tend to increase and to reach 60% in April and 70% in August, as visible in probe #114 (see Charts 8.1 and 8.6b).

The overall pattern of the microclimate in the space between the wooden ceiling and the reinforced concrete structure above is similar to that measured below. However, it should be noted that there are significant differences:

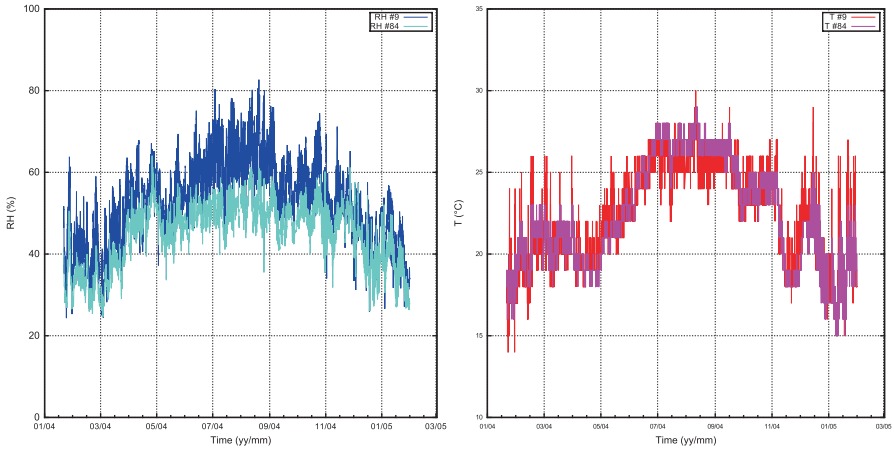


Chart 8.6a Comparison between the RH values (left) and T (right) of sensors placed over and below the ceiling (#9 and #84)

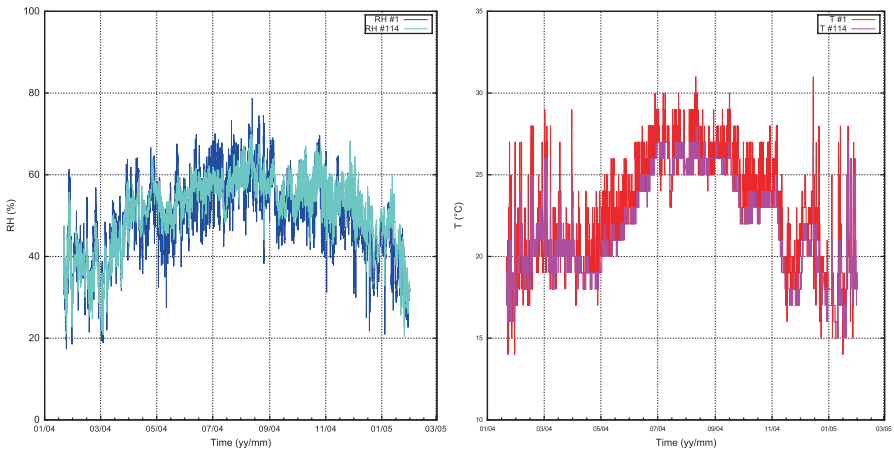


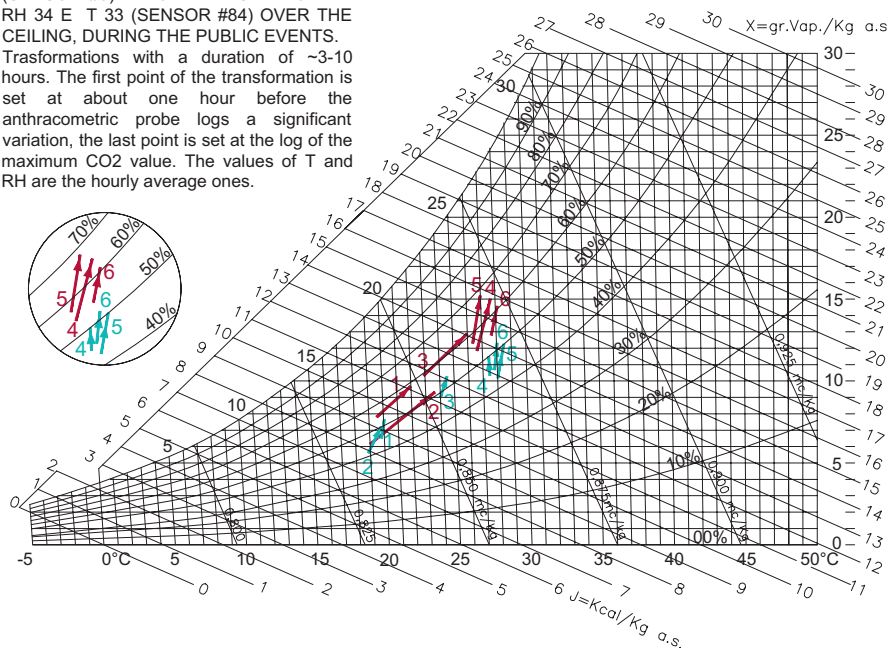
Chart 8.6b Comparison between the RH values (left) and T (right) of sensors placed over and below the ceiling (#1 and #114)

1. In the area below the floor the maximum RH, reached in the month of August, is about 82%, while in the upper space it never exceeded 70% (see Chart 8.1).
2. The absolute humidity oscillations detected by the probes placed above the floor resemble those occurring in the part underneath the floor, however they are considerably damped (see Charts 8.6a, 8.6b, 8.7a, and 8.7b).
3. Comparing the values of the two probes (n.114 and n.1), one placed over the ceiling and the other immediately below it, significant differences happened among the RH values logged at the same moment, sometimes exceeding 20% (see Chart 8.6b).

CHART 8.7a

SPRING AND SUMMER MONTHS,
 PROBES CHANNELS: RH 30 AND T 29
 (SENSOR #9) BELOW THE CEILING AND
 RH 34 E T 33 (SENSOR #84) OVER THE
 CEILING, DURING THE PUBLIC EVENTS.

Transformations with a duration of ~3-10 hours. The first point of the transformation is set at about one hour before the anthracometric probe logs a significant variation, the last point is set at the log of the maximum CO₂ value. The values of T and RH are the hourly average ones.



LEGEND

- 1) 05/04/04 09:00-13:00 (max CO₂ value 1088 ppm)
- 2) 07/04/04 09:00-19:00 (max CO₂ value 1018 ppm)
- 3) 07/06/04 08:00-12:00 (max CO₂ value 1591 ppm)
- 4) 28/06/04 09:00-11:00 (max CO₂ value 1105 ppm)
- 5) 09/07/04 07:00-11:00 (max CO₂ value 1212 ppm)
- 6) 15/09/04 11:00-19:00 (max CO₂ value 1826 ppm)

SENSOR #9 (BELOW THE CEILING)

SENSOR #84 (OVER THE CEILING)

Chart 8.7a Psychrometric chart showing variations during conferences in spring and summer, as logged by sensors #9 and #84

8.2.4 Conclusive Considerations

From the data reported above it can be highlighted that there are various thermohygro-metric dynamics inside the room that produce critical events both in the winter and in the summer months: very low values of RH were often logged in winter while in summer the opposite problem occurred, reaching thermohygro-metric values that involve a risk of mold growth on the wooden elements.

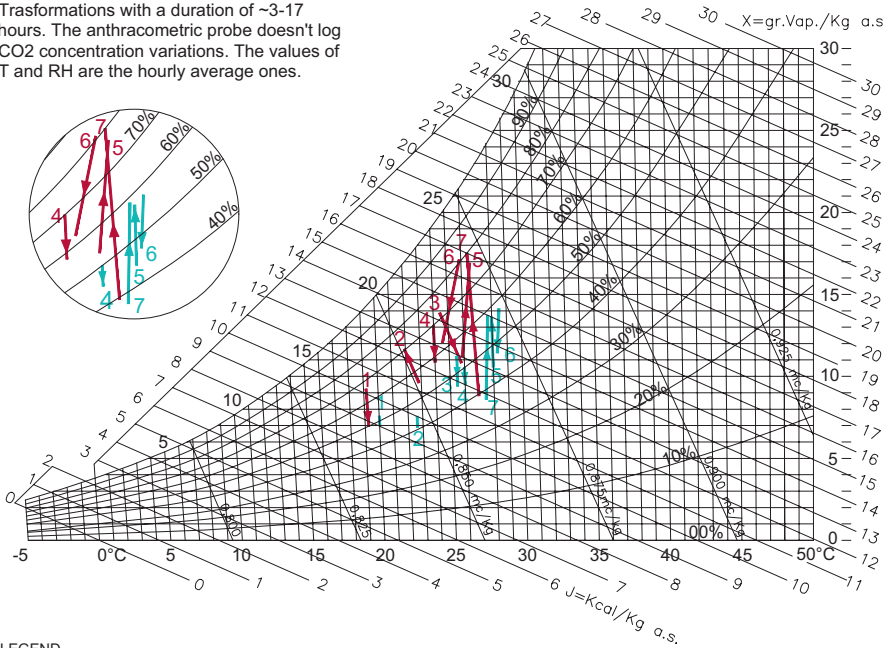
The calculated wood EMC values are also very close in summer to the thresholds that can make the wooden ceiling elements susceptible to biological attack (see Chart 8.8).

Strong daily fluctuations in RH occurred throughout the period considered, especially below the ceiling. These fluctuations are linked to different perturbation factors. Some hypotheses have been formulated that are summarized below:

CHART 8.7b

SPRING AND SUMMER MONTHS,
 SENSORS #9 E #84 (RH 30 E T 29, RH 34
 E T 33).

Trasformations with a duration of ~3-17 hours. The anthracometric probe doesn't log CO2 concentration variations. The values of T and RH are the hourly average ones.



LEGEND

- 1) 12/04/04 08:00-17:00 (last event 08/04/04 11:00)
- 2) 21/05/04 08:00-20:00
- 3) 13-14/06/04 22:00-10:00 (last event 12/06/04 10:00-12:00)
- 4) 16-17/07/04 15:00-8:00 (last event 09/07/04 09:00-17:00)
- 5) 24/07/04 08:00-11:00
- 6) 13-14/08/04 13:00-7:00 (last event 21/07/04 10:00-11:00)
- 7) 26/08/04 05:00-19:00

SENSOR #9 (BELOW THE CEILING)
SENSOR #84 (OVER THE CEILING)

Chart 8.7b Psychrometric chart showing the transformations in spring and summer, as logged by sensors #9 and #84.occupants

1. Conferences, the frequency of which can be seen in Chart 8.8, represent an important factor in the oscillation of absolute humidity and, in many cases, also of RH.
2. A second factor is the uncontrolled input of external air flows with a very unstable hygrometric content.
3. Lastly, it should be noted that the fan coil system, lacking of a humidity control system, besides not assuring a sufficiently stable level of RH, represents a source of considerable variation of RH in dry winter periods.

Such fluctuations can be a factor of increase of the degradation of the painted panels, the higher they are in intensity and frequency, due to the consequent phenomena of shrinkage and swelling of the supports following changes in potential

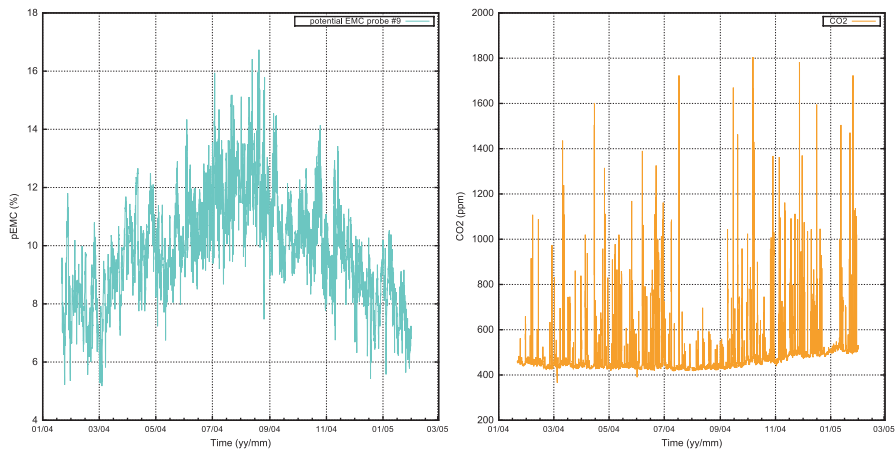


Chart 8.8 (left): RH and T integrated in the potential EMC line calculated from the values logged by sensor #9, (right): Distribution of events with presence of occupants obtained by the CO₂ concentration values logged by the anthracometric sensor



Fig. 8.6 Detail of a painted panel, with evidence of past degradation of the support

EMC. It is therefore appropriate to evaluate them carefully in order to implement, as far as possible, all the necessary corrective solutions.

8.2.5 Choice of the Range of Climate Fluctuations Adopted as Set Points of the New HVAC System

The design of the air conditioning system and monitoring of the *Sala Magna* has as its main goal the creation of an optimal microclimate for the conservation of precious painted panels that cover the ceiling of the room and the prevention of hygro-mechanical stresses and biological infestations that have seriously compromised the integrity of the painted surfaces and of their wooden supports (Fig. 8.6). The hall has long been used as a conference room and is currently heated with a fan coil system working at intermittent intervals and without an air renewal system.

The previously described micro-climatic data monitoring carried out in the *Sala Magna* between 2004 and 2005 has actually shown that, during the occupation of the room, RH between 70% and 80% has often been achieved, therefore exceeding the acceptable limits for the welfare of the occupants and creating extremely dangerous conditions even for mold growth on the building walls and on the wooden trusses of the ceiling. The potential EMC of the wood (converted using the Hailwood-Horrobin function) has fluctuated between 4% and 17%, with significant differences between the two faces of the painted boards. With the purpose of ensuring a geometric-dimensional stability of the painted panels it could be more efficient to maintain a stable moisture content of wood and to avoid thermo-hygrometric differences between the two faces of the boards, thus preventing or minimizing asymmetric moisture diffusion gradients in the panels.

Hence, from the system design point of view, reasoning on the interaction between T and RH can be particularly effective. Rather than moving within the ranges of independent and predetermined T and RH as proposed in standards, that in some cases could be very expensive and could also introduce dangerous conditions for the hygro-mechanical stability of the ceiling's painted panels when the system works on an intermittent regime.

The decision to refer directly to the EMC instead may allow for a more targeted use of energy resources. The Italian and international regulations that deal with the storage conditions of artistic objects, recommend RH fluctuations between ± 2 and ± 5 percentage points: a maximum range of 4% (in the range from 50% to 60% with no seasonal fluctuations) is required for example from [7]. With respect to the thermal oscillations the same standard prescribes a range of variation of only 1.5 °C (within the range from 19 to 24 °C) for painted wooden objects.

Analyzing these recommendations combining the values in a potential reference moisture content value using the Hailwood-Horrobin function (1956), it is evident that while a variation of 4% of RH in isothermal conditions produces a change of about 0.7% of EMC, a change of 1.5 °C at stable RH determines a difference of just

0.05% EMC. The progress and the lack of different models in describing the way wood achieves a moisture content in equilibrium with the surrounding air are the subject of a scientific review published in 2013 [18]. Even though this paper considers the Hailwood-Horrobin model as not deeply accurate in describing the sorption dynamic phenomena, it remains easily implementable at controller level. Furthermore, because of the small range of variations that will affect the ceiling, the delayed effects (hysteresis and mechano-sorption) will be negligible.

A broader range of T and RH is proposed by the ASHRAE Handbook [19] for the class of museum objects more exposed to the risk of mechanical damage called “AA”: $\pm 5\%$ without seasonal fluctuations while a seasonal fluctuation of temperature $\pm 5\text{ }^\circ\text{C}$ is allowed.

The opportunity of establishing wide seasonal variations in the room temperature actually allows a flexible adaptation to various needs, including the mitigation of the effects of the presence of occupants during conferences and energy savings in the room during closing periods, when the temperature can fluctuate widely, but still remain below the threshold of potentially harmful degradation processes. For instance, a variation of $10\text{ }^\circ\text{C}$ actually causes a variation of about 0.3% of potential EMC. This drift can be offset with small adjustments of the RH ($\sim 2\text{--}3\%$), without significant energy consumption. In this way it is possible to keep the moisture content of the painted panels stable, establishing an acceptable fluctuation range that will be experimentally determined thanks to a hygromechanical monitoring of the floor [20], necessary to evaluate its deformation response in different T-RH conditions.

When choosing the moisture content reference value to be kept, the microclimate parameters to which the ceiling of the *Sala Magna* has been preserved up to now must also be taken into account. Using *a priori* museum standards for particular artifacts, as the ceiling of the *Sala Magna*, does not guarantee the best results, both for energy efficiency and for conservation.

The local climatic conditions of the site, the specific thermodynamic behaviour of the building and the destination of the air conditioned rooms can require different energy saving criteria: for instance, a conference room in the Palermo climate in winter may often require a dehumidification process of the so-called “primary air”, i.e. the outdoor air, rather than humidification.

Therefore, during public events, the set points could be different from the ones adopted in Canada or in Northern Europe regions, where the need to humidify the outdoor air (with low absolute humidity values) in winter may determine a different set point strategy. Energy savings should therefore be pursued by developing algorithms that allow the building automation system installation to adopt from time to time the most convenient temperature set point as a function of the outdoor conditions, of the indoor microclimate and of the room’s use.

During the closing period of the room T will be free to fluctuate within much broader ranges, while the system will only adjust the RH in the ceiling air volume, which is 8 m high over the floor, in order to maintain the EMC values stable with no stress for the painted panels in the ceiling. It is important to stress that the RH will be the same over and below the wooden ceiling, thanks to the positive pressure of

the treated air, that flows from the upper part to the lower one through the existing gaps. The energy saved thanks to an appropriate choice of temperature can improve the efficiency of a continuous use of the air-conditioning system, thus assuring the stability of the exhibiting conditions of the artifact.

8.3 Conclusions

The proposed approach represents an innovation in the air-conditioning field aiming to a more sustainable preventive conservation of wooden cultural heritage without renouncing tight climate control. The experimental results obtained by a hygro-mechanical monitoring system applied to the wooden structure will allow accurate validation of the response of the panels to the conditions that will be established in the *Sala Magna*. Hopefully it will be possible to compare the response differences between uncontrolled (*ante*) and controlled microclimate (*post*) with the new air conditioning strategy. The results will be the focus of future scientific publications.

Acknowledgments This work has been carried out thanks to the support of Eng. Antonio Sorce, Technical Area Head, and Arch. Costanza Conti, Architectural Restoration Department Head from the Technical Area of the University of Palermo. The data provided by the 2004 monitoring have been a useful support for the technical decisions adopted in this intervention and the Authors thank therefore Professors Costanzo, Cusumano, Giaconia C., Giaconia G., Trapani and Barbaro for their precious work.

References

1. Hailwood, A.J. and S Horrobin. 1946. Absorption of water by polymers. Analysis in terms of a simple model. *Transactions of the Faraday Society*, 42B: 84–102
2. Brunauer, S., P.H. Emmett and E. Teller, 1938. Adsorption of gases in multi molecular layers. *Journal of the American Chemical Society*. 60: 309–319, DOI:<https://doi.org/10.1021/ja01269a023>
3. Guggenheim, E.A. 1966. *Applications of statistical mechanics*. Oxford: Clarendon Press.
4. Anderson, R.H. 1946. Modification of the BET equation. *Journal of the American Chemical Society*, 68, 689–691.
5. de Boer, J.H. 1953. The dynamic character of adsorption. 2nd Ed. Oxford: Clarendon Press
6. Dionisi-Vici P., M. De Vincenzi., and L. Uzielli. 2011, An analytical method for the characterization and the determination of the climatic distance of the microclimates for the conservation of wooden Cultural Heritage objects, *Studies in Conservation*, 56:41–57, DOI: <https://doi.org/10.1179/sic.2011.56.1.41>
7. UNI 10829: 1999, *Beni di interesse storico e artistico - Condizioni ambientali di conservazione - Misurazione ed analisi*, Italian Standard
8. EN 15757:2010, Conservation of Cultural Property - Specifications for temperature and relative humidity to limit climate-induced mechanical damage in organic hygroscopic materials

9. Jakiela, S., L. Bratasz, and R. Kozłowski. 2008. Numerical modelling of moisture movement and related stress field in lime wood subjected to changing climate conditions, *Wood Science and Technology* 42–1 21–37, DOI:<https://doi.org/10.1007/s00226-007-0138-5>
10. Strlič, M., D. Thickett, J. Taylor and M. Cassar (2013). Damage functions in heritage science. *Studies in Conservation*, 58(2), 80–87. doi:<https://doi.org/10.1179/2047058412y.0000000073>
11. Strojceki, M., M. Łukomski, L. Krzemień, J. Sobczyk and Ł. Bratasz. 2014. Acoustic emission monitoring of an eighteenth-century wardrobe to support a strategy for indoor climate management, *Studies in Conservation*, 59: 4, 225–232, DOI:<https://doi.org/10.1179/2047058413Y.0000000096>
12. Kramer, R.P., M.P.E. Maas, M.H.J. Martens, A.W.M. van Schijndel, and H.L. Schellen, 2015, Energy conservation in museums using different setpoint strategies: A case study for a state-of-the-art museum using building simulations, *Applied Energy* 158, 446–458, DOI: <https://doi.org/10.1016/j.apenergy.2015.08.044>
13. Anaf W. and O. Schalm, 2019. Climatic quality evaluation by peak analysis and segregation of low-, mid-, and high-frequency fluctuations, applied on a historic chapel, *Building and Environment*, 148, 286–293 DOI: <https://doi.org/10.1016/j.buildenv.2018.11.018>
14. Klein L. S. Bermudez, A. Schrott, M. Tsukada, P. Dionisi-Vici, L. Kargère, F. Marianno, H. Hamann, V. López and M. Leona, 2017. Wireless Sensor Platform for Cultural Heritage Monitoring and Modeling System, *Sensors*, 17(9), 1998, doi:<https://doi.org/10.3390/s17091998>
15. Allegretti O., and P. Dionisi-Vici 2018. Technological improvements in creating controlled thermo-hygrometric conditions in sealed microenvironments: the Dew Point Climatic Generator, 2018 *IOP Conf. Ser.: Materials. Science and Engineering*. 364 012026, doi:<https://doi.org/10.1088/1757-899X/364/1/012026>
16. Costanzo S, A. Cusumano, C. Giaconia, G. Giaconia, S. Trapani and S. Barbaro. 2004. La salvaguardia dei beni artistici e culturali. Un caso studio: la sede del Rettorato dell'Università di Palermo. Paper presented at 59° Congresso Nazionale ATI, Genova.
17. Costanzo S., A. Cusumano, C. Giaconia, G. Giaconia, 2006. Preservation of the artistic heritage within the seat of the Chancellorship of the University of Palermo: A proposal on a methodology regarding an environmental investigation according to Italian Standards, *Building and Environment*, 41, 12, 1847–1859 doi:<https://doi.org/10.1016/j.buildenv.2005.06.010>
18. Engelund E. T., L.G. Thygesen, S. Svensson, and C. A. S. Hill. 2013., A critical discussion of the physics of wood–water interactions, *Wood Science and Technology*, 2013, 47–1, doi:<https://doi.org/10.1007/s00226-012-0514-7>
19. ASHRAE Handbook, HVAC application, Chapter 21, 2007
20. Uzielli L., L. Cocchi, P. Mazzanti, M. Togni, D. Jullien, and P. Dionisi-Vici, 2012, The Deformometric Kit: A method and an apparatus for monitoring the deformation of wooden panels, *Journal of Cultural Heritage*, 13, 3, S94–S101, DOI: <https://doi.org/10.1016/j.culher.2012.03.001>
21. Avramidis, St. and J. F. Siau, 1987. Experiments in nonisothermal diffusion of moisture in wood Part 3, *Wood Science and Technology*, 21, 4, 329–334 DOI: <https://doi.org/10.1007/BF00367738>
22. Schito E., P. Conti, and D Testi, Robust microclimate control for artwork preservation in response to extreme climatic conditions: simulation of museum halls for temporary exhibitions with a validated dynamic tool, 2018. *IOP Conf. Ser.: Materials. Science and Engineering* 364 012008, DOI: <https://doi.org/10.1088/1757-899X/364/1/012008>

Chapter 9

The Influence of Low Temperature on Moisture Transport and Deformation in Wood: A Neglected Area of Research



Charlotta Bylund Melin

Abstract The aim of this paper is to compile knowledge on how wooden objects respond to cold, fluctuating indoor environments. Indoor environments, in less-climate controlled historic buildings, may be both cold and humid during winter as well as severely fluctuating on a daily and seasonal basis. The paper discusses both moisture transport as well as deformation of wood. It has been shown that moisture diffusion is retarded by low temperatures, due to lower vapour pressure, in comparison with higher temperatures. Some studies demonstrate that a change in moisture content and subsequent deformation is not aligned. In a fluctuating environment, wooden objects rarely, or never, reach a moisture content which is in equilibrium with the ambient air. Hence, the assumed maximum deformation will not be reached. This tendency is further enhanced by cold environments. High relative humidity, often associated with low temperatures, has a higher breaking strain than in the lower humidity ranges. It is possible that these combinations are the reason why wooden objects are in a fairly good state of preservation in less-climate controlled buildings. Focused research on these conditions are rare. Combined studies of moisture transport and deformation, *in situ* and in laboratories are needed to increase the knowledge on how to make the best preservation strategy for wooden objects in historic buildings and to reduce energy consumption.

Keywords Historic buildings · Wood · Relative humidity · Low temperature · Moisture content · Energy efficiency

9.1 Introduction

A significant number of heritage wooden objects are housed in historic buildings. In contrast to climate-controlled museums, the indoor environment in historic buildings is often more difficult to control to the same standards as in museums. Historic

C. B. Melin (✉)

Department of Preservation and Photography, Nationalmuseum, Stockholm, Sweden
e-mail: charlotta.bylund.melin@nationalmuseum.se; <https://www.nationalmuseum.se/en/>

buildings frequently have large interior volumes with a high air infiltration rate, which obstructs efforts to regulate indoor relative humidity (RH) and temperature [52]. The buildings themselves are often of high cultural heritage value and therefore interventions, such as installation of air conditioning plants or alterations to the building envelope to limit air infiltration, may be restricted. Heritage wooden objects in historic buildings, as in museums, are often on display, being part of immobile interiors, or for instance as a part of the liturgy in churches.

A variety of heating or climate-control strategies are found in historic buildings; background heating is often used to keep a low general temperature above the freezing point; intermittent heating is used by many churches and results in cold and humid climates during the weeks and higher temperature and reduced RH during Sunday services [35]. Conservation heating or hygrostatic heating uses the temperature to regulate RH [7]. There are also several examples of buildings which are dehumidified with no temperature control, for instance Läckö castle in southern Sweden [16]. Combinations and variations of these strategies exist, for instance background heating and intermittent heating in rural churches. There are buildings which have no active climate control and still keep cultural heritage collections, protected only by the building envelope. Hence, in temperate zones, these interiors are often cold and can reach sub-zero temperatures during parts of the year, often in combination with high and fluctuating RH. Finally, there are buildings which are heated to human comfort year-round without controlling RH, resulting in a very low RH in the winter periods. The term *dynamic indoor environment* used in this paper refers to the on-going, combined RH and temperature fluctuations on both daily, sometimes weekly or monthly as well as seasonal changes found in less-climate-controlled buildings (Fig. 9.1).

After World War II many churches and other historic buildings became permanently heated with their indoor climate changing from generally cold and humid to warmer and dryer. The consequence was alarming. Wooden objects, such as medieval altarpieces and polychrome sculptures of high cultural heritage value became desiccated and seriously damaged in a short period of time [14, 46, 51, 58]. In recent years it has been observed that painted wooden objects in non-heated historic buildings with an indoor environment far from the climate-controlled museums are often in a surprisingly good state of preservation [2, 13, 57].

It is known that extreme fluctuations of ambient RH and temperature are one major threat to objects of hygroscopic materials and substances. Objects made of hygroscopic, organic materials are particularly influenced by the indoor environment. Wood, for instance, responds to changes in the ambient air. With an increase in RH the material will gain moisture (adsorb) from the ambient air and swell; with a decrease in RH (desorption) the material will release moisture and shrink. If objects are restrained and changes in RH and temperature are large enough, mechanical deformation may become permanent and cause damage such as warping, cupping or cracking. High RH and temperatures also promote chemical and biological degradation. The moisture content (MC) in wood is defined as the mass of water in relation to the oven-dried wood, expressed as a percentage. In the hygroscopic range (0–99% RH), it includes only the bound water in the cell walls. Equilibrium mois-

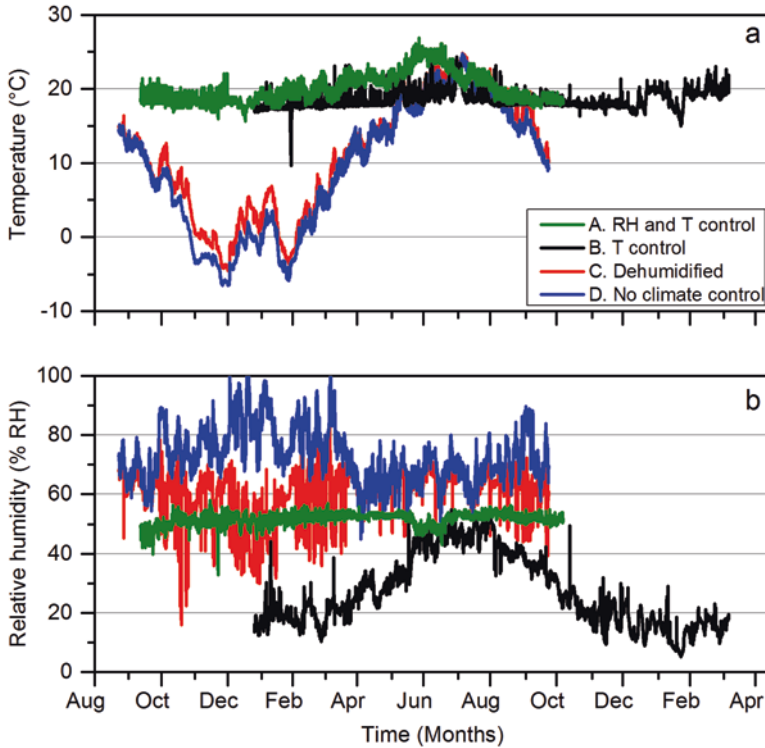


Fig. 9.1 RH and temperature during 1 year in different buildings with different types of climate control. (A) Illustrates a museum building environment with both RH and temperature control aiming to keep RH at 50% and temperature at 20 °C. (B) is a church environment with temperature control, programmed not to drop below 18 °C. RH is not controlled, resulting in very low RH during winter periods. (C) is a historic building with dehumidification which turns on if RH exceeds 70%. Temperature is not controlled and drops below 0 °C. (D) is the same building as C but from a part of the building with neither RH nor temperature control

ture content (EMC) is defined as the MC at which the wood is neither adsorbing nor desorbing moisture from the ambient air. This will only occur if RH and temperature is constant for a long-enough period of time for the wood to be fully acclimatised to the ambient air throughout. This may take a very long time and during real-life conditions it is uncertain if EMC is ever reached [25]. Instead, moisture gradients develop in the wood and during dynamic, fluctuating climate the MC profile constantly changes [20]. One would assume that deformation in wood would correlate with the adsorption and desorption of moisture of the ambient air. However, this is not always the case and these processes are often more complicated, as described for instance by Dionisi-Vici et al. [23]. An attempt to explain some of these processes are found in Bylund Melin [21].

The recommended climate ranges as they are known today are mainly derived from the results of laboratory experiments [2]. Extensive research has been per-

formed since the 1980s starting with systematically-performed laboratory experiments at the Smithsonian Institution among others [40]. The aim was to develop rational guidelines for the control of the air-conditioning systems in museums. The method was to determine the maximum deformation for a large number of materials to determine the elastic (reversible) range, meaning the maximum stress a material can undergo without exceeding the yield point, in order not to risk plastic (permanent) deformation. In these tests the response rate of a RH change was not critical. The maximum strains were found to be achieved at full EMC due to a change in RH. Experiments were primarily performed at room temperature [26, 41]. The conclusion of their work was that the yield point is approximately 0.4% for most polymers. Using the yield point as the limit, variations within the range 30–60% RH are mechanically safe for general collections [41, 44]. The yield strain has since been considered to be the threshold to what wood and other hygroscopic materials can withstand. Whilst the yield strain is rather constant in the entire RH range, the breaking strain (1.0–2.0%) is constant in the low and mid-RH ranges. Above 80% RH it dramatically increases [27]. Although these environmental ranges have been criticised for being too wide [28] the yield strain value has been regarded by others as very conservative considering that the wood can be stretched considerably more before it actually breaks [10].

These recommended climate ranges are aimed at museum collections. To a much lesser degree, have there been systematic studies of the conditions which apply for objects in historic buildings with indoor environments much different from climate-controlled museums. Such factors are the rate at which sorption and deformation occurs upon a change in RH and the influence of temperature on RH and MC. In wood science, for instance, which critically studies moisture transport in relation to wood drying, these factors are well known. Time-dependant sorption, which plays a significant role in the process, is crucial in drying wood without causing permanent damage. It is known that at low RH ranges, bound-water diffusion is a relatively slow process, and the moisture transport is governed by moisture diffusion (the movement of molecules from a region of high concentration to an area of low concentration). In the mid-RH range, a relatively fast sorption of bound water occurs. At high RH levels the bound-water diffusion becomes more predominant although the sorption rate decreases [38].

It seems clear that the temperature potentially has greater influence on deformation of hygroscopic, organic materials than to solely regulate RH of the ambient air. Solitary experimentation and modelling of the effect of low temperatures has been performed. It showed that lower temperature (5 °C) allowed larger fluctuations before critical strain was reached compared to critical strain at higher temperature (20 °C) Rachwał et al. [54]. However, these types of experiments are aimed to support mathematical modelling and hence they need to use full EMC values and assumed maximum deformation for the equations. In reality, especially during fluctuating environments, the effects are likely different. Here the impact of temperature on the actual rate of diffusion and deformation is vital. Response rate and response delay upon changes in RH and temperature, as well as stress relaxation, are other factors which influence the actual deformation. Despite the knowledge on the ben-

efits of low temperatures the area has not been studied in any detail. Factors such as critical temperature thresholds are not fully understood but are important for the preservation of hygroscopic objects and not least for energy efficiency measures in historic buildings.

The aim of this review paper is to focus on the influence of cold temperatures on RH and thereby also MC and subsequent deformation of wood exposed to cold temperatures as found in historic buildings.

9.2 Review

Low temperature has been reported to have a positive impact on wood in that it decreases the rate of chemical reactions as well as biological activity and therefore reduces the chemical and biological degradation of organic materials [9, 35, 47, 48]. It is also known that moisture diffusion is retarded by lower temperatures due to corresponding lower vapour pressure, which in turn reduces and delays deformation in wood [15, 33]. Unger et al. [64] pointed out that lower temperatures allow for larger RH amplitudes because the strength of wood increases with reduced temperatures.

Since the influence of RH and temperature on wood is closely related, the purpose of this section is to both describe the influence of temperature on moisture transport and deformation as a single parameter, as well as in combination with RH.

9.2.1 Interaction Between Temperature and MC

Wood has a low *thermal conductivity* (a measure of the rate of heat flow through the thickness of the material) and a low *thermal diffusivity* (a measure of how quickly a material can absorb heat from its surroundings) [31]. One approach to the varying temperature has been its potential to cause stress and dimensional change to materials in the same way as varying RH.

When subjecting dry wood (less than 3–4% MC) to changing temperatures it responds dimensionally: expanding on heating (thermal expansion) and contracting on cooling (negative thermal expansion). Wood at intermediate moisture levels (8–20% MC) will at first expand on heating because of increased distance between water molecules, due to an initial increased oscillation. Gradually the wood will shrink as it loses moisture at increased temperatures. Hence, for wood at usual moisture levels, the net change in dimension will be negative at elevated temperatures [31, 50]. Richard [55] describes that, at a constant RH, wood will have a higher EMC at a lower temperature and lower EMC at a higher RH. In a sealed package containing an oak panel, both a drop in RH as well as a slight shrinkage (0.08%) of the wooden panel occurs on a drop in temperature from 20 °C to 0 °C. Because the coefficient of thermal expansion (a measure for the relative

change in dimension caused by temperature change) is much smaller compared to moisture-related deformation, in the context of climate-induced mechanical damage, it is often ignored [31, 34, 40, 56]. According to Richard [55], a 20 °C change in temperature is equivalent to approximately 2.3% RH change. At low temperatures Michalski concluded that in the case of wood, the effect of a slightly higher EMC due to a lower temperature overrides the thermal shrinkage completely [45]. The dimension of wooden object is of course of importance. Because wood is a natural insulator, the larger the piece of wood, the more time is needed to equilibrate the core temperature with the ambient air, and further this does not change evenly [59].

However, the interaction between temperature and MC in wood on a macroscopic as well as and microscopic level is complex and not fully understood. According to thermodynamics, adsorption of moisture on the wood surface is accompanied by an evolution of heat (exothermic reaction) [3] and the opposite endothermic reaction is expected during desorption of moisture. In desorption experiments of wood, Avramidis et al. [5] observed that in the beginning of the experiments, just below the surface at which evaporation takes place, an increased moisture front developed which seemed to move towards the core of the specimen as desorption progressed. Traditionally, MC gradients have been assumed to be the driving forces for diffusion, but the authors stress the importance, when modelling moisture transport and gradients in wood under unsteady-state, non-isothermal conditions, to consider heat and moisture transport as coupled processes and thermally-induced mass transfer (The *Soret effect* or thermophoresis). Moisture transport which creates temperature and MC gradients in the material results in additional phenomena. One example is when the temperature on the surface of the wood is higher in comparison to the core simultaneously as MC is higher in the core compared to the surface; the moisture potentials will have opposite directions and, in some situations, may level each other out [30].

On the microscopic level, MC gradients are also found through the cell walls during moisture transport through the material. A phase change of water from vapour in the lumen to bound water in the cell walls, and the reverse will occur. This phase transition is followed by a change in temperature. In the case of adsorption, the released energy results in a local temperature increase. For desorption the situation is reversed [24].

9.2.2 *Temperature's Influence on Deformation*

Only occasional studies on the influence of temperature on deformation have been found in conservation science. However, Michalski [48] compiled information on incorrect temperatures for cultural heritage objects resulting in chemical and biological degradation as well as mechanical damage. From the perspective of indoor environments in historic buildings, low, fluctuating temperatures are most relevant. For low temperatures Michalski concluded that some materials, such as wood,

benefit from low temperatures while for instance acrylic paints and oil paints, often associated with wood, are more sensitive to low temperatures. According to the author, two situations which can lead to damage due to fluctuating temperatures are when the components of a complex assembly have different coefficients of expansion, and when an object is subjected to a fluctuation more rapid than its ability to respond to it. However, single fluctuations of 30–40 °C are not considered harmful. Sensitive materials will not suffer from fatigue stresses (progressive damage that occurs in materials subjected to cyclic loading) when subjected to daily fluctuations of 10 °C over thousands of years. Less sensitive materials can even tolerate fluctuations of 20–40 °C [48]. In wood science, thermal expansion coefficients can be considered independent of temperatures in the range –51 °C to 54 °C [31].

Studies show that creep (time-dependent deformation exhibited by a material under constant load) is higher at higher temperature levels and is accelerated by a temperature increase. However, the creep acceleration is difficult to study as the MC of the wood will also change with temperature [49]. Another laboratory experiment by Rachwał et al. [54] showed that the critical RH amplitude influencing a panel painting increased significantly at lower temperatures in that it increases the time of the panel to respond. The effect of lower temperature was more pronounced for short-term fluctuations and gradually less important for long-term fluctuations. This demonstrates that moisture diffusion is retarded by low temperatures.

However, it should also be mentioned that there are results on temperature dependence which are opposite to the above results showing that lower temperatures reduce deformation. A study by Yang et al. [68] investigating MC changes and dimensional responses of wood at constant RH (60% RH) with repeated step-changes in temperatures (25–40 °C) gave surprising results that contrast with those from other studies. The shrinkage coefficient showed that wood suffers 1.5 times as many dimensional changes per unit degree Celsius compared to unit % RH for samples of the same size. In another study by the same authors, their experiments showed that MC exchange due to fluctuating RH between 45% and 75% RH was lower at 40 °C compared to 25 °C, which was explained as due to the decrease in hygroscopicity of wood with increasing temperature that accompanies the loss of sorption sites [67].

9.2.3 *Sub-zero Temperatures*

One possible risk for wood located in sub-zero environments is freezing of water in the wood capillary, lumen and cells. Previously it has been assumed that liquid water could also exist due to capillary condensation below the fibre saturation point (FSP) in contact with ambient moisture [25]. However, nuclear magnetic resonance (NMR) analysis has shown that no significant amount of liquid water is present below 99.5% RH, as long as wood is only in contact with moisture from ambient air [63]. Therefore, it is uncertain if damage due to freezing of water actually occurs in wood. One of the few studies found of the influence of low and sub-zero

temperatures is by Hedlin [32]. He showed that, for 12 different types of wood species, EMC was substantially lower at 99% RH at $-12\text{ }^{\circ}\text{C}$ in comparison to the same RH at $21\text{ }^{\circ}\text{C}$. Therefore, wood stored under such cold conditions will tend to have a MC below that of the fibre saturation point (FSP) during the winter season. It has also been shown by Bodig & Jayne [8] that the E-modulus (a materials resistance to being deformed elastically (i.e., non-permanently) when a stress is applied to it) continues to increase below the freezing point and that the larger effect of low temperatures is more predominant in combination with higher MC ranges. Carrlee [22], who has reviewed the risks from low temperatures and freezing of museum objects, concluded that there should not be any significant structural damage to wooden objects which are repeatedly frozen for pest control.

9.2.4 *The Influence of Low Temperature on Painted Wooden Objects*

In the cultural heritage sector, wooden objects frequently have a painted, varnished or gilded surface. Studies have shown that for instance wooden panels painted on one side only are particularly sensitive to a changing RH. This is due to the paint layer creating a moisture barrier, resulting in asymmetrical moisture gradients and subsequent warping (out-of-plane deformation) of the panel [12, 23]. The influence of temperature on this complex problem has not been found.

However, research has been performed to study the impact of low temperatures on the various paint constituents. Varnishes, lacquers, oil, alkyd and acrylic paints are at risk when exposed to low temperatures. These materials show much lower dimensional response to temperature compared to RH and therefore low temperatures could be considered not to be harmful. However, paints such as acrylics, alkyds and oil, undergo a glass transition or phase transition (T_g) from *rubbery* via the *leathery* region to the *glassy* state at low temperatures, where these materials become very brittle. In this leathery region the materials are still able to partly deform elastically [42, 45]. The leathery transition can occur during a temperature interval from $0\text{ }^{\circ}\text{C}$ to $-30\text{ }^{\circ}\text{C}$ for different types of oils, with and without pigments, aged and not aged. Not until $-30\text{ }^{\circ}\text{C}$ does full glassy response occur [45].

Different studies give different information on the T_g for paints, which might be due to the large variety and constituents of paints that exist, in addition to age and history, which may also have influenced the paint. Traditional oil paints have a T_g of around $-15\text{ }^{\circ}\text{C}$ and for alkyd paints T_g is about $-5\text{ }^{\circ}\text{C}$ according to Mecklenburg and Tumosa [43]. Young and Hagan [69] tested a range of modern alkyd and acrylic primers and showed that, despite there being a variation among the tested paints, the E-modulus and ultimate tensile strength increased and the strain to failure decreased with temperatures ranging from $20\text{ }^{\circ}\text{C}$ to $-10\text{ }^{\circ}\text{C}$. T_g , was shown in this test to be $10\text{ }^{\circ}\text{C}$ for alkyds and $0\text{ }^{\circ}\text{C}$ for acrylics.

Fig. 9.2 Detail of a gilded picture frame. The grain of the wood is vertical in the picture and the craquelure run mostly horizontally in the gilded surface, which is perpendicular to the grain. This damage is therefore assumed to be a result of low temperatures



Damage to painted or varnished wooden objects subjected to low temperatures are according to Mecklenburg seen as craquelure in the surface layer, running predominantly perpendicular to the wooden grain (Fig. 9.2). The explanation for this behaviour is that the dimensional response of most materials to changes in temperature is low and remarkably consistent from one material to another. However, because wood has an anisotropic behaviour it will only deform to a minor degree in the direction of the grain upon a fall in temperature. In the cross-grain direction it will instead contract and thereby release stresses and strains in the surface layers in the cross-grain directions. Temperature-induced cracking in the varnished or painted layer can occur as soon as the object has reached the new temperature equilibrium [42].

Low temperatures and sub-zero temperatures are commonly used for museum objects for eradication of insect infestations or mould. During these circumstances the freezing process is of course thoroughly controlled in a way not occurring in historic buildings. In these situations, Strang [59] agrees that oil paint and polymers become brittle when cooled down to low temperatures. However, painted wooden objects down to $-20\text{ }^{\circ}\text{C}$ are considered safe. Below this point there is a small but real possibility of increased craquelure in painted and varnished objects. As mentioned earlier, wood that is only in contact with moist air does not contain liquid water [63] and therefore theoretical freeze/thaw cycles should not cause damage.

9.2.5 *Combined Effects of Low Temperatures and High RH*

During natural conditions a temperature change without a subsequent RH change is not likely to happen in any other environments than in a tightly-sealed and buffered show case or transport crate [53]. Therefore, in any natural environment there will always be an influence of temperature on RH and thereby MC, both on a daily as well seasonal basis. Because the RH and temperature levels in non-heated buildings vary with the seasons and in relation to each other it is not straightforward to separate the two parameters during dynamic conditions so as to be able to evaluate the impact of RH and temperature separately. Moreover, the moisture transport processes in the higher RH range are much more complex compared to the central RH range. The reason is that water vapour in the lumen and bound water in the cell wall are not always in equilibrium because diffusion of vapour is almost instant compared to bound water diffusion [37]. Experiments which study the mechanical impact on wood of low temperatures and high RH are few. Three considerations argue that this combination is likely to have a positive influence on wooden heritage objects:

- It has been shown that the rate of sorption is lower at higher RH range, which is opposite to the general belief that transversal diffusivities are constant or increase in the higher RH range [4, 33, 54, 65].
- Several studies have shown that moisture diffusion is retarded by low temperatures due to lower vapour pressure at lower temperatures. [15, 20, 33].
- Although the yield strain is rather constant in the entire RH range, the breaking strain which is constant in the low and mid-RH ranges dramatically increases above 80% RH. [10, 27].

To what degree this combined effect is beneficial or not is uncertain. Erhardt et al. [26] for instance, contradicts that high RH avoids mechanical damage because the material is softer and more flexible. Damage occurs but is more likely to lead to deformation rather than to fracture.

A few studies have observed the effect of combined effect of RH and temperature. Olstad [51] monitored deformation of wooden objects and wooden walls in two stave churches in Norway. One was heated and the other non-heated. The deformation in the non-heated church was lower compared to the heated church and Olstad also pointed out that the objects in the non-heated church was in better state of preservation compared to the heated church. Bratasz et al. [11] monitored the response of different parts of a polychrome sculpture in a church. On a sudden heating episode where the temperature was raised from 4 to 21 °C and RH subsequently dropped from 54% to 27%, the wood expanded during a time frame of approximately 2 h. It was explained as an initial response to temperature rise followed by shrinkage due to a RH reduction [11]. It is possible that this phenomenon was the *Sorets effect* described in Sect. 9.2.1. In a laboratory study investigating micro-displacements in the surface of a model painting, Bernikola et al. [6] observed that the deformation was larger upon desorption compared to adsorption. Monitoring

deformation of a nineteenth century icon, a linear relationship was found on a step-change from 23% to 58% RH at a constant temperature of 26 °C, but an exponential relationship when the temperature decreased from 34 °C to 22 °C and RH simultaneously rose from 22% to 47% RH. No explanation for this behaviour was given.

To specifically study the influence of the combined effect of RH and temperature on moisture transport in wood, a method was used whereby small RH and temperature data loggers were inserted in wood at different depths [19]. It showed that low temperature had a clear impact on moisture diffusion in wood. Low temperatures (7 compared to 25 °C) reduced the moisture diffusion rate, resulting in MC fluctuations inside the wood of smaller amplitudes, both regarding daily fluctuations and for step-changes. Further, the response delay increased at lower temperatures compared to higher temperatures. Combined fluctuating RH and temperature showed that, for daily fluctuations, the MC amplitude size was between those at constant 7 °C and 25 °C. Moreover, experiments showed that the effect of MC in wooden samples on daily RH fluctuations of the same magnitude with a set point of 50% RH at 20 °C were similar to situation with a set point of 70% RH at 7 °C. This confirms that low temperatures also at high RH levels retards sorption. [20].

Another approach is found through population studies to explore the cause and effect relationship between indoor environment and damage. In one study the state of preservation of 16 painted wooden pulpits were related to the energy consumption of the medieval churches the pulpits were located in. It showed slight correlations in that craquelure in the painted layers were less frequent in churches which had not been heated compared to those with larger energy consumption [17, 18]. An explanation for this may be found in a study by Erlebacher et al. [29] on the combined influence of low temperature and high RH. It showed the correlation between low temperatures and brittleness of acrylic paint. It suggested that there is a difference in T_g which is due both to RH and temperature. They noted that T_g was passed near 5 °C at 50% RH and 10 °C at 5% RH. The ambient moisture in the air would then act like a plasticizer, resulting in a lower T_g . This may even produce a lower T_g in the higher RH range, common in the winter periods in unheated historic buildings. Further, Unger et al. [64] showed that lower temperatures allow for larger RH amplitudes because the strength of wood increases with reduced temperatures.

9.3 Discussion

The results from most of the literature cited in this paper, along with the author's own work, suggest that low temperatures are beneficial for preservation of wooden objects. The combination of high RH and low temperature may also be less harmful than assumed.

However, not all studies are in favour of the advantages of low temperatures. The reported results on the effects of low temperatures vary from causing damage to varnish, paint or gilded layers on wood, to having no or little impact, or to be beneficial in combination with high levels of RH. Which temperature levels can be recom-

mended, or which should be avoided, must be studied in more detail. It is uncertain whether dynamic historic building environments are more harmful or less harmful to wooden objects than the environments commonly studied in laboratory experiments. During a full year, or more, in a less climate-controlled building, it is likely that there are periods that are both better and others which are worse compared to the yield strain scenario defined in laboratory-based studies.

The area of research is complex and does not always give clear research results. Common to objects found in both historic buildings and museums is that they are often of a substantial age and may have been subjected to a variety of different indoor environments, either because of transfers between different locations or due to changes of indoor environment in the one building. To link the damage and deterioration visible today to indoor environment is not a straight-forward task [60]. The environmental impact can result in chemical and biological deterioration or mechanical damage either as an individual response to deteriorating agents or as complex synergetic or antagonistic responses [36]. One way to tackle this problem is to reduce the number of variables in scientific experiments. However, the more the experiments are designed in order to be reproducible the less they resemble observations in reality [1]. Although, yield strain upon a step-change in RH or temperature can be measured accurately in laboratory experiments, this is much more complicated for actual objects. Mechanical damage, such as cracks, craquelure or detachment of paint layers, visible to a naked eye or using portable microscope, must be considered permanent damage as a result of strain to failure. Slight warping in wood can indicate either permanent damage or a transient elastic change wherein the material has not yet reached the yield strain. To distinguish between objects which have undergone permanent deformation or yield strains but not yet strain to failure appears thus to be difficult. Hence, at the moment this correlation between laboratory experiments and actual damage to objects in their own environments is missing. Therefore, in order to fully understand how wooden objects respond to the indoor environment, it is suggested that laboratory experiments and modelling be complemented with, and closely related to, observations and monitoring of actual objects and experimental specimens in museums and historic buildings. As an example, the Getty Conservation Institute is currently working on the 'Managing Collection Environments Initiative' taking those aspects in to their research [62].

One could argue that to study moisture transport in wood is unnecessary because what is important is deformation. However, it is shown that the relationship between moisture diffusion in terms of weight change in wood and deformation is not always non-linear or consistent. In contrast to what would be assumed, deformation appears to occur faster than moisture exchange [23, 39]. Stress has also been monitored to remain in the wood also after EMC was reached [61]. Studying the two parameters simultaneously may therefore give a better understanding on the mechanisms behind deformation of dynamic RH and also the effect of temperatures.

Although conservation heating in historic buildings has been used for decades and been thoroughly investigated, a deeper knowledge on how hygroscopic materials respond to intermittent heating and dehumidification would also be valuable. Wessberg et al. [66] have shown that dehumidification is more energy-consuming

than conservation heating and also the more effective in reducing mould growth. If colder temperatures may be allowed in historic buildings, this will certainly influence energy efficiency measures.

References

1. Ashley-Smith, J., 2011. Risk analysis. In C. Caple, ed. *Preventive Conservation in Museums*. London: Routledge, pp.39–50.
2. Atkinson, J.K., 2014. Environmental conditions for the safeguarding of collections: A background to the current debate on the control of relative humidity and temperature. *Studies in Conservation*, 59(4), pp.205–212. doi: <https://doi.org/10.1179/2047058414Y.0000000141>
3. Avramidis, S., 1997. The basics of sorption. In *International Conference of COST Action E8, Mechanical Performance of Wood and Wood Products, Theme: Wood -water relations, Copenhagen Denmark, June 16–17 1997*. Copenhagen, pp.3–16.
4. Avramidis, S., 2007. Bound water migration in wood. In P. Perré, ed. *Fundamentals of Wood Drying*. Nancy: European COST, A.R.BO.LOR., pp.105–125.
5. Avramidis, S., Hatzikiriakos, S.G. & Siau, J.F., 1994. An irreversible thermodynamics model for unsteady-state nonisothermal moisture diffusion in wood. *Wood Science and Technology*, 28, pp.349–358. doi: <https://doi.org/10.1007/BF00195282>.
6. Bernikola, E., Nevin, A. & Tornari, V., 2009. Rapid initial dimensional changes in wooden panel paintings due to simulated climate-induced alterations monitored by digital coherent out-of-plane interferometry. *Applied Physics A*, 95(2), pp.387–399. doi: <https://doi.org/10.1007/s00339-009-5096-3>.
7. Blades, N., Lithgow, S., Staniforth, S. Hayes, B. 2018. Conservation Heating 24 Years On. *Studies in Conservation*, 3630, pp.15–21. Available at: <https://doi.org/10.1080/00393630.2018.1504457>.
8. Bodig, J. & Jayne, B.A., 1982. *Mechanics of wood and wood composites*, New York: Van Nostrand Reinhold Company Inc.
9. Bordass, W.T., 1994. Museum environments and energy efficiency. In M. Cassar, ed. *Museums Environment Energy*. London: HMSO Publications, pp.5–16.
10. Bratasz, L., 2013. Allowable microclimatic variations for painted wood. *Studies in Conservation*, 58(2), pp.65–79. doi: <https://doi.org/10.1179/2047058412Y.0000000061>.
11. Bratasz, L., Kozłowski, R., Camuffo, D., & Pagan, E., 2007. Impact of Indoor heating on painted wood: Monitoring the altarpiece in the Church of Santa Maria Maddalena in Rocca Pietore, Italy. *Studies in Conservation*, 52(3), pp.199–210. doi: <https://doi.org/10.1179/sic.2007.52.3.199>.
12. Brewer, A. & Forno, C., 1997. Moiré fringe analysis of cradled panel paintings. *Studies in Conservation*, 42(4), pp.211–230. doi: <https://doi.org/10.1179/sic.1997.42.4.211>.
13. Brunskog, M., 2003. *Japanning in Sweden 1680s–1790s. Characteristics and preservation of orientalized coatings on wooden substrates*. [Doctoral thesis]. University of Gothenburg. Acta Universitatis Gothoburgensis, Gothenburg Studies in Conservation 11.
14. Brunskog, M., 2012. Paint failure as potential indicator of cool indoor temperature. In T. Broström & L. Nilsen, eds. *Postprints from the Conference Energy Efficiency in Historic Buildings, Visby February 9–11, 2011*. Visby: Gotland University Press 15, pp.30–36.
15. Buck, R.D., 1961. The use of moisture barriers on panel paintings. *Studies in Conservation*, 6(1), pp.9–20. doi: <https://doi.org/10.1179/sic.1961.003>.
16. Bylund Melin, C., Bjurman, J., Brunskog, M., & von Hofsten, A., 2010. Painted wood as a climate indicator? Experiences from a condition survey of painted wooden panels and environmental monitoring in Läckö Castle, a dehumidified historic building. In M. Sawicki, ed.

- Multidisciplinary Conservation: A Holistic View for Historic Interiors. Rome 23–26 March 2010. ICOM-CC Interim-Meeting.* Rome: ICOM.
17. Bylund Melin C, Legnér M. (2013). Quantification, the link to relate climate-induced damage to indoor environments in historic buildings. In *Ashley-Smith J, Burmester A, Eibl M, eds. Climate for Collections Standards and Uncertainties, Post Prints of the Munich Climate Conference, 7–9 November 2012.* London: Archetype Publisher Ltd.; 2013:311–323. Available at: http://www.doernerinstitut.de/downloads/Climate_for_Collections.pdf.
 18. Bylund Melin C. and Legnér M. 2014. The relationship between heating energy and cumulative damage to painted wood in historic churches. *Journal of the Institute of Conservation* 37(2):94–109, doi:<https://doi.org/10.1080/19455224.2014.939096>.
 19. Bylund Melin C., Gebäck T., Heintz A. and Bjurman J. 2016. Monitoring dynamic moisture gradients in wood using inserted relative humidity and temperature sensors. *E-Preservation Science*, 13:7–14. Available at: http://www.morana-rtd.com/e-preservation-science/2016/ePS_2016_a2_Bylund_Melin.pdf.
 20. Bylund Melin C. and Bjurman J. 2017. Moisture gradients in wood subjected to RH and temperatures simulating indoor climate variations as found in museums and historic buildings. *Journal of Cultural Heritage*, 2017, 25:157–162, doi: <https://doi.org/10.1016/j.culher.2016.12.006>
 21. Bylund Melin, C. 2017. *Wooden object in historic buildings: Effects of dynamic relative humidity and temperature.* [Doctoral thesis]. University of Gothenburg. Gothenburg: Acta Universitatis Gothoburgensis, Gothenburg Studies in Conservation 43. Available at: <https://gupea.ub.gu.se/handle/2077/54179>.
 22. Carrlee, E., 2003. Does low-temperature pest management cause damage? Literature review and observational study of ethnographic artifacts. *JAIC*, 42, pp.141–166.
 23. Dionisi-Vici, P., Mazzanti, P. & Uzielli, L., 2006. Mechanical response of wooden boards subjected to humidity step variations: Climatic chamber measurements and fitted mathematical models. *Journal of Cultural Heritage*, 7, pp.37–48. doi: <https://doi.org/10.1016/j.culher.2005.10.005>.
 24. Eitelberger, J., Svensson, S. & Hofstetter, K., 2011. Theory of transport processes in wood below the fiber saturation point. Physical background on the microscale and its macroscopic description. *Holzforschung*, 65, pp.337–342. doi: <https://doi.org/10.1515/hf.2011.041>.
 25. Engelund, E.T., Garbrecht Thygesen, L., Svensson, S., & Hill C.A.S., 2013. A critical discussion of the physics of wood–water interactions. *Wood Science and Technology*, 47, pp.141–161. doi: <https://doi.org/10.1007/s00226-012-0514-7>.
 26. Erhardt, D., Mecklenburg, M.F., Tumosa, C.S. & McCormick-Goodhart, M.H., 1995. The determination of allowable RH fluctuations. *WAAC Newsletter*, 17(1).
 27. Erhardt, D., Mecklenburg, M.F., Tumosa, C.S. & McCormick-Goodhart, M., 1997. The determination of appropriate museum environments S. Bradley, ed. *The British Museum Occasional Paper No. 116. The Interface between Science and Conservation*, 16, pp.153–163.
 28. Erhardt, D., Tumosa, C.S. & Mecklenburg, M.F., 2007. Applying science to the question of museum climate. In T. Padfield & K. Borchersen, eds. *Museum Microclimates, Contributions to the Conference in Copenhagen, 19–23 November 2007.* Hvidovre: The National Museum of Denmark, pp.11–18.
 29. Erlebacher, J.D., Mecklenburg, M.F. & Tumosa, C.S., 1992. The mechanical behavior of artists' acrylic paints with changing temperature and relative humidity. In M. C. Steele, ed. *AIC Painting Speciality Group: Postprints. Twentieth Annual Meeting of the American Institute for Conservation or Historic and Artistic Works, June 5th, 1992.* Buffalo, New York: AIC, pp. 35–41.
 30. Esping, B., 1992. *Drying wood 1a: Basics in drying.* [in Swedish]. Göteborg: Träteknik.
 31. Glass, S. V & Zelinka, S.L., 2010. Moisture relations and physical properties of wood. In *Wood handbook: Wood as an engineering material.* Forest Products Laboratory. General Technical Report FPL-GTR-190. Madison, WI: U.S. Department of Agriculture, Forest Service, Forest

- Products Laboratory, pp. 4:1–4:19. Available at: https://www.fpl.fs.fed.us/documnts/fplgtr/fplgtr190/chapter_04.pdf [Accessed January 16, 2019]
32. Hedlin, C.P., 1966. Sorption isotherms of twelve woods at subfreezing temperatures. *Forest Products Journal*, 17(12), pp.43–48.
 33. Håkansson, H., 1998. *Retarded sorption in wood: Experimental study, analyses and modeling*. [Doctoral thesis] Lund University. Report TABK --98/1012.
 34. Jakiela, S., Bratasz, Ł. & Kozłowski, R., 2008. Numerical modelling of moisture and related stress field in lime wood subjected to changing climate conditions. *Wood Science and Technology*, 42, pp.21–37. doi: <https://doi.org/10.1007/s00226-007-0138-5>.
 35. Klenz Larsen, P. & Broström, T., 2015. *Climate control in historic buildings*. Uppsala University and National Museum of Denmark. Available at: http://eprints.sparaochbevara.se/862/1/Climate_control_in_historic_buildings.pdf [Accessed December 27, 2019].
 36. Koestler, R.J. Brimblecombe, P., Camuffo, D., Ginell, W.S., Graedel, T.E., Leavengood, P., Petushkova, J., Steiger, M., Urzì, C., Vergès-Belmin, V. & Warscheid, T., 1994. How do external environmental factors accelerate change? In W.E. Krumbein et al., eds. *Durability and Change: The Science, Responsibility and Cost of Sustaining Cultural Heritage*. Chichester: John Wiley & Sons Ltd., pp.149–163.
 37. Lund Frandsen, H., 2005. *Modelling of moisture transport in wood: State of the art and analytical discussion*, Aalborg: Aalborg University. Available at: http://orbit.dtu.dk/files/115532281/ModOfMoistTransInWood_HLF.pdf [Accessed December 28, 2018].
 38. Lund Frandsen, H., 2007. *Selected constitutive models for simulating the hygromechanical response of wood*. [Doctoral thesis] Aalborg University. Available at: http://vbn.aau.dk/files/13648994/Selected_Constitutive_Models_for_Simulating_the_Hygromechanical_Response_of_Wood [Accessed December 28, 2018].
 39. Ma, E., Nakao, T. & Zhao, G., 2010. Technical note: Responses of vertical sections of wood samples to cyclical relative humidity changes. *Wood and Fiber Science*, 42(4), pp.550–552.
 40. Mecklenburg, M.F., 1991. Applied mechanics of materials in conservation research. *Materials Issues in Art and Archaeology II*, 185, pp.105–122.
 41. Mecklenburg, M.F., 2007a. Determining the acceptable ranges of relative humidity and temperature in museums and galleries: Part 1, structural response to relative humidity. *Report of the Museum Conservation Institution, the Smithsonian Institute*. Available at: <http://www.si.edu/mci/downloads/reports/Mecklenburg-Part1-RH.pdf> [Accessed January 3, 2019].
 42. Mecklenburg, M.F., 2007b. Determining the acceptable ranges of relative humidity and temperatures in museums and galleries: Part 2, structural response to temperature. *Report of the Museum Conservation Institution, the Smithsonian Institute*. Available at: <http://www.si.edu/mci/downloads/reports/Mecklenburg-Part2-Temp.pdf> [Accessed January 10, 2019].
 43. Mecklenburg, M.F. & Tumosa, C.S., 1999. Temperature and relative humidity effects on the mechanical and chemical stability of collections. *ASHRAE Journal*, (April), pp.69–74.
 44. Mecklenburg, M.F., Tumosa, C.S. & Erhardt, D., 1998. Structural response of painted surfaces to changes in ambient relative humidity. In V. Dorge & F. C. Howlett, eds. *Painted Wood, History and Conservation. Proceedings of a symposium organized by the Wooden Artifacts Group and the American Institute for Conservation of Historic and Artistic Works and The Foundation of the AIC, held at the Colonial Williamsburg Foundation*. Los Angeles: The Getty Conservation Institute, pp.464–483.
 45. Michalski, S., 1991. Paintings: Their response to temperature, relative humidity, shock, and vibration. In M. F. Mecklenburg, ed. *Art in Transit: Studies in the Transport of Paintings. Conference on The Packing and Transportation of Paintings, London 9–11 September 1991*. Washington: National Gallery of Art, pp.223–248.
 46. Michalski, S., 1993. Relative humidity in museums, galleries, and archives: Specification and control. In W. B. Rose & A. TenWolde, eds. *Bugs, Mold & Rot II. A Workshop on Control of Humidity for Health, Artifacts, and Buildings, November 16–17, 1993: Proceedings*. Washington DC: The National Institute of Building Science, pp.51–62.

47. Michalski, S., 2002. Double the life for each five-degree drop, more than double the life for each halving of relative humidity. In R. Vontobel, ed. *ICOM-CC, 13th Triennial Meeting, Rio de Janeiro, 22–27 September 2002, vol. I*. London: James & James Ltd., pp.66–72.
48. Michalski, S., 2009. Agent of Deterioration: Incorrect Temperature. *Government of Canada*. Available at: <https://www.canada.ca/en/conservation-institute/services/agents-deterioration/temperature.html> [Accessed January 18, 2019].
49. Mohager, S., 1987. Creep and relaxation of wood at constant and cyclic climatic conditions [in Swedish]. [Doctoral thesis] Tekniska högskolan, Stockholm.
50. New, B., 2014. The painted support: Properties and behaviour of wood. In N. Kos & P. van Duin, eds. *The conservation of panel paintings and related objects. Reserach agenda 2014–2020*. The Hague: Netherlands Organisation for Scientific Research (NWO), pp. 19–60.
51. Olstad, T.M., 1994. Mediaeval wooden churches in a cold climate: Parish churches or museums? In A. Roy & P. Smith, eds. *Preventive Conservation Practice, Theory and Research: Preprints of the Contribution to the Ottawa Congress, 12–16 September 1994*. London: IIC, pp. 99–103.
52. Oreszczyn, T., Cassar, M. & Fernadez, K., 1994. Compative study of air-conditioned and non air-conditioned museums. In A. Roy & P. Smith, eds. *Preventive Conservation Practice, Theory and Research: Preprints of the Contribution to the Ottawa Congress, 12–16 September 1994*. London: IIC, pp.144–148.
53. Padfield, T., Burke, M. & Erhardt, D., 1984. A cooled display case for George Washington's commission. In D. de Froment, ed. *ICOM Committee for Conservation, 7th Triennial meeting, Copenhagen, 10–14 September 1984: preprints*. Paris: ICOM in association with the J. Paul Getty Trust, pp.84.17.38–84.17.42.
54. Rachwał, B., Bratasz, Ł., Łukomski, M. & Kozłowski, R., 2012. Response of wood supports in panel paintings subjected to changing climate conditions. *Strain*, 48(5), pp.366–374. doi: <https://doi.org/10.1111/j.1475-1305.2011.00832.x>.
55. Richard, M., 2007. The benefits and disadvantages of adding silica gel to microclimate packages for panel paintings. In T. Padfield & K. Borchersen, eds. *Museum Microclimates, Contributions to the Conference in Copenhagen, 19–23 November 2007*. Hvidovre: The National Museum of Denmark, pp.237–243.
56. Richard, M., 2011. Further studies on the benefit of adding silica gel to microclimate packages for panel paintings. In A. Phenix & S. A. Chui, eds. *Proceedings from the Symposium Facing the Challenges of Panel Paintings Conservation: Trends, Treatments and Training, The Getty Center, Los Angeles, May 17–18, 2009*. Los Angeles: The Getty Conservation Institute, pp.140–147.
57. Schulze, A., 2013. How the usual museum climate recommendations endanger our cultural heritage. In J. Ashley-Smith, A. Burmester, & M. Eibl, eds. *Climate for Collections Standards and Uncertainties 2013, Post prints of the Munich Climate Conference, 7–9 November 2012*. London: Archetype Publisher Ltd., pp.81–92.
58. Staniforth, S., Hayes, B. & Bullock, L., 1994. Appropriate technologies for relative humidity control for museum collections housed in historic buildings. In A. Roy & P. Smith, eds. *Preventive Conservation Practice, Theory and Research: Preprints of the Contribution to the Ottawa Congress, 12–16 September 1994*. London: IIC, pp.123–128.
59. Strang, T.J.K., 1997. Controlling insect pests with low temperature. *CCI Notes*, 3(3), pp. 1–4. Available at: <https://www.canada.ca/en/conservation-institute/services/conservation-preservation-publications/canadian-conservation-institute-notes/controlling-insects-low-temperature.html> [Accessed February 3, 2014]
60. Strlič, M., Thickett, D., Taylor, J. & Cassar, M., 2013. Damage functions in heritage science. *Studies in Conservation*, 58(2), pp.80–87. doi: <https://doi.org/10.1179/2047058412Y.0000000073>.
61. Svensson, S. & Toratti, T., 2002. Mechanical response of wood perpendicular to grain when subjected to changes of humidity. *Wood Science and Technology*, 36, pp. 145–156. doi: <https://doi.org/10.1007/s00226-001-0130-4>.

62. The Getty Conservation Institute, 2015. Managing Collection Environments Initiative. Available at: http://www.getty.edu/conservation/our_projects/education/managing/overview.html [Accessed January 20, 2019].
63. Thygesen, L.G., Englund, E.T. & Hoffmeyer, P., 2010. Water sorption in wood and modified wood at high values of relative humidity. Part I: Results for untreated, acetylated, and furfurylated Norway spruce. *Holzforschung*, 64, pp.315–323. doi: <https://doi.org/10.1515/HF.2010.044>.
64. Unger, A., Schniewind, A.P. & Unger, W., 2001. *Conservation of wood artifacts: A handbook*, Berlin Heidelberg New York: Springer Verlag.
65. Wadsö, L., 1993. Measurements of water vapour sorption in wood. *Wood Science and Technology*, 28, pp.59–65. doi: <https://doi.org/10.1007/BF00193877>.
66. Wessberg, M., Leijonhufvud, G. & Broström, T., 2016. An evaluation of three different methods for energy efficient indoor climate control in Skokloster Castle. In M. de Bouw et al., eds. EECHB-2016, Energy Efficiency and Comfort of Historic Buildings, Brussels Belgium, 19th–21st October 2016. Brussels: Belgian Building Research Institute, pp. 144–150.
67. Yang, T. & Ma, E., 2016. Moisture sorption and thermodynamic properties of wood under dynamic condition. *International Journal of Polymer Science*, pp.1–8. doi: <https://doi.org/10.1155/2016/2454610>.
68. Yang, T., Ma, E. & Shi, Y., 2015. Dimensional responses of wood under cyclical changing temperature at constant relative humidity. *Journal of Korean Wood Science Technology*, 43(5), pp.539–547. doi: <https://doi.org/10.5658/WOOD.2015.43.5.539>.
69. Young, C. & Hagan, E., 2008. Cold temperature effects of modern paints used for priming flexible supports. In J. H. Townsend et al., eds. *Preparation for Painting: Artist's Choice and Its Consequences*, vol. 163. London: Archetype, pp.172–179.

Chapter 10

Conservation and Technological Research of a Polychrome Sculpture of *Christ on a Donkey* from the Workshop of Michel and Gregor Erhart



Katarzyna Męczyńska and Anna Michnikowska

Abstract The National Museum in Poznań (MNP) undertook research and restoration of a medieval sculpture Christ on a donkey. Research was undertaken following detailed observation of the sculpture's surface and interior as well as the X-radiographs. The examinations of wood fibres, grounds, pigments, binding materials and metals via microscopic and microchemical methods along with many stratigraphic cross-sections allowed the determination of the original polychromy under multiple underpaintings and to adopt an appropriate conservation program. The violet mineral fluorite was identified in the paint layer of Christ's robe by microscopy and SEM-EDS analysis. This pigment was used most frequently in Central Europe (Southern Germany, Lower Silesia, Bohemia and Austria) during relatively short period (1470–1520). Based on the discovery of fluorite, we were able to confirm the earlier attribution of the sculpture to the workshop of Michel and Gregor Erhart of Ulm.

Keywords Christ on a donkey · Sculpture · Wood · Conservation · Erhart · Fluorite · SEM-EDS · X-radiography

K. Męczyńska

Studio of Painting and Polychrome Sculpture Conservation, National Museum in Poznań, Poznań, Poland

e-mail: katarzynameczyńska@tlen.pl; <https://www.mnp.art.pl>

A. Michnikowska (✉)

Conservation and Technological Research Laboratory, National Museum in Poznań, Poznań, Poland

e-mail: a.michnikowska@mnp.art.pl

© Springer Nature Switzerland AG 2019

A. Nevin, M. Sawicki (eds.), *Heritage Wood*, Cultural Heritage Science, https://doi.org/10.1007/978-3-030-11054-3_10

10.1 Introduction

One of the most valuable exhibits of Medieval Art Gallery in National Museum in Poznań is Christ on a donkey sculpture (Figs. 10.1 and 10.2.), completed in the period between 1493 and 1494 in the workshop of Michel and Gregor Erhart of Ulm, southern Germany [5]. This solid, polychrome depiction became a part of the collection of the National Museum in Poznań and was registered in the museum handbook on 17 June 1945. It was transported from the stockpile in Gębice, nearby Czarnków in the Poznań voivodship, where during World War II the Nazi authorities stored works of art looted from different places. The sculpture's earlier history is unknown, but it is certain that its place of origin lies outside of Wielkopolska region.

10.2 History of Iconographic Depiction

The sculpture portrays Christ, sitting on a donkey and raising his right hand in blessing. His left probably held leather reins that are not preserved. Christ is dressed in a loose tunic, currently painted brown with a white trim. The donkey, with its head held low, is depicted standing stiffly on a platform that had once been wheeled to allow for the sculpture to be paraded. Holes drilled on both sides of the horse's



Fig. 10.1 *Christ on a donkey* (inv. no. MNP P 1), the sculpture before conservation treatment, ©MNP



Fig. 10.2 *Christ on a donkey* (inv. no. MNP P 1), the sculpture after conservation treatment, © MNP

muzzle confirm that it had once held a curb with reins attached in its mouth. The oldest known sculptural portrayals of Christ on a donkey are from the twelfth century C.E. They reached the height of popularity in fifteenth and the beginning of sixteenth c. in the German-speaking lands as well as northern Italy, Bohemia and Poland [[1], 169].

The sculpture was mobile, fastened to a wheeled platform and paraded around city streets on Palm Sundays during processions referencing biblical texts that describe Christ's arrival at Jerusalem. During the Reformation the processions with Christ on a donkey were considered idolatrous and were ultimately banned by the Catholic Church in 1782.

This type of sculpture is very rare in Poland. There are only 3 known, complete statues: in the National Museum in Kraków [2], the convent of the Order of Saint Clare in Stary Sącz, and the National Museum in Poznań. Each one of the aforementioned sculptures is of different construction. Christ's figure was hollowed out from its bottom side and was placed on the donkey's trunk that is made of two halves in the work from Kraków, while the sculpture from Nowy Sącz is solid according to the director Robert Ślusarek. Two other sculptures have been preserved only partially (Christ's torsos only) in the Tarnów Diocesan Museum, dated to the first half of sixteenth century from Nowe Rybie, as well as a work from Rzepiennik Biskupicollection in the storage of the National Museum in Kraków.

10.3 Construction, Manufacture Technique and the State of Preservation of the Sculpture

10.3.1 Methodology of Study

Conservation of the sculpture was informed by a complex research program. An examination of the technology and sculpting technique allowed the identification of both the original and secondary materials: wood, fibres, grounds, pigments, binders and metals.

The donkey's belly was opened along the old joints and thorough visual documentation of the interior was performed with numerous photographs of the interior and X-radiographs. This enabled the technical study of the interesting original construction, later additions, repairs and previous conservation efforts. Data obtained during this research strongly influenced the planning of conservation of the sculpture.

The following examinations were carried out:

1. Visual observations and photography of the sculpture and its interior under an raking and diffused daylight, carried out by Marek Peda, MNP.
2. X-ray examinations, undertaken by Roman Stasiuk (equipment Baltospot) and Wojciech Pawlicki, Euromed Poznań (equipment AJEX 240H, scanner FireCR+40).
3. Identification of wood and fibres under microscope by Anna Michnikowska (AM), Conservation and Technological Research Laboratory, National Museum in Poznań (MNP) and Małgorzata Zimniewska, Institute of Natural Fibres, Poznań
4. Stratigraphic cross-sections of samples (AM)
5. Examination of materials – grounds, pigments and binders – using microchemical and microcrystaloscopic methods (AM)
6. Examination of purple pigment from Christ's robe using SEM-EDS was carried out by Jacek Michniewicz, *Institute of Geology, Adam Mickiewicz University in Poznań*. A Hitachi S-3700 N scanning electron microscope (SEM) equipped with a *Noran EDS spectrometer*; analysis was performed in a low vacuum mode.

10.3.2 Construction and Woodworking

The sculpture measures: 150 × 145 × 40 cm. It stands on a wooden platform (length: 119 cm, width: 37.5–38.5 cm, thickness: 2.5 cm).

The statue was carved from lime wood and consists of 2 larger and 14 smaller pieces. The largest part is the body of the donkey from its rump to the muzzle, along with a part of the robe that covers Christ's legs down to his knees. This piece had been carved from a block of wood (45 × 45 × 150 cm), from a quarter of a trunk with

fairly regular annual rings, with the pith probably close to the animal's right side according to master carpenter Dominik Murawski. Another block was used for Christ's upper body part, from the hips to the head. A line between the two main parts is clearly visible.

The two main pieces were joined together in an interesting way. Inside the sculpture, Christ's body was connected with that of the donkey by a solid wooden block of a coniferous tree ($9 \times 9.5 \times$ approximately 18 cm), as seen in Fig. 10.3. The block was stabilized with splints. Upper and lower parts of sculpture are joined with an interior block with four long wooden dowels. The X-radiographs seen in Fig. 10.4 show that the tips of the dowels are rounded and their heads are square (1.4×1.4 cm).

The smaller pieces of the sculpture are the platform, the four legs of the donkey, its tail, ears, the lower part of its neck, Christ's left hand, his two feet and lower hems of his robe as seen in Fig. 10.5. The donkey's ears along with the feet and left hand of Christ are attached with dowels.

The sculpture contains three separate hollow spaces: the interior of the donkey as well as Christ's torso and head. Wood material was carved out from donkey's body from the side of the belly. Semicircular chisel marks are visible inside the statue (see Fig. 10.3). Hollow spaces in the Christ's head and his back were cut out from the back side of the sculpture. All hollow spaces were closed by fitted, rectangular,

Fig. 10.3 The block connecting the two main parts of the sculpture, marks of tools and the elements added during restoration visible inside the donkey's trunk and neck, © MNP



Fig. 10.4 An X-radiograph showing the join of the two main parts of the sculpture; wooden block, long dowels, inserts and fillings are visible, © R. Stasiuk

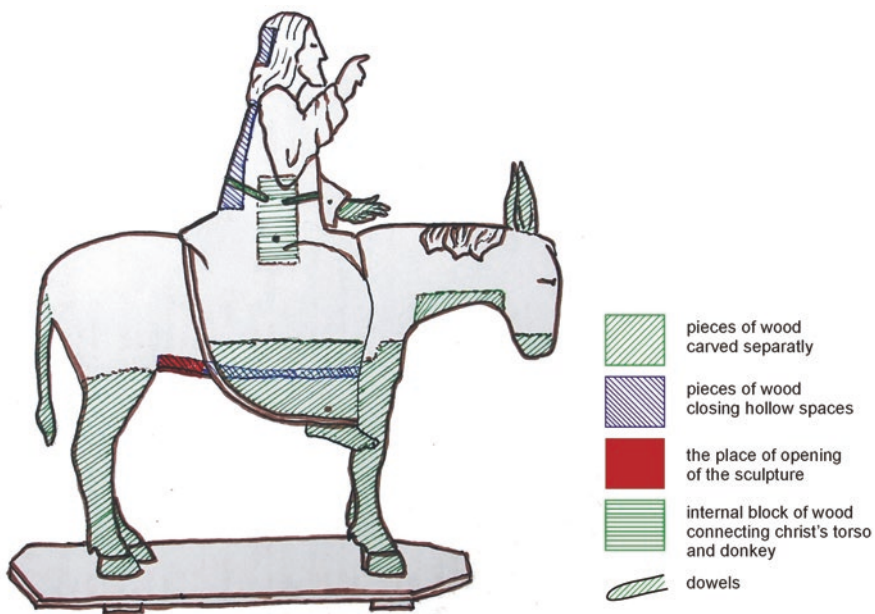


Fig. 10.5 The schematic drawing of sculpture's construction © K.Męczyńska

sculpted pieces of wood. The joint areas have been reinforced with pulped linen fibres, that are visible in many places (see Fig. 10.6). The thickness of the walls of the sculpture vary to a great degree – the back of the donkey next to Christ’s back is 7.7 cm thick, whereas the side walls are much thinner at between 4 and 5 cm. The top of Christ’s head and the donkey’s forehead have holes from mounting which are currently plugged with wooden spigots, which suggest that during sculpting the piece was mounted on a carpentry bench (see Fig. 10.7).



Fig. 10.6 Christ’s back with fibres reinforcing the connections of parts © MNP



Fig. 10.7 Christ’s head with the hole from mounting in a carpenter bench plugged with wooden spigot © MNP

Through careful examination of the sculpture the tools used could be deduced and included semicircular chisels, hatchets, saws, drills and rasps. The bold chisel work, regular strokes, and smooth details suggest that the artist was highly skilled, as he understood their material and could predict stresses and warps of the wood.

10.3.3 *Original Ground and Paint Layers*

10.3.3.1 **Ground**

The colour of the ground ranges between white and cream. It consists of chalk and glue and was applied in multiple layers using the ‘wet-on-wet’ method. In its thickest area the ground is 400 µm thick and consists of 6 layers.

10.3.3.2 **Painting Layer**

Christ’s flesh is painted in pink (lead white + vermilion + organic red). The painting layer contains tempera or glue medium. As both foundation and painting layer are strongly bound, it is probable that paint must have been applied immediately after an application of the ground layers. In the area of Christ’s hair, beard and robes as well as the donkey’s hair the paint was applied in two layers: a greyish-black or black underpainting in tempera followed by proper paint layer containing greater amount of oil in the binding medium as seen in Fig. 10.8. This layer has likely been finished with layers of oil-resin glazes. From examination of cross-sections it can be seen that the original paint layer in the areas of donkey’s coat was grey. The mane was slightly brown. In the area of Christ’s robe the aforementioned black underpainting was covered with brownish-red paint, which in some regions was more purple.

This layer is rather grainy and contains large black grains (organic, plant black), white grains (lead white) as well as at least two types of red grains. These are: a small-grain iron-containing red and another pigment composed of flat, glassy, optically isotropic particles. The colour of these particles ranges from pale to dark purple. Some particles display an unusual, striped colouration (Fig. 10.9). Pink and pale blue particles are also present. Optical properties and a significant level of chemical resistance strongly suggests that the particles are fluorite (CaF_2). Examination of the individual pigment crystals using SEM-EDS confirmed the identification of fluorite.

Fluorite was used as a pigment in the 1470–1520 period, mostly, but not exclusively, in mountainous regions of Europe where it was mined, i.e. in southern Germany, the area of Bohemia, in Lower Silesia in Poland, in Austria, Tyrol, Switzerland and France [[4], 318; [3]]. The use of fluorite in paint layers of our *Christ on a donkey* sculpture confirms therefore both the time of its creation to the late fifteenth C. as well as its region of origin (southern Germany) as established during earlier iconographic examinations.



Fig. 10.8 Cross-section of a sample from the borderline of Christ's robe and hair; original layer containing fluorite lies on the black underpainting; above a few layers of overpainting, magnification 30× © MNP

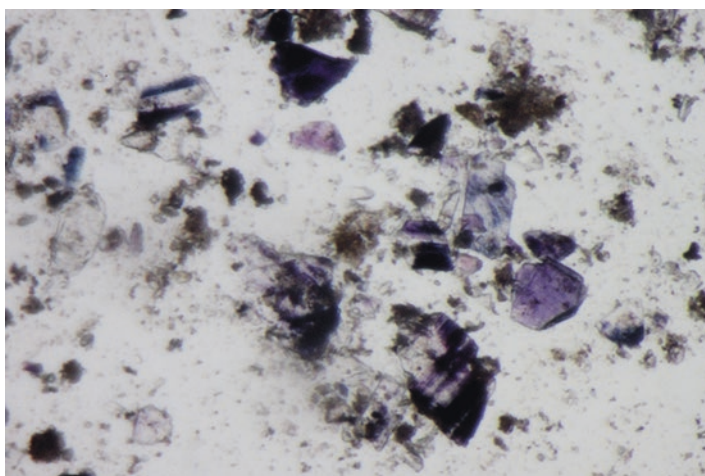


Fig. 10.9 The purple pigment – flurite from the Christ's robe; magnification 100 × © MNP

The current colour of Christ's robe is brownish, however the original colour was probably cleaner, more vivid, and more purple, as demonstrated from images of a cross-section (Fig. 10.6). It seems that the ultimate colouring of the robe was also influenced by the black underpainting, since fluorite has poor hiding strength,

especially with bound in an oil medium. Only some particles of this pigment have an intense colour, as most are either colourless or slightly coloured. The effect of an application of a fluorite layer on a black underpainting appears similar to that often found with blue layers.

A small amount of a turquoise (mineral copper blue) layer of the lining of Christ's robe was discovered in a sample from the edge of the robe along with traces of dark red glaze. It is possible that this glaze was covering the whole of the robe, but it was not preserved.

The original layer on the edge of the robe was also not preserved. Traces of secondary gilding have been discovered, possibly indicating that gilding appeared in original layers.

Overall, in the original paint layers the following pigments were identified: lead white, iron red, vermilion, organic red, fluorite violet, copper blue and large grain plant black.

10.3.4 *Halo*

The original sculpture had probably possessed a cross halo, which is currently missing. A similar halo in an analogical South German sculpture dated to the last quarter of fifteenth century, conserved in the Cluny Museum in Paris. The four metal hobnails and a larger, flat element embedded in Christ's head are likely traces of its fastening mechanism. These metal elements are not externally visible and can be observed only through examination of X-radiographs as seen in Fig. 10.10.

10.3.5 *State of Conservation of Original Elements*

The original wood is fairly well preserved. Damage and cavities on the donkey's back and neck as well as on Christ's head indicate that the sculpture might once have been exposed to unfavourable weather conditions, and perhaps even displayed outdoors.

The wheels and axles were not preserved and nor were the reins (probably in leather).

The sculpture had been attacked by anobium larvae at some stage, and later underwent repairs to treat the damage. The original polychrome is preserved in very small fragments underneath multiple layers of overpaintings. This is well illustrated by a mosaic of lighter and darker spots as visible in X-ray images. (Fig. 10.8).

Fig. 10.10 An X-radiograph of Christ's head and torso revealing metal elements in the head as well as the mosaic of layers from different periods, © R. Stasiuk



10.4 Previous Conservation, Repairs and Modifications

10.4.1 *Wood Repairs*

The sculpture was repaired and repainted many times. It is known that in the nineteenth or twentieth century a large-scale conservation programme was carried out. During this treatment the statue was dismantled and repaired to a great extent. Badly damaged fragments of the donkey's trunk were removed and wooden inserts were glued in their place. The donkey's tail was also replaced.

The legs of the donkey have also been repaired. We were unable to unequivocally determine that the current legs are not original. The legs have only a single layer of secondary ground. Inside the sculpture, there is an evidence of attempt to affix the front right leg with two large blocks of wood. A secondary large block was also glued in the rear quarters of the donkey. These elements were carved out of coniferous wood, most likely pine. They bear traces of mechanical tools that were in use since the beginning of eighteenth century.

The fastening mechanism of Christ's right hand and left foot were replaced, and square dowels were replaced with round ones.

Inside the sculpture plenty of wood shavings with evidence of woodworms remain as traces of restoration work performed during the nineteenth C. In addition to the wood shavings, we noted a walnut inside the work which was probably left by the restorers.

10.4.2 Secondary Grounds

Secondary grounds are preserved only in fragments. Different layers of white or cream secondary grounds were discovered on the surface of the sculpture. For instance, the ground layer on the donkey's legs and in the lower part of the animal's body was prepared with a very strong binder, and has a tendency to crack and peel in large fragments.

10.4.3 Secondary Painting Layers

Before conservation the polychrome was a mosaic of numerous layers of overpaintings that differed in both texture and colour, all covered by light brown layer. Stratigraphic examinations and cross-sections show three complete and a few areas of local overpainting, none of which is completely preserved. Secondary layers were often applied without a ground, directly onto the wood. The two oldest overpaintings of Christ's robe were probably performed between the sixteenth and eighteenth centuries, since both contain smalt, which was widely used during the period. The third overpainting of both Christ's robe and skin are laying on thick white ground. This layer contains no traces of lead white and therefore must have been painted either at the end of nineteenth or at the beginning of twentieth century.

The skin of the donkey presents the most varied surface. Four painting layers in different shades of grey are visible on its side, ranging in shades from very light to very dark.

The colour tone of Christ's robe had previously been more uniform, with a maroon oil overpainting. There are also numerous dark brown, grainy and imprecisely layered spots of overpainting. Between these layers there are traces of blue polychrome on a thin, white ground, preserved in numerous, but fragmented areas.

On Christ's face and limbs there are three layers of overpainting in varying shades of pink.

10.5 Conservation

The surface of the sculpture was very uneven and dirty before restoration, and the numerous white stains of secondary ground had a disruptive effect on the overall form of the piece. Before conservation work was started it was intended to reveal the original polychrome of the entire sculpture. However, during examinations and research it became clear that the original layers are only preserved in microscopic

fragments (e.g. 1 mm × 0.5 mm), and were only found in about half of all samples. A decision was then made that the primary objective of conservation work will be to achieve an aesthetic effect with a unified appearance.

The sculpture was preliminarily cleaned first. Flakes were reattached and the surface of the sculpture was consolidated. The semi-transparent, brown layer was removed. We decided to attempt to unify the colouring of the sculpture without removing the layers of overpainting. It was decided that the cavities in the ground layer on the donkey's body and legs should be filled and new and old putty should be delicately retouched. Unfortunately, it was impossible to reveal the original layers as they are only preserved in traces. Conservation work thus consisted of the removal of the secondary, light brown overpainting surface layer as well as careful reintegration of losses.

10.6 Conclusion

The greatest outcome of this project was the recognition of the sculpture's complex structure and the masterful craftsmanship through the use of X-ray examinations and an interior inspection. The examinations of wood, fibres, grounds, pigments, binding media and metals using both microscopic and microchemical methods along with the numerous stratigraphic cross-sections allowed us to establish the sculpture's original appearance, as well as the history and extent of the numerous restorations it had undergone. The mineral pigment fluorite was identified in the painting layer of Christ's robes. A microscopic identification of this pigment was then confirmed using SEM EDS. Due to the relatively short period of time during which this pigment was in use – from the end of fifteenth to the beginning of sixteenth century – coupled with the region of its most frequent use – southern Germany, Lower Silesia, Bohemia and Austria, – we were able to attribute our sculpture to the workshop of Michel and Gregor Erhart of Ulm. Consequently, the earlier attribution made on the basis of an examination of style was confirmed.

Acknowledgements The authors would like to thank the following people and institutions for their help:

Mr. Robert Ślusarek from the Nowy Sącz District Museum and priest Tadeusz Bukowski from the Tarnów Diocesan Museum for information regarding the sculptures of Christ on a donkey in their collections, Mr. Roman Stasiuk from the Academy of Fine Arts in Warsaw and Mr. Wojciech Pawlicki from Euromed, Poznań for X-ray photographs, Ms. Katarzyna Przewoźna and Małgorzata Zimniewska from the Institute of Natural Fibres and Medicinal Plants in Poznań for fibre analysis, Mr. Jacek Michniewicz from the Institute of Geology of the Adam Mickiewicz University in Poznań for SEM-EDS examinations, Mr. Dominik Murawski for carpentry consultations.

References

1. Chrzanowski, T. M. Kornecki 1989 'Sztuka w Krakowie po Stwoszu. Epilog Gotyku Mieszczańskiego' *Folia Historiae Artium*, 25, 169
2. Marcinkowski W. National Museum in Krakow, Galeria Sztuki Dawnej Polski 12-18 wiek, file no. 20, page 5, http://www.muzeum.krakow.pl/uploads/media/20_Chrystus_na_osiolku_z_Szydlowca.pdf accessed 14.08.2013
3. Richter, M. O. Hahn and R. Fuchs. 2001. Purple fluorite: a little known artists' pigment and its use in late gothic and early renaissance painting in Northern Europe, *Studies in Conservation* 46, 1-13
4. Wisła, E. T. Żurkowska-Mastalerz. 1987. Fiolet śląski. Identyfikacja nie znanego pigmentu wym na podstawie materiału uzyskanego w czasie prac konserwatorskich w latach 1978-1985, *Ochrona Zabytków* 40(4), 318
5. Wozniński A. 1992. Rzeźba Chrystusa na osiołku z Muzeum Narodowego w Poznaniu', *Studia Muzealne MNP*, 16, 75-92.

Chapter 11

Multi-Disciplinary Complex Research to Reconsider Basic Questions on Attribution and Dating of the *Last Judgment* Triptych from National Museum in Gdańsk by Rogier van der Weyden and Hans Memling



Iwona Szmelter and Tomasz Ważny

Abstract A multi-disciplinary study of the *Last Judgment* triptych in the National Museum in Gdansk considers the oak support, underdrawing, paint and the interpretation of the artistic process, shedding new light on the work and its creation. Cutting-edge in situ analysis and the examination of micro-samples has been undertaken. The results demonstrate that the work had been created following the Flemish tradition of painting in the Low Countries in the second half of the fifteenth century. Dendrochronology has provided data on the earliest date for the preparation of the oak support to ca. 1460. Infrared reflectography reveals underdrawings showing that in the Christological centre of the composition there were major changes. The triptych was first attributed to brothers van Eyck, then Rogier van der Weyden, in 1843 to Hans Memling. In light of analytical results we suggest that the triptych is the posthumous completion of a work designed and composed by Rogier van der Weyden and finished by Hans Memling.

Keywords Technical study · Attribution · Rogier van der Weydan · Hans Memling · Triptych

I. Szmelter (✉)

Faculty of Conservation-Restoration of Artworks, Academy of Fine Arts, Warsaw, Poland
e-mail: iwona.szmelter@asp.waw.pl

T. Ważny

Faculty of Fine Arts/Conservation and Restoration of Works of Art, Nicolaus Copernicus University, Torun, Poland

Laboratory of Tree-Ring Research, University of Arizona, Tucson, AZ, USA

11.1 Introduction

Multi-disciplinary complex methodology is used to reconsider basic questions on attribution and dating of the *Last Judgment* triptych from the National Museum, Gdansk (Fig. 11.1). The only date about the triptych that is confirmed by the archives connected with the theft of a triptych by pirates in 1473 [38]. The triptych was first attributed to brothers van Eyck, then Rogier van der Weyden, and in 1843 by Mr. Hotho to Hans Memling, though the authorship of the work is still questioned. A systematic study of the painting materials and technique has been undertaken starting with non-invasive analytical methods and is the focus of this work.

11.2 Examination of the Wood Support

The *Last Judgment* triptych was painted following with strict rules of the Low Countries - on a wood ground carefully made of oak. The central section is made up of six vertical boards with a total width of 180 cm. Dendrochronology has often contributed to the solving of important art-historical questions and controversies [37]. Dendrochronological examination of the oak is based on the analysis of annual rings of wood and is therefore completely independent of the other chronological indicators. Roger Van der Weyden died in June 1464. Thus if the wood used by the



Fig. 11.1 Triptych *The Last Judgment*; the panels present (from left): reverse – donor’s wife, Caterina Tanagli; obverse: panel “Heaven” – march of the ransomed; central panel – Christ the Judge, Michael the Archangel and the scene of weighing souls; panel “Hell” – pushing sinners down to Hell. On the reverse side of the side leaves there are depicted donors: Angelo Tani with his wife, Caterina Tanagli. The triptych is painted in tempera and oil on oak; exhibited at the National Museum in Gdańsk (inventory No. MNG/SD/413/M). Image in visible light taken by Roman Stasiuk 2010, Archives of the Faculty of Conservation and Restoration of Works of Art of the Academy of Fine Arts in Warsaw

Table 11.1 Detailed results of dendrochronological analysis of the *Last Judgment*

Number of plank	Number of rings	Average ring width /mm	Dating of tree-ring series
1	152 (+2)	1.89	1257–1410
2	161	1.76	1252–1412
3	237 (+1)	1.15	1204–1441
4	240 (+1)	1.11	1208–1448
5	243 (+1)	0.87	1196–1439
6	236 (+1)	0.98	1210–1446

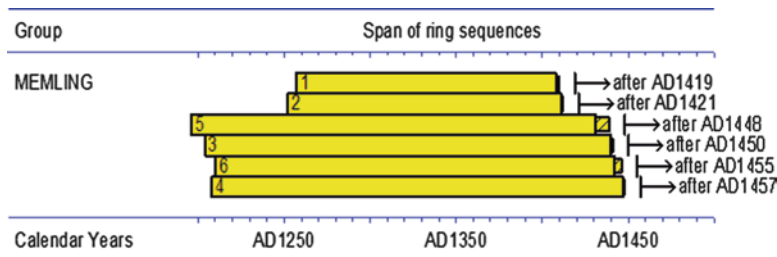


Fig. 11.2 Schematic diagramme of tree-ring dating of six oak boards representing the middle of *The Last Judgment*

author of the triptych were younger, the authorship of van der Weyden would be automatically excluded.

Dendrochronological analysis was performed in 2003 in the National Museum in Gdansk (measurements) and the Institute for the Study, Conservation and Restoration of Cultural Heritage at the Nicolaus Copernicus University in Toruń (laboratory examination). We measured ring widths from all six boards with an accuracy of 0.05 mm. Tree-ring series were compared with a set of European oak chronologies, which allowed the dating of wood and an estimation of the origin if the oak. Detailed results are provided in Table 11.1 and their graphical presentation on diagram in Fig. 11.2.

Boards No. 1 and No. 2 are from the same tree. Wood was characterized by relatively wide annual rings and exactly radially oriented boards. Also, boards 3 and 4 were made from one tree. The average ring width of boards 3, 4, 5 and 6 was approximately 1 mm, with deviation of the radial direction of up to 20 °. Board thickness ranged from 1.1 to 2.0 cm.

The youngest preserved annual ring is dated to 1448. There were no remnants of the outer layer of wood - sapwood, which was cut off during the preparation of the boards as a layer with reduced durability and susceptibility to attack by wood-destroying insects.

11.2.1 *Origin of Timbers*

All boards forming the painting support are derived from so-called Baltic oak. Boards 3 and 4 originate from central Poland, other boards came from different areas East or Northeast of the current Polish border, most likely the Niemen river basin. Comparative analyses with other works from the Low Countries, which were subjected to dendrochronological examination, did not allow the detection of wood from the same trees in any other painting.

11.2.2 *Missing Sapwood*

Three trees, which were cut to make boards number 3–6 used to construct the panel were 250 + years old. From the sapwood statistics made for 206 oak samples from Gdansk Pomerania with preserved complete sapwood, the oaks representing this age-class had from 9 to 30 sapwood rings [37]. After the rejection of 5% of the extreme values we obtain a number of sapwood rings between 11–29 and median of 17. However, there are some regional differences, probably related to differences in the influence of the continental climate.

For example, recent (still growing) oaks of north-eastern and eastern Poland (age 100–280 years) and the central part of the country (aged between 160 and 340 years) have the number of sapwood rings listed in Table 11.2.

The wood used as material for the production of panels used in *The Last Judgment* does not come from the coast, but from the middle part of the country and the areas

Table 11.2 Relationship between sapwood and geographical origin of trees

Number of sapwood rings	Number of trees from NE and E Poland with corresponding number of sapwood rings	Number of trees from central Poland with corresponding number of sapwood rings
8	2	0
9	6	0
10	12	0
11	13	3
12	10	4
13	11	9
14	2	3
15	4	3
16	4	6
17	2	4
18	1	3
19	2	2
20	2	0

to the east and northeast of the Białowieża Forest, which is why it seems most appropriate to adopt a number 9 after the rejection of the extreme value.

Pascale Fraiture of the Royal Institute for Cultural Heritage (KIK/IRPA) in Brussels set the extreme value of eight sapwood rings as a minimum for the Baltic oak. Miles [22] writes that “generally, medieval woodworkers would have trimmed off only the minimum amount of heartwood along with the sapwood when preparing boards and planks. This would normally vary between 1/2 and 1 inch (13 mm to 25 mm).” To confirm, Miles gives numerous examples of calculation for the boards of Baltic origin used in English churches and cathedrals. If we confine ourselves only to the wood from the fifteenth century, 73 boards examined by Miles had from 15 to 178 missing heartwood rings. Artists working on the *Last Judgment* had to treat the wood much more economically, but it is difficult to assume that the both younger boards (#4 and #6) were cut sapwood with accuracy exactly along the line dividing sapwood and heartwood. With a length of boards of 242 cm it can be assumed, however, that one side of the board may be very close to the sapwood/heartwood border or even touch it. The difference in results of the dating of the upper and lower edge of the boards of up to 21 years reinforces this assumption. If only sapwood is assumed to be missing, the earliest possible date for the sapwood/heartwood border is the year 1449.

11.2.3 Sapwood Statistics of the Baltic Oaks

The values shown in Tables 11.1 and 11.2 above require taking nine sapwood rings as the minimum value for the 250-year-old oaks of Mazovia, Podlasie and the former Duchy of Lithuania. We omit the statistical calculations and models made by Miles [22]. Although Miles’ statistics are based on 447 samples of oak with bark or waney-edge from Poland, he relied mainly material from Gdansk Pomerania and Western Pomerania, so in other geographical regions from the region of origin of the wood from *The Last Judgment*. Assuming, that the oaks had only the minimum number of nine sapwood rings, 1458, or the fall or winter of 1458/1459 was the earliest possible date for felling trees, of which the boards 3 and 4 were made.

11.2.4 Transport and Oak Seasoning

In 1459 semi-products made of fresh logs (wainscot) could be ready for transportation down the river to the nearest Baltic harbour. Timber from trees felled in winter could be found as a wainscot and planks at the lumber-yards in the Low Countries after a few months. After a few weeks of spring rafting to the port, timber was re-loaded to the sea-going ship and during the navigation season transported to the West. Customs records are evidence of former timber trade.

Oak was an important and expensive commodity, and was usually bought for a specific purpose. It should be considered that the main reason of massive transportation of oak timbers was shipbuilding, and shipyards consumed enormous amounts of high-quality timbers in the very beginning of “The Age of Discovery”. The forest resources of the main sea-powers were already heavily exploited.

Timber used for production of painted panels should be perfectly seasoned. The old craftsman’s handbooks or artists’ treatises provide us recommendations how to select “well-seasoned” wood taken even from dismantled ships for production of high-quality painting panels, but such material was so far decayed and deteriorated in extremely wet conditions, that in reality it had a value of firewood only. The time for seasoning was dependent on workshop procedures and Klein provides the following numbers: from 2 to 8 years for oak panels from the 16th and seventeenth century and 10–15 years of seasoning time for fifteenth-century panels [15]. In this later case however, Klein draws attention to the limited number of studies of signed and dendrochronologically dated fifteenth c. panels. Uzielli claims that “the golden rule of the craft states that the equilibrium moisture content (EMC) of the wooden support at the time of manufacturing or painting should be as close as possible to the average EMC predicted in its subsequent environment” [34]. In our experience we have noted an exceptional case of the painting with the cutting year of the tree equal to the date on the signature. Thus, it seems to be acceptable to apply 2 years as a minimal time between the felling of the tree and creation of the painting. After 2010 Klein subsequently modified his calculation and in catalogue of early Netherlandish paintings from the Rijksmuseum in Amsterdam, applying the following formula for 15th and sixteenth c. paintings on Baltic oak: “earliest possible creating date: 9 sapwood rings + 2 years for seasoning.”

Short and intense seasoning plus the time required for panel-making theoretically allow for the delivery of the support to the artist’s workshop at the end of 1460. The different origin of boards suggest that they were not a specially ordered timber for production of a particular painting panel, but that this was a material purchased at the timber yard.

Dendrochronological analysis and determination of the earliest possible production date of the painting support at the end of 1460 hence does not preclude van der Weyden’s participation in the creation of *The Last Judgment*.

11.2.5 Research by Faculty of Conservation of the Academy of Fine Arts, Warsaw

Through the use of infrared reflectography, researchers from Faculty of Conservation at Academy of Fine Arts in Warsaw have discovered significant underdrawings, several changes in the composition of the work, the use of different tools and materials for drawing, and different stylistic changes in the painting layers. This provided the first information that the triptych had been created by artists of different artistic

temperament and style. The results of the analysis by infrared reflectography and radiography in 2010 contributed to the thesis of the existence of several chronological layers and the stylistic differences between the underdrawing and priming layers, and thus leading to the need to discovery of the authorship of various artists. Subsequent studies also confirm the conclusions of the research carried out in 2010 [32].

Different scientific analysis was undertaken providing new revelations concerning the several stages of the artistic process [31]. The new information confirmed the thesis of a change in the composition and underdrawing of the work with the priming layers probably made by Rogier van der Weyden and his workshop, which was the norm in the fifteenth century painting workshops, while the completion of the painting and its details was the work of Hans Memling, for whom this work was one of the earliest and most important in his oeuvre.

This paper presents the results of multidisciplinary research. Contemporary conservation methodology requires a properly trained specialist to investigate a work of visual art and in a broader view, cultural property in general, based on a variety of criteria. A spectacular example in Poland is the case described below of investigations of *The Last Judgment* triptych in the National Museum in Gdansk. These were begun in 1959–1961, and conducted with the use of different types of light sources and with the analysis of samples. Since, the triptych has been investigated several times, culminating in the multidisciplinary research project described in this paper. Later the triptych was examined by the series of condition reports.

11.3 Historical Context

11.3.1 *Origin of the Panel*

Very little has been discovered about the origins of *The Last Judgment* triptych from the archival sources. The earlier history of the work has thus not been confirmed in the sources and archives, so far only partially analysed, even though the painting has long been of interest to many generations of art historians. The first information relates only to the seizure of the painting on April 27, 1473, during the boarding by pirates of the galleon “San Matteo” sailing from Bruges to Italy under Italian colours which had been transporting the panel [38]. This was connected to the wars between the Hanseatic League and England (1470–1474). Captain Paul Benecke of the “Peter von Danzig”, a caravel from Gdańsk, won a sea battle off the coast of England and the triptych, just one of the properties seized, was given to the church of the Virgin Mary in Gdańsk. The masterpiece remained in St Mary’s Church, despite the protests of representatives of the Medici, who suffered financial damage as a result of the loss of the transported goods, and despite the support for the idea of revindication by Duke Charles the Bold of Burgundy and Pope Sixtus IV.

The triptych was appropriated as a war trophy several times in its subsequent history. In 1807, it was taken to France by Napoleon, in 1815 it was taken to Berlin. Finally, in 1817, after many attempts to recover it, the painting was placed in the chapel of St Dorothy in St. Mary's Church in Gdańsk. The triptych was hidden by the Nazis during the Second World War, but was taken out of hiding by the Red Army in 1945 and first carried off to the Hermitage. Only after the Polish political thaw in 1956 did the painting return to Poland. First it was exhibited at the National Museum in Warsaw, and finally it went back to Gdansk, this time to the National Museum, while a copy hangs in St Mary's Church.

11.3.2 The Technology and Style of Early Flemish Renaissance Painting

The significance for early modern Europe of the tempera-oil technique and style of art developed in the Low Countries is undoubted. The order of the triptych by Angelo Tani, a representative of the Medici in Flanders in the years 1450–1464 coincided with the flowering of painting in Flanders, the southern part of the Netherlands, the heart of cultural changes in the arts in Northern Europe in the fifteenth century. The explosion of Flemish painting was related to the growth of the so-called Low Countries (a union of Burgundy and the Netherlands) under the rule of the Dukes of Burgundy which became one of the richest parts of Europe until the dissolution of the union in 1477 [13]. The artistic progress and technological progress made in Flanders in painting, also visible in our study of the Gdansk triptych, demonstrates the importance of the need for reassessment of a forgotten power of late medieval northern Europe in the development of proto-Renaissance culture. In this area, the cultural patronage due to the new humanist aspirations and commissions of the dukes, Church and the nascent urban patricians in Dijon, Brussels, Bruges, Ghent, Antwerp and other northern cities nurtured lively artistic centres. This led to the creation of important works by highly skilled artists, humanists and musicians, and gave rise there to the birth of what many authors consider to the early stages of a Northern Renaissance [3]. Works were commissioned from the most talented painters who oversaw workshops producing paintings and polychrome sculptures with impressive new forms of expression, full of psychological reflection, utilizing vibrant colours of oil paints and recent technological improvements [9], which were widely admired when compared with the contemporary Italian paintings with their matte tempera technique [20]. There was a demand for Flemish paintings and tapestries in Italy and other cultural centres in the fifteenth century.

11.3.3 *The Commissioning of the Triptych*

The Italian donor of the *Last Judgment*, who is shown on the left outer wing of the triptych picturesquely draped in a brown robe was Angelo Tani. He was an agent of the Flanders branch of the Medici family bank from 1450, and in the 1455–1464, he was the head of the branch in Bruges [38], recognized on the basis of the coat of arms on the reverse of the panels. Unfortunately, the complete reconstruction of the events surrounding the creation of the triptych is impossible in the absence of archival data. Angelo Tani was one of the pillars of society in the Italian colony in Flanders. The triptych was intended for his family chapel in the church of San Michele San Bartolomeo in Badia Fiesolana near Florence, the dedication of which had been delayed. When the church was consecrated 1466–1467 it coincided with the wedding in 1466 in Florence of Angelo Tani, then of somewhat advanced age, with a young wife, Caterina Tanagli - the couple is represented on the reverse of the side wings of the triptych. For these reasons, many authors link this date to the commissioning of the triptych, but equally the triptych could have been ordered in advance. Tani left Flanders in 1464 after 14 years of residence there and moved back to Florence. There is no evidence to support the hypothesis that he could have ordered the painting while on a visit to one of the bank's branches in London in 1467 when he might have passed through Bruges: did he visit the newly established workshop of Hans Memling, whose existence was first mentioned in 1465? On his return to Italy in 1468, did Tani participate in the wedding ceremony of Charles the Bold and Elizabeth of York in Bruges?

One fact that we know from the archives is that Tommaso Portinari was appointed to his position in Bruges and in 1473, he sent a ship with goods to Italy, including the triptych in the transport [38]. For this reason, the small portrait of the head of an unknown man painted on tin and applied to the picture of the saved man on the scales of the Archangel Michael is often interpreted as the so-called "Portrait of Portinari". It should be added that the long features of the face of the redeemed man which result from a nineteenth century reconstruction of the damage to the face could have been influenced by the known portrait of Portinari from the brush of Memling (now in the Metropolitan Museum in New York, see the section on the history of conservation and current findings (Fig. 11.3)). The chronology of the commissioning and the creation of the triptych is therefore an open question.

Angelo Tani would most likely have been able to order the triptych before returning to Florence in 1464. For years he had known of Rogier van der Weyden's success in northern Europe and in Italy and the works ordered from him. He knew the dimensions of his family chapel and the planned size of the altarpiece. Determining the needs of the donor and the ordering of the work must have preceded the beginning of the painting work, which could have started after from 1460, the earliest date at which the support could have been ready according to the data from dendrochronology. The analysis of the style of the underdrawings and large parts of the lower paint layers which represent the most important iconographic figures also indicate the authorship of Rogier van der Weyden. By contrast, the examination of

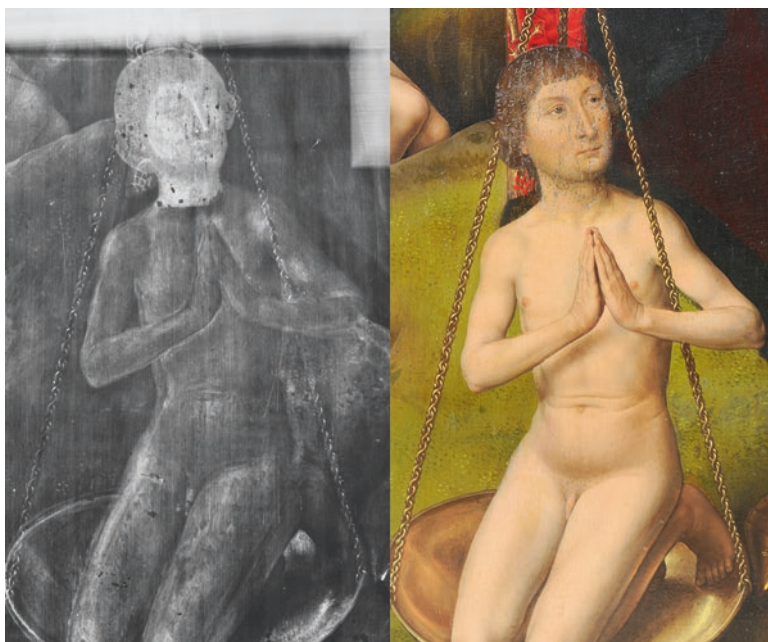


Fig. 11.3 The figure of a saved men on the scale of Michael the Archangel painted in multi-layer technique on wood; the portrait was painted on tin, affixed to the original work of art in the place of the former underpainting in part of complexion. The portrait is interpreted as a depiction of Tommaso Portinari, the successor at the branch of the Medici Bank in Bruges of Angelo Tani (donor of the triptych): Left (X-radiograph), Right, image in visible light. Imaging by Roman Stasiuk, Archives of the Faculty of Conservation and Restoration of Works of Art of the Academy of Fine Arts in Warsaw

the reverse of the triptych in multispectral infrared reflectography (MNIR) indicate the preparation of the panels and the paintings of the figures and robes of the donors by the usual method of underdrawings, but the heads, portraits of the donors in the *alla prima* technique. The figures of the donors have careful underdrawing and a multi-layered painting technique while their faces are painted almost without drawing (see Fig. 11.9). They are different, added later, after their marriage in 1466. Thus, the triptych could have been painted in stages over many years, like many other polyptychs in the fifteenth century.

11.3.4 Context and History of the Attribution of the Work

The Gdańsk *Last Judgment* has been associated with the name of a variety of artists. Starting from the seventeenth century, it was attributed to the most famous artists such as Jan van Eyck (1390–1441) and Rogier van de Weyden (1400–1464). The hypothesis linking the creation of the work on stylistic grounds to Hans Memling

(1430? -1494 Bruges) was first proposed in 1843 by the Berlin philosopher and pioneer of the history of art Heinrich Gustav Hotho. In 1864, another German art historian, Ernst Foerster, who knew both the Gdansk triptych and the *Last Judgment* in Beaune, painted for the Chancellor Rolin by Rogier van der Weyden, argued, however, that the work was designed and started by Rogier and completed by Memling. For nearly two hundred years, these two opinions were accompanied by a variety of other hypotheses by different authors. The discourse was not about facts, because there are still many gaps in our knowledge of Memling. Nothing is known about the course of his artistic training, and we do not even know his date of birth. We only learn of Memling, when, as “Jan van Mimelinghe, son of Hamman, born in Seiligenstadt” he bought citizenship of Bruges on 30th January 1465, and first appears in the pages of history [38].

An open question is the attribution by scholars of the influences of many painters (the van Eyck brothers, Petrus Christus, Hugo van der Goes, Stefan Lochner and mainly Rogier van der Weyden and also Dieric Bouts) on the training and style of painting by Hans Memling [18, 19]. In his comments to the Memling exhibition in the Quirinale Stables in Rome opened on 10 October 2014, the curator Till Holger Borchert suggested that: “it is quite likely that Memling finished his studies as a painter in Cologne before travelling to the Netherlands. His knowledge of the composition and patterns of work of Dieric Bouts and Rogier van der Weyden, clearly visible in his paintings, however, suggests that Memling worked in Leuven and Brussels before opening his own workshop in Bruges in 1465” [5].

Unusually, Hans Memling created his best monumental works at the beginning of his career, according to many studies. These are large-scale works such as the *Triptych of John Crabbe* of 1465–7(?)¹ after settling in Bruges, clearly influenced by Rogier’s manner of representation of the Crucifixion, which is known from earlier works – a triptych of Rogier van der Weyden and two triptychs from the van der Weyden workshop. Another monumental early work is the altar created for Ferry de Clugny, Bishop of Tournai, of which has survived the panel representing the Annunciation, now in the Metropolitan Museum in New York. According to the curator, Maryan W. Ainsworth, the composition is based on the representation of the Annunciation designed by Rogier van der Weyden. The painting is accompanied in the museum in New York by the information that the *Annunciation* was probably ordered before Rogier’s death in 1464, and painted by Memling who probably also worked in the workshop of Rogier before settling in Bruges in 1465 [1].

Many researchers ask why Memling, a previously unnoticed artist, would have received his most important commissions immediately after settling in Bruges. There is also no explanation as to why, after not receiving any large orders, he was distanced from the painters’ guild, which Ziemba notes in his description of Memling after his arrival in Bruges [38]. Till Holger Borchert suspected that Memling sought more commercial gains in a strategy of serving a private clientele more interested in small devotional retables and small portraits in lyrical style [6].

¹ Triptych in oils on a wooden panel 78 × 63 cm (central panel), 83.3 × 26.7 cm (each side wing). Currently in the Museo Civico in Vicenza.

In contemporary art history there are two main hypotheses about the authorship of the early work: the first is that the work is by Rogier van der Weyden, continued by Hans Memling, the second is that the entire work is by Hans Memling. The archival evidence alone cannot resolve these hypotheses. There is an interesting distribution of attributions, German art historians mostly accepted the hypothesis about Memling's sole authorship and British, American and Flemish scholars have disputed it. McFarlane defined the triptych as a posthumous work of Rogier over Memling worked, and referred to the 1864 thesis of Foerster [21].

A list of specific questions to allow the identification of the author of the Gdansk triptych were proposed by Trzeciak [28, 29]: *“From whom would Angelo Tani, the rich banker, the head of the northern branch of the most important bank in Europe of the Medici family, who lent money to monarchs, commission a painting for his family chapel in a Florence church? Would it be from a young artist who had only just opened a workshop in Bruges, or would it be more likely that he would order it from the famous master Rogier, of whose talent he had heard in the Medici court [...] it is more likely that it was from Rogier and not Hans.”* The results of the multidisciplinary analyses reported below serve to supply an answer to these questions.

11.3.4.1 Past Restoration and Early Research

In the course of its history, the triptych has been subjected to several restorations dating from the eighteenth century. Restoration has been performed at least three times: in 1718 by the painter Krey from Gdansk (he inscribed his work on the glass step to Paradise *“Renovirt Anno 1718 den Julius Christhop Krey”*). It was then restored in Berlin – in 1815 by Prof. J. Bock, then in 1851 by Prof. Ch. Xeller in collaboration with the painter Stuebe [4]. The history of the triptych after 1956 has increasingly involved technical studies, which shed new light on the work and its history. The documentation of the most recent conservation both in Saint Petersburg and Poland has been lost and we know little about the results of their research, as are studies by Prof. K. Kwiatkowski, which fortunately have been described in the literature by himself and by Prof. Jan Białostocki.. The results of the present study have been deposited with the directors of the National Museum in Gdansk in 2013.

11.3.4.2 Previous Instrumental Analytical Studies of the Triptych

The results of tests made on the Gdansk triptych in 1960 by the conservator and investigator of painting technology, Prof. Kazimierz Kwiatkowski produced some basic information about the work following examination under analytical lighting – in UV luminescence, in IR light and radiography [16]. Following examination Białostocki posed questions about the reasons for the changes observed in the underdrawing of the triptych [4]. This was the first piece of modern research which produced descriptions of underdrawing in the light of

analysis of IR photographs and it allowed the identification of three different types of drawings, as seen in Figs. 11.3, 11.4, 11.5, 11.6, 11.7, 11.8 and 11.9. The first of these consists of sharply defined modeling with long graphic lines for example the lines in the folds of the drapery of the angels in heaven and St Peter. The second type of underdrawing is indecisive, delicate and uncertain, for example in the revision of the modeling of the angel with a trumpet flying on the horizon. It was first noted at this time that originally both wings of the angel were higher in the underdrawing and the pattern of the folds of the drapery of the robes of the angels had been changed. The third type of drawing is done rather carelessly, sketched quickly, without precision. Commenting on the numerous



Fig. 11.4 Imaging of the changes of the portrait of Michael the Archangel. Top left: image of the composition in visible light (VIS); Top right: X-ray image showing the first version of the portrait with open eyes and in the polyptych of Rogier van der Weyden from Beaune; Bottom left: image of changes in infrared reflectography (IRR) at 1200 nm; Bottom right: image of changes and drawing details in infrared reflectography (MNIR) of the painting at 2265 nm. registration and imaging of test results in infrared reflectography with MNIR scanner CHARISMA MOLAB project 2013, Archives of the Faculty of Conservation and Restoration of Works of Art of the Academy of Fine Arts in Warsaw. infrared reflectography with MNIR scanner CHARISMA MOLAB project 2013



Fig. 11.5 Imaging of the changes of the composition of the group of apostles on the right side of Christ, presenting different draft and former composition of angels of *Arma Christi*: Top left: image in visible light (VIS); Bottom left: underpainting is visible X-radiograph; Top right: image of the changes the author introduced to the drawing in infrared reflectography, around 1200 nm; Bottom right: precisely presented angels and details in infrared reflectography (MNIR) around 2265 nm. Image in visible light taken by Roman Stasiuk 2010, Archives of the Faculty of Conservation and Restoration of Works of Art of the Academy of Fine Arts in Warsaw. Infrared reflectography was acquired with a MNIR scanner CHARISMA MOLAB project 2013



Fig. 11.6 Visualization of changes in the underpainting of the triptych from Gdańsk, developed probably by the author of the draft of detailed underdrawings and underpaintings: left: underpainting of the group of apostles on the left-hand side of Christ in X-radiography – showing the former version of this composition presenting the underpainting and “psychologization” of the portraits of apostles; right: the same person introduced later considerable changes to e.g. facial features and hair of the apostle on the right hand – visible in infrared reflectography (MNIR) around 2265 nm. Infrared reflectography was acquired with a MNIR scanner CHARISMA MOLAB project 2013



Fig. 11.7 Comparison of infrared imaging of similarities of the composition of angels from *Arma Christi* on the both sides of Christ in the polyptych from Beaune (ca. 1443–1452) (left) courtesy of C2RMF in Paris as part of the CHARISMA ARCHLAB project 2013. Centre and right: the triptych from Gdańsk (ca. 1460–1470). The first composition from Gdańsk in form of draft drawings of angels was similar to the version from Beaune; afterwards, as a result of exploring new forms and iconography by the artist, in the second version the groups of apostles replaced angels and gilt, whereas underdrawings of angels are located on the bottom corners of the central panel; infrared reflectography imaging (MNIR) around 1700 nm



Fig. 11.8 Comparison of infrared imaging of Christ in the polyptych from Beaune (ca. 1443–1452) and in the triptych from Gdańsk (ca. 1460–1470). Left, infrared imaging of the polyptych *The Last Judgment* from Beaune from 1953; centre and (MIR around 1000 nm) and right (MNIR around 2265 nm) the triptych from Gdańsk. Results from infrared reflectography were recorded with the MNIR scanner CHARISMA MOLAB project 2013, Archives of the Faculty of Conservation and Restoration of Works of Art of the Academy of Fine Arts in Warsaw



Fig. 11.9 Imaging of the portrait of Catarina Tanagli, the donor's wife; similarly to the portrait of the donor Angelo Tani, the compositions differ from careful underdrawings of their robes thanks to minimal drawing and *alla prima* technique, later than chronology of the work of art: From left: image in visible light; image in MNIR reflectography around 1000 nm; MNIR around 1700 nm; MNIR around 2265 nm. Infrared reflectography with MNIR scanner CHARISMA MOLAB project 2013

stylistic, iconographic and compositional changes, however, other authors have treated them all together, in terms of overall processes such as the increase in the size of the hands, the larger keys of St Peter at the entrance to Paradise, changes in the position of the arms of the Apostles. Białostocki suggested that 'the author expanded forms and shapes of bodies at the expense of surrounding space'. Also noted however were the surprising discovery in the underdrawing of two portrait busts on the line of the horizon, probably of two bearded Apostles which had been painted over in the final version, the women starting to climb the steps to Paradise (on the obverse of the right wing) originally wore wreaths on their heads that were lost in the final version of the painting (Fig. 11.5). The changes observed by Kwiatkowski in the x-ray photographs show analogies with, for example, the representation of the figure of Archangel Michael, having open eyes in the underdrawing, staring at the viewer in the same way as in the *Last Judgment* polyptych of Rogier van der Weyden painted for the hospital in Beaune, while in the final version the Archangel has downcast eyes. This change is clearly shown in Fig. 11.4, based on the newer, more accurate imaging.

Another important analysis of the underdrawings was made by Molly Faries in 1994 in situ in the National Museum in Gdansk [11]. IR analysis of the underdrawings showed that, in addition to the changes recorded 30 years earlier and described by Białostocki, there were alterations to the greenery visible in parts which had previously been opaque, and in the position and the wings of Satan. In the part showing the saved souls there were a number of completely changed portraits, for example men have been changed into women and an older man was originally drawn as a woman, and another young woman in the underdrawing later became a bearded man. The drawing was made with a brush and was carefully executed, but there was more sketchy underdrawing done with black chalk, especially in parts of

the apostles and the robes of the angel holding a cross. Faries noticed that the underdrawing was similar to that employed by the workshop of Rogier van der Weyden and faithfully followed motifs typical of it, even though the development of the final painting was different [11].

In parallel, as mentioned above, Ainsworth discovered the double authorship of the Annunciation attributed to Memling in the Metropolitan Museum in New York. She showed that the underdrawings visible in the construction of the work in infrared reflectography are evidence of the participation of different authors. In numerous studies over the past three decades, Ainsworth [2] has noted a large number of preparatory drawings similar to the style of Rogier van der Weyden in the paintings attributed to Memling. Following significant investigations in the laboratory of the Metropolitan Museum in New York, and on the basis of the analysis of many paintings, Ainsworth has shown that black chalk was used for the underdrawings of later works of Memling after 1475. In contrast to Faries [11], whose results were ignored by the Gdansk museum, Ainsworth changed the description under the exhibited *Annunciation* in the Metropolitan Museum in New York to indicate it was “a painting begun by Rogier van der Weyden and completed by Hans Memling, as a journeyman, a wandering painter.”

A different position is taken in the erudite humanistic research study of Barbara Lane in [17]. Lane suggested that the reasons why Memling knew the Weyden preparatory drawings was an open question. Lane points to the lack of data in the archives of the stay of Memling in any workshop and draws attention to the possibilities that he had an opportunity to learn about the models and patterns of Rogier van der Weyden because some of them, especially Marian ones, were in the art trade. Further research led Lane to amend attributions, suggesting that some of the motifs of the creative activity of Memling had their origins in a period spent in the atelier of Dirk Bouts [18, 19].

The results of a study, presented in Flik and Świetlik-Olszewska [12], devote much space to the problems of interpretation of the several kinds of tools used for underdrawings through the reproduction of various drawing materials. Investigations of details and style of the underdrawings revealed little more than previous studies. There was a partial examination of drawings of various areas of the triptych, including the robes and the hand of Caterina Tanagli, so far described as made of black chalk, while destructive testing in the field of instrumental analysis showed characteristic elements of vegetable charcoal, thus dry material. Attempts were made by Flik and Świetlik-Olszewska to create replicas using various materials from which it was concluded that the underdrawings of the Gdansk triptych were done using a brush and a black water-based paint, charcoal, and possibly a metal stylus (replicated by the lead mineral galena). On the triptych, incomprehensible swirls of lines were noted on the torso of the Apostle on the left of the centre panel and in a few other places. According to the Flik and Świetlik-Olszewska the lines of the garments were carefully defined, but there were numerous other changes, drawn in black chalk or charcoal which suggested the “impetuous nature of the drawings.”

11.3.5 *Recent Studies of Technique, Material and the Multi-Stage Creative Process*

The *Last Judgment* triptych is a typical multi-layered painting; from the preparation of the oak support, the preparation of the ground, the underdrawing, the sizing, gilding and the painted layers. These features are consistent with our knowledge of the typical manner of the preparation of such paintings, including a reading of a number of surviving treatises on painting and guild regulations. During study, however, unexpected features were found hidden in the lower layers. The design of the composition of the central panel of the triptych had been changed three times, the underdrawing and underpainting were changed repeatedly. Analysis of the data from the mosaic of IR examinations obtained in 2010 from the entire surface of the face of the panel indicated that we are dealing with a unique object, concealing significant changes in the composition and evidence of preparatory drawings made by many authors. The studies in 2010 yielded the idea that the first and second phases of the underdrawings related to the planned composition of this work, and involved changes of the whole character of parts of the composition made by the same author. They had a very different character from the third phase indicating the involvement of another author and not only due to the use of different materials.

Non-destructive examination was based on a complex mosaic of full-size images from infrared reflectography in the range of 800–1200 nm (IRR), which were then supplemented with X-ray radiography.² The results showed significant changes in the composition of the central panel and numerous other small changes throughout the triptych. Underneath the compositions of the Apostles either side of the figure of Christ and the Archangel Michael (Fig. 11.4) were found other drawings which revealed the positions of angels, lines showing the folds of their robes and position of their wings drawn in the first phase. Large format prints on a scale equivalent to the original composed of a mosaic of images of the work produced by infrared reflectography clearly demonstrated a completely different earlier composition in the central part of the triptych. This comprised a pair of angels with the *Arma Christi* now hidden by the Apostles depicted in the later version of the composition on both sides of Christ.

The chronology of changes was established on the basis of the stylistic features and materials. The earliest, first and second stage underdrawings exhibit the characteristics of the style of Rogier van der Weyden. In particular, these are manifested in long, thin carefully executed lines, which terminate in breaks in the pattern of folds in a T-shaped form or intersecting sharply or in hook-like patterns, and the hatching in the shadows [28]. These characteristics are consistent with the nature of his other underdrawings known from the infrared reflectography known works by Rogier van der Weyden in the New York Metropolitan Museum, the National Gallery, and elsewhere. In the Gdansk triptych, the third phase of the

²Conducted by Roman Stasiuk, archives of the Faculty of Conservation and Restoration of Works of Art (WKiRDS), Academy of Fine Arts in Warsaw.

underdrawing is characterized by sketchy marks done in black chalk or charcoal, similar to those of *The Portrait of an Old Woman* in the Louvre painted by Hans Memling in 1470–1472.

Comparison of the style of these drawings shows the extremely different artistic temperament of their two authors. In contrast to the careful draughtsmanship of the earliest of the two compositions, the other author who left only a correction in the form of a quick charcoal sketch did not attach much importance to the drawings. It seems he only continued a triptych which he received already in an advanced stage of the artistic process, with most of the underdrawing completed, and most importantly, on which in some areas the first layers of paint had already been applied (Fig. 11.6). In addition, in the radiographs made in 2010 it was noted that in the groups of Apostles the painting of the figures was already well advanced, and this had probably taken place in the workshop of Rogier. In these intermediate layers of paint there are clear differences in the psychological expressiveness of the physiognomy of the Apostles. However, in both the older and newer versions, the form of portraits of the faces are similar to other works of Rogier van der Weyden, for example the *Braque Family Triptych* (now in the Louvre), dating to 1460 - the year of Rogier's death. The degree to which the final painted version of the multi-layer layer altarpiece was done by Rogier is uneven in different parts of the Gdansk triptych and defining his personal participation would require further study. It seems that work in the style of Rogier dominates all the major iconographic scenes. The artist created the design of the composition of the *Last Judgment*, made careful underdrawings, and laid the first painted underlayers. These repeat the characteristic features of his usual model of work. Perhaps the painting process of all the main characters had even been completed by him. This cannot be categorically stated since the multi-layer technique commonly applied in the fifteenth century, allowed for constant changes to be made in the composition. The degree to which the painting was done by the master himself is difficult to define in view of the fact that it was common for the students of the master to execute the parts of the scenes of lesser importance. In the case of the Beaune *Last Judgment*, Rogier van der Weyden's co-workers continued the work in the years 1443–1452 despite the master's long trip to Italy. The role of the master was still predominant in the fifteenth century workshop, but was in accord with the known manner of executing orders. Work in their ateliers had the form of "one workshop, many names," as Nadolny succinctly defines their practice [26].

In general, we may state on the basis of comparing the underdrawings and the differing final painted version, that the main part of the whole work is by Rogier, but parts of it have the lyricism of the art of Memling, especially in the portion depicting Hell, the painted version of which tones down and harmonizes the very expressive original composition defined by the original underdrawing. This is confirmed by numerous details in all the panels of the triptych. Many small changes have been registered. For example in the central panel in the Psychomachia motif, in the scene of the struggle of an angel and the devil for the soul of a man, the final version has been toned down. The woman in the foreground at the foot of the Archangel has

loose hair in the underdrawing but in the finished painting it is done up in a bun. In the figures of the saved and the damned, the latter presented falling kinetically into Hell, the final expression has been relaxed in comparison with the oldest underdrawings. The women in Paradise were originally depicted with wreaths in the hair, and differently draped. Perhaps Memling took over a painting already largely completed in parts of the most important parts and only added to the finishing of parts of the background. Changes of a more fundamental nature were noted in the central portion of Rogier's initial composition as a result of the work in 2010 and partly confirmed the above-mentioned by Faries [11]. This laid a moral obligation on the research team of 2010 to revisit this question in the form of a multi-disciplinary project.

11.3.6 New Investigations of the Triptych

A systematic study of the materials and techniques of painting co-ordinated by the author as executed 2012. Analysis was carried out in four campaigns. The advantage of studies in Gdansk was the ability to make use of the latest MOLAB equipment and the large experience of the team of researchers [24]. In situ investigations were based both on imaging studies obtained by scanning multispectral near infrared reflectography (MNIR) and on multipoint analyses by near and mid-infrared reflectance spectroscopies (near-FTIR and mid-FTIR, respectively), X-ray fluorescence spectroscopy (XRF), UV-vis reflectance and fluorescence spectroscopies, and measurements of luminescence lifetimes (time-correlated single photon counting—TCSPC). Samples which were taken from a few points in order to answer specific questions that arose during the first, non-invasive research and related primarily to information about the painting's stratigraphy. During the analysis of the results, comparison of the data with the results obtained in the previous MOLAB study of another important painting attributed to Hans Memling and assistants: *Christ with singing and music-making Angels* (dated ca. 1487–1490, towards the end of the artist's career), conserved at the Royal Museum of Fine Arts in Antwerp [35]. Investigations correlated the results of X-ray diffraction (XRD) and X-ray fluorescence (XRF) investigations, and new data was acquired from multi-spectral infrared reflectography (MNIR), of the entire triptych, obverse and reverse [31, 32]. Below the main results of the recent work on the Gdańsk *Last Supper* are summarised.

11.3.7 New Information Provided by the MNIR Scanning

A multispectral scan in infrared reflectography (MNIR) was conducted of the whole Gdansk triptych using a prototype device developed by the National Institute of Optics in Florence (CNR-INO) [8]. Compared to conventional reflectography

bandwidths, multi-spectral technique improves the ability to detect underdrawings several-fold. The MNIR scanner allows the acquisition of a set of monochrome images at different wavelengths in the NIR spectral region from 850 to 2300 nm. Information is acquired from radiation reflected by the painting point by point with a spatial resolution of 16 pixels/mm². The images, each of which represents a response in a particular wavelength are spatially registered and can be accurately superposed on each other in a mosaic-like manner, to make comparisons between different results.

The main changes in composition and drawing registered in the MNIR study were found in the central panel. The central figure of Christ (see Fig. 11.7) is placed between two horizontal groups of Apostles on the left and right, flanked by Mary kneeling on one side and on the other by St. John the Baptist. In these places the MNIR imaging of the underlayers shows that in the first stage of the panel's design there was a different Christological composition. In this, the figure of Christ was surrounded by groups of two angels with the *Arma Christi*, as in Rogier's representation of the *Last Judgment* in the polyptych in Beaune. They can be seen under the figures of the Apostles, parts of them are partially obscured by the layer of gilding applied to the panel.

In the earlier composition, an angel bearing a cross and a second angel with the crown of thorns can be seen underneath the group of apostles, the lines defining the angels are visible under the faces and torsos of the Apostles. The angels are meticulously shown with delicate lines, a careful description of the intended image. The artist's long thin lines end with droplets of binder, which is characteristic for the use of a brush. Such precise drawing of a thin line expresses more than just manual dexterity and a talented drawing hand, but it shares similarities with the signature of the author, stating the author's declaration of intent for the project - *circum scriptio, disegno*.

However, in the corners of the middle panel, the corrections executed in the angels of the upper parts of the left and right side of the composition were done in a different material, a dry medium such as charcoal. As previously mentioned, such a dry material was the most widely used in the very latest phase of correction of the underdrawing. Dozens of such sketchy drawing change were recorded by the longest wavelength (2265–2300 nm). During the interpretation of these details, it was noted that the effect of changes in the drawing softened the form of expression, but increased the size of the figures at the expense of the background.

The MNIR results generally confirmed the hypothesis concerning the three phases (stages) of the design of the centre panel with a first phase which was subsequently corrected by the first author in a second phase who used a liquid material to draw the lines. In particular, the lines of the folds of the drapery were boldly drawn with long lines, the folds dynamically culminating with hooked or T-shaped folds, typical of Rogier van der Weyden. It is possible to see how the author was searching for form, light and shadow through dynamic shading in the figures and the folds of the drapery wonderful forms and draperies. In many of his paintings such a development of style is almost identical. The style of drawing can be analyzed in the same way as a graphologist studies handwriting. The many changes of a dynamic charac-

ter in the underdrawing of the side panels have a similar character, in the later phases, the faces are a little larger and their physiognomies have a somewhat milder expression, which invests the top layer of paint with the form visible to the eye.

It is worth noting that the only area of the painting of the Gdansk triptych which differs in that it has an underdrawing which is conducted in a simple and very static manner is the figure of Christ, which lacks the small changes and adjustments that are visible in the rest of the triptych (Fig. 11.7). For this reason it is probable that the composition of the triptych began from the central figure of Christ (Fig. 11.8). It is very similar to the depiction of Christ by Rogier van der Weyden in the polyptych of the *Last Judgment* in the Hôtel-Dieu in Beaune, painted between 1443 and 1452, with the exception of the face which is more gentle. It can be assumed that the most important figure of Christ is a canonical form taken straight from the model, which is derived from the Beaune panel. Comparing the underdrawing of the depiction in the Beaune *Last Judgment* with the results from IR examinations in 1951³ and the IR results from 2010, together with the MNIR results from Gdańsk of 2013, we see clear similarities, even though the rest of the drawings have a more sketchy form. The large presentation of the results, in a scale similar to 1:1 enhanced our understanding of the artistic process. A more accurate comparison would be possible using the same research tool using infrared for both *Last Judgment* panels to assess whether, in the case of the figure of Christ the same drawing had been used as the pattern, or whether the degree of similarity between the two figures is to be interpreted as variations in the form in which the figure was drawn by master Rogier (Fig. 11.8).

11.3.7.1 Materials and Technology of the Painting

Taking into account the results of all the techniques used in-situ, over 6000 points were recorded in the study and 350 analyses were conducted in the central and lateral panels of the triptych [31, 32].

Analytical data provided by a combination of different research techniques have enhanced our understanding of the work of art through the description of the palette: the characteristics of author-specific pigments, the pigments used for repainting, analysis of organic compounds (adhesives and varnishes) and studies on painting technique (structure, stratigraphy). The results of the tests confirm the 2005 study, with the exception of an alternative diagnosis of the binder. In addition, samples were analysed with scanning electron microscopy (SEM), equipped with an energy dispersion spectrometer (EDS), micro-FTIR spectroscopy where paint layer stratigraphy of five micro-samples were studied, and two other micro-samples were analyzed with Surface Enhanced Raman Spectroscopy (SERS).

³In the archives of the Louvre, C2RMF Centre de Recherche et de Restauration des Musées de France, Palais du Louvre, Paris, the author found documentation of an examination of the “Last Judgment” of Rogier van der Weyden of Beaune which had been carried out in 1951.

The results obtained place the Gdansk triptych painting firmly in the tradition of early Flemish style of the second half of the fifteenth century. In addition, studies have confirmed the generally good condition of the paint layers by detecting low quantities of degradation products (unfortunately, with the exception of the catastrophic condition of the so-called Portinari Portrait) and were used for the evaluation of past restoration treatments. This knowledge is useful for dating and attribution of the work and is used for delineation of conservation strategies, preventive maintenance and defining the conditions of exposure of this masterpiece.

A synoptic view was obtained of the most important results and the palette used for the *Last Judgment* that could be compared with that of *Christ and Music-making Angels* from the workshop of Hans Memling and assistants, dated late, c. 1487/1490 [35]. The affinities between the two images are clear. The exceptions are different grounds. The material under the *Last Judgment* is chalk or calcite (CaCO_3) and lead white (lead carbonate, present as cerussite PbCO_3 and hydrocerussite, $2\text{PbCO}_3 \cdot \text{Pb}(\text{OH})_2$) which was observed by diffuse reflection FTIR spectroscopy and X-ray diffraction (XRD). This is according to the tradition of western and northern European painting, where chalk was generally used as a ground, mixed with lead white. Lead white is present in all the samples from the object in the first layer of underpainting. Meanwhile, a different composition was noted from the substrate layer under a late painting of Memling from Antwerp, that is made of gypsum (CaSO_4) and calcite (CaCO_3). The result of research on this painting was rather unexpected, because gypsum was traditionally used in the South-European school.

The gilding of the central image in the background of the triptych was done with pure gold foil (thickness less than 1 mm) with mission gilding. This also was rather surprising in the light of the dominance then of the well-known technique of gilding on bole and shiny burnishing, which was considered 'noble'.

In terms of the pigment used, the typical range available at that time was utilized. White lead is present throughout the triptych as the white pigment used in the paint layers and priming. A very wide range of colours incorporating ochre, from shades of yellow, orange, red to brown and mixed shades with additives of varying composition to modulate the hue - cinnabar, minium, white lead were documented. Tin-lead yellow type I was used for a more vivid yellow and as an additive in some orange and green areas in a manner similar to that in the image from Antwerp. Organic reds, probably Madder lake (alizarin) were used in glazes. Vermilion and red lead were added to skin tones. Purple tones, used for example in shades of draperies were clearly of organic origin. All the examined green pigments are based on copper, but their identification is uncertain due to the difficulty in discriminating analysis of the compounds belonging to this class of pigments [7].

The blue pigments were both azurite and ultramarine blue pigments, the main ones used in the details, such as the valuable brooch. This was identified (the study of X-ray diffraction XRD and near-FTIR) as natural lapis lazuli. A similar result was obtained in the case of a similar brooch from Antwerp [23]. Smalt is used in the places where there was later retouching, such as the sky in the middle panel (detected by non-invasive XRF analysis and in SEM-EDS of micro-samples). There was also found a large amount of retouching of the sky in the background using Prussian blue

(used since the mid-eighteenth century) [9]. It is present in varying amounts in the three panels of the triptych and in the greatest quantity in the depiction of hell.

Analyses of the varnishes revealed both natural and synthetic resins. The presence of thick layers of varnish over the entire surface of the triptych inhibited the use of mid- FTIR analysis, making it difficult to precisely investigate the composition of the painting materials. Analysis of the binder showed the presence of both lipid and, to a lesser degree, protein components, which suggests the use of techniques of oil painting with small areas of tempera. The dissemination of the technology of oil painting went hand in hand with the development of the ability to combine it with tempera to preserve the freshness of colours depending on the characteristics of pigments and binders suitable for them from the twelfth century long before the van Eycks, according to Theophilus. Antonio Averlino ('Filarete'), names Rogier van der Weyden and van Eyck as the painters who are most skilled in the application these media [10]. Research is currently being carried out on the binders used in the *Altar of the Mystic Lamb* in Ghent by the brothers Van Eyck. This research is hindered by the occurrence of varnishes blocking access, and it is only after removal of this varnish during conservation that we will be able to say more about the methods used in the famous Van Eyck workshop to which Vasari ascribed to a revolutionary character, rather than a masterful technique [36].

The attention of researchers has been focused on the study of the so-called Portinari Portrait (see Fig. 11.2), which is in alarmingly bad condition. There is an ongoing process of the separation of the layers of paint at its contact with the metal surface below due to oxidation of the metal as observed in X-ray diffraction (XRD) [14]. Due to the continued deterioration of the paint layers, the portrait has been reconstructed several times which hinders our ability to determine the scope of the retouching or repainting (the reconstruction does not contain pigments of types used at a later date). It is interesting that the stratigraphic analysis of the lower portion of a sample reveals that under a layer of tin leaf, there is an earlier layer of paint (containing lead white, tin-lead yellow, azurite and cinnabar), which comprised the skin tones of a the previous oval portrait painted on tin. Analysis of the upper layers above the second tin layer by optical coherence tomography (OCT) indicated the the use of multiple layers of glazes and varnishes in the upper layers of the portrait of the Saviour, as well as the large losses as mentioned above [33].

The curious method of the application of portraits on tin plates to polyptychs painted on a wooden support is adopted by several artists, including those of Rogier van der Weyden. The investigation of eleven such added small portraits in his *Seven Sacraments Altarpiece* in Antwerp has confirmed the very bad state of preservation of the inserts [30]. According to results of XRF/XRD analyses, the cause of the damage is the presence of oxidized tin (romarchite SnO and cassiterite SnO₂) [32]. Through analysis only relatively small areas of later repainting were identified. The conservation recommendations were to remove the unsightly darkened retouching in Prussian blue in the panel depicting hell. Interestingly, in the Gdansk image, as in the case of that in Antwerp, oxalates of copper were found below the layer of varnish, but a much smaller amount than in the damaged Antwerp image [25]. While metal oxalates are typical products of the oxidative degradation of organic compo-

nents and their formation in the structure of paintings may vary depending on the type of pigment but the mechanism leading to the formation of these compounds is unclear.

The results of this research, confirmed that the triptych was executed with techniques of Flemish paintings of the second half of the fifteenth century, and data from multi-spectral infrared studies confirmed that the Gdańsk *Last Judgment* was painted in several stages. The different nature of the central composition of the triptych, as indicated by the underdrawings and several other drawings, indicates the hands of different authors.

11.4 A New Attribution and Dating of the Triptych

In the multi-criteria studies of the Gdansk *Last Judgment* described in this work, scientific analysis revealed the age of the oak support, underdrawings, paint and the interpretation of the artistic process, shedding new light on the work and its creation. The challenge for researchers was to create a broad cooperation between specialists from various fields, to establish a common terminology for research and communication in the course of subsequent discoveries, and also the need to formulate further questions.

The analytical results from the study of the *Last Judgment* shows that the work had been created in accordance with all rules of the Flemish tradition of painting in the Low Countries in the second half of the fifteenth century. Dendrochronology has provided data on the earliest date possible for the preparation of the oak support to ca. 1460. The MNIR infrared reflectography discovered underdrawings showing that in the Christological centre of the composition there were major changes probably made by the same person who designed the composition of the triptych. A chronological sequence of three phases of changes in the underdrawing was documented (MNIR) and changes in the underpainting (X-ray radiography) allow us to track the changes in the composition of Rogier van der Weyden (Fig. 11.9). The composition of the painting is modelled on his work *the Altar of the Last Judgment* of Beaune. This concerns the composition of the Divine Judgment as a panorama with the centrally presented figures of Christ with sword and lily motifs, The Archangel Michael and the presentation of the intercessors: the Virgin Mary and St. John the Baptist. Key changes were made by the hand of the first author on the previous underdrawings of the group of angels with the *Arma Christi*, originally located in the central panel around Christ and the Archangel Michael on the left and the right. In the Gdansk image the golden background is reduced in extent, first by the moving of the angels with the *Arma Christi* into the sky, and then the angelic group are moved higher. Two rows of Apostles were introduced on a background created by mission gilding. Another difference from the composition at Beaune, is that in the scene of the Divine Judgment in the Gdansk panel, God is showing as winning on the scales of the Archangel Michael, the balance pan shows that it is heavier. Here too, at first the gaze of the Angel was aimed directly at the viewer, as in the

Beaune panel - but in Gdansk the image the gaze was subsequently changed, the eyes are downcast. The two versions are characterized by careful underdrawing using long lines, dramatic shading and characteristic breaks in the folds of drapery. The underpainting in the central part of the triptych and the most important iconographic representations is in Rogier's style. The next, third phase of changes in the drawing is done carelessly, diagrammatically and using dry chalk or carbon black. The corrections mainly have the character of shorthand indications of the location and indicating the general lines of the composition, especially in those parts where there is no detectable underpainting. The last phase of the finishing of the work is almost done painting *alla prima*, quickly and decisively.

There are reasonable grounds to believe that the triptych was ordered from the renowned workshop of Rogier van der Weyden at the time of its heyday, and the painting was begun around 1460 (as shown by the earliest dating of the wooden support by dendrochronological analysis). It was there that the composition was established with reference to the experience of the artist gained a few years previously during painting the *Last Judgment* from Beaune, but with a more complex composition. In its creation, two phases of underdrawings were done and then the underpainting applied while in the workshop of master Rogier. It was Rogier who created its form, modified his previous composition on the same subject. The painting was then continued by Hans Memling [29]. In the tradition of fifteenth century art, the central parts of the composition, the underdrawing and the painting of the most important figures were usually done by the main artist, who directed the workshop and the rest was delegated to assistants.

The chronology of the process of creation has primary importance in any discussion of the Gdańsk *Last Judgment* triptych. The facts discovered in the research shed light on the artistic process and determine that the creators were working in a style which is a clear continuation of that of the polyptych of Beaune. The commission at an unknown date could have been of Rogier van der Weyden, whose work was also famous in Italy and, as noted above, may have dated as early as 1460 or may have been just before his death in June 1464. Memling probably completed the work after settling in Bruges in January 1465, the most important of his paintings were created soon after his debut as an artist. It is worth remembering that in this case and in other large works, such as the *Last Judgment* by Rogier van der Weyden in Beaune (ca.1443–1452), work on retables took years and teamwork under the direction of a master was the norm, which modern interpreters looking for the presence of a single artist should bear in mind.

In the composition of Rogier van der Weyden, in the careful underdrawings and underpaintings, we see that although he had had experience with the *Last Judgment* from Beaune, he started with a similar vertical composition of Christ and the Archangel Michael, but did not stop seeking new resolutions. He changed the design of the work slightly, moving a group of angels up and in their place he put the figures of the Apostles, a more developed group in relation to the composition of Beaune. In some parts of the work the underpaintings had reached quite a developed state before his death in June 1464 in Brussels. Hans Memling probably continued the work. From what we know he came to Bruges in January 1465. The short dashes

registered by MNIR indicate the places where the artist continuing the work wanted to finish the painting in a similar manner to his corrections of the hand in his *Portrait of an Elder Woman*, from the years 1470 to 1472, now in the Louvre.

Generally, the most important analogies in the recorded images of the *Last Judgment* triptych from Gdansk are to the work of Rogier van der Weyden, including in particular the *Last Judgment* in Beaune and the *Braque Family Triptych*. In these works the masterly development of the composition can be perceived, dynamic and skilful underdrawings, the nature of the figures (for example see Fig. 11.7). The representations of Christ have a similar layout and drawing characteristic of Rogier van der Weyden. This is a new, expanded depiction of the *Last Judgment*, but still in the style of Rogier. The big surprise was the discovery of the portraits of the donors on the back side of the triptych which had been produced without careful drawings and portrayed only sketchily. The creative process of the portrait of Caterina Tanagli is comprised of the sketch and an *alla prima* technique of early-Renaissance character which is shown in the mosaic of infrared reflectography registration in various wavelengths (MNIR at 800–2265 nm) (Fig. 11.9). The two milieus, the Florentine school and that of the Netherlands communicated with one another, emphasizing the role of northern European art in the development of Renaissance painting in Florence and not, as once commonly believed, that the north only imitated Italian art [27]. The research results shed light on the original proto-Renaissance pedigree of fifteenth century Flemish painting with its identity born in the north of Europe. Contemporary theories allow parallel development of Renaissance thought and art in many local European centres going beyond “italo-centrism.”

11.5 Conclusions

This proposed attribution of the Gdansk triptych and the alteration of the chronology of its creation follows significant multidisciplinary research. The results imply the need for archival research on the dating of the commissioning of the triptych, after the arrival of the donor in Flanders (1450) and his directorship of the Medici Bank (1455–1464), as well as in the years before the journey of the triptych in 1473. This will give new information on the operation of the workshops in Brussels and later Bruges of Rogier van der Weyden, the most important painter after the van Eyck's.

There should be a revision of the concept of a single artist, routinely accepted in the twentieth century and today, which is not without significance in the case of the *Last Judgment* triptych in Gdansk. At the end of this paper let me quote the opinion of Przemysław Trzeciak: “Today, even more than in 1960, I am convinced that the description of this painting should read: ‘Probably the work of Rogier van der Weyden, completed by Hans Memling, created c.1460-1470’ [...]”.

In the light of the research presented here on the materials and techniques employed in the Gdansk *Last Judgment* triptych we read its provenance as the post-humous completion of a work designed and composed by Rogier van der Weyden

and finished by Hans Memling. The results of research have also shed light on the original proto-Renaissance pedigree of fifteenth century Flemish painting, with its own specific identity born in the north of Europe.

Acknowledgements The authors thank colleagues from the Academy of Fine Arts in Warsaw, Prof. Przemysław Trzeciak for valuable comments and cooperation, and Roman Stasiuk, Piotr Zambrzycki for the tests. Thanks to many foreign collaborators for their commitment to the CHARISMA-MOLAB research campaigns: Prof. Antonio Sgamellotti, Prof. Bruno Brunetti, Dr. Constanza Miliani, Dr. Laura Cartechini, Dr. Aldo Romani, Dr. Chiara Anselmi, Dr. Brenda Doherty and Dr. Francesca Rosi of CNR-ISTM in Perugia, to Dr. Mattia Patti at the University of Pisa, Dr. Luca Pezzati of INOA, Florence. I would also like to thank Laboratorio Universitario di Nanomaterials (Luna), the Department of Physics, University of Perugia for the SEM measurements. Special thanks are due to Dr. Philippe Walter, Helene H. Rousselière, E. Van Elslande, the CHARISMA-MOLAB-FIXLAB LAMS-CNRS, Laboratoire d'Archéologie Moléculaire et Structurale-UPMC-UMR of France. I would also like to express my thanks to scholars from Poland: Prof. Piotr Targowski.

References

1. Ainsworth, M. W. 1994. Hans Memling as a Draughtsman in: *Hans Memling: Essays*, ed. D. DeVos, 78–87, Ghent: Ludion.
2. Ainsworth, M.W. 2001. Early Netherlandish painting at the crossroads: a critical look at current methodologies in Proceedings of a Metropolitan Museum of Art symposium on 7 November 1998, New Haven: Yale University Press.
3. Belozerskaya, M. 2002. *Rethinking the Renaissance: Burgundian Arts across Europe*, Cambridge: Cambridge University Press.
4. Białostocki, J. 1970. 'Sąd Ostateczny' Hansa Memlinga. Spostrzeżenia i analizy w oparciu o badania technologiczne, *Rocznik Historii Sztuki*: 35–37.
5. Borchert, T-H, ed. 2014 *Memling, Rinascimento fiamingo*, Milan: Skira.
6. Borchert, T-H, ed. 2015. *Memling's Portraits*, Thames & Hudson: New York.
7. Buti D. F. Rosi, B. G. Brunetti and C. Miliani, 2013. In-situ identification of copper-based green pigments on paintings and manuscripts by reflection FTIR. *Analytical and Bioanalytical Chemistry*, 405, 2699.
8. Daffara, C. E. Pampaloni, L. Pezzati, M. Barucci and R. Fontana, 2010. Scanning Multispectral IR Reflectography SMIRR: An Advanced Tool for Art Diagnostics, *Accounts of Chemical Research*, 43, 847.
9. Eastaugh, N. V. Walsh, T. Chaplin and R. Siddall, 2004. *Pigment Compendium: A Dictionary and Optical Microscopy of Historical Pigments*, Amsterdam: Elsevier.
10. Effmann, E. 2006. Theories about the Eyckian painting medium from the late-eighteenth to the mid-twentieth centuries, *Reviews in Conservation* 7, 17.
11. Faries, M. 1998. The Underdrawings of Memling's *Last Judgment* Altarpiece in Gdańsk, in *Memling Studies. Proceedings of the International Colloquium* (Bruges, 10–12 November 1994), 248, ed. H. Verougstraete-Marcq, R. van Schoute, and M. Smeyers, Leuven: Uitgeverij Peeters.
12. Flik, J. J. Olszewska-Świetlik, 2005. *Tryptyk "Sąd Ostateczny" Hansa Memlinga z Muzeum Narodowego w Gdańsku — technologia i technika malarska*, Toruń: Wydawnictwo Naukowe Uniwersytetu Mikołaja Kopernika.
13. Folie, J. 1963. Les oeuvres authentifiées des Primitifs flamands, *Bulletin de l'Institut royal du Patrimoine artistique* 6, 183–256.

14. Gianoncelli, A. J. Castaing, L. Ortega, E. Dooryhée, J. Salomon, P. Walter, J.-L. Hodeau, P. Bordet, 2008, A portable instrument for in situ determination of the chemical and phase compositions of cultural heritage objects, *X-ray Spectrometry*, 37, 418–42
15. Klein P. 2003. Dendrochronological analyses of Netherlandish paintings. In: *Recent developments in the technical examination of early Netherlandish painting: Methodology, limitations & perspectives*, eds. M. Faries and R. Spronk, 65–81. Cambridge: Harvard University Art Museums.
16. Kwiatkowski, K. 1960. Tryptyk Hansa Memlinga 'Sąd Ostateczny' w świetle zagadnień warsztatowych. Appendix to the catalogue of the exhibition *Malarstwo Niderlandzkie w zbiorach polskich (1450–1550)*, 23, Warszawa: Muzeum Narodowe w Warszawie
17. Lane, B.G. 1991. The Patron and the Pirate; the Mystery of Memling's Gdansk 'Last Judgment', *The Art Bulletin* 4, 628.
18. Lane, B.G. 2009a *Hans Memling: Master Painter in Fifteenth-Century Bruges*, parts II and III, Turnhout: Brepols.
19. Lane, B.G. 2009b. *Hans Memling: Master Painter in Fifteenth-Century Bruges*. Turnhout: Brepols Publisher.
20. MacBeth R. and R. Spronk, 1997. A Material History of Rogier's *St. Luke Drawing the Virgin*: Conservation Treatments and Findings from Technical Examinations, in *Rogier van der Weyden, St. Luke Drawing the Virgin: Selected Essays in Context*, ed. C.J. Purtle, 103–34 and 211–219, Turnhout: Brepols Publisher.
21. McFarlane, K.B. 1971. The Authorship of the Danzig 'Last Judgment', in *Hans Memling*, 16–27, Oxford: Clarendon Press.
22. Miles D.H. 2005. , New Developments in the interpretation of dendrochronology as applied to oak timbers building, PhD Dissertation, University of Oxford.
23. Miliani C. A. Daveri, B. G. Brunetti, A. Sgamellotti, 2008. CO₂ entrapment in natural ultramarine blue, *Chemical Physics Letters*, 466, 148.
24. Miliani, C. F. Rosi, B.G. Brunetti, A. Sgamellotti, 2010. In Situ Noninvasive Study of Artworks: The MOLAB Multitechnique Approach, *Accounts of Chemical Research*, 43, 6, 728.
25. Monico, L. F. Rosi, C. Miliani, A. Daveri and B.G. Brunetti, 2013. Non-invasive identification of metal-oxalate complexes on polychrome artwork surfaces by reflection mid-infrared spectroscopy, *Spectrochimica Acta, Part A, Molecular and Biomolecular Spectroscopy* 116: 270–280.
26. Nadolny, J. 2008. One craft, many names: gilders, preparers, and polychrome painters in the 15th and 16th centuries in *Proceedings of the Triennial ICOM-CC Conference*, New Delhi, Vol. I, 10–17.
27. Nutgall P. 2004. *From Flanders to Florence. The Impact of Netherlandish Painting, 1400–1500*, New Haven: Yale University Press.
28. Trzeciak, P. 1990. Tryptyk Sądu Ostatecznego w Gdańsku, *Zeszyty Naukowe Akademii Sztuk Pięknych w Warszawie* 2.
29. Trzeciak, P. 2014, Kto to namalował?, *Zdanie* 1–2: 96–97.
30. Steyaert, G. The Seven Sacraments' Some Technical Aspects Observed During Restoration, in Rogier van der Weyden in Context. Papers presented at the Seventeenth Symposium for the Study of Underdrawing and Technology in Painting held in Leuven, 22–24 October 2009, eds. L. Cambell, C. Reynolds, J Van Der Stock, L. Watteeuw. (Paris-Leuven-Walpole, Ma: Peeters Publishers, 2012), 124–127.
31. Szmelter, I. L. Cartechini, A. Romani and L. Pezzati, 2014. Multi-criterial Studies of the Masterpiece 'The Last Judgment' attributed to Hans Memling, at the National Museum of Gdańsk (2010–2013), in *Science and Art: The Painted Surface*, ed. A. Sgamellotti, B. G. Brunetti, C. Miliani, 230–249. Cambridge: Royal Society of Chemistry.
32. Szmelter, I. P. Walter and H. Rousselière, 2015, *New Information Provided by Radiography, XRD and XRF as heuristic approaches in the multicriterial studies of the triptych 'The Last Judgment' attributed to Hans Memling from National Museum in Gdansk*, *Opuscula Musealea* 23 61–73.

33. Targowski P. and M. Iwanicka, 2012. Optical Coherence Tomography: its role in the non-invasive structural examination and conservation of cultural heritage objects – a review, *Applied Physics A* 106: 265–277.
34. Uzielli, L. 1998. Historical overview of panel-making techniques in central Italy. in *The Structural Conservation of Panel Paintings*, eds K. Dardes and A. Rothe, 110–135. Los Angeles: Getty Conservation Institute.
35. van der Snick, G. C. Miliari, K. Janssens, B.G. Brunetti, A. Romani, F. Rosi, P. Walter, J. Castaing, W. De Nolf, L. Klaassen, I. Labarquee and R. Wittermann, 2011. Material analyses of s: Getty Conservation Institute. aking Angelslyses of s: Getty Conservation Institute.d to Hans Memling and assistants: Part I. non-invasive in situ investigations, *Journal of Analytical Atomic Spectrometry*, 26, 2216
36. van Grevenstein, A. and R. Spronk, *An interdisciplinary research project to assess the structural condition of the Ghent Altarpiece*, Final project report, October 9, 2011, 20, accessed March 30, 2019, <http://closertovaneyck.kikirpa.be/?doc=Final%20project%20report.pdf>.
37. Weislogel, A.C. V. Utermohlen, L. Ferri, and T. Wazny. 2001. *Unknown World: Art, Exploration and Trade in the Dutch Golden Age*. Ithaca: Cornell University Press.
38. Ziemba A. 2011. *Sztuka Burgundii I Niderlandów (Burgundian and Netherlands Art, 1380–1500)*, volume II, 545–551, Warsaw: Warsaw University Press